Nicolaus Copernicus University in Toruń
Faculty of Earth Sciences and Spatial Management

Forest Fragmentation Dynamics in Tuchola Forest, Poland. A Multiscale Analysis Using Remote Sensing

By **Sanjana Dutt**

Doctoral thesis completed at
The Department of Geoinformation
and Environmental Remote Sensing

under the supervision of

Dr. hab. **Mieczysław Kunz**, prof. of NCU

Toruń, 2025

To my Parents

Table of Contents

Once, I heard an Indian mystic say that if you give a flower to a scientist, the first instinct is to take it apart—study its parts, its functions, its design. In doing so, we uncover its structure but lose the soul of the flower.

I have always feared becoming that scientist.

Acknowledgments

Centuries ago, explorers like Ibn Battuta and Marco Polo set out to understand the world, mapping cultures, landscapes, and ways of life. Their curiosity hooked me as a teenager and set me on my own trail of questions—like why sands near rivers and seas feel so different, or why trees in Kolkata and the Himalayas grow with such contrasting logic. I kept an atlas close and decided geography would be my passport. I didn't know how to make a living out of curiosity—only that I loved the quest and dreaded a 9–5. For this stubbornness, I owe my *father*, who never discouraged asking questions; my *mother*, who believed in me; and everyone who declined to help—they pushed me to find my own way.

Fast forward to 2021—I started my PhD in a town where an astronomer once wandered. Leaving a metropolis for a place with more trees than people was intimidating, but I'm so glad I did. I want to thank the campus trees—the forest where I found my solitude—which saw the real struggles and somehow held me anyway. And to the souls who made these years buoyant and indelible: *Kinga*, who always had my back; *Aunt Hanna* for warm Easters and Christmases; *Arameh* for never missing a birthday; *Aniqa*, whose food felt like home; *Vivek* and *Rahul*, for their academic advice and a horrible sense of humour; and the lively crew of *Dormitory 10, 6th floor*. To my childhood friends—*Debapriya*, *Sohini*, and *Ishani*—for being one call away, and to *Irfan*, my travel co-conspirator, for turning every trip into a story worth keeping. And to the most brutally honest peer reviewers of all—the weights at the *gym*—thank you for tearing my muscles and somehow rewiring my brain.

On the academic side, I'm grateful to *Professor Wiesław Nowak*, a mentor far beyond his director's role, and to my supervisor, *Professor Mieczysław Kunz*, for the freedom to work independently, for his guidance, and for always backing me with recommendations. Thanks to *Dr. Radosław Golba*, *Dr. Eng. Dominika Daab*, *Dr. Barbara Szyda*, and the NCU Statistical Analysis Center—especially *Jakub Wojtasik*—for handling my endless requests. I'm thankful to *Professor Andrzej Nienartowicz* for welcoming me to the *Ecological Questions* review team; to the Department of International Partnerships and Educational Mobility of NCU for shepherding my academic travels; and to the IDUB, AST, and PROM programs for funding. The Doctoral School of Exact and Natural Sciences of NCU, and our wonderful secretary, *Agnieszka Górska-Pukownik*, made this journey far smoother than it might have been.

I'm deeply grateful to my collaborators—*Dr. Amit Batar* (Japan), *Dr. Dimitri Justeau-Allaire* (France), *Dr. Carlos Rivas* (Spain), and *Professor Tarmo K. Remmel* (Canada). Their ideas, patience, and good humor shaped this thesis at every turn. Many others from conferences and late-night emails helped spark new paths; their influence threads quietly through these pages.

Above all, to my *brother*—thank you for mocking my clumsy attempts, brushing off failures with a casual "*meh*" and cheering the loudest for every win. This thesis, like every journey, is just another step in my lifelong quest to understand forests, the earth, and *life itself.*

Abstract

Forest fragmentation significantly affects biodiversity, carbon sequestration, and ecosystem resilience. Yet temperate forests—such as those in northern Poland within the Tuchola Forest Biosphere Reserve (TFBR; Polish: RBBT)—remain understudied compared with tropical systems. This dissertation analyzes fragmentation dynamics in the TFBR, a landscape shaped by monocultural forest management, strong land-use pressure, and extreme events, notably the August 2017 windstorm. Using satellite remote sensing at multiple resolutions (Sentinel-2, ALOS PALSAR, Landsat-8, CORINE), advanced landscape metrics (e.g., Forest Area Density, FAD), and machine-learning methods, I examine multiscale and multitemporal patterns, ecological consequences, and monitoring strategies to support adaptive protection and increase resilience.

The thesis addresses four questions: (i) How have methods for assessing forest fragmentation evolved? (ii) How do fragmentation and multiscale disturbances alter forest structure and landscape coherence? (iii) Which ecological processes dominate across fragmentation zones (core, transition, sparse)? (iv) Which vegetation indicators best support monitoring, prioritization, and conservation effectiveness? Across five articles, the dissertation: traces a methodological shift from patch-based metrics to connectivity-oriented approaches (Article 1); establishes reference conditions for pre-disturbance baselines and the onset of fragmentation assessment (Article 2); quantifies post-2017 loss of core forest and expansion of edge zones (Article 3); maps susceptibility to hurricane-force winds using a proprietary fragmentation-risk framework that highlights interfaces with agricultural land (Article 4); and identifies water stress and related processes using Sentinel-2 indices and machine learning (Article 5).

This work provides a scalable, open analytical framework that integrates remote sensing, landscape metrics, and machine learning to assess structural and functional fragmentation, with applications to core-area protection and corridor restoration. Limitations include the lack of LiDAR for 3-D validation, dependence on detailed inventory data, and computational constraints for large-scale modeling. Future research should incorporate voxel-based metrics, deep learning, and continuous validation with high-quality field data.

The methodology is transferable beyond the Tuchola Forest Biosphere Reserve to temperate and boreal forests using cloud platforms (e.g., Google Earth Engine). It supports the Kunming–Montreal Global Biodiversity Framework (30×30 by 2030) and REDD+ MRV objectives, and advances SDGs 15 (Life on Land), 13 (Climate Action), and 6 (Clean Water and Sanitation) by providing practical elements for biodiversity conservation and climate adaptation in temperate forests.

Keywords: Forest fragmentation, landscape metrics, connectivity, remote sensing, machine learning, Tuchola Forest, TFBR, temperate forests, conservation planning, Kunming–Montreal Framework, REDD+ MRV.

Streszczenie

Fragmentacja lasów znacząco wpływa na bioróżnorodność, sekwestrację węgla i odporność ekosystemów, jednak lasy strefy umiarkowanej, takie jak te położone w północnej Polsce w granicach Rezerwatu Biosfery Bory Tucholskie (RBBT), pozostają niedostatecznie zbadane w porównaniu z innymi systemami, np. tropikalnymi. Niniejsza rozprawa analizuje dynamikę fragmentacji w RBBT, krajobrazie ukształtowanym przez monokulturową gospodarkę leśną, intensywną presję użytkowania ziemi oraz ekstremalne zjawiska klimatyczne, takie jak nawałnica z sierpnia 2017 roku. Wykorzystując teledetekcję satelitarną różnej rozdzielczości (Sentinel-2, PALSAR, Landsat-8, CORINE), zaawansowane metryki krajobrazowe (np. gęstość obszaru leśnego, ang. *forest area density*; FAD) oraz uczenie maszynowe, przeanalizowano wzorce wieloskalowe i wieloczasowe, konsekwencje ekologiczne oraz strategie monitorowania, które powinny wspierać adaptacyjną ochronę środowiska i zwiększać odporność ekologiczną.

Praca odpowiada na cztery pytania badawcze: (i) Jak ewoluowały metody oceny i analizy fragmentacji lasów? (ii) Jak fragmentacja i wieloskalowe zaburzenia zmieniają strukturę i spójność krajobrazu leśnego? (iii) Jakie procesy ekologiczne dominują w wyróżnianych strefach fragmentacji, tj. strefie rdzennej, przejściowej i rzadkiej? (iv) Które wskaźniki wegetacji najlepiej wspierają monitorowanie oraz priorytetyzację i efektywność działań ochronnych? Podsumowując pięć załączonych artykułów, rozprawa doktorska prezentuje rozwój metodologii od metryk opartych na płatach do podejścia zorientowanego na spójności krajobrazu (Artykuł 1), wskazuje poziomy odniesienia przed wystąpieniem zaburzeń w krajobrazie i rozpoczęciem oceny fragmentacji (Artykuł 2), szacuje utratę zwartych (rdzennych) obszarów leśnych i ekspansję stref krawędziowych w krajobrazie po wystąpieniu nawałnicy w 2017 roku (Artykuł 3), wskazuje (mapuje) obszary wysokiego ryzyka na skutki huraganowych wiatrów, spowodowane bliskością gruntów rolnych i podatną ekspozycją terenu za pomocą autorskiej koncepcji oceny krajobrazu z wykorzystaniem „modelu podatności na fragmentację" (ang. *Fragmentation Susceptibility Modeling Framework*) (Artykuł 4) oraz identyfikuje stres wodny i inne wybrane parametry, jako efekt dominujących procesów ekologicznych analizowanych przy wykorzystaniu wskaźników teledetekcyjnych opartych na danych obrazowych Sentinel-2 i metodach uczenia maszynowego (Artykuł 5).

Rozprawa doktorska jest pionierskim opracowaniem, które wykorzystuje skalowalne, otwarte ramy analityczne, integrujące teledetekcję satelitarną, metryki krajobrazowe i uczenie maszynowe w celu analizy fragmentacji pod kątem struktury i funkcjonalności, zwłaszcza w kontekście celowej ochrony stref rdzeniowych i odbudowy korytarzy ekologicznych. W trakcie prac zauważono ograniczenia wynikające z braku danych LiDAR do walidacji modelu 3D, zależność wyników analiz od szczegółowych danych inwentaryzacyjnych oraz ograniczenia obliczeniowe w tworzonym modelowaniu wielkoskalowym. Przyszłe badania nad podjętą problematyką, zwłaszcza w zakresie ekologicznym, powinny już wykorzystywać metryki oparte na wokselach, uczenie głębokie i ciągłą walidację modelu w oparciu o dokładne dane terenowe.

Opracowana metodologia ma zastosowanie także poza obszarem analizy – Rezerwatem Biosfery Bory Tucholskie, w monitorowanie lasów umiarkowanych i borealnych z wykorzystaniem danych satelitarnych i platform chmurowych (np. Google Earth Engine; GEE). Narzędzia te wspierają globalne ramy różnorodności biologicznej zawarte w ramach *Porozumienia Kunming-Montreal* (2022), które zakłada odbudowę do 2030 roku 30% zdegradowanych ekosystemów i ochronę 30% obszarów lądowych, oraz działania zapisane w protokole REDD+ (*Reducing Emissions from Deforestation and Forest Degradation*) w celu pomiaru i monitorowania pokrywy leśnej oraz zapasów węgla z wykorzystaniem mechanizmu MRV (*Measurement, Reporting and Verification*) dla łagodzenia zmian klimatycznych. Praca doktorska wspiera *Cele Zrównoważonego Rozwoju ONZ* (ang. *Sustainable Development Goals UN*; SDG) w szczególności SDG 15 (*Życie na lądzie*), SDG 13 (*Działania w dziedzinie klimatu*) oraz SDG 6 (*Czysta woda i warunki sanitarne*), dostarczając praktycznych elementów strategii dla ochrony bioróżnorodności i adaptacji klimatycznej w lasach strefy umiarkowanej.

Słowa kluczowe: fragmentacja lasów, metryki krajobrazowe, spójność krajobrazu, teledetekcja satelitarna, uczenie maszynowe, Bory Tucholskie, RBBT, lasy strefy umiarkowanej, ochrona krajobrazu, Porozumienie Kunming-Montreal, REDD+, MRV.

List of Scientific Publications Related to the Thesis with Impact Factor (IF) and Polish Ministry of Science and Higher Education (MNiSW) Points

Article	Journal / Publisher	IF (2024)	MNiSW Points
Dutt, S., Remmel, T.K., Rivas, C.A., Mazziotta, A., & Kunz, M. (2025). *Advancing Forest Fragmentation Analysis: A Systematic Review of Evolving Spatial Metrics, Software Platforms, and Remote Sensing Innovations.*	*Landscape Ecology* (Under review)	5.1	140
Dutt, S., & Kunz, M. (2022). *Land use/cover changes using Corine Land Cover data following hurricanes in the last 10 years: A case study on Tuchola Forest Biosphere Reserve.*	Book Chapter, [In:] Młynarczyk, A. (ed.): *Środowisko przyrodnicze jako obszar badań*. Vol. IV. Bogucki Wydawnictwo Naukowe, Poznań: 25–42.	–	20
Dutt, S., & Kunz, M. (2024). *Landscape metrics of the Brusy Commune before and after wind-storm: An assessment based on Landsat-8 data.*	*Bulletin of Geography. Physical Geography Series* 26: 19–33.	0.8	40
Dutt, S., Batar, A.K., Sulik, S., & Kunz, M. (2024). *Forest ecosystem on the edge: Mapping forest fragmentation susceptibility in Tuchola Forest, Poland.*	*Ecological Indicators* 161: 111980.	7.4	200
Dutt, S., Wojtasik, J., Justeau-Allaire, D., & Kunz, M. (2025). *How does fragmentation reshape forests? Tracking dominant ecological processes across core, transitional, and rare zones.*	*GIScience & Remote Sensing* (Under review)	6.9	100

Other Scientific Contributions with Impact Factor (IF) and Polish Ministry of Science and Higher Education (MNiSW) Points

Article	Journal / Publisher	IF (2024)	MNiSW Points
Gebrie, A., Mohan, M., Karpowicz, D.A., ... **Dutt, S.,** ... & Hendy, I. (2025). *Potential benefits of biodiversity corridors for fragmented mangrove ecosystems.*	*Biological Conservation* 310: 111309.	4.4	140
Kowal, M., Sorokowski, P., Gjoneska, B., ... **Dutt, S.,** ... & Zumárraga-Espinosa, M. (2025). *Cross-cultural data on romantic love and mate preferences from 117,293 participants across 175 countries.*	*Scientific Data* 12(1): 1103.	6.9	140
Dutt, S. (2024). ***Face to face with the Supercyclone Amphan–Kolkata, 20 May 2020.***	Book Chapter, [In:] N. Abhayawickrama, A. Baird, R.A. Bellingham, S.L. Chakraborty, B. Christie, ... & J.S. Yates (Eds.), *Planetary justice: Stories and studies of action, resistance and solidarity*. Bristol University Press. Policy Press: 155–160.	–	–
Saha, U.D., Bhattacharya, S., Bhattacharya, H.N., Islam, A., Jaiswal, M., Narzary, B., & **Dutt, S.** (2023). *Development of a hyper-avulsive river course during the Holocene on the Himalayan frontal plains.*	*Catena* 231: 107279.	5.7	140
Ghazi, B., **Dutt, S.,** & Torabi Haghighi, A. (2023). *Projection of future meteorological droughts in Lake Urmia Basin, Iran.*	*Water* 15(8): 1558.	3.3	100

Kowal, M., Sorokowski, P., Pisanski, K., ... **Dutt, S.,** ... & Mišetić, K. (2022). *Predictors of enhancing human physical attractiveness: Data from 93 countries.*	*Evolution and Human Behavior* 43(6): 455–474.	3.2	140
Saha, U.D., Saheb, A.M., Islam, A., Barman, S.D., **Dutt, S.,** & Islam, A.R. M. T. (2022). *Characterizing the trend of channel braiding of a tropical transboundary river using spatial growth component analysis and ARIMA model.*	*Advances in Space Research* 70(7): 1773–1794.	2.8	70
Saha, U.D., Bhattacharya, S., Bhattacharya, H.N., & **Dutt, S.** (2022). *Development of the Dharala River Course and Its Response to Neotectonic Indentations-Evidences from Old Data Inventory, Satellite Images and Sedimentary Architecture.*	Book Chapter, [In:] Bhattacharya Harendra Nath (ed.), *Himalayan Neotectonics and Channel Evolution*. Springer International Publishing: 207–237.	–	20

Chapter 1: Introduction

Forest fragmentation—*the rearrangement* of forest into smaller, more isolated patches—reshapes ecological processes even when total forest area stays constant. By changing patch size, isolation, and edge exposure ("fragmentation per se"), it intensifies light and wind at boundaries, elevates vapor-pressure deficits, and raises fire and biotic stress (Arroyo-Rodríguez et al., 2017; Fletcher et al., 2018; Fahrig, 2019; Ma., et al. 2023). Globally, edge proximity is now pervasive—more than two-thirds of forests lie within ~1 km of an edge—so edge-mediated impacts are rarely local anomalies but system-wide constraints (Siegel et al., 2024). Against this backdrop, the Tuchola Forest Biosphere Reserve (TFBR) offers a stringent temperate test case: its even-aged Scots pine (*Pinus sylvestris*) monoculture and shallow rooting accentuate susceptibility to edge-driven moisture stress, wind exposure, and fire, especially after the 2017 derecho (Wulder et al., 2009; Britton et al., 2024).

This thesis positions fragmentation not only as a structural patterning problem but as a **pattern → process → action** workflow: role-based and density metrics (MSPA, FAD) diagnose structure; Sentinel-2 vegetation indices (e.g., NDRE for pigment stress; NDMI/NDWI for moisture) capture functional responses; and zone-specific management (protect, buffer, restore) follows logically for **Core**, **Transitional**, and **Rare** areas. Articles 1–5 build this case across scales and sensors, and here I frame the ecological motivation, methodological evolution, TFBR context, conservation implications, and the research questions, objectives, and hypotheses that guide the work.

1.1 Background and Motivation

Forests sustain biodiversity, carbon storage, and hydrological regulation (Mazziotta et al., 2025). Yet land-use pressures and intensifying disturbances reconfigure forest into smaller, more exposed units that disrupt connectivity and processes (Fahrig, 2003; Fletcher et al., 2018). Temperate systems like **TFBR** remain under-represented relative to tropical case studies, even though their **even-aged pine structure (>90%)** increases edge sensitivity and limits rooting depth, amplifying moisture stress and fire risk compared to mixed deciduous stands (Wulder et al., 2009; Britton et al., 2024). Leveraging high-resolution remote sensing (Sentinel-2; PALSAR), fixed-window density (FAD), role-based morphology (MSPA), and interpretable machine learning, this thesis develops **scalable, auditable** monitoring tools aligned with Kunming–Montreal targets and REDD+ MRV (Haneda et al., 2025; Mazziotta et al., 2025).

Definitions & Parameters used throughout the thesis (authoritative summary)

- **Forest definition / MMU:** FAO/HRL-FTY — ≥ 0.5 ha, ≥ 10% canopy cover, trees ≥ 5 m at maturity.
- **Edge width (for edge-based metrics/MSPA): 100 m**; "core" is **≥ 200 m** from edges.
- **FAD/FOS rolling window (harmonised):** Sentinel-2 10 m: **51×51 px** (~510 m); Landsat-8 30 m: **17×17 px** (~510 m); CORINE 100 m: **5×5 px** (~500 m). *Sensitivity:* ± 20% reported.
- **FAD zones: Core ≥ 90%**, **Transitional 40–60%**, **Rare ≤ 10%** forest cover.

- **Compositing (Sentinel-2): Medoid, leaf-on DOY ~180–260**; S2 cloud/shadow mask + snow filter; despiking via robust z-score.
- **Change detection (where applied): LandTrendr** on NDVI/NDMI with standard segmentation and recovery constraints (full params: Appendix A).
- **Model evaluation: Spatial block CV (k = 5)** + held-out test (by year/area); metrics AUC, Kappa (and OOB-R^2 where relevant); permutation FI + PDP/ICE.

1.2 Ecological Impacts of Fragmentation

Edge environments alter light, wind, and moisture regimes, accelerating pigment decline and desiccation, and increasing vulnerability to fire and pests (Arroyo-Rodríguez et al., 2017; Fletcher et al., 2018). Figure 1 illustrates this as an "iceberg" cascade: the visible ecological changes at edges trigger knock-on effects below the waterline—shifts in biodiversity, losses in ecosystem services (carbon, water, recreation), risks to people, and long-term evolutionary consequences. In TFBR, the 2017 derecho sharply expanded edges and reduced cores, compromising interior-dependent species and services like carbon and hydrological buffering (Ahmad et al., 2025). While small patches can act as stepping-stones for mobile taxa, population stability of interior specialists still requires large, connected cores (Blake & Karr, 1984; Fahrig et al., 2019). To avoid confounding composition with configuration, I stratify the landscape into Core, Transitional, and Rare zones using FAD, then read functional responses with Sentinel-2 indices: NDRE and CIred-edge/GARI for pigment dynamics, NDMI/NDWI for canopy water status, and NDVI/EVI for greenness/biomass (Lausch et al., 2016; Wang et al., 2010; Xue & Su, 2017).

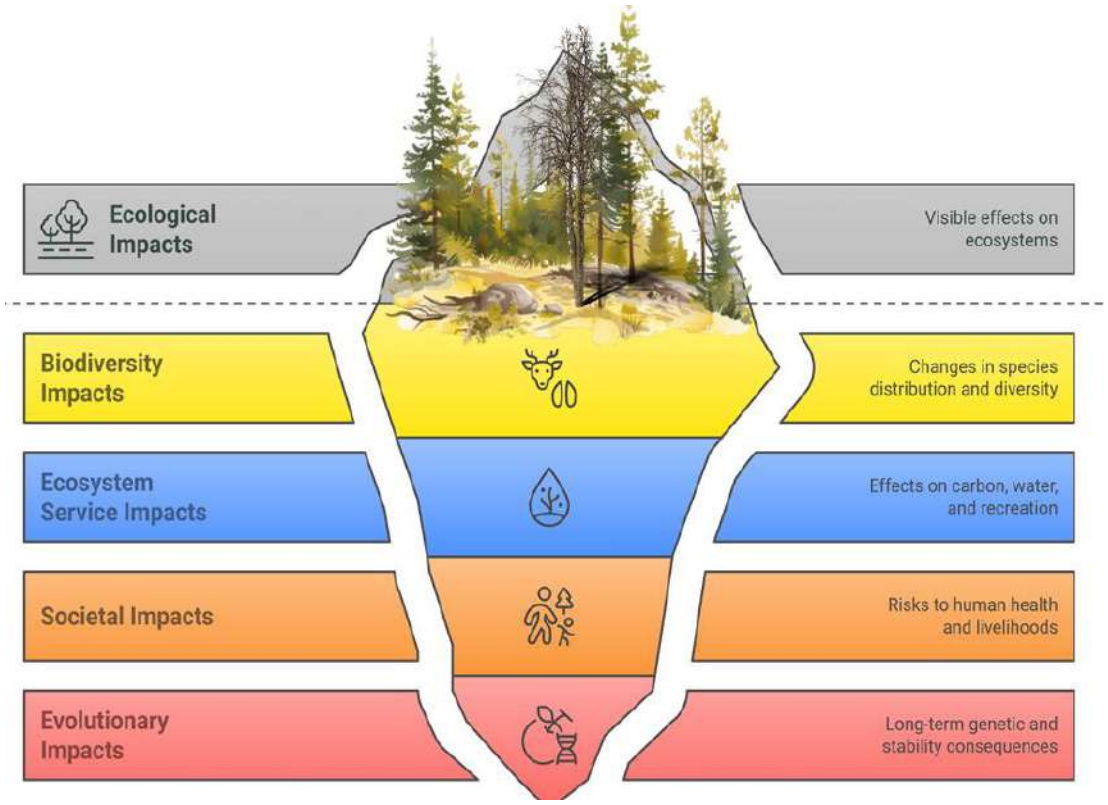

Figure 1: Fragmentation's "iceberg" of impacts: edge-driven microclimate changes → visible ecological effects → deeper consequences for biodiversity, ecosystem services, society, and evolution.

1.3 Evolution of Fragmentation Analysis

Methods progressed from patch/edge/shape metrics (e.g., FRAGSTATS) and neutral landscape models to role-based morphology (MSPA), fixed-window density (FAD/FOS), and connectivity graphs that generalize to policy scales (McGarigal, 1995; Vogt et al., 2007; Vogt & Riitters, 2017). Advances in remote sensing (Sentinel-2; lidar for canopy height/structure) and change detection (VCT, LandTrendr) enable multi-decadal, multi-sensor tracking of structural change (Maier et al., 2006; Zald et al., 2016; Kennedy et al., 2018). Open, scriptable tools (landscapemetrics, PyLandStats, GuidosToolbox; Google Earth Engine) make workflows auditable and scalable, addressing long-standing issues of scale dependence and reporting inconsistency when paired with explicit parameter disclosure (Hesselbarth et al., 2019; Bosch, 2019; Vogt et al., 2022). This thesis adopts that open pipeline to link structure and function in TFBR.

1.4 Tuchola Forest Context

Designated a UNESCO Biosphere Reserve in 2010, Tuchola Forest Biosphere Reserve spans post-glacial lowlands and wetlands but is dominated by even-aged Scots pine (~96–97%), creating homogeneous canopies and shallow rooting that amplify edge effects and reduce resilience (Jastrzębski et al., 2010; Ahmad et al., 2025). Superimposed windstorms (e.g., 2017 derecho; see photo 1 and 2) intensified fragmentation, particularly along cropland–forest and road interfaces. TFBR's core–buffer–transition zoning provides a natural scaffold for FAD-based stratification and for testing how fragmentation alters ecological processes across zones.

Photo 1: View of the landscape of the Tuchola Forest after a catastrophic storm in August 2017 (courtesy of Daniel Jańczyk)

Photo 2: View of the landscape of the Tuchola Forest after a catastrophic storm in August 2017 (courtesy of Daniel Jańczyk)

1.5 Conservation Implications

A zone-specific reading of fragmentation (see photo 3) translates directly into action: Core zones require strict protection (≥ 200 m from edges) to maintain interior conditions as described by Pfeifer., et al. (2017) and carbon stocks; Transitional zones benefit from buffers and ecological corridors to stabilize pigment and moisture dynamics; Rare zones—highly fragmented and edge-exposed—call for passive rewilding and stepping-stones, with species mixes that improve rooting depth and moisture retention. Early-warning signals from NDRE (pigment) and NDMI/NDWI (moisture) help target interventions before structural decline is visible. These tools align with Kunming–Montreal Targets 2 and 3 and strengthen REDD+ MRV by providing reproducible, high-resolution condition and risk layers for temperate forests (Ye et al., 2020; Haneda et al., 2025; Mazziotta et al., 2025).

Photo 3: View of the forest landscape of the Tuchola Forest demarcating the Core, Transitional, and Rare areas based on canopy continuity vs. openings from field study by the author (not a computed FAD surface) (photo: Mieczysław Kunz).

1.6 Research Questions, Objectives, and Hypotheses

This thesis synthesizes five empirical articles (2016–2024) analyzing TFBR's forest fragmentation using remote sensing datasets (CORINE Land Cover, Landsat-8, PALSAR, Sentinel-2), landscape metrics, and ecological ground data (Polish Forest Data Bank) (Pekkarinen et al., 2009; Altunel & Celik, 2025).

Research Questions (RQ):

- **RQ1:** How have forest fragmentation definitions and measurement methods evolved, and which are most effective for temperate forest landscapes?
- **RQ2:** How do fragmentation dynamics (e.g., core loss, edge expansion) and the 2017 derecho affect ecological processes across TFBR's Core, Transitional, and Rare zones?
- **RQ3:** What are the ecological impacts of fragmentation on vegetation health and ecosystem function across TFBR's fragmentation zones?
- **RQ4:** Which Sentinel-2-derived vegetation indices, integrated with machine learning, best support monitoring and prioritized conservation (e.g., core protection, transitional buffering, rare restoration) in TFBR?

Objectives (O):

- **O1:** Synthesize the evolution of fragmentation analysis to establish a methodological foundation for temperate forests (Article 1).
- **O2:** Quantify temporal and spatial fragmentation changes in TFBR driven by the 2017 derecho (Articles 2–3).
- **O3:** Assess fragmentation's ecological impacts on vegetation health and ecosystem function across Core, Transitional, and Rare zones using FAD zoning (Articles 2–4).
- **O4:** Develop Fragmentation Susceptibility Models using Bayesian Weight-of-Evidence (WoE) and machine learning to predict risk from drivers like cropland proximity and windstorm exposure (Article 4).
- **O5:** Identify sensitive Sentinel-2-derived vegetation indices (e.g., NDWI, GNDVI, EVI) using machine learning to support conservation prioritization (Article 5).

Hypotheses (H):

- **H1:** Fragmentation increased post-2017 derecho, reducing core forest areas and expanding edge zones, as measured by FAD and MSPA.
- **H2:** Vegetation health, assessed via NDWI, GNDVI, and EVI, is negatively correlated with fragmentation intensity, particularly in Transitional and Rare zones.
- **H3:** Advanced landscape metrics (e.g., FAD, MSPA) and Bayesian WoE models, integrated with PALSAR and Sentinel-2 data, accurately predict fragmentation susceptibility, guiding conservation.
- **H4:** Sentinel-2-derived indices (NDWI, GNDVI, EVI), combined with machine learning, robustly predict ecological conditions across TFBR's zones, enhancing monitoring.

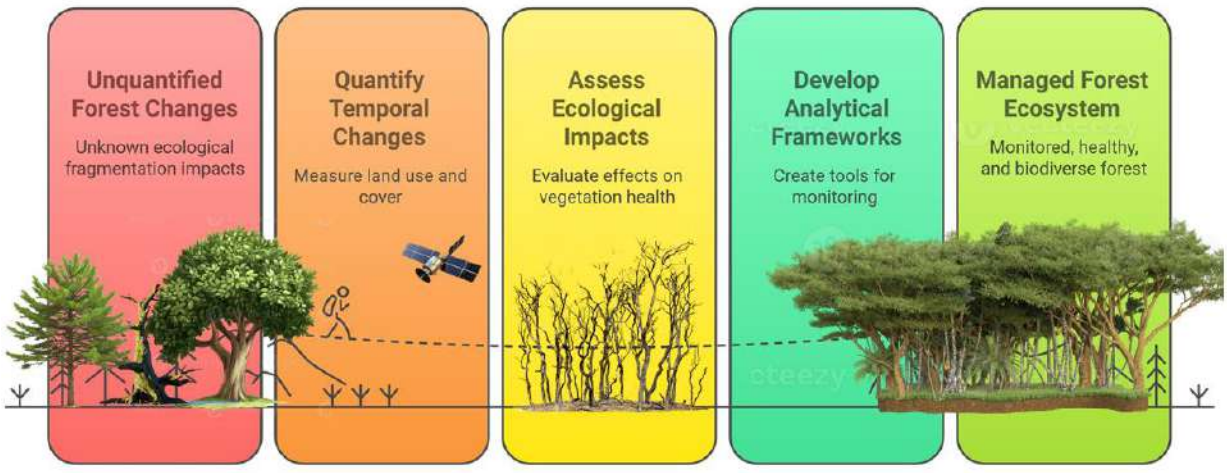

Figure 2: Conceptual roadmap for forest fragmentation monitoring in Tuchola Forest. The framework highlights five research goals: identifying unknown ecological impacts, quantifying temporal change, assessing vegetation health, building analytical tools, and informing sustainable forest management.

1.7 Structure of the Thesis

Here I outline how the thesis unfolds and how the embedded articles fit together. The structure moves from concepts to context, from methods to results, and finally to synthesis. Part I motivates the problem and situates this work within the methods literature; Part II details the TFBR study area and analytical workflow that underpin all analyses; Part III compiles the empirical articles into a coherent narrative of dynamics, drivers, and monitoring; and Part IV integrates findings, limitations, and implications for management and policy. This roadmap is intended to help readers navigate cross-references between chapters and articles and to see how each component contributes to the overarching research aims.

The thesis is organized into four parts:

- **Part I: Conceptual Framework (Chapters 1)**: Introduces fragmentation impacts, research objectives, and a systematic methodological review (Article 1).
- **Part II: Study Area and Analytical Framework (Chapters 2–3)**: Describes TFBR's ecological context and outlines methodologies, datasets, and analytical tools.
- **Part III: Empirical Analyses (Articles 2–5, Chapter 4)**: Presents findings on fragmentation dynamics, disturbance impacts, susceptibility mapping, and ecological monitoring.
- **Part IV: Conclusions (Chapter 5)**: Integrates insights, evaluates contributions and limitations, and provides recommendations for research and management.

This synthesis advances understanding of temperate forest fragmentation, delivering actionable tools for sustainable management and global conservation goals.

Chapter 2: The Tuchola Forest Biosphere Reserve

The Tuchola Forest Biosphere Reserve (TFBR), designated by UNESCO in 2010, is a key case study for analyzing forest fragmentation dynamics in temperate landscapes. This chapter details TFBR's geographical, ecological, and conservation contexts, emphasizing its postglacial landscape, pine-dominated monoculture, and UNESCO zonation as a framework for studying fragmentation and climatic disturbances. Detailed ecological analyses, such as Forest Area Density (FAD) zoning and vegetation stress, are deferred to Articles 2–5 (Chapter 5), aligning with the thesis's empirical findings. By highlighting TFBR's unique features, this chapter underscores its significance for global temperate forest research and conservation policies, including the Kunming–Montreal Global Biodiversity Framework and REDD+ MRV protocols (Haneda et al., 2025; Mazziotta et al., 2025).

2.1 Geographical Context

The TFBR spans 3,195 km² across Poland's Pomeranian and Kuyavian-Pomeranian voivodeships, covering 22 communes (Nienartowicz et al., 2010; Nienartowicz & Kunz, 2018), see figure 4. Its postglacial lowland landscape, featuring sandy outwash plains, lakes, and peat bogs, creates a distinctive ecological setting for fragmentation studies (Kistowski, 2020). Organized into a core zone (78.8 km², including Tuchola Forest National Park and 25 nature reserves), a buffer zone (1,046 km²), and a transition zone (2,069 km²), TFBR's UNESCO zonation, shown in Figure 3, supports multi-scale fragmentation analyses and restoration planning (Kunz & Nienartowicz, 2013; Kunz, 2020). The reserve's six physical regions—Wysoczyzna Świecka, Równina Charzykowska, Pojezierze Kaszubskie, Pojezierze Starogardzkie, Bory Tucholskie (Tuchola Forest), and Dolina Brdy—host diverse ecological conditions, with Bory Tucholskie as the forested core and Dolina Brdy supporting critical wetlands (Kistowski, 2020). This structure positions TFBR as a model for assessing temperate forest responses to land-use and climatic pressures (Kunz & Nienartowicz, 2021; Ahmad et al., 2025).

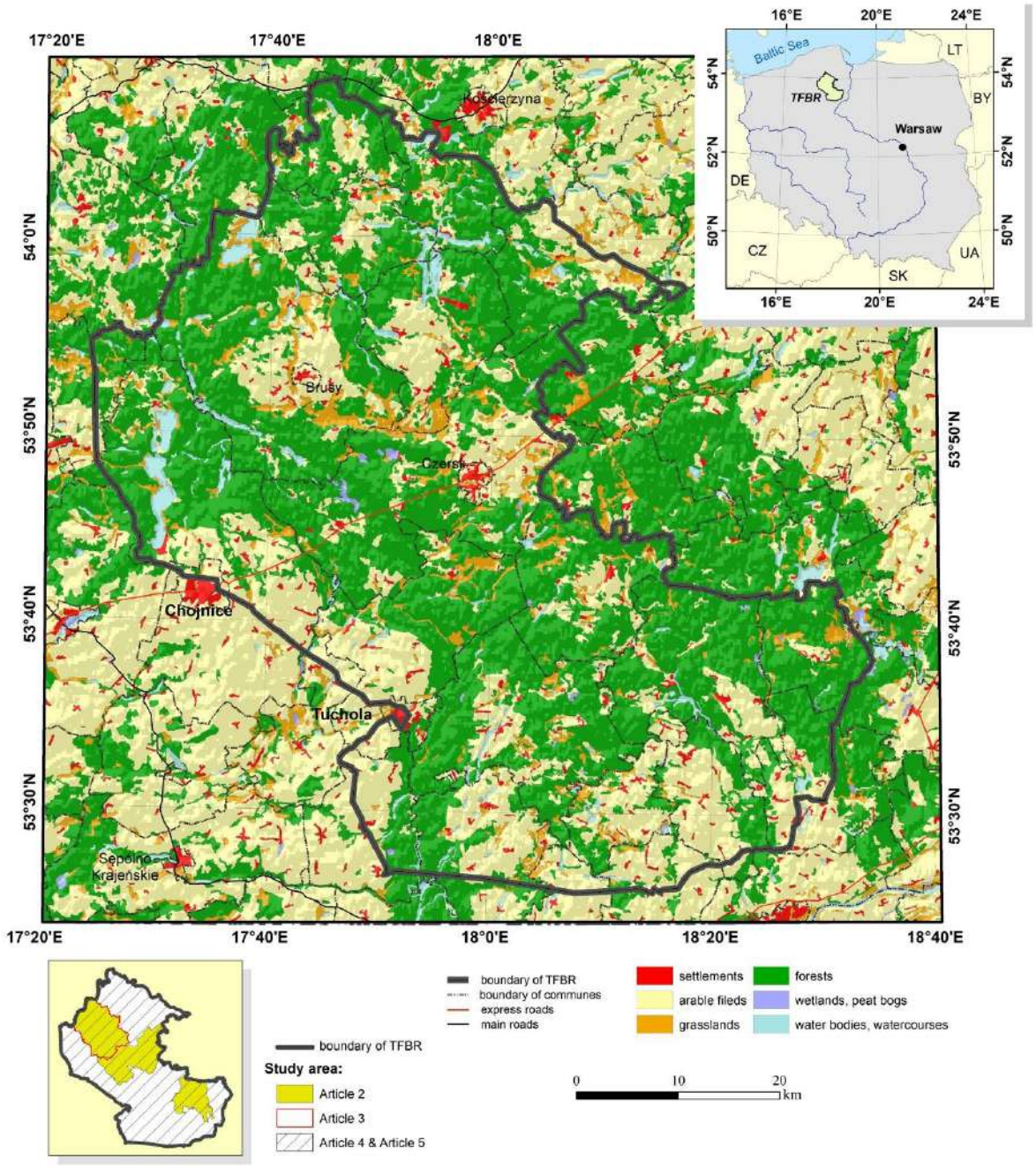

Figure 4: Map of the Tuchola Forest Biosphere Reserve (TFBR) with detailed research areas.

2.2 Ecological Characteristics

Dominated by a Scots pine (*Pinus sylvestris*) monoculture (96.8% of forest cover), TFBR's historical forestry practices amplify its vulnerability to fragmentation and climatic disturbances like the 2017 derecho (Jastrzebski et al., 2010; Ahmad et al., 2025). This homogeneity, unlike mixed temperate or tropical forests, intensifies edge effects and connectivity loss, reducing resilience (Fahrig, 2003; Blanchard et al., 2023). The 2017 derecho exacerbated core forest loss and edge expansion, with impacts analyzed in Articles 2–4 (Chapter 5) (Taszarek et al., 2019; Mazziotta et al., 2025). TFBR's biodiversity, including unique wetlands and lobelia lakes,

supports vital ecological functions, but fragmented patches threaten species like the hazel grouse, facing dispersal barriers (Rutkowski et al., 2016; Peterson et al., 2025). These traits make TFBR a compelling case for studying disturbance-driven fragmentation, with global implications (Kunz et al., 2023; Saura, 2021).

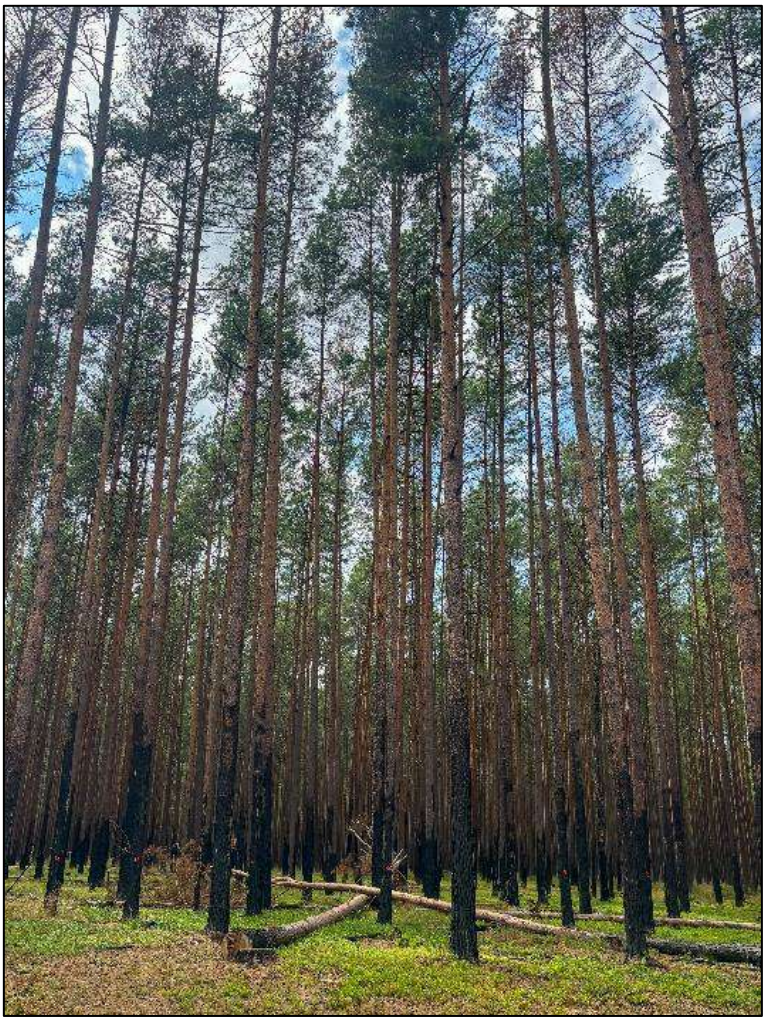

Photo 4. Disturbance evidence in TFBR (field view). Basal charring on even-aged Scots pine (*Pinus sylvestris*) with scattered windthrow indicates recent fire activity and edge-amplified stress typical of Transitional/Rare FAD zones (photo: Sanjana Dutt).

2.3 Conservation Challenges and Policy Context

TFBR faces conservation challenges from its pine monoculture, climatic stressors, and pressures from agriculture and forestry (Referowska-Chodak & Kornatowska, 2021; Ahmad et al., 2025). As a Natura 2000 site, it reflects Poland's biodiversity commitments, but the lack of legal status for biosphere reserves limits management (Referowska-Chodak & Kornatowska, 2021). The thesis's tools, including fragmentation susceptibility mapping and vegetation monitoring (Articles 4–5), offer solutions, aligning with global policies:

Photo 5. Timber extraction in TFBR. Harvest operations create new/temporary edges and access tracks that can influence fragmentation metrics and spectral signals (photo: Sanjana Dutt).

- **Kunming–Montreal Global Biodiversity Framework (2022)**: Targets 2 (30% ecosystem restoration) and 3 (30% protected areas) are supported by TFBR's need for ecological corridors and core zone protection. The thesis's remote sensing and machine learning tools (Articles 4–5) prioritize conservation actions, such as mapping high-risk zones (Mazziotta et al., 2025; Ye et al., 2020).
- **REDD+ MRV Protocols**: These require precise forest cover and carbon stock monitoring. The thesis's integration of Sentinel-2 and PALSAR data (Articles 4–5) enhances REDD+ compliance in temperate forests (Haneda et al., 2025).
- **United Nations Sustainable Development Goals (SDGs)**: The research supports SDG 15 (Life on Land) via habitat conservation, SDG 13 (Climate Action) through carbon mapping, and SDG 6 (Clean Water) by linking fragmentation to hydrological resilience (Haneda et al., 2025; Mazziotta et al., 2025).

These alignments position TFBR as a model for integrating local and global conservation efforts, providing scalable tools for temperate forest management, see photo 5.

Chapter 3: Materials, Methods, and Analytical Framework

We quantify forest fragmentation in the Tuchola Forest Biosphere Reserve (TFBR) using a scalable, open workflow that links structure (FAD/MSPA and classical landscape metrics) to function (Sentinel-2 vegetation indices) and to action (susceptibility mapping and zone-specific guidance), refer to figure 5. All parameters affecting scale and comparability (minimum mapping unit, edge width, rolling-window sizes, compositing policies, resampling rules, and cross-validation design) are declared here to ensure full reproducibility and policy-grade reporting. Choices are aligned with Kunming–Montreal Targets 2 and 3 and with REDD+ MRV practices.

Figure 5: Conceptual workflow for forest fragmentation analysis in the Tuchola Forest Biosphere Reserve. The framework illustrates the stepwise integration of satellite inputs,

preprocessing, classification, landscape metrics, advanced analytics, spatial tools, ground validation, and ecological interpretation to produce spatially explicit outputs that inform conservation planning.

3.1 Evolution of Fragmentation Analysis

Early work emphasized patch/edge/shape statistics (e.g., FRAGSTATS), which are replicable but weakly linked to connectivity and processes. Subsequent advances introduced (i) **role-based morphology** (MSPA) that distinguishes core/edge/bridge roles; (ii) **fixed-scale density** (e.g., Forest Area Density, FAD) that standardizes configuration across sensors and eras; and (iii) **connectivity indicators** and graph/circuit analogues that generalize to corridor planning. In parallel, disturbance "feeders" (LandTrendr, VCT, CCDC) stabilized time-series diagnostics, and open pipelines (R, Python, GEE) made analyses auditable at scale. This study adopts that trajectory: MSPA + FAD for structural diagnostics, paired with interpretable ML on Sentinel-2 indices to read **zone-specific functional responses** in Core, Transitional, and Rare contexts.

3.2 Datasets and Satellite Platforms

We use multi-sensor data to span **regional (100 m)**, **local (30 m)** and **fine (10–20 m)** scales:

- **CORINE Land Cover (1990–2018, 100 m)** — regional baselines for composition/configuration, cautioning under-detection of fine fragmentation. *Use:* Article 2 baselines.
- **Landsat-8 OLI (30 m)** — local trajectories for the 2017 derecho context; atmospherically corrected (Collection 2 L2), cloud/shadow masked, composited to annual leaf-on medoids. *Use:* Article 3.
- **ALOS PALSAR (25 m, L-band SAR)** — structure under clouds/debris; radiometric calibration to γ^0, terrain correction, and Refined-Lee speckle filtering prior to FAD/MSPA and susceptibility modeling. *Use:* Article 4.
- **Sentinel-2 MSI (10–20 m, L2A)** — fine-scale VIs and FAD zoning; QA60 + cloud/shadow masks; **leaf-on medoid** composites (DOY ≈ 180–260) to harmonize phenology. Bands: B2 (Blue), B3 (Green), B4 (Red), B5–B7 (Red-edge), B8 (NIR), B11/B12 (SWIR). *Use:* Article 5.
- **Polish Forest Data Bank (BDoL)** — stand attributes for validation/interpretation (degradation, moisture/site type, age), acknowledging variable thematic granularity.

Preprocessing common to all rasters. Reprojection to EPSG:2180 (PUWG 1992); alignment to a common extent/grid; resampling rules: nearest-neighbour for categorical (classes/MSPA), bilinear for continuous (indices); explicit data lineage and parameter files. Compositing policy (optical). Annual medoid of leaf-on stack to suppress outliers; sensitivity ±DOY 20 d reported. Rolling-window harmonization. FAD/FOS windows standardized at ~500 m across sensors:

- Sentinel-2 (10 m): 51×51 px,
- Landsat-8 (30 m): 17×17 px,

- CORINE (100 m): 5×5 px.
  Edge width = 100 m; *Core* defined as ≥200 m from edge. Sensitivity ±20% reported.

Alternative datasets, such as Dynamic World (10 m, Sentinel-2, near real-time), World Cover (10 m, Sentinel-2), and Esri Land Cover (10 m, Sentinel-2), offer high accuracy for forest classes (72–75%) but were not used due to limited historical coverage for TFBR's long-term analysis (Brown et al., 2022, 2023; Venter et al., 2022; Altunel & Celik, 2025). MODIS (250–1000 m) and Sentinel-1 (10 m, SAR) were excluded for coarser resolution or limited spectral bands for vegetation analysis (Radeloff et al., 2024). High-resolution platforms like PlanetScope or Pléiades Neo were considered but deemed cost-prohibitive (Mazziotta et al., 2025). Preprocessing, including atmospheric correction and cloud masking, was conducted using Google Earth Engine (GEE), chosen over proprietary platforms like ENVI or ArcGIS for scalability and accessibility (Mutanga & Kumar, 2019; Zhao et al., 2021). Specific dataset applications are detailed in Articles 2–5.

Table 1: Evolution of toolsets and datasets for forest fragmentation analysis (1990–2025).

Period	Tools/Datasets	Characteristics	Thesis Application
1990–2000	FRAGSTATS, Landsat	Patch-based, coarse resolution	Baseline metrics (Article 2)
2000–2010	GuidosToolbox, MODIS	Landscape connectivity focus	Connectivity analysis (Article 3)
2010–2025	GEE, Sentinel-2, PALSAR	High-resolution, process-oriented	Susceptibility modeling, ecological monitoring (Articles 4–5)

3.3 Landscape Metrics

Landscape metrics quantify TFBR's fragmentation patterns across core, buffer, and transition zones using the R package *landscapemetrics* (Kupfer, 2012; McGarigal et al., 2012, as cited in Ahmad et al., 2025). Key metrics include Number of Patches (NP), Edge Density (ED), and Shannon's Diversity Index (SHDI), with FAD zoning classifying areas into Core (≥90% forest cover), Transitional (40–60%), and Rare (≤10%) zones (Riitters et al., 2000, as cited in Article 3). MSPA, implemented via GuidosToolbox, enhances core-edge-bridge analysis, supporting connectivity assessments (Vogt & Riitters, 2017; Ye et al., 2020). Functional metrics, such as least cost distance and graph-based connectivity (e.g., node degree, centrality), were evaluated but not used due to data constraints and TFBR's focus on structural patterns (Kupfer, 2012; Fletcher et al., 2018). Alternatives like ArcGIS or QGIS were considered but excluded for open-source preference. Metric calculations and ecological implications are detailed in Articles 3–5.

3.4 Remote Sensing Analysis

Remote sensing datasets were processed to map forest cover, detect disturbances, and assess ecological conditions. Sentinel-2 and PALSAR data generate FAD maps and monitor structural changes, while Landsat-8 provides temporal context for the 2017 derecho's impacts (Articles

3–4) (Altunel & Celik, 2025; Radeloff et al., 2024). GEE facilitates cloud-free composite generation and time-series analysis, outperforming proprietary platforms due to its scalability and open access (Mutanga & Kumar, 2019; Zhao et al., 2021). Dynamic World's near real-time capabilities and probability scores were considered but not used due to TFBR's historical focus (Brown et al., 2022, 2023). Sentinel-1 and GOES were excluded for lower optical resolution or regional focus (Radeloff et al., 2024). Change detection algorithms, including LandTrendr for NDVI breakpoints, are detailed in Articles 2–5 (Mazziotta et al., 2025).

3.5 Statistical and Machine Learning Methods

Here I outline the statistical and machine-learning toolbox used in this thesis and the principles guiding model selection, training, and evaluation. Section 3.5.1 motivates the use of tree-based ensembles for high-dimensional, non-linear relationships in Sentinel-2 and ancillary predictors, while Section 3.5.2 introduces a Bayesian Weight-of-Evidence approach to quantify driver contributions and produce interpretable susceptibility maps. Across methods, I specify data partitioning, cross-validation, and performance metrics, and indicate how model outputs are interpreted alongside vegetation indices (Section 3.6) and integrated into the end-to-end pipeline (Section 3.7). This subchapter thus links algorithms to ecological questions, balancing predictive accuracy with transparency and reproducibility.

We framed prediction problems for four Forest Ecological Attributes (FEAs): Degradation (ordinal), Moisture content (ordinal), Site type (ordinal), Stand age (continuous).

3.5.1 Ensembles

- **Extra Trees (ET)** for primary modeling (robust to high-dimensional, non-linear interactions; fast; low variance through randomized splits).
- **LightGBM (LGBM)** as a secondary comparator (gradient-boosted trees).
- Hyperparameters: tuned via Bayesian or coarse-to-fine grid (trees, max depth, min samples per split/leaf, subsampling where applicable).
- Class imbalance: stratified sampling / class weights for ordinal FEAs.

3.5.2 Spatial evaluation & interpretability

- Leakage control: spatial block cross-validation (k=5) + held-out test split by year/area.
- Metrics: AUC and Cohen's Kappa for ordinal FEAs, OOB-R^2/MAE for stand age; distributional diagnostics (boxplots of normalized errors).
- Explanations: Permutation Feature Importance (FI), Partial Dependence (PDP) and ICE; interpretation is zone-aware (Core vs Transitional vs Rare).

3.5.3 Bayesian Weight-of-Evidence (WoE)

For fragmentation susceptibility, WoE quantifies the log-odds contribution of drivers (e.g., distance to cropland/roads, wind speeds, slope, tree height/age). Categories are constructed to minimize multicollinearity (checked by correlation matrices) and maximize monotonic interpretability. Outputs: susceptibility map + ROC/Kappa validation.

3.6 Vegetation Indices

Vegetation indices, derived from Sentinel-2, monitor ecological health across TFBR's fragmentation zones. We standardize VI usage and terminology (Sentinel-2 bands in parentheses):

- **NDVI** = (B8−B4)/(B8+B4) — greenness/biomass; saturates at high LAI.
- **EVI** = 2.5·(B8−B4)/(B8+6·B4−7.5·B2+1) — greenness with aerosol/soil correction; less saturation.
- **GNDVI** = (B8−B3)/(B8+B3) — chlorophyll-leaning greenness
- **NDRE** = (B8−B5)/(B8+B5) [alt: B6/B7] — **early pigment stress**, red-edge sensitive (pine-appropriate).
- **CIred-edge** = (B8/B5) − 1 [alt: B6/B7] — chlorophyll proxy, very sensitive.
- **NDMI** = (B8−B11)/(B8+B11) — **canopy water status**; we use this as the **moisture index**.
- **GARI** = (B8 − [B3 − (B2 − B4)])/(B8 + [B3 − (B2 − B4)]) — pigment stress, atmospherically resistant.

Detailed analyses and conservation applications are presented in Article 5.

3.7 Analytical Integration

The analytical framework integrates datasets, metrics, and models to address RQs 1–4 (Chapter 1), as summarized in Table 2. Figure 6 illustrates the pipeline, from data acquisition to conservation recommendations, ensuring traceability across Articles 2–5. The framework supports Kunming–Montreal Targets 2 and 3 and REDD+ MRV by providing scalable tools for temperate forest management, addressing edge effects and connectivity thresholds (Haneda et al., 2025; Peterson et al., 2025; Saura, 2021).

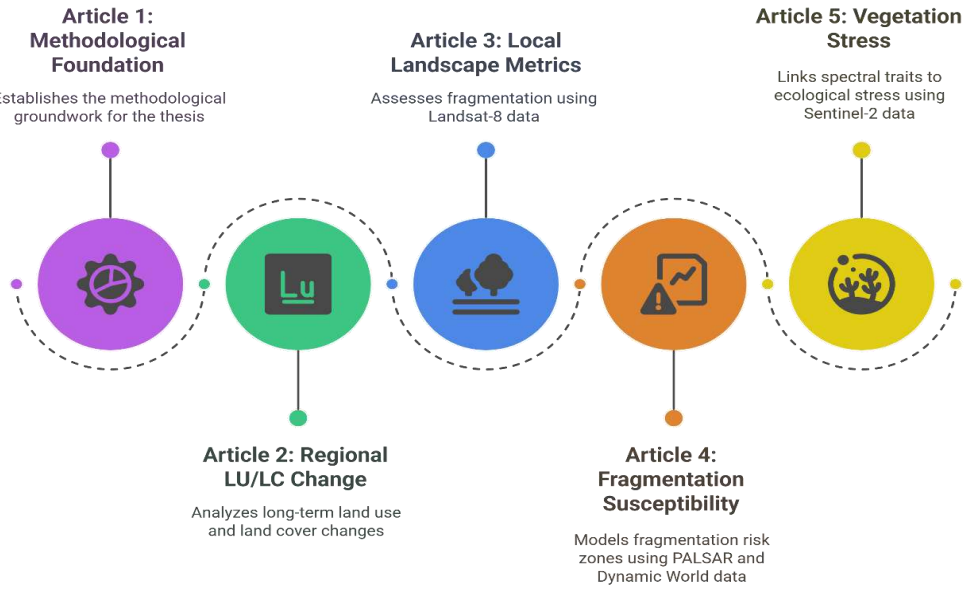

Figure 6: Conceptual framework linking the five core research articles. Article 1 provides the methodological foundation, while Articles 2–5 apply and extend specific techniques (e.g., FAD,

RF, WOE, NDVI/GNDVI) to map fragmentation dynamics, model susceptibility, and assess ecological condition.

Table 2: Summary of Articles' Contributions and Methodological Links

Article	Focus	Data	Methods	Key outputs	Links to other articles
1	Methodological evolution	Literature review	Systematic review, synthesis	Tool and index evolution	Framework for 2–5; justifies tool selection
2	Regional LU/LC change (1990–2018)	CORINE	FAD (GuidosToolbox), NP, ED, SHDI (FRAGSTATS)	62% to 55% Intact decline, SHDI rise to 1.6	Baseline for Articles 3–5
3	Local fragmentation (Brusy)	Landsat-8	FAD, RF (GEE), NDVI, ED (Patch Analyst)	12% Intact loss, 67% ED increase	Supplies inputs to 4, supports validation in 5
4	Fragmentation susceptibility	PALSAR, Dynamic World	WOE, RF, FAD	High-risk Patchy zones mapped	Extends 2–3, inputs ecological zones for 5
5	Vegetation stress and index analysis	Sentinel-2	Extra Trees, NDWI, GNDVI, SVH	25% canopy loss, stress in Patchy zones	Synthesizes 2–4; applies ST/STV framework

3.8 Methodological Gaps and Future Directions

Limitations include the absence of LiDAR for 3D canopy analysis, reliance on Polish Forest Data Bank for validation, and computational constraints in large-scale machine learning (Blanchard et al., 2023; Haneda et al., 2025). Emerging methods, such as deep learning (e.g., convolutional neural networks), voxel-based LiDAR for carbon stock estimation, and graph-based connectivity metrics, could enhance TFBR's monitoring capabilities, as discussed in Chapter 4 (Brown et al., 2022; Kupfer, 2012; Mazziotta et al., 2025). Dynamic World and GEE advancements offer potential for real-time integration, while small patch conservation could boost biodiversity, per landscape-scale findings (Riva & Fahrig, 2023; Venter et al., 2022). These gaps highlight opportunities to refine tools and support global conservation efforts (Peterson et al., 2025).

Chapter 4: Synthesis, Contributions, and Future Directions

This chapter synthesizes findings from five empirical articles (Articles 1–5, Chapter 5) examining forest fragmentation in the Tuchola Forest Biosphere Reserve (TFBR), a temperate landscape shaped by the 2017 derecho, intensive forestry, and agricultural pressures. Addressing four research questions (RQs) through a multi-scale framework integrating remote sensing (CORINE, Landsat-8, PALSAR, Sentinel-2), landscape metrics (e.g., Forest Area Density [FAD]), and advanced analytics (machine learning, Bayesian modeling), it highlights ecological impacts and methodological advancements. Contributions to science and conservation are outlined, alongside limitations and future research directions, aligning with global policy frameworks like the Kunming–Montreal Global Biodiversity Framework and REDD+ MRV protocols (Haneda et al., 2025; Mazziotta et al., 2025).

4.1 Synthesis of Key Findings

This section integrates evidence across Articles 1–5 to answer RQs 1–4, merging structural diagnostics (FAD, MSPA, connectivity) with functional signals from Sentinel-2 vegetation indices and SAR–optical comparisons. Regionally (CORINE), intact forest declined even before 2017; locally (Landsat-8), the derecho accelerated edge expansion and patch proliferation; at fine scale (Sentinel-2), Transitional and Rare FAD zones carry the brunt of pigment decline (NDRE/GARI) and moisture stress (NDMI/NDWI). SAR (PALSAR) improves classification of Rare/Patchy states under post-disturbance/cloudy conditions, while interpretable ensembles (Extra Trees/LightGBM) expose zone-specific processes that translate directly into management actions.

4.1.1 Cross-Scale Ecological and Methodological Patterns

RQ1: Methodological evolution (Article 1).

The field has moved from patch/edge/shape + fractal descriptors to role-based morphologies (MSPA), fixed-window density (FAD/FOS), and connectivity graphs, implemented in reproducible, open pipelines (R/Python/GEE). This shift matters for temperate forests because fixed-window density stabilizes policy-scale comparisons and role classes (core/edge/bridge) scale to regional reporting.

RQ2 & RQ3: Processes & disturbance (Articles 2–4).

• **Regional/Landsat-8 (Brusy):** Post-2017, Number of Patches +38%, Mean Patch Size −30%, Edge Density up, with a 177.5% increase in damaged forest and −25.2% forest cover in one year—classic fragmentation signatures.

• **FAD zones (S2):** Core shows stable PDPs (buffered), Transitional/Rare show steep, volatile PDPs—consistent with edge microclimates, desiccation, nutrient drawdown. NDRE & GARI are strongest for early degradation in Rare; NDMI/NDRE best capture moisture dynamics (sharp contrasts in Rare; stable in Core).

• **Drivers:** Proximity to cropland (≤200 m), roads, high wind speeds (25–27 km/h), and younger/shorter stands elevate susceptibility; gentler slopes coincide with more fragmented patches.

• **Species context:** Pine dominance buffers some responses but increases edge vulnerability; birch and oak exhibit higher edge sensitivity—relevant for restoration mixes.

RQ4: Monitoring tools (Article 5).

• **Predictors:** NDRE, GARI, GRNDVI flag pigment decline (degradation); NDMI/NDRE capture soil–canopy moisture interplay; NDVI/NDRE support site-type filtering; CVI/NDRE track age but can confuse rapid edge regrowth with maturity.

• **Models:** Extra Trees/LightGBM + PDPs give directional, zone-aware insights.

• **Optical vs SAR:** PALSAR outperforms Dynamic World for Rare/Patchy detection post-storm; SAR–optical fusion is advantageous where clouds or debris complicate optical-only mapping.

Table 3: Cross-Scale Fragmentation Patterns and Conservation Implications

Scale	Data Source	Key Finding	Conservation Implication
Regional	CORINE	Gradual intact forest decline pre-2017 (Article 2)	Prioritize corridor restoration
Local	Landsat-8	67% edge density increase post-derecho (Article 3)	Protect core zones (>200 m from edges)
Fine	Sentinel-2	25% canopy loss in Rare zones (Article 5)	Monitor vegetation stress for restoration

4.2 Contributions to Science and Conservation

This thesis contributes (i) a joined-up, open workflow that ties morphology (FAD/MSPA) and connectivity to functional VIs via interpretable ensembles; (ii) a validated susceptibility model that elevates SAR where optical is limited; and (iii) a reporting canon that addresses the field's L1–L5 issues (scale, regional tuning, validation, bio-links, reporting).

4.2.1 Methodological Innovations

- **Fragmentation Susceptibility (Article 4).** WoE + FAD + environmental drivers using PALSAR & Sentinel-2 maps high-risk zones (AUC 0.82; Kappa 0.68). Iterative refinement lifted ROC from 0.64 → 0.82 by removing non-forest confounders and multicollinear variables, and by aligning to wind severity patterns.
- **Interpretable ML for processes (Article 5).** Extra Trees/LightGBM link NDRE/NDMI/NDVI to degradation, moisture, site type, and age, with PDPs exposing zone-specific response regimes (stable Core vs volatile Rare).
- **Open, reproducible stack.** R/Python/GEE workflows + parameter disclosure (windows, edges, MMU, compositing, CV) make results auditable and portable.

4.2.2 Management Strategies

- **Core:** Strict protection (≥200 m from edges), minimize new edges; preserve carbon & interior specialists.
- **Transitional:** Buffers + corridors to damp pigment/moisture volatility; selective thinning where it moderates extremes.
- **Rare:** Passive rewilding + stepping-stones**,** mixed-species (incl. deeper-rooted) plantings; prioritize patches proximate to cropland/roads and high-wind corridors.

4.2.3 Global Policy Alignment

Beyond local and regional insights, the thesis engages directly with international frameworks for biodiversity and climate action. By situating its findings within the SDGs, the Kunming–Montreal Global Biodiversity Framework, and REDD+ MRV protocols, the research demonstrates how temperate forest monitoring can contribute to broader sustainability goals and reporting mechanisms.

The thesis aligns with:

- **SDGs**: Supports SDG 15 (biodiversity), SDG 13 (carbon mapping), and SDG 6 (hydrological resilience) (Haneda et al., 2025).
- **Kunming–Montreal Global Biodiversity Framework (2022)**: Targets 2 (30% ecosystem restoration) and 3 (30% protected areas) are supported by tools for mapping high-risk zones and monitoring stress (Mazziotta et al., 2025).
- **REDD+ MRV Protocols**: High-resolution mapping and vegetation index analysis track fragmentation-driven carbon loss, enhancing temperate forest monitoring (Haneda et al., 2025).

4.3 Applicability Beyond TFBR

The approach generalizes to temperate/boreal forests and can be adapted to tropics with region-tuned windows/thresholds and cloud-robust SAR–optical fusion. Practical on-ramps: (i) free S2 L2A + PALSAR mosaics; (ii) open code; (iii) a standard reporting checklist. Priorities differ: pine-dominated systems emphasize edge buffering; mixed broadleaf/tropical mosaics require stricter validation to mitigate spectral confusion and stronger graph-connectivity components.

4.4 Limitations

While the thesis advances both methodology and ecological understanding, several limitations must be acknowledged. These include data and resource constraints, methodological sensitivities, and reliance on existing field datasets. Recognizing these boundaries is essential for interpreting the findings appropriately and for charting a realistic path forward in future work.

- **Data & scale.** Sentinel-2 (10 m) and Landsat-8 (30 m) cannot resolve microhabitats; CORINE under-detects fine-scale change, and SAR–optical performance varies with disturbance context and cloud/debris conditions. The absence of LiDAR restricts explicit 3D canopy and vertical connectivity analyses (Blanchard et al., 2023; Pekkarinen et al., 2009).
- **Modeling choices.** Treating categorical ecological attributes as continuous improves gradient detection and PDP interpretability, but may obscure ecological thresholds in edge-dominated **Rare** zones. Ensemble ML is computationally demanding and sensitive to feature sets, partitioning schemes, and hyperparameters.
- **Validation.** Reliance on the Polish Forest Data Bank provides consistent labels but limited physiological detail; broader field/biodiversity validations would strengthen causal inference and reduce site-specific bias (Ahmad et al., 2025).
- **Transferability.** Results are derived from a pine-dominated temperate system; applying thresholds, windows, and susceptibility drivers elsewhere requires regional calibration and local validation.
- **Parameter sensitivity.** Outcomes depend on rolling-window size (FAD/FOS) and edge width; reported ±20% sensitivity tests bracket this uncertainty. Compositing and change-detection policies (e.g., BAP vs. medoid; segmentation/recovery thresholds) also influence detected trends.
- **Computing constraints.** Large-area ML pipelines and SAR–optical fusion incurred processing bottlenecks that limited the breadth of model comparison and frequency of re-runs.

Net effect: these limitations do not overturn the main conclusions, but they bound precision at fine scales, argue for expanded validation (including LiDAR/GEDI and biodiversity data), and motivate region-tuned parameterization before transfer to non-temperate, mixed-species forests.

4.5 Future Research Directions

To push this framework from "very good" to "decision-grade," next steps should (i) add missing **data dimensions** (vertical structure, traits, climate), (ii) adopt **richer models** that link pattern→process→action, (iii) harden **pipelines** for repeatable operations at scale, and (iv) test **generalisation** across biomes and disturbance regimes.

1) Enrich the data stack (what to add)

- **Vertical structure & biomass:** GEDI L2A/L4B, ICESat-2 ATL08, country airborne/UAV LiDAR, ESA Biomass/CCI Aboveground Biomass → resolve edge regrowth vs. true maturity; quantify vertical connectivity.

- **Traits & chemistry:** PRISMA/EnMAP hyperspectral (red-edge/pigments; water absorption), Sentinel-3 OLCI; field leaf traits where available → tighten VI–process links.
- **Moisture & heat:** SMAP soil moisture; ERA5-Land (met), ECOSTRESS/LST (thermal) → couple microclimate with edge stress.
- **SAR for all-weather change:** Sentinel-1, ALOS-2 PALSAR-2; (near-term) NISAR → robust in cloudy/post-disturbance periods.
- **Disturbance & alerts:** GLAD/Global Forest Watch, RADD, FIRMS → near-real-time disturbance feeders.
- **Biodiversity & field networks:** GBIF/eBird occurrences, ICP Forests, national plot networks → external validation for L3/L4.

2) Strengthen methods (how to model)

- **Edge–process coupling:** Joint models of **NDRE/NDMI/LST/soil moisture** with distance-to-edge; estimate thresholds where stress accelerates (segmented regression/Bayesian change points).
- **Multi-hazard risk:** Spatio-temporal models combining **wind (reanalysis), drought (SPI/SM), biotic pressure**; stack into a composite hotspot index with uncertainty.
- **Connectivity that "thinks":** Integrate MSPA with **Circuitscape/Omniscape** and **graph neural networks** for species-aware corridors; parameterise by dispersal distances.
- **Hybrid physics–ML:** Couple **PROSAIL/RTM** simulations with Extra Trees/LightGBM (or NGBoost) to reduce confounding and improve extrapolation; report SHAP for mechanism hints.
- **Causal & design-based inference:** Use **design-based area estimation**, spatial block CV, and (where data permit) difference-in-differences/causal forests to separate drivers from correlates.
- **Restoration optimisation:** Multi-objective siting (cost, carbon, connectivity, drought refuge) via **prioritizr/Marxan**; outputs = ranked corridor/buffer portfolios.

3) Production-grade pipelines (how to run)

- **Workflow & versioning:** Snakemake/Airflow + **DVC/MLflow** for data/model lineage; containerise (Docker) for portability.
- **Cloud & cadence:** Earth Engine for ingestion/compositing; batch ML on HPC/cloud (AWS/GCP). Publish quarterly/seasonal updates.
- **FAIR & reproducibility:** Pin **window sizes, edge widths, MMU, compositing policies**, CV schemes in a machine-readable config; emit a "model card" per run (metrics, features, SHAP/PDP, sensitivity).
- **Policy hooks:** Export **KM-GBF T2/T3 indicators**, **REDD+ MRV** layers (activity data + emission factors), and **NFMS**-ready summaries.

4) Where to test next (geographies & contexts)

- **Temperate/boreal:** Carpathians, Białowieża, Baltic & Scandinavian storm corridors → wind–edge interactions; spruce/birch–pine mixes.
- **Mediterranean:** Fire-prone mosaics (Portugal/Spain/Italy) → add burn severity & post-fire recovery to fragmentation dynamics.
- **Tropical pilots:** Western Kenya, Amazon sub-basins → high cloud; rely on SAR–optical fusion and strong local validation.
- **Interfaces:** Urban–forest fringes and **cropland ecotones** (your highest-risk context) for corridor/stepping-stone effectiveness.
- **Peatland–forest ecotones:** Coupling fragmentation with hydrological stability (SDG-6 co-benefits).

5) Concrete, near-term studies (fit to your thesis)

- **Voxels at the edge:** Fuse GEDI with S2 over TFBR to quantify vertical permeability vs. NDRE-inferred maturity (resolve the age misclassification in Rare zones).
- **Corridor short-list:** Run **Omniscape + prioritizr** for TFBR Transitional zones; deliver a top-10 corridor list with costs and expected NDMI/NDRE gains.
- **Alert-to-action pilot:** Trigger workflows from GLAD/RADD alerts → update FAD + risk layer within 7–14 days; produce a one-page "Ops Bulletin."
- **Species-specific connectivity:** Parameterise corridors for **pine, birch, oak** using dispersal kernels and patch quality (NDRE/NDVI + LiDAR height).

Deliverables to aim for

- A **public checklist + config template** (scale, edge, MMU, compositing, CV, validation).
- A **sensor/method trade-off table** (PALSAR vs S2 vs CORINE) bundled with the code.
- Quarterly **risk & condition maps** (Core/Transitional/Rare) with uncertainty bands.

These additions make the framework more **mechanistic, transferable, and operational**, while staying compatible with your current stack (S2, PALSAR, FAD/MSPA, Extra Trees/WoE).

Chapter 5. Conclusions

This chapter synthesizes the thesis into clear answers, contributions, and actionable guidance. First (Section 6.1), I distill what the results show by explicitly addressing each research question and linking structural diagnostics to functional responses and management actions. I then summarise methodological contributions (Section 6.2) and translate findings into practical strategies and policy relevance (Section 6.3). Finally, I delineate limitations and boundary conditions (Section 6.4) and outline a focused roadmap for future work that would elevate the framework to decision-grade operations (Section 6.5).

5.1 What this thesis shows

Forest fragmentation in the Tuchola Forest Biosphere Reserve (TFBR) is not merely a patterning issue but a coupled **pattern → process → action** problem. By combining fixed-window density and role-based morphology (FAD, MSPA) with Sentinel-2 vegetation indices and interpretable machine learning, this thesis demonstrates that structural configuration reliably anticipates functional stress—especially in edge-dominated parts of the landscape—and that these insights can be operationalised into concrete conservation choices.

RQ1 — How have methods for assessing forest fragmentation evolved?

The field has moved from patch/edge/shape metrics toward **density-based diagnostics (FAD/FOS), role classes (MSPA), and connectivity-aware thinking**, implemented in **open, auditable pipelines** (R/Python/GEE). This evolution matters for temperate systems such as TFBR because:

- fixed windows stabilise comparisons across sensors and scales,
- role classes (core/edge/bridge) translate naturally to management units,
- explicit parameter disclosure (edge width, window size, MMU) improves reproducibility and reporting.

RQ2 — How do fragmentation and the 2017 derecho change forest structure/coherence?

Across scales, TFBR exhibits classic fragmentation signatures: **core loss and edge proliferation**, with post-2017 acceleration. Regional products (CORINE) indicate pre-storm erosion of intactness; Landsat-8 resolves the derecho-triggered jump in edge density and patch number; within Sentinel-2, FAD zoning makes the spatial redistribution of core, transitional, and rare states explicit. Coherence declines are strongest along **cropland–forest and road interfaces**, aligning with known exposure pathways.

RQ3 — What ecological processes dominate Core/Transitional/Rare zones?

Functional signals track structural context. **Core** zones show buffered, stable partial-dependence responses; **Transitional and Rare** zones show steep, volatile responses consistent with **edge microclimates (higher VPD, wind/light), pigment decline, and moisture stress**. Among indices, **NDRE/GARI** are most sensitive to early pigment degradation, while

NDMI/NDWI capture canopy–soil water coupling; NDVI/EVI assist with greenness/biomass but can conflate rapid edge regrowth with maturity without additional constraints.

RQ4 — Which vegetation indicators and models best support monitoring and prioritisation?

An interpretable ensemble (Extra Trees / LightGBM), paired with **NDRE + NDMI (± NDWI/NDVI)** and a small set of environmental drivers, provides **directional, zone-aware** predictions suitable for decision support. **PALSAR** strengthens mapping of Rare/Patchy states under cloudy or debris-rich conditions, and **SAR–optical fusion** improves robustness in post-disturbance periods. The resulting layers—stress, susceptibility, and zone maps—prioritise **core protection**, **buffering and corridor restoration in Transitional**, and **passive rewilding with stepping-stones in Rare**.

5.2 Methodological contributions

1. **A joined-up, open workflow** that links morphology (FAD/MSPA) and connectivity concepts to functional VIs via interpretable ML, with parameter transparency (edge width, window size, MMU, compositing, CV).
2. **Fragmentation Susceptibility Modeling Framework**: Bayesian Weight-of-Evidence plus ensembles integrates **drivers (cropland/roads/wind corridors)** with SAR/optical features to map high-risk zones (reported AUC/Kappa indicate strong discrimination), offering an auditable alternative to black-box risk scores.
3. **Zone-aware interpretation**: Partial-dependence/ICE curves read differently by FAD class, turning models into **process hints** (stable Core vs. volatile Rare) rather than opaque predictions.
4. **Operational scaling**: Harmonised FAD windows across sensors (S2/L8/CORINE) and Earth Engine–based compositing make the approach **portable across time, sensors, and reporting units**.

5.3 Implications for management and policy

- **Protect the interior you still have**: Maintain ≥200 m edge offsets in remaining Core; avoid new perforations that convert Core → Transitional.
- **Stabilise the middle**: In Transitional zones, **buffers and corridors** lower pigment/moisture volatility; prioritise connectors across **cropland–forest** breaks and wind corridors.
- **Repair where fragmentation dominates**: In Rare zones, emphasise **passive rewilding and stepping-stones**, with **deeper-rooted, mixed-species** plantings to improve water retention and reduce edge desiccation.
- **Routine, reproducible monitoring**: Publish seasonal/annual **stress + susceptibility** updates using the same parameters, enabling transparent progress toward **Kunming–Montreal Target 2 & 3** and strengthening **REDD+ MRV** with condition-aware layers for temperate forests.

5.4 Limitations and boundary conditions

Precision at fine scales is bounded by sensor resolution (10–30 m), CORINE's coarseness for historical baselines, and the **absence of LiDAR** for 3-D canopy validation. Ensemble models remain sensitive to feature sets, partitioning, and parameter choices; although spatial block CV mitigates leakage, **site-specific labels** from the Forest Data Bank limit physiological generality. Thresholds and windows are **calibrated for a pine-dominated temperate system**; transferring to other biomes requires re-tuning and local validation. None of these caveats overturn the main conclusions; they define **where and how** the framework should be extended.

5.5 Outlook: from good diagnostics to decision-grade operations

The fastest path to a production-grade programme is to (i) **add vertical structure** (GEDI/ICESat-2/LiDAR) to separate edge regrowth from true maturity, (ii) **couple stress drivers** (soil moisture/LST/wind) with distance-to-edge to identify thresholds, (iii) **harden pipelines** (versioned configs, scheduled updates), and (iv) **validate with biodiversity networks** (ICP Forests/GBIF/eBird) to link spectral stress to living systems. In TFBR, a targeted follow-up could:

- deliver a **top-10 corridor short-list** for Transitional zones (Omniscape + prioritizr),
- run a **quarterly "condition & risk" bulletin** (NDRE/NDMI + susceptibility) with uncertainty bands,
- fuse **GEDI + Sentinel-2** to quantify **vertical permeability** across FAD classes, clarifying management thresholds for interior integrity.

References:

Ahmad, A., Ahmad, S.R., Gilani, H., & Nowosad, J. (2025). Assessment of forest fragmentation and ecological dynamics in Western Himalayan Region over three decades (1990–2020). *Environmental Monitoring and Assessment*, *197*(2), 1–19.

Altunel, A.O., & Celik, D.A. (2025). Comparison of SAR and optical derived data used in forest cover detection; PALSAR-FNF vs. ESRI Land-Cover over North Central Türkiye. *International Journal of Environmental Science and Technology*, *22*(5), 3641–3654.

Arroyo-Rodríguez, V., Saldana-Vazquez, R.A., Fahrig, L., & Santos, B.A. (2017). Does forest fragmentation cause an increase in forest temperature? *Ecological Research*, *32*, 81–88.

Blanchard, G., Barbier, N., Vieilledent, G., Ibanez, T., Hequet, V., McCoy, S., & Birnbaum, P. (2023). UAV-Lidar reveals that canopy structure mediates the influence of edge effects on forest diversity, function and microclimate. *Journal of Ecology*, *111*(7), 1411–1427.

Bosch, M. (2019) PyLandStats: An open-source Pythonic library to compute landscape metrics. *PLoS One*, 14(12), e0225734. https://doi.org/10.1371/journal.pone.0225734

Britton, J., Abatzoglou, J.T., et al., (2024). Explaining MODIS NDVI drought responses with tree-based models and SHAP. *J. Appl. Serv. Climatol.*, *5*, e009001. https://doi.org/10.46275/JOASC.2024.09.001

Brown, C.F., Brumby, S.P., Guzder-Williams, B., Birch, T., Hyde, S.B., Mazzariello, J., ... & Tait, A. M. (2022). Dynamic World, near real-time global 10 m land use land cover mapping. *Scientific Data*, *9*(1), 251.

Dutt, S., Batar, A.K., Sulik, S., & Kunz, M. (2024). Forest ecosystem on the edge: Mapping forest fragmentation susceptibility in Tuchola Forest, Poland. *Ecological Indicators, 161*, 111980. https://doi.org/10.1016/j.ecolind.2024.111980

Dutt, S., & Kunz, M. (2024). Landscape metrics of the Brusy Commune before and after wind-storm: An assessment based on Landsat-8 data. *Bulletin of Geography. Physical Geography Series, 26*, 19–33. https://doi.org/10.12775/bgeo-2024-0002

Dutt, S., & Kunz, M. (2022). Land use/cover changes using Corine Land Cover data following hurricanes in the last 10 years: A case study on Tuchola Forest Biosphere Reserve. [In:] Młynarczyk, A. (ed.): *Środowisko przyrodnicze jako obszar badań*. Vol. IV. Bogucki Wydawnictwo Naukowe, Poznań, 25–42.

Dutt, S., Remmel, T.K., Rivas, C.A., Mazziotta, A., & Kunz, M. (*under review*). Advancing Forest Fragmentation Analysis: A Systematic Review of Evolving Spatial Metrics, Software Platforms, and Remote Sensing Innovations. *Landscape Ecology*, Springer Nature, 1–21.

Dutt, S., Wojtasik, J., Justeau-Allaire, D., & Kunz, M. (*under review*). How does fragmentation reshape forests? Tracking dominant ecological processes across core, transitional, and rare zones. *GIScience & Remote Sensing*, Taylor & Francis, 1–18.

Fahrig, L. (2003). Effects of habitat fragmentation on biodiversity. *Annual Review of Ecology, Evolution, and Systematics*, *34*(1), 487–515.

Fahrig, L., Arroyo-Rodríguez, V., Bennett, J.R., Boucher-Lalonde, V., Cazetta, E., Currie, D. J., ... & Watling, J.I. (2019). Is habitat fragmentation bad for biodiversity? *Biological Conservation*, *230*, 179–186.

Fletcher, R.J., Jr., Didham, R.K., Banks-Leite, C., Barlow, J., Ewers, R.M., Rosindell, J., ... & Haddad, N.M. (2018). Is habitat fragmentation good for biodiversity? *Biological Conservation*, *226*, 9–15.

Haneda, L.E., Brancalion, P.H., Valle, D., Silva, C.A., Gorgens, E.B., Prata, G.A., ... & de Almeida, D.R.A. (2025). Edge effect impacts on forest structure and carbon stocks in REDD+ projects: An assessment in the Amazon using UAV-LiDAR. *Forest Ecology and Management*, *585*, 122646.

Hesselbarth, M.H., Sciaini, M., With, K.A., Wiegand, K., & Nowosad, J. (2019). landscapemetrics: An open-source R tool to calculate landscape metrics. *Ecography*, *42*(10), 1648–1657.

Jastrzębski, M., Nienartowicz, A., Deptula, M., Bubnicki, J.W., & Domin, D.J. (2010). Past, current and potential resources of carbon and above-ground plant biomass in the landscape with heaths in some selected areas of the Tuchola Forest. *Ecological Questions*, *13*, 9–27. https://doi.org/10.12775/v10090-010-0012-1

Kennedy, R.E., Yang, Z., Cohen, W.B., et al. (2018). Implementation of the LandTrendr algorithm on Google Earth Engine. *Remote Sensing*, 10(5), 691. https://doi.org/10.3390/rs10050691

Kistowski, M. (2020). Regionalizacja fizycznogeograficzna Rezerwatu Biosfery Bory Tucholskie w świetle aktualnych doświadczeń badawczych. [In]: M. Kunz (Ed.), *Rola i funkcjonowanie parków krajobrazowych w rezerwatach biosfery* (pp. 39–55). Wyd. Naukowe UMK, Toruń.

Kunz, M. (Ed.). (2020). *Rola i funkcjonowanie parków krajobrazowych w rezerwatach biosfery [The role and functioning of landscape parks in biosphere reserves]*. Wyd. Naukowe UMK, Toruń, 1–452.

Kunz, M., & Nienartowicz, A. (2021). Remote sensing imagery in monitoring spatial pattern changes in forest landscape. In *Observing our environment from space: New solutions for a new millennium* (pp. 391–398). CRC Press.

Kunz, M., & Nienartowicz, A. (Eds.). (2013). *Biosphere Reserves in Poland / Rezerwaty Biosfery w Polsce*. Wyd. Naukowe UMK, Toruń, 1–211.

Kunz, M., Nienartowicz, A., & Kamiński, D. (2023). Loss in CO_2 assimilation by forest stands relative to its emissions generated by the economic sector as an indicator of ecological consequences of a windstorm in the municipality of Brusy, NW Poland. *Bulletin of Geography. Socio-Economic Series*, *59*, 41–56. https://doi.org/10.12775/bgss-2023-0003

Kupfer, J.A. (2012). Landscape ecology and biogeography: Rethinking landscape metrics in a post-FRAGSTATS landscape. *Progress in physical geography*, *36*(3), 400-420.

Lausch, A., Erasmi, S., King, D.J., Magdon, P., & Heurich, M. (2016). Understanding forest health with remote sensing—Part I: Spectral traits, processes and characteristics. *Remote Sensing*, *8*(12), 1029.

Ma, J., Li, J., Wu, W., & Liu, J. (2023). Global forest fragmentation change from 2000 to 2020. *Nature Communications*, *14*(1), 3752.

Maier, B., Tiede, D., & Dorren, L. (2006) Assessing mountain forest structure using airborne laser scanning and landscape metrics. International Archives of Photogrammetry, *Remote Sensing and Spatial Information Sciences*, *36*(4), C42.

Mazziotta, A., Francini, S., & Parisi, F. (2025). Monitoring habitat fragmentation and biodiversity in forest ecosystems. In *Ecological connectivity of forest ecosystems* (pp. 171–186). Springer.

McGarigal, K. (1995). FRAGSTATS: Spatial pattern analysis program for quantifying landscape structure. *General Technical Report PNW-GTR-351*. U.S. Department of Agriculture, Forest Service, Pacific Northwest Research Station, Portland, OR, 1–122.

Mutanga, O., & Kumar, L. (2019). Google Earth Engine applications. *Remote Sensing*, *11*(5), 591.

Nienartowicz, A., & Kunz, M. (2018). *Tuchola Forest Biosphere Reserve 2.0 – The grounds and the scope of the proposed changes* / *Rezerwat Biosfery Bory Tucholskie 2.0 – Uzasadnienie wniosku o powiększenie i zakres proponowanych zmian*. LGB „Sandry Brdy", 1–88.

Nienartowicz, A., Domin, D.J., Kunz, M., & Przystalski, A. (2010). *Rezerwat Biosfery Bory Tucholskie. Formularz nominacyjny* / *Biosphere Reserve Tuchola Forest, Nomination Form*. LGD „Sandry Brdy", 1–168.

Pekkarinen, A., Reithmaier, L., & Strobl, P. (2009). Pan-European forest/non-forest mapping with Landsat ETM+ and CORINE Land Cover 2000 data. *International Journal of Remote Sensing*, *30*(6), 1365–1379.

Peterson, M.C., Bradham, J., Ferraro, K., Guillet, M., Keuroghlian, A., Ribeiro, M., & Jorge, M.L.S. (2025). Modeling movement patterns to identify thresholds of functional connectivity in fragmented forest landscapes. *Biological Conservation*, *307*, 111177.

Pfeifer, M., Lefebvre, V., Peres, C.A., Banks-Leite, C., Wearn, O.R., Marsh, C.J., ... & Ewers, R.M. (2017). Creation of forest edges has a global impact on forest vertebrates. *Nature*, *551*(7679), 187–191.

Radeloff, V.C., Roy, D.P., Wulder, M.A., Anderson, M., Cook, B., Crawford, C.J., ... & Zhu, Z. (2024). Need and vision for global medium-resolution Landsat and Sentinel-2 data products. *Remote Sensing of Environment*, *300*, 113918.

Referowska-Chodak, E., & Kornatowska, B. (2021). Effects of forestry transformation on the ecosystem level of biodiversity in Poland's forests. *Forests*, *14*(9), 1739.

Riva, F., & Fahrig, L. (2023). Landscape-scale habitat fragmentation is positively related to biodiversity, despite patch-scale ecosystem decay. *Ecology Letters*, *26*(2), 268–277.

Rutkowski, R., Jagołkowska, P., Zawadzka, D., & Bogdanowicz, W. (2016). Impacts of forest fragmentation and post-glacial colonization on the distribution of genetic diversity in the Polish population of the hazel grouse *Tetrastes bonasia*. *European Journal of Wildlife Research*, *62*, 293–306.

Saura, S. (2021). The Habitat Amount Hypothesis implies negative effects of habitat fragmentation on species richness. *Journal of Biogeography*, *48*(1), 11–22.

Siegel, T., Magrach, A., Laurance, W.F., & Luther, D. (2024). A global meta-analysis of the impacts of forest fragmentation on biotic mutualisms and antagonisms. *Conservation Biology*, 38(3), e14206. https://doi.org/10.1111/cobi.14206

Taszarek, M., Pilguj, N., Orlikowski, J., Surowiecki, A., Walczakiewicz, S., Pilorz, W., ... & Półrolniczak, M. (2019). Derecho evolving from a mesocyclone—A study of 11 August 2017 severe weather outbreak in Poland: Event analysis and high-resolution simulation. *Monthly Weather Review*, *147*(6), 2283–2306.

Venter, Z.S., Barton, D.N., Chakraborty, T., Simensen, T., & Singh, G. (2022). Global 10 m land use land cover datasets: A comparison of Dynamic World, World Cover and Esri Land Cover. *Remote Sensing*, *14*(16), 4101.

Vogt, P., & Riitters, K. (2017). GuidosToolbox: Universal digital image object analysis. *European Journal of Remote Sensing*, *50*(1), 352–361.

Vogt, P., Riitters, K.H., Rambaud, P., d'Annunzio, R., Lindquist, E., & Pekkarinen, A. (2022) GuidosToolbox Workbench: spatial analysis of raster maps for ecological applications. *Ecography*, *45*(3), 000–000. https://doi.org/10.1111/ecog.05864

Vogt, P., Riitters, K.H., Estreguil, C., Kozak, J., Wade, T.G., & Wickham, J.D. (2007). Mapping spatial patterns with morphological image processing. *Landscape Ecology*, *22*(2), 171–177.

Wang, K., Franklin, S.E., Guo, X., & Cattet, M. (2010). Remote sensing of ecology, biodiversity and conservation: A review from the perspective of remote sensing specialists. *Sensors*, *10*(11), 9647–9667.

Wulder, M.A., White, J.C., Andrew, M.E., Seitz, N.E., Coops, N.C., 2009. Forest fragmentation, structure, and age characteristics as a legacy of forest management. *For. Ecol. Manage. 258*(9), 1938–1949. https://doi.org/10.1016/j.foreco.2009.07.041

Xue, J., & Su, B. (2017). Significant remote sensing vegetation indices: A review of developments and applications. *Journal of Sensors*, *2017*, 1353691.

Ye, H., Yang, Z., & Xu, X. (2020). Ecological corridors analysis based on MSPA and MCR model—A case study of the Tomur World Natural Heritage Region. *Sustainability*, *12*(3), 959.

Zald, H.S.J., Wulder, M.A., White, J.C., Hilker, T., Hermosilla, T., & Hobart, G.W. (2016). Integrating Landsat time series and LiDAR to map forest structure and biomass. *Remote Sensing of Environment*, *176*, 188–201.

Zhao, Q., Yu, L., Li, X., Peng, D., Zhang, Y., & Gong, P. (2021). Progress and trends in the application of Google Earth and Google Earth Engine. *Remote Sensing*, *13*(18), 3778.

Appendix

Full-text of 5 Publications

Article	Journal / Publisher	IF (2024)	MNiSW Points
Dutt, S., Remmel, T.K., Rivas, C.A., Mazziotta, A., & Kunz, M. (2025). *Advancing Forest Fragmentation Analysis: A Systematic Review of Evolving Spatial Metrics, Software Platforms, and Remote Sensing Innovations.*	*Landscape Ecology* (Under review)	5.1	140
Dutt, S., & Kunz, M. (2022). *Land use/cover changes using Corine Land Cover data following hurricanes in the last 10 years: A case study on Tuchola Forest Biosphere Reserve.*	Book Chapter, [In:] Młynarczyk, A. (ed.): *Środowisko przyrodnicze jako obszar badań*. Vol. IV. Bogucki Wydawnictwo Naukowe, Poznań: 25–42.	–	20
Dutt, S., & Kunz, M. (2024). *Landscape metrics of the Brusy Commune before and after wind-storm: An assessment based on Landsat-8 data.*	*Bulletin of Geography. Physical Geography Series* 26: 19–33.	0.8	40
Dutt, S., Batar, A.K., Sulik, S., & Kunz, M. (2024). *Forest ecosystem on the edge: Mapping forest fragmentation susceptibility in Tuchola Forest, Poland.*	*Ecological Indicators* 161: 111980.	7.4	200
Dutt, S., Wojtasik, J., Justeau-Allaire, D., & Kunz, M. (2025). *How does fragmentation reshape forests? Tracking dominant ecological processes across core, transitional, and rare zones.*	*GIScience & Remote Sensing* (Under review)	6.9	100

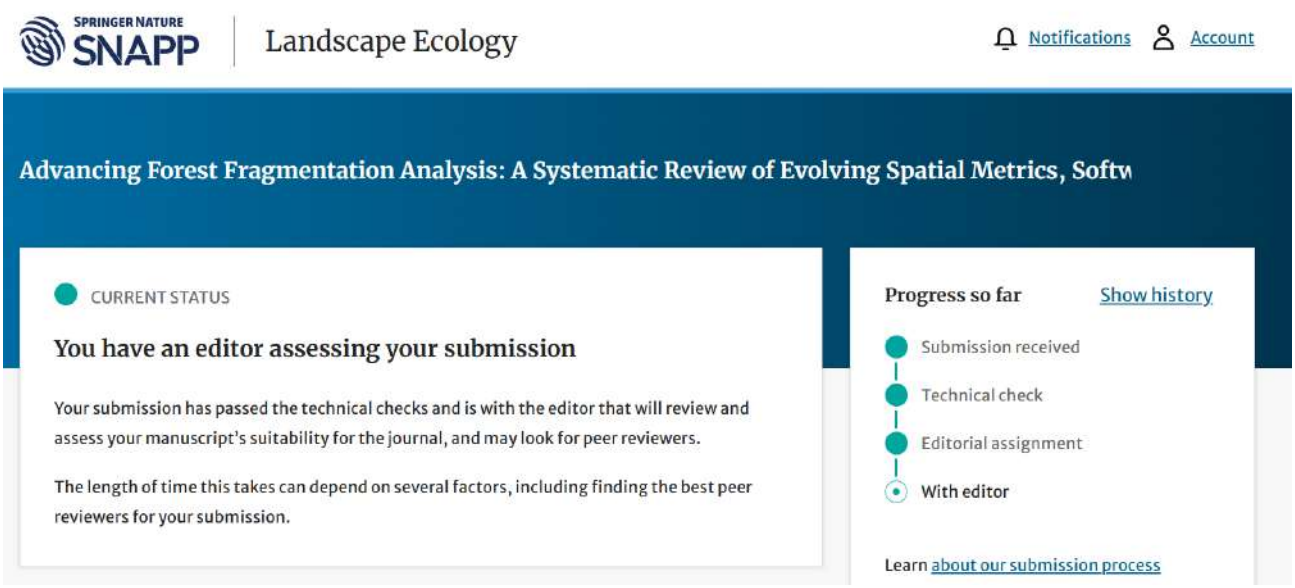

Your submission

Title

Advancing Forest Fragmentation Analysis: A Systematic Review of Evolving Spatial Metrics, Software Platforms, and Remote Sensing Innovations

Type

Review

Journal

Landscape Ecology

Submission ID

94200a57-f4ea-43e5-bc57-b8964d30b8a7

Submission version

v.1.0

Advancing Forest Fragmentation Analysis: A Systematic Review of Evolving Spatial Metrics, Software Platforms, and Remote Sensing Innovations

Sanjana Dutt[1]*, Tarmo K. Remmel[2], Carlos A. Rivas[3], Adriano Mazziotta[4], Mieczysław Kunz[1]

[1] Faculty of Earth and Environmental Sciences, Nicolaus Copernicus University, Toruń, Poland
[2] Faculty of Environmental & Urban Change, York University, Toronto, Ontario, Canada
[3] Mediterranean Forest Global Change Observatory (GLOBAM), DigiFoR+—ERSAF, Department of Forestry Engineering, University of Córdoba, Campus de Rabanales, Crta. IV Km 396, 14071 Córdoba, Spain
[4] Natural Resources Institute Finland (Luke), Latokartanonkaari 9, FI-00790 Helsinki, Finland

Corresponding author:* sanjana.dutt@doktorant.umk.pl

ABSTRACT

Context
Forest fragmentation—the breakup of continuous habitat into isolated patches—alters landscape processes and biodiversity. Rapid advances in sensors and computing have diversified diagnostic methods, but comparability and ecological linkage remain uneven.

Objectives
Synthesize 138 methodological studies (1990–2025) to: (i) chart shifts in metric families, including emerging 3-D approaches; (ii) assess how data and processing choices shape indicator performance; and (iii) distill limits and reporting practices that improve portability.

Methods
We reviewed studies using lidar/TLS and Sentinel-2 inputs, change detection, and indicators implemented in *landscapemetrics*, *GuidosToolbox*, and *Google Earth Engine*, tracing transitions from patch/edge metrics to morphology-aware roles, connectivity, fixed-window density, and 3-D/voxel measures.

Results
The field is moving toward morphology-aware roles, multiscale connectivity, fixed-scale density, and vertical structure. Five recurring limits are: scale sensitivity and habitat-amount confounding; region-tuned parameters that hinder transfer; scarce field validation of global/automated products; weak or inconsistent biotic links of structural metrics; and incomplete reporting that curbs reproducibility. Gaps include uneven tropical coverage and limited 2-D/3-D cross-walks. Priorities are transparent parameterization and sensitivity checks, precise documentation of spatial/detector settings, region-specific benchmarking, shareable workflows, and integration of field data.

Summary
Standardizing documentation, validation, and cross-scale linkages can improve the reliability of fragmentation measures for monitoring and conservation. Emphasis should be on refining and harmonizing existing methods rather than proposing new indices

Keywords: forest fragmentation; landscape metrics; change detection; lidar; open-source workflows; methodological synthesis

1. Introduction

Forest fragmentation—the division of continuous forest into smaller, more isolated patches—creates edge environments, reshapes ecological processes, and can accelerate biodiversity loss (McGarigal & Marks, 1995;

Heilman et al., 2002; Riitters et al., 2007; Bennett & Radford, 2008). Over two-thirds of global forests now lie within 1 km of an edge (Haddad et al., 2015; Siegel et al., 2024), with pressures most pronounced in tropical and subtropical regions (Lung & Schaab, 2006; Giriraj et al., 2010). Fragmentation is distinct from habitat loss: loss reduces area, whereas fragmentation concerns how a fixed amount of forest is arranged by patch size, shape, and isolation (Fahrig, 2003, 2019, 2024; Fardila et al., 2017). Connectivity—the degree to which landscape structure facilitates or restricts movement—adds a further interpretive layer (Bogaert et al., 2000; Vogt et al., 2007; Lausch et al., 2015). Although patch-scale edge effects are well documented, landscape-scale responses do not always follow directly from local patterns (Fletcher et al., 2018; Fahrig, 2024), underscoring the need for scale-declared, method-transparent assessments that can be linked to ecological data where available (Bennett & Radford, 2008).

Methodologically, practice has progressed from early patch/edge/shape tallies to morphology- and connectivity-aware approaches, fixed-window density measures, and first-generation 3-D/voxel indicators. FRAGSTATS and Patch Analyst established a common language for pattern quantification (McGarigal & Marks, 1995; Elkie et al., 1999). Role-based morphology—exemplified by morphological spatial pattern analysis (MSPA)—made cores, edges, bridges, corridors, and perforations legible at reporting scales (Vogt et al., 2007; Wickham et al., 2010). Advances in remote sensing, including lidar/TLS for canopy structure, together with robust time-series change detection (e.g., Vegetation Change Tracker, LandTrendr, Two-Thresholds Method), have enabled consistent disturbance trajectories that feed downstream indicators (Maier et al., 2006; Huang et al., 2010; Zald et al., 2016; Kennedy et al., 2018; Giannetti et al., 2020). Open, scriptable ecosystems and cloud platforms—*landscapemetrics*, PyLandStats, GuidosToolbox, and Google Earth Engine—now support auditable pipelines from data ingestion to indicators. In parallel, neutral landscape generators (e.g., Landscape Generator; flsgen) provide realistic, controlled mosaics to test sensitivity and to separate composition from configuration (van Strien et al., 2016; Peura et al., 2018; Justeau-Allaire et al., 2022).

Despite this expansion in capability, five recurring issues complicate inference and comparability across studies: (i) sensitivity to grain and extent and the attendant conflation with habitat amount; (ii) regional dependence of thresholds and assumptions; (iii) gaps in external/empirical validation—especially for global products and emergent 3-D indicators; (iv) loose coupling to biological responses; and (v) incomplete parameter reporting (O'Neill et al., 1999; Hernando et al., 2017; Zatelli et al., 2019; Fletcher et al., 2018; Vergara et al., 2021; Feleha et al., 2025). Recent families—fixed-window density measures such as Forest Area Density (FAD), role-based morphology paired with graph metrics, and voxel/3-D approaches—address parts of this problem yet introduce assumptions that must be declared and tested.

This review analyzes 138 methodological studies (1990–2025) to:

1. map the evolution from patch-based measures to connectivity, shape complexity, fixed-window density, and emerging 3-D approaches;
2. evaluate how remote sensing and time-series/change-detection methods—together with compositing/segmentation choices and cloud platforms—condition the accuracy and comparability of fragmentation indicators; and
3. diagnose common limitations and summarize practical reporting elements (e.g., grain/extent, edge width, window size, detector settings, MMU, validation) that make results more portable across regions and scales.

2. Methodology

2.1 Literature search

We followed PRISMA 2020 (Page et al., 2021) to ensure a transparent, reproducible process. We targeted peer-reviewed journal articles published 1990–2025 and ran searches from 3 Oct 2024 to 9 Sep 2025 using Publish or Perish (Harzing, 2010) across Google Scholar, Scopus, and Web of Science. We limited results to English and article document types; conference papers, theses, books/chapters, and reports were excluded. Studies were included if they proposed, evaluated, or systematically applied methods/metrics/workflows for forest fragmentation (e.g., structural/configurational metrics, change-detection feeding fragmentation indicators, graph/MSPA/fixed-window/3-D approaches), and excluded if purely ecological case studies without methodological contribution or non-forest

contexts unless methods were demonstrated for forests. To keep scope forest-specific we filtered out terms such as "urban," "animal*," and "bird*" unless paired with "forest." Database searches returned 1,160 records; Litmaps/Connected Papers, citation chasing, and colleague recommendations added 46, for 1,206 records prior to deduplication. Title/abstract and full-text screening applied the criteria above; reasons for exclusion are shown in PRISMA Figure 1, and verbatim database search strings are provided in Supplementary Table S1.

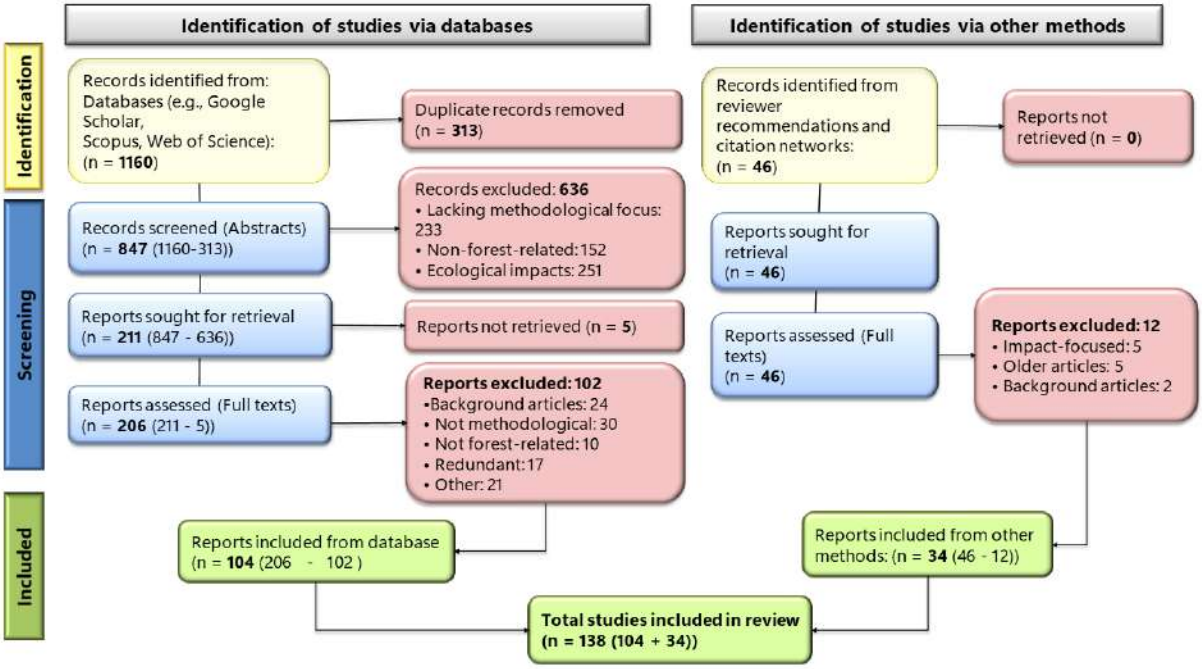

Figure 1. PRISMA 2020 flow diagram for a systematic review of methods to assess forest fragmentation (1990–2025).

2.2 Screening Process

We removed 313 duplicate records using Rayyan (Ouzzani et al., 2016), leaving 847 unique articles. Title/abstract/keyword screening excluded 233 items without a methodological focus, 152 outside a forest context, and 251 that reported ecological impacts only without a fragmentation-methods component. We sought 211 full texts; 5 could not be retrieved, leaving 206 for full-text assessment. In parallel, we identified 46 additional records via reference tracking (Litmaps, Connected Papers) and colleague recommendations, which were included at the full-text stage.

2.3 Study Selection

Full texts were assessed against predefined criteria: (i) proposes, evaluates, or systematically applies methods to measure forest fragmentation (spatial/configurational metrics, remote-sensing/change-detection feeding fragmentation indicators, graph/MSPA/fixed-window/3-D approaches); (ii) forest context or forest-reporting subset; (iii) peer-reviewed journal article; (iv) publication 1990–2025; (v) English, full text available; and (vi) unique contribution.

Of the 206 database-sourced articles, 96 were excluded: 24 background/narrative, 28 not methodological, 10 not forest-related, 17 redundant (repetitive case applications of standard landscape-metrics workflows—e.g., FRAGSTATS or Patch Analyst—without methodological novelty or evaluation), and 17 other reasons (insufficient methodological detail or peripheral scope).

Of the 46 additional records, 12 were excluded at full text (5 impact-focused only, 5 outside scope/publication window, 2 background). The final set comprised 138 methodological studies: 110 from databases and 34 from other sources (see PRISMA Figure 1).

2.4 Limitations

This review is limited to English-language, peer-reviewed journal articles. While this may omit some regional contributions, English dominates publication in this domain, and citation chasing in our included papers did not repeatedly surface non-English methodological keystones. Our search emphasized method/tool terms (e.g., FRAGSTATS, GuidosToolbox) to capture studies that develop or evaluate fragmentation methods; broader ecological terms would have inflated returns with impact-only studies and diluted the methodological focus. This emphasis could favor papers that explicitly name software; we countered it through snowballing (Litmaps, Connected Papers) and colleague recommendations. By design, we prioritized methods-focused work and excluded descriptive case studies that simply reuse existing metrics, which limits ecological context but preserves a clear methods synthesis. Finally, full-text screening was conducted by one reviewer using predefined criteria and Rayyan, with co-author oversight at inclusion; this does not remove selection bias entirely, but it provides a consistent and auditable screen.

3. Results

3.1 Scope and Organization

This review synthesizes 138 studies (1990–2025) on methodological approaches to quantifying forest fragmentation. We organize findings along three linked components: (i) data sources (remote-sensing and ground-based inputs), (ii) change-detection methods (time-series analyses that derive disturbance/transition signals), and (iii) landscape pattern indicators (metrics of configuration and connectivity). In practice, data sources feed change detection, which then supports indicator calculation (Fig. 2). The columns in Fig. 2 group periods by sensor-era shifts, showing a progression from early, primarily Landsat-based work to multi-sensor approaches that integrate increasingly higher spatial and temporal resolution sensors, including lidar, to improve temporal fidelity and structural sensitivity.

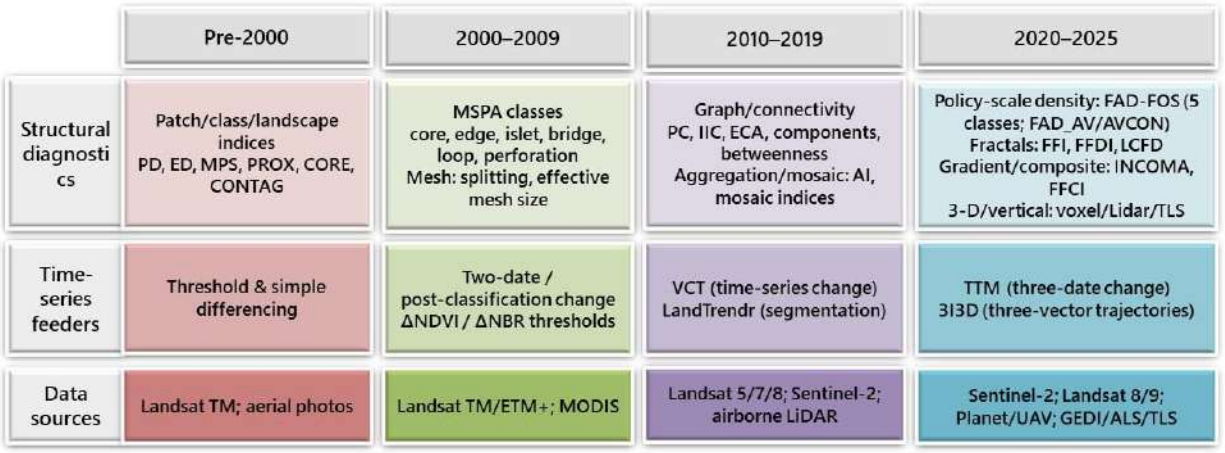

Figure 2. Evolution of forest-fragmentation methods (1990–2025). Rows depict the chain from data sources (bottom) → change-detection methods (middle) → landscape pattern indicators (top). Columns group eras by sensor availability and resolution, illustrating the transition from early single-sensor paradigms to multi-sensor integrations (including lidar) that enhance change detection and indicator robustness.

3.2 Evolution of Landscape Pattern Indicators

Initial investigations in the 1990s emphasized two-dimensional assessments of forest patches, including patch counts, area metrics, edge lengths, and core area delineations (Ripple et al., 1991; McGarigal & Marks, 1995; Jorge & Garcia, 1997; Walker & Kenkel, 1998). These methodologies, while systematically replicable, offered limited insight into ecological connectivity or species dispersal potential. By the early 2000s, the introduction of effective mesh size provided a more nuanced metric for evaluating landscape subdivision (Jaeger, 2000). Subsequent developments

around 2007 incorporated role-based classifications—such as core areas, edge zones, and connective bridges—enhancing the spatial resolution of forest network analyses (Vogt et al., 2007; Tejaswi, 2007).

Post-2010, connectivity-focused indicators, including Probability of Connectivity (PC) and Integral Index of Connectivity (IIC), gained prominence, featuring in approximately 25% of studies, particularly for informing wildlife corridor design (Estreguil & Mouton, 2009; Ye et al., 2020; Lin et al., 2021; Ramezani & Ramezani, 2021). Recent advancements have diversified into three categories: (1) fixed-scale density metrics, exemplified by Forest Area Density (FAD), enabling inter-regional comparability (Vogt & Caudullo, 2025); (2) shape and connectivity indices, such as Forest Fragmentation Index (FFI) and Local Connectedness (LCFD), which account for patch morphology and local linkages while mitigating data inaccuracies (Alage et al., 2025); and (3) three-dimensional assessments leveraging lidar to elucidate canopy structure and vertical connectivity, addressing limitations of planar analyses (Zald et al., 2016; Nowosad & Stepinski, 2021; Remmel, 2022; Zhen et al., 2023; Lin et al., 2024). A comprehensive overview of these tools is presented in Table 1 and Supplementary Table S2.

Table 1. Evolution of toolsets for forest fragmentation—concise view. Grouped by period, showing key tools, their contributions, and tags. Full details in Supplementary Table S2.

Period	Exemplary toolsets	What it adds	Key refs
Pre-2000	FRAGSTATS; Patch Analyst; pMAP	Baseline patch/class metrics (area, edge, shape, core); early proximity/contagion (RS/GIS)	McGarigal & Marks (1995); Elkie et al. (1999)
	Khoros	Simulated patterns; metric correlation; early eco-response tests	Hargis et al. (1999)
2000–2009	GUIDOS/APACK	MSPA roles; moving-window (FAD/entropy); continental mapping (QGIS/Prog)	Vogt et al. (2007); Wulder et al. (2008); Soverel et al. (2010)
	ERDAS/IDRISI/eCognition	object-based image analysis **(**OBIA**)** segmentation; Lidar-derived metrics; early CA–Markov	Maier et al. (2006); Meddens et al. (2008)
	ArcIMS + FRAGSTATS	Web-mapping + classical metrics (Web-GIS)	Wang (2002); Southworth et al. (2004)
2010–2019	LFT	Core/edge/perforated/patch; morph segmentation (ArcGIS)	Kopecká & Nováček (2010);
	Conefor + Circuitscape/Linkage	Connectivity (PC/IIC/dI; circuit/least-cost corridors) (Graph/Circuit)	Saura & Torné (2009); McRae et al. (2008)
	landscapemetrics; motif; PyLandStats; LecoS; ShrinkShape2	Reproducible pipelines; pattern signatures; rotation-invariant shape (R/QGIS/Py)	Hesselbarth et al. (2019); Remmel (2015)
	PolyFrag; FRAGSTATS v3.3	Vector-aware metrics; custom edge width (GIS)	MacLean & Congalton (2013)
	Feeders: VCT; LandTrendr; CCDC; TTM	Stable time-series disturbance detection (GEE/RS)	Huang et al. (2010);
2020–2025	GUIDOS—GuidosToolbox; GWB—Graph-Based Workflow	MSPA expansions; distance/similarity (Jensen–Shannon multiscale) (QGIS/C/GDAL)	Vogt & Riitters (2017); Vogt et al. (2022); Dutt et al., (2024)
	FAD–FOS pipelines	Fixed-scale density classes; policy-scale comparability	Vogt & Caudullo (2025)
	Patternbits; geodiv; Intra	Config elements & KL; gradient surface metrics; CWA intra-patch connectivity (R)	Remmel (2020, 2022); Justeau-Allaire et al. (2024)
	VecLI; VARLI; LDTtool/LDT4QGIS	Vector indices; composition/configuration change typologies; perimeter-area fixes (Py/QGIS)	Yao et al. (2022); Huang et al. (2024)
	flsgen	Neutral landscapes with controlled fragmentation (API/R/CLI)	Justeau-Allaire et al. (2022)

ENVI+GeoDa; MapBiomas+IDRISI (FFCI)	PCA/ANN/CA–MC composite fragmentation; forecasting (RS)	Lin et al. (2024); Moreira et al. (2024); Wu et al. (2024)
Fiji/ImageJ2 + ComsystanJ	3-D voxel fragmentation; fractal dim; succolarity (3-D)	Andronache (2024)
ESIS/Imalys; AMAPVox	Hybrid PMM–GM; TLS-PAI; phenology impacts (3-D/TLS)	Selsam et al. (2024); Nunes et al. (2022)
ProNet scripts	PA-network connectivity metric; simple bounded index (Py/R)	Theobald et al. (2022)
LandTrendr (apps)	Recent provincial apps to 2025 (feeder in practice)	Qiu et al. (2025)

3.3 Change-Detection Methods

Change detection supplies the time-stamped events that feed downstream fragmentation indicators; contemporary practice matches the detector family to the disturbance regime (abrupt vs. gradual) and documents compositing/parameter choices.

Trajectory segmentation: *Vegetation Change Tracker (VCT)* formalizes long Landsat histories with strict filtering, and *LandTrendr* fits piecewise trends to locate breakpoints and recovery segments at scale on cloud platforms (Huang et al., 2010; Kennedy et al., 2018). These approaches work best when long, relatively clean series are available and when both loss and recovery matter.

Tri-date detectors: When time series are sparse or disturbances are short and sharp, calibrated three-date methods perform well. The *Two-Thresholds Method (TTM)* applies paired loss and recovery thresholds on ΔNBR (delta Normalized Burn Ratio), and *3I3D* uses Sentinel-2 vector angles and magnitudes to flag clear-cuts with minimal tuning (Giannetti et al., 2020; Francini et al., 2021).

Continuous/harmonic models: *Continuous Change Detection and Classification (CCDC)* models seasonal cycles and longer-term trends, capturing gradual or compound deviations that step/tri-date detectors may miss; implementations in *Google Earth Engine* enable regional coverage (Gorelick et al., 2017; Mahapatra et al., 2025).

Across all families, data handling choices strongly shape outputs. Compositing strategies (e.g., Best Available Pixel vs. medoid) trade noise suppression against radiometric consistency and day-of-year proximity, which can shift estimated break timing and raise edge-adjacent false positives if not reported (Francini et al., 2023). Sensor stacks have moved from Landsat-only to Landsat+Sentinel-2, with commercial very-high-resolution small-sat constellations (e.g., Dove/Skysat) used selectively for fine-scale confirmation and lidar for canopy structure/validation (Zald et al., 2016; Nunes et al., 2022). Global baselines such as Global Forest Change provide standardized context but require local checks for omission/commission—especially in coppice, selective logging, and fire landscapes (Hansen et al., 2013). Recent provincial deployments (e.g., Guangdong) route detector outputs directly into fragmentation indices and driver analyses (Qiu et al., 2025).

3.4 Software and Reproducibility

The earliest implementations of fragmentation metrics were deeply tied to GIS workstations. In the Cascade Range, Ripple et al. (1991) used the *pMAP GIS* to introduce GISfrag, one of the first spatially explicit fragmentation indices, combining proximity mapping with edge removal to estimate interior habitat. By the late 1990s, *ArcView GIS* linked directly to *FRAGSTATS* outputs, allowing stand attributes to be translated into spatial metrics in boreal systems (Vernier & Cumming, 1999). National-scale studies soon followed: Heilman et al. (2002) integrated *FRAGSTATS* with *ArcGIS* and TIGER road data to derive intactness scores, while Wang (2002) prototyped *ArcIMS* as an early web-based GIS for fragmentation services. Continuous and discrete classifications were also tested in Western Honduras, where Southworth et al. (2004) combined *FRAGSTATS* with local indicators of spatial association in GIS, showing how socioeconomic context shaped patterns. Remote sensing platforms were integrated next: Lung and Schaab (2006) paired *ERDAS IMAGINE* time-series clustering with moving-window GIS metrics in Kenyan rainforests, and Maier

et al. (2006) combined airborne laser scanning with object-based segmentation in *eCognition* and *ArcGIS* to relate canopy structure to fragmentation indices. At continental scales, Wickham et al. (2008) advanced multi-scale forest density mapping using GIS-based moving windows on NLCD data, highlighting scale sensitivity.

Legacy metric calculators such as *FRAGSTATS* and *Patch Analyst* codified patch/class metrics and seeded reproducibility by standardizing formulas (McGarigal & Marks, 1995; Elkie et al., 1999). The *GuidosToolbox* lineage expanded role-based morphology (MSPA) and fixed-scale density (FAD), making edge, core, and corridor classes directly comparable across regions (Vogt et al., 2007; Vogt & Riitters, 2017; Vogt et al., 2022). In India's Western Ghats, Ramachandra, Setturu, and Chandran (2016) applied *FRAGSTATS* with Riitters' indices to quantify biodiversity-rich fragmentation, illustrating how classical software remained embedded in regional GIS workflows. Predictive modeling extended this further, with *IDRISI*'s CA–Markov used alongside *FRAGSTATS* to forecast degradation trajectories (Malhi et al., 2020).

Since ~2018, open ecosystems in R and Python have standardized reproducible workflows. *landscapemetrics* and motif embed FRAGSTATS-style indices in tidy pipelines, while *PyLandStats*, *LecoS*, and *ShrinkShape2* extend analysis into Python/QGIS contexts and provide rotation-robust shape descriptors (Hesselbarth et al., 2019; Nowosad, 2021; Bosch, 2019). Vector-native frameworks (e.g., *VecLI*) and raster–vector integrators (e.g., *VARLI*) mitigate biases from rasterization, and connectivity platforms such as *Conefor* and *Circuitscape* now link directly to morphology roles. General-purpose GIS platforms have become orchestration hubs: *QGIS* (with *Processing*, *GRASS GIS*, and *SAGA*), *ArcGIS Pro* (via ModelBuilder and *ArcPy*), and companion spatial-statistical software such as *GeoDa* allow analysts to integrate patch metrics, network measures, and machine-learning scripts within auditable environments. Increasingly, these analyses are distributed through cloud infrastructures like *Google Earth Engine*, which couples detectors to downstream metrics while preserving reproducible logs.

Reproducibility now extends beyond tool choice to parameter transparency. Analysts increasingly report grain, extent, edge width, compositing policy, and detector settings, and share code or notebooks alongside outputs. This mitigates reporting inconsistency (L5 in Fig. 4) by making studies portable and comparable, while enabling sensitivity checks—such as varying window sizes or compositing rules—without re-engineering full workflows (Marchesan et al., 2018; Yao et al., 2022; Huang et al., 2024; Munhoz et al., 2025). Overall, the trajectory has been from workstation calculators to documented, interoperable pipelines that allow independent verification and cross-study synthesis.

3.5 Advances in New Methods (post-2016)

This subsection emphasizes methodological expansions since 2016, grouped into arcs that show how capabilities accreted.

2016–2019: from 2-D patterns to structure and information.
The first shift was explicit incorporation of vertical structure. Lidar-based methods captured canopy height and porosity, reframing connectivity as three-dimensional rather than planar (Zald et al., 2016; Remmel, 2018). In parallel, information-theoretic approaches gained ground: Nowosad and Stepinski (2019) described landscapes as configuration distributions rather than lists of indices, and Remmel (2020) formalized hyper-local configuration elements for pattern diagnostics. During this period, GIS platforms still anchored workflows, with Ramachandra et al. (2016) using *FRAGSTATS* within *ArcGIS* and PCA environments to analyze forest hotspots in India.

2020–2022: connectivity inside patches and networks between them.
Connectivity refinements unfolded at multiple scales. Within patches, Complexity-Weighted Patch Area (CWA) and related formulations weighted area by form/roughness, capturing intra-patch navigability in ways comparable to classical graph indices (Justeau-Allaire et al., 2024). At broader scales, ProNet provided a bounded, report-ready index for protected-area systems (Theobald et al., 2022). Representation also matured: vector-native indices (*VecLI*) reduced raster biases, and *GuidosToolbox/Workbench* introduced multiscale distance–similarity operators that integrate directly with MSPA roles (Vogt, 2015; Yao et al., 2022; Vogt et al., 2022). Integration with GIS remained central, with predictive CA–Markov modeling in *IDRISI* tied to FRAGSTATS outputs for long-term forecasts (Malhi et al., 2020).

2023–2025: composites, edges, density at policy scale, and controlled experiments. Recent years have seen consolidation across pattern, trajectory, and driver domains. Composite indices such as the Forest Fragmentation Comprehensive Index (FFCI) combine spectral change, configuration, and context to separate loss from recovery (Wu et al., 2024; Lin et al., 2024). The Forest Edge Index (FEI) standardizes edge-centric states for driver analyses, and the Multiscale Similarity Index (MSI) applies Jensen–Shannon similarity to benchmark observed mosaics against fully forested references (Zhen et al., 2023; Netzel et al., 2024). At the policy scale, FAD–FOS pipelines have matured into tools for inter-regional comparability with explicit spatial supports (Vogt & Caudullo, 2025). Methodological frameworks have also tightened raster–vector integration (*VARLI*) and coupled detailed indicators with machine learning to attribute processes (Huang et al., 2024; Lin et al., 2024).

Where time series underpin inference, operational feeders such as provincial *LandTrendr* applications now pipe disturbance segments directly into fragmentation indicators, and sensitivity tests quantify how fixed-scale choices affect outcomes—relevant to scale sensitivity (L1 in Fig. 4) (Qiu et al., 2025; Zhang et al., 2025). Neutral generators such as *flsgen* permit stress-testing of metrics under controlled fragmentation mosaics before transfer to real landscapes (Justeau-Allaire et al., 2022). Recent case studies also demonstrate tighter GIS integration: Zhang et al. (2024) combined *GuidosToolbox*, *Conefor*, and *ArcGIS* to construct ecological security patterns; Lin et al. (2024) fused *FRAGSTATS*, *ENVI*, and *GeoDa* with machine learning in R; and Netzel et al. (2024) used *GDAL/OGR* and custom C code to implement MSI. Together these highlight how GIS platforms are not superseded but remain the backbone environments in which fragmentation innovations are operationalized.

4. Discussion — overview

Across 138 studies, forest-fragmentation methods progress from patch tallies to role-aware, connectivity-explicit, and increasingly 3-D representations. We interpret this trajectory through five recurring *limitations (L1–L5)* that affect transferability: **L1**—scale sensitivity and habitat-amount conflation; **L2**—region-specific thresholds and assumptions; **L3**—weak empirical validation (especially for global products); **L4**—limited linkage to biological responses; and **L5**—incomplete parameter reporting. Figure 3 is a schematic of these limitations; evidence and implications appear below.

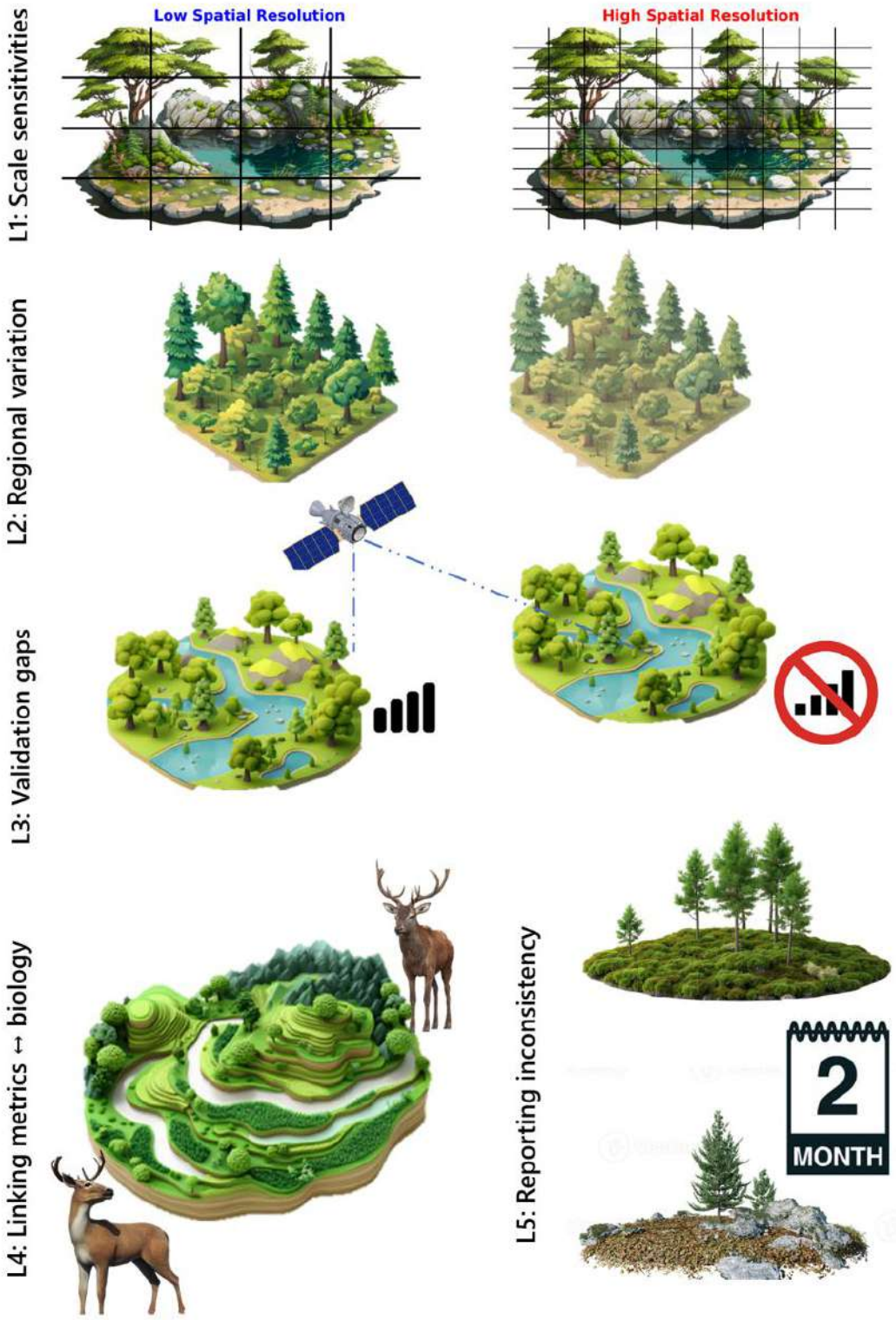

285

286 **Figure 3.** Visual summary of five limitations (**L1–L5**) in forest-fragmentation methods: L1 scale sensitivities; L2
287 regional parameterization; L3 validation gaps; L4 metric–biology linkage; L5 reporting inconsistency. Interpretation
288 is developed in 4.1–4.4.

4.1 Tracing the evolution of metric suitability

Ripple et al. (1991) showed early on that GIS-derived indices could reveal fragmentation trajectories, and the FRAGSTATS era formalized patch, edge, shape, and core metrics for reproducible mapping (McGarigal & Marks, 1995; Walker & Kenkel, 1998; Remmel & Csillag, 2003; Sun & Southworth, 2013). The central weakness—**L1**—is that many indices vary with grain and extent, so differences can reflect pixel size or window choice rather than ecological change (O'Neill et al., 1999; Long et al., 2010; Pe'er et al., 2013). Remmel (2009) explains part of the mechanism: coincidence matrices summarize composition well but capture little about configuration unless augmented, making composition–configuration conflation likely when one class dominates.

MSPA reframed maps into roles—cores, edges, bridges, corridors, perforations—useful at reporting-unit and continental scales (Vogt et al., 2007; Estreguil & Mouton, 2009; Wickham et al., 2010). Connectivity metrics followed. Roberts et al. (2000) and later Lin et al. (2021) and Theobald et al. (2022) translated dispersal and resistance assumptions into graph-based indicators (PC, IIC, dI; *ProNet*) with clearer decision relevance, while surfacing **L2** (context dependence of species/guild parameters) and **L4** (the gap to observed responses).

Recent families aim to curb conflation and tighten links to process. Fixed-scale density (FAD/FOS) declares spatial support up front, stabilizing inter-regional comparisons (Vogt & Caudullo, 2025). Information-theoretic and local-connectedness measures separate form complexity from neighborhood linkage (Peptenatu et al., 2023; Alage et al., 2025). And voxel/3-D approaches bring canopy permeability and edge penetration into scope, advancing structure–function hypotheses but raising data and validation demands (Remmel, 2020, 2022). Across these arcs, results travel best when spatial support, thresholds, and connectivity parameters are stated and stress-tested; otherwise, method settings masquerade as ecological differences (Wang et al., 2012; Fahrig, 2019; Nunes et al., 2022; Zhang et al., 2025).

4.2 Transforming accessibility through open-source, GIS, and cloud ecosystems

Open, scriptable ecosystems have turned isolated metric runs into auditable pipelines. In R, *landscapemetrics* and motif expose FRAGSTATS-style indices within reproducible workflows; in Python, *PyLandStats* and *LecoS* fill a similar role; and *GuidosToolbox* with its Graph-based Workflow Builder scales role-based morphology for large reporting units (Hesselbarth et al., 2019; Nowosad, 2021; Vogt & Riitters, 2017; Vogt et al., 2022). General-purpose GIS—*QGIS* (with *Processing*, *GRASS GIS*, *SAGA*) and *ArcGIS Pro* (ModelBuilder, *ArcPy*)—now acts as the orchestration layer where parameters are modeled, batched, and versioned, while *GeoDa* provides spatial-autocorrelation diagnostics. *Google Earth Engine* has democratized compositing and change detection at scale without bespoke infrastructure (Wulder et al., 2008; Coops et al., 2010; Gorelick et al., 2017).

Two practice gaps persist. First, **L5**: key parameters are too often omitted—grain, extent, edge rules, windowing, compositing policy, detector settings—with our screen suggesting roughly a sixth of papers miss at least one (Hernando et al., 2017; Zatelli et al., 2019). Second, **L3**: reliance on global products without local checks (e.g., *Global Forest Change*) risks omission/commission errors in selective logging, coppice, and fire mosaics (Hansen et al., 2013; Nunes et al., 2022). Addressing both rarely requires new software; it requires concise parameter logs and validation notes attached to each map product. Ramachandra et al. (2016) offer a good template, combining *FRAGSTATS* and PCA in *ArcGIS* to surface regional drivers in India's Western Ghats.

Machine learning extends these pipelines from description to attribution. Zanella et al. (2017) and Zhen et al. (2023) demonstrate how Random Forest applied to PD, LPI, Division, or FFCI composites can illuminate drivers, while Moreira et al. (2024) and Lin et al. (2024) show forward scenarios via ANN or CA-Markov. The same features that add explanatory power raise the bar for transparency: credible ML use reports features and neighborhoods, data partitioning and cross-validation, model settings and interpretability steps, and—crucially—external or hold-out checks (Hansen et al., 2013; Hernando et al., 2017; Zatelli et al., 2019).

4.3 Elevating fidelity with advanced data sources

Multi-sensor regimes sharpen structural detection and help separate composition from configuration (Maier et al., 2006; Long et al., 2010; Zald et al., 2016; Mshelia et al., 2022). Airborne and terrestrial laser scanning reveal vertical

heterogeneity that 2-D indicators miss—central for permeability and microclimate—while detector families (*VCT*, *LandTrendr*, *TTM*, tri-temporal Sentinel-2) stabilize disturbance trajectories before indicators are computed (Huang et al., 2010; Kennedy et al., 2018; Giannetti et al., 2020; Francini et al., 2021, 2023). These gains amplify familiar trade-offs: finer spatial and temporal support heightens **L1** sensitivities and can invite over-interpretation without ecological corroboration (Ostapowicz et al., 2008; Fahrig, 2024). Voxel/3-D formulations promise tighter links to structure and biomass but are data-hungry and demand stronger validation beyond instrumented sites (Remmel, 2022; Mazziotta et al., 2025). In practice, high-fidelity inputs work best when paired with explicit parameter disclosure and targeted field or higher-resolution checks.

4.4 Bridging research and practice: targeted fixes for L1–L5

Validation first (addresses L3, L4). Mac Nally (2008) argued for design-based estimation when mapping prevalence; following that guidance, fragmentation workflows should link indicators to field plots, biodiversity proxies, or independent structure data and report design-based or model-assisted area estimates where feasible (Nunes et al., 2022).

Standardized reporting (addresses L1, L5). Rather than rely on defaults, specify the spatial support and thresholds that govern outputs: grain, extent, edge width, and window size for rolling measures (for FAD, stabilization typically occurs at tens to low hundreds of pixels in dissected landscapes: Zatelli et al., 2019; Zhang et al., 2025); forest definitions and MMU (e.g., FAO/HRL-FTY; Vogt & Caudullo, 2025); compositing policy (Best Available Pixel vs. medoid, target phenology, sensor priority, despiking; Francini et al., 2023); and detector settings—*VCT* masking/IFZ, *LandTrendr* segmentation/recovery, *TTM* cross-validation, tri-temporal Sentinel-2 cut-offs (Huang et al., 2010; Kennedy et al., 2018; Giannetti et al., 2020; Francini et al., 2021).

Region-tuned implementations (addresses L2). Calibrate thresholds, windows, and resistance/dispersal assumptions to local disturbance regimes and canopy architecture so metrics reflect regional realities rather than imported defaults (Geri et al., 2010; Rosa et al., 2017; Kozak et al., 2018; Osewe et al., 2022). Ramachandra et al. (2016) exemplify this tuning in a biodiversity hotspot.

Multi-scale integration (addresses L1, L4). Combine complementary families to reduce conflation and expose process: pair MSPA roles with graph metrics for movement potential; deploy fixed-window FAD–FOS for policy comparability; use INCOMA/gradient surfaces for heterogeneous mosaics; and add voxel morphology where vertical connectivity matters (Nowosad & Stepinski, 2021; Remmel, 2022; Vogt & Caudullo, 2025).

Open, cloud-based reproducibility (enables L1–L5). Share R/Python/GEE workflows—*landscapemetrics*, motif, *geodiv*, *VecLI/VARLI*, *LDT4QGIS*—so parameters are visible, versioned, and re-runnable, making sensitivity checks straightforward and enabling like-for-like comparisons (Mairota et al., 2013; Hesselbarth et al., 2019, 2021; Yao et al., 2022; Smith et al., 2021; Paixão & Machado, 2023).

5. Summary statements

Across three decades and 138 studies, fragmentation analysis has shifted from patch/edge tallies to role-aware, connectivity-explicit, and increasingly three-dimensional descriptions. The most useful way to read that shift is as a linked chain—data sources → change detectors → pattern indicators—where choices made upstream condition what indicators can say downstream.

Five limitations repeatedly shape inference. Scale sensitivity and habitat-amount dependence remain the main source of comparability problems (L1). Parameters tuned in one region do not travel cleanly to another (L2). Adoption of global or automated layers without local checks is still common (L3). Structural metrics are too rarely tied to biological responses (L4). And key settings—spatial support, edge rules, compositing policy, detector thresholds—are inconsistently reported (L5).

What works in practice is incremental rather than novel. Declaring spatial support (e.g., fixed-window density) stabilizes comparisons; pairing role-based morphology with connectivity metrics clarifies movement options; and, where vertical structure matters, targeted lidar/TLS or voxel summaries add needed realism. The common denominator is transparent parameterization with light-weight sensitivity checks, so that apparent differences reflect landscapes rather than hidden settings.

Evidence gaps are evident. Validation is often lacking and could benefit from design-aware, independent approaches; methods might be more effective when tuned to regional disturbance regimes and canopy architecture; and clearer cross-walks between 2-D indicators and 3-D/voxel measures could enhance understanding. Geographic coverage also remains uneven, with several tropical regions under-represented.

Looking ahead, future progress may hinge less on new indices and more on refining existing ones through precise specification and validation. Key considerations include: (i) documenting spatial support and detector settings as metadata, (ii) exploring region-balanced benchmarking and neutral-landscape challenges to assess sensitivity, (iii) developing simple, shareable workflows for inspection, and (iv) integrating field or high-resolution data where possible. Adopting these approaches could strengthen fragmentation measures' reliability for ecological interpretation, monitoring, and decision-making amid accelerating habitat change.

Reference list

Adamczyk, J., & Tiede, D. (2017) ZonalMetrics—a Python toolbox for zonal landscape structure analysis. Computers & Geosciences, 99, 91–99. https://doi.org/10.1016/j.cageo.2016.11.005

Alage, I. L., Tan, Y., Akande, A. W., Olugbenga, H. J., Suprijanto, A., & Lodhi, M. K. (2025). Fractal Metrics and Connectivity Analysis for Forest and Deforestation Fragmentation Dynamics. Forests, 16(2), 314. https://doi.org/10.3390/f16020314

Andronache, I. (2024) Analysis of Forest Fragmentation and Connectivity Using Fractal Dimension and Succolarity. Land, 13(2), 138. https://doi.org/10.3390/land13020138

Atkins, J. W., Stovall, A. E., & Silva, C. A. (2022) Open-source tools in R for forestry and forest ecology. Forest Ecology and Management, 503, 119813. https://doi.org/10.1016/j.foreco.2021.119813

Batar, A. K., Shibata, H., & Watanabe, T. (2021) A novel approach for forest fragmentation susceptibility mapping and assessment: a case study from the Indian Himalayan region. Remote Sensing, 13(20), 4090. https://doi.org/10.3390/rs13204090

Bennett, A. F., & Radford, J. Q. (2008). Emergent properties of land mosaics: Implications for landscape management and restoration. In Managing and Designing Landscapes for Conservation (pp. 201–209). Wiley-Blackwell.

Bogaert, J., Van Hecke, P., Van Eysenrode, D. S., & Impens, I. (2000) Landscape Fragmentation Assessment Using a Single Measure. *Wildlife Society Bulletin (1973-2006)*, *28*(4), 875–881. http://www.jstor.org/stable/3783842

Bonhomme, V., Castets, M., Ibanez, T., Géraux, H., Hély, C., & Gaucherel, C. (2017) Configurational changes of patchy landscapes dynamics. Ecological Modelling, 363, 1–7. https://doi.org/10.1016/j.ecolmodel.2017.08.007

Bosch, M. (2019) PyLandStats: An open-source Pythonic library to compute landscape metrics. PLoS One, 14(12), e0225734. https://doi.org/10.1371/journal.pone.0225734

Coops, N. C., Gillanders, S. N., Wulder, M. A., et al. (2010) Assessing changes in forest fragmentation following infestation using time series Landsat imagery. Forest Ecology and Management, 259(12), 2355–2365. https://doi.org/10.1016/j.foreco.2010.03.008

Dutt, S., Batar, A. K., Sulik, S., & Kunz, M. (2024) Forest ecosystem on the edge: Mapping forest fragmentation susceptibility in Tuchola Forest, Poland. Ecological Indicators, 161, 111980. https://doi.org/10.1016/j.ecolind.2024.111980

Elkie, P. C., Rempel, R. S., & Carr, A. P. (1999) Patch Analyst User's Manual: A tool for quantifying landscape structure. Ontario Ministry of Natural Resources, Northwest Science and Technology, Thunder Bay, Ontario. TM-002.

436 Estreguil, C., & Mouton, C. (2009) Measuring and reporting on forest landscape pattern, fragmentation, and
437 connectivity in Europe: methods and indicators. JRC Scientific and Technical Reports. Luxembourg: Office for
438 Official Publications of the European Communities.

439 Fahrig, L. (2003) Effects of habitat fragmentation on biodiversity. Annual Review of Ecology, Evolution, and
440 Systematics, 34(1), 487–515. https://doi.org/10.1146/annurev.ecolsys.34.011802.132419

441 Fahrig, L. (2019) Habitat fragmentation: A long and tangled tale. Global Ecology and Biogeography, 28(1), 33–41.
442 https://doi.org/10.1111/geb.12839

443 Fahrig, L. (2024) Patch-scale edge effects do not indicate landscape-scale fragmentation effects. Conservation
444 Letters, 17, e12992. https://doi.org/10.1111/conl.12992

445 Fardila, D., Kelly, L. T., Moore, J. L., & McCarthy, M. A. (2017) A systematic review reveals changes in where and
446 how we have studied habitat loss and fragmentation over 20 years. Biological Conservation, 212, 130–138.
447 https://doi.org/10.1016/j.biocon.2017.04.031

448 Feleha, D. D., Tymińska-Czabańska, L., & Netzel, P. (2025). Forest Fragmentation and Forest Mortality—An In-
449 Depth Systematic Review. Forests, 16(4), 565. https://doi.org/10.3390/f16040565

450 Fletcher Jr, R. J., Didham, R. K., Banks-Leite, C., Barlow, J., Ewers, R. M., Rosindell, J., ... & Haddad, N. M.
451 (2018). Is habitat fragmentation good for biodiversity?. *Biological conservation*, *226*, 9-15.
452 https://doi.org/10.1016/j.biocon.2018.07.022

453 Francini, S., Hermosilla, T., Coops, N. C., Wulder, M. A., White, J. C., & Chirici, G. (2023). An assessment
454 approach for pixel-based image composites. ISPRS Journal of Photogrammetry and Remote Sensing, 202, 1–12.
455
456 Francini, S., McRoberts, R. E., Giannetti, F., Marchetti, M., Mugnozza, G. S., & Chirici, G. (2021). The Three
457 Indices Three Dimensions (3I3D) algorithm… International Journal of Remote Sensing, 42(12), 4693–4711.

458 Frazier, A. E., & Kedron, P. (2017) Comparing forest fragmentation in Eastern US forests using patch-mosaic and
459 gradient surface models. Ecological Informatics, 41, 108–115. https://doi.org/10.1016/j.ecoinf.2017.08.002

460 Geri, F., Rocchini, D., & Chiarucci, A. (2010) Landscape metrics and topographical determinants of large-scale
461 forest dynamics in a Mediterranean landscape. Landscape and Urban Planning, 95(1–2), 46–53.
462 https://doi.org/10.1016/j.landurbplan.2009.12.001

463 Giannetti, F., Pegna, R., Francini, S., McRoberts, R. E., et al. (2020). Two Thresholds Method (TTM)… Remote
464 Sensing, 12(22), 3720. https://doi.org/10.3390/rs12223720

465 Giriraj, A., Murthy, M. S. R., & Beierkuhnlein, C. (2010) Evaluating forest fragmentation and its tree community
466 composition in the tropical rainforest of Southern Western Ghats (India) from 1973 to 2004. Environmental
467 Monitoring and Assessment, 161(1–4), 29–44. https://doi.org/10.1007/s10661-008-0724-5

468 Gorelick, N., Hancher, M., Dixon, M., Ilyushchenko, S., Thau, D., & Moore, R. (2017). Google Earth Engine:
469 Planetary-scale geospatial analysis for everyone. Remote Sensing of Environment, 202, 18–27.
470 https://doi.org/10.1016/j.rse.2017.06.031

471 Haddad, N. M., Brudvig, L. A., Clobert, J., Davies, K. F., Gonzalez, A., Holt, R. D., ... & Townshend, J. R. (2015).
472 Habitat fragmentation and its lasting impact on Earth's ecosystems. *Science advances*, *1*(2), e1500052.
473 10.1126/sciadv.1500052

Hansen, M. C., Potapov, P. V., Moore, R., et al. (2013). High-resolution global maps of 21st-century forest cover change. Science, 342, 850–853. https://doi.org/10.1126/science.1244693

Hargis, C. D., Bissonette, J. A., & Turner, D. L. (1999) The influence of forest fragmentation and landscape pattern on American martens. Journal of Applied Ecology, 36(1), 157–172. https://doi.org/10.1046/j.1365-2664.1999.00377.x

Harzing, A. W. (2010) The Publish or Perish Book. Melbourne: Tarma Software Research Pty Limited.

Heilman, G. E., Strittholt, J. R., Slosser, N. C., & Dellasala, D. A. (2002) Forest fragmentation of the conterminous United States: Assessing forest intactness through road density and spatial characteristics. BioScience, 52(5), 411–422. https://doi.org/10.1641/0006-3568(2002)052[0411:FFOTCU]2.0.CO;2

Hernando, A., Velázquez, J., Valbuena, R., Legrand, M., & García-Abril, A. (2017) Influence of the resolution of forest cover maps in evaluating fragmentation and connectivity to assess habitat conservation status. Ecological Indicators, 79, 295–302. https://doi.org/10.1016/j.ecolind.2017.04.031

Hesselbarth, M. H., Nowosad, J., Signer, J., et al. (2021) Open-source Tools in R for Landscape Ecology. Current Landscape Ecology Reports, 6, 97–111. https://doi.org/10.1007/s40823-021-00067-y

Hesselbarth, M. H., Sciaini, M., With, K. A., Wiegand, K., & Nowosad, J. (2019) landscapemetrics: an open-source R tool to calculate landscape metrics. Ecography, 42(10), 1648–1657. https://doi.org/10.1111/ecog.04617

Huang, C., Goward, S. N., Masek, J. G., Thomas, N., Zhu, Z., & Vogelmann, J. E. (2010). An automated approach for reconstructing recent forest disturbance history using dense Landsat time series stacks. Remote Sensing of Environment, 114(1), 183–198. https://doi.org/10.1016/j.rse.2009.08.017

Huang, Y., Zheng, M., Li, T., Xiao, F., & Zheng, X. (2024) An integrated framework for landscape indices' calculation with raster–vector integration and its application based on QGIS. ISPRS International Journal of Geo-Information, 13(7), 242. https://doi.org/10.3390/ijgi13070242

Jaeger, J. A. (2000) Landscape division, splitting index, and effective mesh size: new measures of landscape fragmentation. Landscape Ecology, 15, 115–130. https://doi.org/10.1023/A:1008129329289

Jorge, L. A. B., & Garcia, G. J. (1997). A study of habitat fragmentation in Southeastern Brazil using remote sensing and GIS. Forest Ecology and Management, 98(1), 35–47. https://doi.org/10.1016/S0378-1127(97)00076-8

Jung, M. (2016) LecoS—A QGIS plugin for automated landscape ecology analysis. PeerJ Preprints. https://doi.org/10.1016/j.ecoinf.2015.11.006

Justeau-Allaire, D., Blanchard, G., Ibanez, T., Lorca, X., Vieilledent, G., & Birnbaum, P. (2022). Fragmented landscape generator (flsgen): A neutral landscape generator with control of landscape structure and fragmentation indices. Methods in Ecology and Evolution, 13(7), 1412–1420. https://doi.org/10.1111/2041-210X.13859

Justeau-Allaire, D., Ibanez, T., Vieilledent, G., Lorca, X., & Birnbaum, P. (2024). Refining intra-patch connectivity measures in landscape fragmentation and connectivity indices. Landscape Ecology, 39(2), 24. https://doi.org/10.1007/s10980-024-01840-0

Kedron, P. J., Frazier, A. E., Ovando-Montejano, G. A., & Wang, J. (2018) Surface metrics for landscape ecology: a comparison of landscape models across ecoregions and scales. Landscape Ecology, 33, 1489–1504. https://doi.org/10.1007/s10980-018-0685-1

Kennedy, R. E., Yang, Z., Cohen, W. B., et al. (2018). Implementation of the LandTrendr algorithm on Google Earth Engine. Remote Sensing, 10(5), 691. https://doi.org/10.3390/rs10050691

Kopecká, M., & Nováček, J. (2010) Natural forest fragmentation: an example from the Tatra Region, Slovakia. Land Use/Cover Changes in Selected Regions in the World, 5, 51–56.

Kozak, J., Ziółkowska, E., Vogt, P., Dobosz, M., Kaim, D., Kolecka, N., & Ostafin, K. (2018) Forest-cover increase does not trigger forest-fragmentation decrease: Case study from the Polish Carpathians. Sustainability, 10(5), 1472. https://doi.org/10.3390/su10051472

Lausch, A., Blaschke, T., Haase, D., Herzog, F., Syrbe, R. U., Tischendorf, L., & Walz, U. (2015) Understanding and quantifying landscape structure—a review on relevant process characteristics, data models and landscape metrics. Ecological Modelling, 295, 31–41. https://doi.org/10.1016/j.ecolmodel.2014.08.018

Li, M., Xu, Y., Mao, L., & Su, P. (2010) Assessing rates and causes of global forest fragmentation based on Globcover V2.2. In: 2010 3rd International Congress on Image and Signal Processing (Vol. 3, pp. 1077–1082). IEEE. https://doi.org/10.1109/cisp.2010.5646898

Lin, J., Huang, C., Wen, Y., & Liu, X. (2021) An assessment framework for improving protected areas based on morphological spatial pattern analysis and graph-based indicators. Ecological Indicators, 130, 108138. https://doi.org/10.1016/j.ecolind.2021.108138

Lin, X., Zhen, S., Zhao, Q., & Hu, X. (2024) A new paradigm for assessing detailed dynamics of forest landscape fragmentation. Forests, 15(7), 1212. https://doi.org/10.3390/f15071212

Lin, Y., Jin, Y., Ge, Y., Hu, X., Weng, A., Wen, L., … Li, B. (2024) Insights into forest vegetation changes and landscape fragmentation in Southeastern China: From a perspective of spatial coupling and machine learning. Ecological Indicators, 166, 112479. https://doi.org/10.1016/j.ecolind.2024.112479

Long, J. A., Nelson, T. A., & Wulder, M. A. (2010a) Characterizing forest fragmentation: Distinguishing change in composition from configuration. Applied Geography, 30(3), 426–435. https://doi.org/10.1016/j.apgeog.2009.12.002

Long, J. A., Nelson, T. A., & Wulder, M. A. (2010b) Local indicators for categorical data: impacts of scaling decisions. The Canadian Geographer/Le Géographe canadien, 54(1), 15–28. https://doi.org/10.1111/j.1541-0064.2009.00300.x

Lovelace, R., Nowosad, J., & Muenchow, J. (2019) Geocomputation with R (1st ed.). Chapman and Hall/CRC. https://doi.org/10.1201/9780203730058

Lung, T., & Schaab, G. (2006) Assessing fragmentation and disturbance of west Kenyan rainforests by means of remotely sensed time series data and landscape metrics. African Journal of Ecology, 44(4), 491–501. https://doi.org/10.1111/j.1365-2028.2006.00663.x

Mac Nally, R. (2008). Remnant geometry, landscape morphology and their ecological effects. In Managing and Designing Landscapes for Conservation (pp. 55–62). Wiley-Blackwell.

Machado, R., Bayot, R., Godinho, S., Pirnat, J., Santos, P., & de Sousa-Neves, N. (2020) LDTtool: A toolbox to assess landscape dynamics. Environmental Modelling & Software, 133, 104847. https://doi.org/10.1016/j.envsoft.2020.104847

MacLean, M. G., & Congalton, R. G. (2013) PolyFrag: a vector-based program for computing landscape metrics. GIScience & Remote Sensing, 50(6), 591–603. https://doi.org/10.1080/15481603.2013.856537

549 Mahapatra, S., et al. (2025). Understanding forest fragmentation dynamics and identifying drivers… Results in
550 Engineering, 26, 104640.

551 Maier, B., Tiede, D., & Dorren, L. (2006) Assessing mountain forest structure using airborne laser scanning and
552 landscape metrics. International Archives of Photogrammetry, Remote Sensing and Spatial Information Sciences,
553 36(4), C42.

554 Mairota, P., Cafarelli, B., Boccaccio, L., Leronni, V., Labadessa, R., Kosmidou, V., & Nagendra, H. (2013) Using
555 landscape structure to develop quantitative baselines for protected area monitoring. Ecological Indicators, 33, 82–95.
556 https://doi.org/10.1016/j.ecolind.2012.08.017

557 Malhi, R. K. M., Anand, A., Srivastava, P. K., et al. (2020) An integrated spatiotemporal pattern analysis model to
558 assess and predict the degradation of protected forest areas. ISPRS International Journal of Geo-Information, 9(9),
559 530. https://doi.org/10.3390/ijgi9090530

560 Marchesan, J., Pereira, R. S., Alba, E., & Pedrali, L. D. (2018) Spatial analysis of forest fragmentation in the
561 Atlantic Forest biome areas. Journal of Agricultural Science, 10(12), 1–12. https://doi.org/10.5539/jas.v10n12p294

562 Mazziotta, A., Francini, S., & Parisi, F. (2025). Monitoring Habitat Fragmentation and Biodiversity in Forest
563 Ecosystems. In Ecological Connectivity of Forest Ecosystems (pp. 171–186). Cham: Springer Nature Switzerland.

564 McGarigal, K. (1995) FRAGSTATS: spatial pattern analysis program for quantifying landscape structure. General
565 Technical Report PNW-GTR-351. U.S. Department of Agriculture, Forest Service, Pacific Northwest Research
566 Station, Portland, OR, 1–122.

567 McGarigal, K., & Marks, B. J. (1995) Spatial pattern analysis program for quantifying landscape structure. General
568 Technical Report PNW-GTR-351. U.S. Department of Agriculture, Forest Service, Pacific Northwest Research
569 Station, Portland, OR, 1–122.

570 McRae, B. H., Shah, V. B., & Mohapatra, T. K. (2008). Circuitscape user's guide. *The University of California,*
571 *Santa Barbara*.

572 Meddens, A. J., Hudak, A. T., Evans, J. S., et al. (2008) Characterizing forest fragments in boreal, temperate, and
573 tropical ecosystems. AMBIO, 37(7), 569–576. https://doi.org/10.1579/0044-7447-37.7.569

574 Moreira, R. M., Lana, M., Sieber, S., & Malheiros, T. F. (2024) A landscape ecology approach: Modeling forest
575 fragmentation with artificial neural networks and cellular-automata Markov-chain for improved environmental
576 policy in the southwestern Brazilian Amazon. Land Degradation and Development, 35(2), 687–704.
577 https://doi.org/10.1002/ldr.4945

578 Mshelia, Z. H., Aigbokhan, O. J., & Agbor, C. F. (2022) Analysis of forest dynamics using landscape metrics and
579 Markov chain model in Omo Forest Reserve, Ogun State, Nigeria. Journal of Applied Sciences and Environmental
580 Management, 26(9), 1565–1573. https://doi.org/10.4314/jasem.v26i9.16

581 Munhoz, H. M., Francisco, B. S., Prudente, V. H. R., et al. (2025). Forest fragmentation dynamics in the direct
582 influence area of Iguaçu National Park, Brazil. Environmental Monitoring and Assessment, 197, 334.
583 https://doi.org/10.1007/s10661-025-13801-4

584 Netzel, P., Tyminska, L., Feleha, D. D., & Socha, J. (2024) New approach to assess forest fragmentation based on
585 multiscale similarity index. Ecological Indicators, 158, 111530. https://doi.org/10.1016/j.ecolind.2023.111530

Newman, M. E., McLaren, K. P., & Wilson, B. S. (2011) Comparing the effects of classification techniques on landscape-level assessments: pixel-based versus object-based classification. International Journal of Remote Sensing, 32(14), 4055–4073. https://doi.org/10.1080/01431161.2010.484432

Nowosad, J. (2021) Motif: an open-source R tool for pattern-based spatial analysis. Landscape Ecology, 36, 29–43. https://doi.org/10.1007/s10980-020-01135-0

Nowosad, J., & Hesselbarth, M. H. (2024) The landscapemetrics and motif packages for measuring landscape patterns and processes. arXiv preprint https://doi.org/10.48550/arxiv.2405.06559

Nowosad, J., & Stepinski, T. F. (2019) Information theory as a consistent framework for quantification and classification of landscape patterns. Landscape Ecology, 34, 2091–2101. https://doi.org/10.1007/s10980-019-00830-x

Nowosad, J., & Stepinski, T. F. (2021) Pattern-based identification and mapping of landscape types using multi-thematic data. International Journal of Geographical Information Science, 35(8), 1634–1649. https://doi.org/10.1080/13658816.2021.1893324

Nunes, M. H., Camargo, J. L. C., Vincent, G., Calders, K., Oliveira, R. S., Huete, A., … Maeda, E. E. (2022) Forest fragmentation impacts the seasonality of Amazonian evergreen canopies. Nature Communications, 13(1), 917. https://doi.org/10.1038/s41467-022-28490-7

O'Neill, R. V., Riitters, K. H., Wickham, J. D., & Jones, K. B. (1999) Landscape pattern metrics and regional assessment. Ecosystem Health, 5(4), 225–233. https://doi.org/10.1046/j.1526-0992.1999.09942.x

Osewe, E. O., Niță, M. D., & Abrudan, I. V. (2022) Assessing the fragmentation, canopy loss and spatial distribution of forest cover in Kakamega National Forest Reserve, Western Kenya. Forests, 13(12), 2127. https://doi.org/10.3390/f13122127

Ostapowicz, K., Vogt, P., Riitters, K. H., Kozak, J., & Estreguil, C. (2008) Impact of scale on morphological spatial pattern of forest. Landscape Ecology, 23, 1107–1117. https://doi.org/10.1007/s10980-008-9271-2

Ouzzani, M., Hammady, H., Fedorowicz, Z., & Elmagarmid, A. (2016) Rayyan—a web and mobile app for systematic reviews. Systematic Reviews, 5, 210. https://doi.org/10.1186/s13643-016-0384-4

Page, M. J., McKenzie, J. E., Bossuyt, P. M., Boutron, I., Hoffmann, T. C., Mulrow, C. D., Shamseer, L., Tetzlaff, J. M., Akl, E. A., Brennan, S. E., Chou, R., Glanville, J., Grimshaw, J. M., Hróbjartsson, A., Lalu, M. M., Li, T., Loder, E. W., Mayo-Wilson, E., McDonald, S., McGuinness, L. A., Stewart, L. A., Thomas, J., Tricco, A. C., Welch, V. A., Whiting, P., & Moher, D. (2021) The PRISMA 2020 statement: an updated guideline for reporting systematic reviews. BMJ, 372, n71. https://doi.org/10.1136/bmj.n71

Paixão, L., & Machado, R. (2023) LDT4QGIS: An open-source tool to enhance landscape analysis. Ecological Informatics, 75, 102073. https://doi.org/10.1016/j.ecoinf.2023.102073

Pe'er, G., Zurita, G. A., Schober, L., Bellocq, M. I., Strer, M., Müller, M., & Pütz, S. (2013) Simple process-based simulators for generating spatial patterns of habitat loss and fragmentation: a review and introduction to the G-RaFFe model. PLoS One, 8(5), e64968. https://doi.org/10.1371/journal.pone.0064968

Peptenatu, D., Andronache, I., Ahammer, H., Radulovic, M., Costanza, J. K., Jelinek, H. F., … Newman, E. A. (2023) A new fractal index to classify forest fragmentation and disorder. Landscape Ecology, 38(6), 1373–1393. https://doi.org/10.1007/s10980-023-01640-y

Peura, M., Burgas, D., Eyvindson, K., Repo, A., & Mönkkönen, M. (2018). Continuous-cover forestry as a cost-efficient tool to increase multifunctionality of boreal production forests. Biological Conservation, 217, 104–112.

Qiu, L., Chang, Z., Luo, X., Chen, S., Jiang, J., & Lei, L. (2025) Monitoring forest disturbances and associated driving forces in Guangdong Province using long-term Landsat time series images. Forests, 16(1), 189. https://doi.org/10.3390/f16010189

Ramachandra, T. V., Setturu, B., & Chandran, S. (2016). Geospatial analysis of forest fragmentation in Uttara Kannada District, India. *Forest Ecosystems, 3*(1), 10. https://doi.org/10.1186/s40663-016-0069-4

Ramezani, H., & Ramezani, A. (2021) Forest fragmentation assessment using field-based sampling data from forest inventories. Scandinavian Journal of Forest Research, 36(4), 289–296. https://doi.org/10.1080/02827581.2021.1908592

Remmel, T. K. (2009). Investigating global and local categorical map configuration comparisons based on coincidence matrices. *Geographical Analysis*, *41*(2), 138-157.

Remmel, T. K. (2015) ShrinkShape2: A FOSS toolbox for computing rotation-invariant shape spectra for characterizing and comparing polygons. The Canadian Geographer/Le Géographe canadien, 59(4), 532–547. https://doi.org/10.1111/cag.12222

Remmel, T. K. (2018) An incremental and philosophically different approach to measuring raster patch porosity. Sustainability, 10(10), 3413. https://doi.org/10.3390/su10103413

Remmel, T. K. (2020) Distributions of hyper-local configuration elements to characterize, compare, and assess landscape-level spatial patterns. Entropy, 22(4), 420. https://doi.org/10.3390/e22040420

Remmel, T. K. (2022) Extending morphological pattern segmentation to 3D voxels. Landscape Ecology, 37, 373–380. https://doi.org/10.1007/s10980-021-01384-7

Remmel, T. K., & Csillag, F. (2003) When are two landscape pattern indices significantly different? Journal of Geographical Systems, 5(4), 331–351. https://doi.org/10.1007/s10109-003-0116-x

Rempel, R. (1999) Natural disturbance analysis and planning tools. [Unpublished manuscript].

Riitters, K. H. (2007) Forest fragmentation. In Forest Health Monitoring: 2005 National Technical Report (pp. 9–15). General Technical Report SRS-104. Asheville, NC: U.S. Department of Agriculture, Forest Service, Southern Research Station.

Riitters, K., Riitters, K. H., Soille, P., & Estreguil, C. (2009) Landscape patterns from mathematical morphology on maps with contagion. Landscape Ecology, 24, 699–709. https://doi.org/10.1007/s10980-009-9344-x

Ripple, W. J., Bradshaw, G. A., & Spies, T. A. (1991) Measuring forest landscape patterns in the Cascade Range of Oregon, USA. Biological Conservation, 57(1), 73–89. https://doi.org/10.1016/0006-3207(91)90108-L

Rivas, C. A., Guerrero-Casado, J., & Navarro-Cerrillo, R. M. (2022) A new combined index to assess the fragmentation status of a forest patch based on its size, shape complexity, and isolation. Diversity, 14(11), 896. https://doi.org/10.3390/d14110896

Roberts, S. A., Hall, G. B., & Calamai, P. H. (2000) Analysing forest fragmentation using spatial autocorrelation, graphs and GIS. International Journal of Geographical Information Science, 14(2), 185–204. https://doi.org/10.1080/136588100240912

Rosa, I. M., Gabriel, C., & Carreiras, J. M. (2017) Spatial and temporal dimensions of landscape fragmentation across the Brazilian Amazon. Regional Environmental Change, 17, 1687–1699. https://doi.org/10.1007/s10113-017-1120-x

Saura, S., & Torné, J. (2009). Conefor Sensinode 2.2: a software package for quantifying the importance of habitat patches for landscape connectivity. *Environmental modelling & software*, *24*(1), 135-139. https://doi.org/10.1016/j.envsoft.2008.05.005

Selsam, P., Bumberger, J., Wellmann, T., Pause, M., Gey, R., Borg, E., & Lausch, A. (2024) EcosystemIntegrity Remote Sensing—Modelling and Service Tool—ESIS/Imalys. Remote Sensing, 16(7), 1139. https://doi.org/10.3390/rs16071139

Siegel, T., Magrach, A., Laurance, W. F., & Luther, D. (2024). A global meta-analysis of the impacts of forest fragmentation on biotic mutualisms and antagonisms. Conservation Biology, 38(3), e14206. https://doi.org/10.1111/cobi.14206

Singh, S., Reddy, C. S., Pasha, S. V., Dutta, K., Saranya, K. R. L., & Satish, K. V. (2017) Modeling the spatial dynamics of deforestation and fragmentation using multi-layer perceptron neural network and landscape fragmentation tool. Ecological Engineering, 99, 543–551. https://doi.org/10.1016/j.ecoleng.2016.11.047

Smith, A. C., Dahlin, K. M., Record, S., Costanza, J. K., Wilson, A. M., & Zarnetske, P. L. (2021) The geodiv r package: Tools for calculating gradient surface metrics. Methods in Ecology and Evolution, 12(11), 2094–2100. https://doi.org/10.1111/2041-210x.13677

Southworth, J., Munroe, D., & Nagendra, H. (2004) Land cover change and landscape fragmentation—comparing the utility of continuous and discrete analyses for a western Honduras region. Agriculture, Ecosystems & Environment, 101(2–3), 185–205. https://doi.org/10.1016/j.agee.2003.09.011

Soverel, N. O., Coops, N. C., White, J. C., & Wulder, M. A. (2010) Characterizing the forest fragmentation of Canada's national parks. Environmental Monitoring and Assessment, 164(1–4), 481–497. https://doi.org/10.1007/s10661-009-0908-7

Sun, J., & Southworth, J. (2013) Remote sensing-based fractal analysis and scale dependence associated with forest fragmentation in an Amazon tri-national frontier. Remote Sensing, 5(2), 454–472. https://doi.org/10.3390/rs5020454

Tang, J., Bu, K., Yang, J., Zhang, S., & Chang, L. (2012) Multitemporal analysis of forest fragmentation in the upstream region of the Nenjiang River Basin, Northeast China. Ecological Indicators, 23, 597–607. https://doi.org/10.1016/j.ecolind.2012.05.012

Tejaswi, G. (2007). Manual on deforestation, degradation, and fragmentation using remote sensing and GIS. MAR-SFM Working Paper, FAO, Rome.

Theobald, D. M., Keeley, A. T., Laur, A., & Tabor, G. (2022) A simple and practical measure of the connectivity of protected area networks: the ProNet metric. Conservation Science and Practice, 4(11), e12823. https://doi.org/10.1111/csp2.12823

van Strien, M. J., Slager, C. T., De Vries, B., & Grêt-Regamey, A. (2016) An improved neutral landscape model for recreating real landscapes and generating landscape series for spatial ecological simulations. Ecology and Evolution, 6(11), 3808–3821. https://doi.org/10.1002/ece3.2145

Vergara, D. G., Lasco, R., Walker, R., Alcantara, A., Ancog, R., Sanchez, P. A., & Tiburan Jr, C. (2021) Fragmentation Trajectories as a review of existing and proposed single-valued fragmentation indices. Journal of Environmental Science and Management, 24(2), 30–47. https://doi.org/10.47125/jesam/2021_2/04

Vernier, P., & Cumming, S. (1999) Predicting landscape patterns from stand attribute data in the Alberta boreal mixedwood. [Technical report, University of Alberta].

Vogt, P. (2015) Quantifying landscape fragmentation. In A. J. Pessoa (Ed.), Simpósio Brasileiro de Sensoriamento Remoto, 17 (SBSR), 2015 (pp. 1239–1246). São José dos Campos: INPE.

Vogt, P., & Caudullo, G. (2025). Pan-European monitoring of local forest fragmentation — Algorithm Theoretical Basis Document (ATBD). Publications Office of the European Union. https://doi.org/10.2760/8260743

Vogt, P., & Riitters, K. H. (2017) GuidosToolbox: universal digital image object analysis. European Journal of Remote Sensing, 50(1), 352–361. https://doi.org/10.1080/22797254.2017.1330650

Vogt, P., Riitters, K. H., Estreguil, C., Kozak, J., Wade, T. G., & Wickham, J. D. (2007) Mapping spatial patterns with morphological image processing. Landscape Ecology, 22, 171–177. https://doi.org/10.1007/s10980-006-9013-2

Vogt, P., Riitters, K. H., Iwanowski, M., Estreguil, C., Kozak, J., & Soille, P. (2007) Mapping landscape corridors. Ecological Indicators, 7(2), 481–488. https://doi.org/10.1016/j.ecolind.2006.11.001

Vogt, P., Riitters, K. H., Rambaud, P., d'Annunzio, R., Lindquist, E., & Pekkarinen, A. (2022) GuidosToolbox Workbench: spatial analysis of raster maps for ecological applications. Ecography, 45(3), 000–000. https://doi.org/10.1111/ecog.05864

Walker, D. J., & Kenkel, N. C. (1998) Fractal analysis of spatio-temporal dynamics in boreal forest landscapes. Abstracta Botanica, 22(1), 13–28.

Wang, F. (2002) Design and implementation of web-based GIS for forest fragmentation analysis. Master's thesis, West Virginia University.

Wang, X., Hamann, A., & Cumming, S. G. (2012) Measuring boreal forest fragmentation after fire: Which configuration metrics are best? Ecological Indicators, 13(1), 189–195. https://doi.org/10.1016/j.ecolind.2011.06.002

Wegmann, M., Leutner, B. F., Metz, M., Neteler, M., Dech, S., & Rocchini, D. (2018) r.pi: A GRASS GIS package for semi-automatic spatial pattern analysis of remotely sensed land cover data. Methods in Ecology and Evolution, 9(1), 191–199. https://doi.org/10.1111/2041-210X.12827

Wickham, J. D., Riitters, K. H., Wade, T. G., & Homer, C. (2008) Temporal change in fragmentation of continental US forests. Landscape Ecology, 23(8), 891–898.

Wickham, J. D., Riitters, K. H., Wade, T. G., & Vogt, P. (2010) A national assessment of green infrastructure and change for the conterminous United States using morphological image processing. Landscape and Urban Planning, 94(3–4), 186–195. https://doi.org/10.1016/j.landurbplan.2009.10.003

Wu, L., Liu, S., Yu, W., Hu, X., & Li, J. (2024) What are the key factors influencing the dynamics of forest edge? An application of a new forest edge index in the southeast of China. Catena, 240, 108009. https://doi.org/10.1016/j.catena.2024.108009

Wulder, M. A., White, J. C., Han, T., et al. (2008) Monitoring Canada's forests. Part 2: National forest fragmentation and pattern. Canadian Journal of Remote Sensing, 34(6), 563–584. https://doi.org/10.5589/m08-081

Yao, Y., Cheng, T., Sun, Z., Li, L., Chen, D., Chen, Z., … Guan, Q. (2022) VecLI: A framework for calculating vector landscape indices considering landscape fragmentation. Environmental Modelling & Software, 149, 105325. https://doi.org/10.1016/j.envsoft.2022.105325

Ye, H., Yang, Z., & Xu, X. (2020) Ecological corridors analysis based on MSPA and MCR model—a case study of the Tomur World Natural Heritage Region. Sustainability, 12(3), 959. https://doi.org/10.3390/su12030959

Zald, H. S. J., Wulder, M. A., White, J. C., Hilker, T., Hermosilla, T., & Hobart, G. W. (2016). Integrating Landsat time series and LiDAR to map forest structure and biomass. Remote Sensing of Environment, 176, 188–201.

Zanella, L., Folkard, A. M., Blackburn, G. A., & Carvalho, L. M. (2017) How well does random forest analysis model deforestation and forest fragmentation in the Brazilian Atlantic forest? Environmental and Ecological Statistics, 24, 529–549. https://doi.org/10.1007/s10651-017-0389-8

Zaragozí, B., Belda, A., Linares, J., Martínez-Pérez, J. E., Navarro, J. T., & Esparza, J. (2012) A free and open source programming library for landscape metrics calculations. Environmental Modelling & Software, 31, 131–140. https://doi.org/10.1016/j.envsoft.2011.10.009

Zatelli, P., Gobbi, S., Tattoni, C., Cantiani, M. G., La Porta, N., Rocchini, D., … Ciolli, M. (2019) Relevance of the cell neighborhood size in landscape metrics evaluation and free or open source software implementations. ISPRS International Journal of Geo-Information, 8(12), 586. https://doi.org/10.3390/ijgi8120586

Zhang, F., Jia, Y., Liu, X., Li, T., & Gao, Q. (2024) Application of MSPA-MCR models to construct ecological security pattern in the basin: A case study of Dawen River basin. Ecological Indicators, 160, 111887. https://doi.org/10.1016/j.ecolind.2024.111887

Zhang, M., Liu, P., Liu, K., & Zhao, Z. (2025) Multiscale sensitivity analysis of landscape fragmentation in plantation forests on the Loess Plateau. Land Degradation & Development. https://doi.org/10.1002/ldr.5469

Zhang, M., Yu, S., & Zhao, Z. (2024) The role of spatial morphology in forest landscape fragmentation: Insights from planted and natural forests of the Chinese Loess Plateau. Land Degradation & Development. https://doi.org/10.1002/ldr.5282

Zhen, S., Zhao, Q., Liu, S., Wu, Z., Lin, S., Li, J., & Hu, X. (2023) Detecting spatiotemporal dynamics and driving patterns in forest fragmentation with a Forest Fragmentation Comprehensive Index (FFCI). Forests, 14(6), 1135. https://doi.org/10.3390/f14061135

Zhu, Z., & Woodcock, C. E. (2014). Continuous change detection and classification of land cover using all available Landsat data. *Remote sensing of Environment*, *138*, 152-171. https://doi.org/10.1016/j.rse.2014.01.011

Statements and Declarations

Funding

The authors declare that no funds, grants, or other support were received during the preparation of this manuscript.

Competing Interests

The authors have no relevant financial or non-financial interests to disclose.

Author Contributions

All authors contributed specific sections to the manuscript and assisted with critical revisions.

Sanjana Dutt led the conceptualization, systematic review, and overall coordination of the manuscript, including preparation of the first and revised drafts.

Tarmo Remmel, Carlos Rivas, Adriano Mazziotta and Mieczysław Kunz contributed to review refinement and provided input on structure, interpretation, and revisions.

All authors read and approved the final version of the manuscript.

Use of Generative AI

During the preparation of this work, Sanjana Dutt used OpenAI's ChatGPT and xAI's Grok to assist with language editing and structural refinement of the manuscript. Napkin AI was used to assist with preliminary visualization design for one figure. All AI-generated content was reviewed, edited, and finalized by the author, who takes full responsibility for the integrity and accuracy of the presented work.

Data Availability

No new data were generated or analyzed in this study. All information is based on published literature cited within the manuscript.

Advancing Forest Fragmentation Analysis: A Systematic Review of Evolving Spatial Metrics, Software Platforms, and Remote Sensing Innovations

Sanjana Dutt[1]*, Tarmo K. Remmel[2], Carlos A. Rivas[3], Adriano Mazziotta[4], Mieczysław Kunz[1]

[1] Faculty of Earth and Environmental Sciences, Nicolaus Copernicus University, Toruń, Poland
[2] Faculty of Environmental & Urban Change, York University, Toronto, Ontario, Canada
[3] Mediterranean Forest Global Change Observatory (GLOBAM), DigiFoR+—ERSAF, Department of Forestry Engineering, University of Córdoba, Campus de Rabanales, Crta. IV Km 396, 14071 Córdoba, Spain
[4] Natural Resources Institute Finland (Luke), Latokartanonkaari 9, FI-00790 Helsinki, Finland

Corresponding author:* sanjana.dutt@doktorant.umk.pl

Corresponding author: sanjana.dutt@doktorant.umk.pl

Supplementary Table S1.
Search queries used for the systematic review across Google Scholar, Scopus, and Web of Science.

Source	Query ID	Mandatory Terms	Alternative Terms (OR)	Excluded Terms
Google Scholar	1	"forest fragmentation"	"new tools", "new methods", "emerging tools", "software for spatial analysis"	–
			"GIS", "remote sensing"	
	2		"FRAGSTATS", "GuidosToolbox", "MSPA", "Patch Analyst", "PolyFrag", "VecLI", "ZonalMetrics", "Landscape Fragmentation Tool", "V-LATE", "morphological image processing"	–
	3		"spatial analysis", "spatial pattern detection", "landscape structure analysis", "landscape metrics", "patch analysis", "morphological analysis", "fragmentation indices"	–

Scopus & Web of Science	1	“forest loss” or “forest fragmentation”	“new tools”, “new methods”, “emerging tools”, “software for spatial analysis”	–
	2		“FRAGSTATS”, “GuidosToolbox”, “MSPA”, “Patch Analyst”, “PolyFrag”, “VecLI”, “ZonalMetrics”, “Landscape Fragmentation Tool”, “V-LATE”, “morphological image processing”	“urban”, “animal”, “bird”, “wetland”, “land use”
	3		“spatial analysis”, “spatial pattern detection”, “landscape structure analysis”, “landscape metrics”, “patch analysis”, “morphological analysis”, “fragmentation indices”	“urban”, “insect”, “bird”, “climate”, “disease”, “soil”, “ecosystem services”, “peatland”, “land use”

Supplementary Table S2. Evolution of software/toolsets for forest fragmentation analysis (by period)

Period	Toolset	Platform Notes	Features	References
Pre-2000	pMAP GIS; **FRAGSTATS**; Patch Analyst & Habitat Analyst	Custom GIS; Arc/Info AML, C; ArcView plug-ins	Patch/class/landscape metrics (area, edge, shape, core); GISfrag proximity; habitat valuation; contagion & nearest-neighbor	Ripple et al. (1991); McGarigal & Marks (1995); Elkie et al. (1999)
2000–2009	**Khoros® Image Processing**	Image-processing environment	Simulated landscapes; metric correlation; ecological response tests	Hargis et al. (1999)
	ArcIMS + FRAGSTATS	Web-GIS; desktop program	Web mapping; LISA integration; patch/class/landscape indices	Wang (2002); Southworth et al. (2004)
	ERDAS IMAGINE, IDRISI, eCognition	RS & GIS; OBIA	Classification/segmentation; early LiDAR-derived canopy metrics; early CA–Markov	Maier et al. (2006); Meddens et al. (2008)
	GUIDOS Toolbox / APACK	Program; command-line	MSPA (core, edge, islet, loop, bridge, perforation); moving-window metrics (FAD, entropy); continental assessments	Vogt et al. (2007); Wulder et al. (2008); Ostapowicz et al. (2008)

Period	Toolset	Platform Notes	Features	References
	RULE (neutral map generator)	Stand-alone	MSPA for phase transitions; (multi)fractal segmentation	Riitters et al. (2009)
	Circuitscape / Linkage Mapper	Python; ArcGIS/QGIS tools	Circuit-theory connectivity; current flow; corridor/linkage mapping	McRae et al. (2008)
	Conefor	GUI/CLI	Graph connectivity (PC, IIC, dI); node/edge prioritization; pairs with MSPA	Saura & Torné (2009)
2010–2019	**Landscape Fragmentation Tool (LFT)**	ArcGIS extension	Core/edge/perforated/patch classes; morphological segmentation of intensity	Kopecká & Nováček (2010); Singh et al. (2017)
	ARC/INFO GRID; FRAGSTATS v3.3; PolyFrag; ZonalMetrics; G-RaFFe	GIS modules; ArcMap toolbox (Python)	Cross-tab & temporal analyses; vector-based metrics; customizable edge width; process-based pattern simulators	Tang et al. (2012); MacLean & Congalton (2013); Pe'er et al. (2013); Adamczyk & Tiede (2017)
	Definiens Developer	Image analysis software	OBIA classification; advanced rulesets	Newman et al. (2011)
	LecoS; ShrinkShape2; landscapemetrics; motif; PyLandStats	QGIS plug-in; R/SAGA; Python	Automated landscape metrics; rotation-invariant polygon shape spectra; tidy/testable pipelines; pattern-based analysis	Jung (2016); Remmel (2015); Hesselbarth et al. (2019); Lovelace et al. (2019); Bosch (2019)
	Landscape Generator (LG); DYPAL	Java; Python	Neutral/optimized landscape generation; parameterizable dilation/erosion	van Strien et al. (2016); Bonhomme et al. (2017)
	SPIP (surface metrics)	Stand-alone	Gradient-surface metrics (roughness, fractal dimension)	Kedron et al. (2018)
	Land-metrics DIY (library)	.NET/C# API (OpenGIS SFA)	~40 vector/raster metrics; extensible, platform-independent programming library	Zaragozí et al. (2012)
	Gradient-surface threshold scalograms (FRAGSTATS + GSM)	FRAGSTATS v4.x + GSM workflow	Thresholded continuous canopy; scalograms of MPS/PD/LPI/ED across density bands	Frazier & Kedron (2017)

Period	Toolset	Platform Notes	Features	References
	r.pi (GRASS GIS)	GRASS add-on	Semi-automatic pattern analysis (core area, PD, connectivity)	Wegmann et al. (2018)
	VCT; LandTrendr; CCDC (change feeders)	Algorithms; GEE/desktop ports	Time-series segmentation (loss/recovery) and continuous change models	Huang et al. (2010); Kennedy et al. (2018); Zhu & Woodcock (2014)
	Google Earth Engine (platform)	Cloud platform	Planetary-scale compositing, time series, and reproducible workflows	Gorelick et al. (2017)
2020–2025	**Patternbits (ShapePattern); geodiv; Intra**	R packages	Configuration elements & KL divergence; 3-D-ready morphological segmentation; gradient surface metrics; complexity-weighted patch area (intra-patch connectivity)	Remmel (2020, 2022); Smith et al. (2021); Justeau-Allaire et al. (2024)
	VecLI; VARLI; LDTtool; LDT4QGIS	Python; QGIS/ArcGIS	Vector indices (area–edge, shape, aggregation); composition/configuration change typologies; perimeter–area corrections	Yao et al. (2022); Machado et al. (2020); Paixão & Machado (2023); Huang et al. (2024)
	flsgen	Java API; R; CLI	Neutral landscape generator with control of 14 indices (incl. MESH, Splitting)	Justeau-Allaire et al. (2022)
	ForestryAnalysisInR; Patch Fragmentation Index (PFI)	R (Shiny)	Forestry/fragmentation workflows; biodiversity & LiDAR structural metrics; simple patch fragmentation index	Atkins et al. (2022); Rivas et al. (2022)
	GUIDOS Toolbox Workbench (GWB)	Program; QGIS plug-in; C/GDAL	MSPA expansions; distance & similarity; Jensen–Shannon multiscale similarity; large-area workbench	Vogt et al. (2022); Netzel et al. (2024); Zhang et al. (2024, 2025)
	FAD–FOS pipelines (fixed-scale density)	GUIDOS + scripts	Forest Area Density classes & summaries (policy-scale, fixed window)	Vogt & Caudullo (2025)
	Fractal/Disorder toolchains (FFI/FFDI/LCFD)	ImageJ2/ComsystanJ; Python/ArcGIS	Compactness & spatial disorder; local connectedness; robust to binary artifacts	Peptenatu et al. (2023); Alage et al. (2025)

Period	Toolset	Platform Notes	Features	References
	ENVI & GeoDa; MapBiomas & IDRISI (FFCI)	RS & spatial analysis	PCA-based composite indices; ANN & CA–Markov forecasting	Lin et al. (2024); Moreira et al. (2024)
	Fiji/ImageJ2 + ComsystanJ (3-D)	Image analysis	Voxel-based 3-D fragmentation; fractal dimension; succolarity	Andronache (2024)
	ESIS/Imalys; AMAPVox (TLS)	Python/C++; TLS processing	Hybrid PMM–GM toolkit; NDVI/NIRv; voxelized TLS for PAI; phenology impacts	Selsam et al. (2024); Nunes et al. (2022)
	LFT (applications)	ArcGIS extension	Recent use-cases of LFT in susceptibility mapping	Batar et al. (2021)
	ProNet scripts; LandTrendr (recent apps)	R/Python; GEE	Protected-area network connectivity metric; provincial LandTrendr deployments	Theobald et al. (2022); Qiu et al. (2025)

W: Młynarczyk A. (red.): Środowisko przyrodnicze jako obszar badań. Vol. IV.
Bogucki Wyd. Nauk., Poznań 2022. ISBN 978-83-7986-411-9.

Sanjana Dutt*, Mieczysław Kunz

Land use/cover changes using Corine Land Cover data following hurricanes in the last 10 years. A case study on Tuchola Forest Biosphere Reserve

Summary: Numerous environmental decisions are predicated on the idea that certain land cover combinations are preferable to others. Given that Corine Land Cover (CLC) database encompasses a detailed three-level hierarchical nomenclature composed of 44 land cover/use classes at its most detailed level, it has been used to analyze temporal changes in the Tuchola Forest Biosphere Reserve as a whole and in three communes that have been severely impacted by hurricanes in the last decade, namely Brusy, Osie, and Czersk. This article compares spatial data from 1990, 2000, 2006, 2012, and 2018 in order to determine the magnitude of land modification caused by hurricanes in 2012, 2017, and 2021. In July 2012, a very strong wind damaged forests covering an area of over 500 ha in the Trzebciny Forest District (Osie Commune). In August 2017, a catastrophic storm swept through Poland, primarily in Pomorze and Kujawy, destroying forest stands across several thousand hectares of Tuchola Forest, most notably in the Rytel, Lipusz, Czersk, Bytów, and Runowo Forest Districts. In July 2021, another hurricane destroyed over 1,000 hectares of forest, primarily in the Osie Forest District. According to the CLC analysis, the entire biosphere reserve lost 140.84 km^2 of forest cover, while the transitional woodland/shrub increased by 726 percent due to forest regeneration. Landscape metrics such as number of patches, mean patch size, edge density, and mean shape index indicate severe fragmentation, whereas Shannon diversity demonstrates an increase in diversity over time. In addition, the Czersk's commune index was chosen to compare the fragmentation percentages with those of the entire TFBR, and the results indicate uniformity.

Keywords: Tuchola Forest, Biosphere Reserve, CLC, land use/cover, spatial indices, landscape structure, hurricane

SD, MK – Department of Geomatics and Cartography, Faculty of Earth Sciences and Spatial Management, Nicolaus Copernicus University in Toruń, Poland
*corresponding author: sanjana.dutt@doktorant.umk.pl

Introduction

News about climate change is no longer as startling as it used to be, neither reading about hurricanes or storms scare us anymore. However, the inevitable consequences that lithosphere faces after any climatic disturbances alters a significant fragment on the landscape, both on a small and a large scale. Studying the relationship between these natural processes on different scales are fundamental to landscape ecology (Chamorro et al. 2015), and integrating it with the temporal aspect to understand the coping mechanism of landscapes is extremely crucial in the current environmental scenario.

Hurricanes leave a permanent impression on forest structure by causing damage to standing inventory, significantly affecting the age class structure and species distribution in an impacted region (Xi et al. 2008). After making landfall, hurricanes can significantly alter the landscape through wind damage, torrential rainfall, and storm surge. Hurricanes (wind speeds over 33 ms^{-1}) are one of the major natural disturbance elements, impacting landscapes by causing property damage, tree mortality, and vegetation degradation (Boose et al. 1994; Juárez et al. 2008). Recent studies indicate that hurricane frequency has increased over the past three decades (Emanuel 2005; Wu, Wang 2008; Walsh et al. 2016; Reed et al. 2022). Recent years (2000–2014) have averaged close to seven hurricanes per year in the North Atlantic which is associated with rising sea surface temperatures (Hurricanes and climate-change 2020).

Although the increase in hurricane intensity has been well recorded, the impact of hurricane forest damage on regional climate has yet to be investigated (Juárez et al. 2008). Research on the coastal ecosystems by Lam et. al. (2011) shows differential rates of land cover changes after repeated hurricane strikes can be used to evaluate the ecosystems' resilience.

In this research, the authors have tried to look into the spatio-temporal changes of the landscape by considering the available Corine Land Cover data of the entire Tuchola Forest in general and thereafter considered three communes, namely Osie, Brusy and Czersk which were reported to have been highly affected after the aforementioned disasters. Spatio-temnporal changes and fragmentation were studied based on these areas. Considering the maximum changes in the Czersk Commune, further analysis of metrics were employed on the entire Tuchola Forest Biosphere Reserve (TFBR) and the Czersk Commune.

Review of approaches regarding land cover changes

"Land use" and "land cover" have different meanings relating to land surface, with the former reflecting human activities and the latter biophysical condition, yet both are dynamic through time (Assaf et al. 2021). Both land use (LU) and land cover (LC) are usually monitored via field surveys, however, only land cover is mostly estimated using remote sensing techniques (United States Department of Agriculture). LULC change assessment is difficult because acquiring ground-based

data at the right time and space resolution is expensive and time-consuming. Remote sensing monitors, quantifies, and models landscape changes and patterns (Joorabian Shooshtari et al. 2020; Gemitzi et al. 2021). Using remote sensing data, several studies have determined local, regional, and global land-cover changes (Wolter 2006; Popovici 2013; Kucsicsa 2019; Karra 2021).

During the past two decades, technological advances in remote sensing have enabled the production of numerous global land cover datasets, facilitating their extensive use in modelling research (Brice Mora et al. 2014). Global economic crisis forces nations to reduce expenditure. However, better environmental data and reporting obligations are growing due to increased awareness. As the value of "free data" spanning large areas grows, it may become necessary to enhance the usage of remote sensing to meet both needs (Manakos et al. 2014).

COoRdination of INformation on the Environment (CORINE) was an EU initiative to standardize land data in the 39 participating countries and produce a European-wide land cover inventory (Land Copernicus; Büttner 2014). CLC maps have a scale of 1:100,000 and classifies land according to a 3-level hierarchical categorization scheme with 44 classes at the third and most specific level (Gemitzi et al. 2021). As CLC is typically updated every six years, it was deemed useful to investigate whether forest fragmentation may be reliably computed using remotely sensed imagery that is available over such temporal intervals. Merely observing the changes in the landscape is not enough, unless we analyze the ecological significance of it, hence selected landscape metrics were applied to the CLC dataset of 5 years.

Since the inception of landscape ecology, the relationship between spatial patterns and ecological processes has been one of its central concerns (Wu, Hobbs 2002). To establish this correlation, the first step is to quantify landscape patterns (Hulshoff 1995), which has received considerable attention from landscape ecologists (Turner 2005).

Review of landscape metrics for forest landscape stability

Metrics are quantitative measurements and features generated from land cover data, such as composition (kinds and area of specific land cover classes) and configuration (spatial organization of land cover classes throughout the landscape, including habitat fragmentation) (Turner 2005).

Landscape ecologists have proposed numerous landscape pattern indicators since the 1970s (Wu 2006), including patch number, patch area, patch form index, fragmentation index, sub-dimension, landscape heterogeneity index, etc. (Turner, Gardner 1991; Kunz 2006). These indicators analyze quantitative data, the composition and spatial distribution of landscape structure, compare the structural characteristics of various landscapes, and reveal the landscape's spatial configuration and changing patterns (Bailey et al. 2007).

Landscape metrics uses categorical data with spatial interruption, while spatial statistics uses quantitative data with spatial continuity (Wu 2000). Landscape

pattern studies usually use categorization maps like vegetation, soil, and land use/land cover (Peng et al. 2010).

Due to the rapid development of GIS and RS technologies, as well as free and upgraded software packages like FRAGSTATS (McGarigal, Marks 1995), APACK and IAN (Mladenoff, DeZonia 2004), and ArcGIS plugins like Patch Analyst (Rempel et al. 2012), landscape ecologists can easily obtain metrics for a particular landscape (Kunz, Nienartowicz 2004; Kunz 2006; Kjelland et al. 2007; Gardner et al. 2008; Messerli et al. 2009; Riitters et al. 2009; Peng et al. 2010; Kelly et al. 2011; Reif, Swannack 2014; Adamczyk, Tiede 2017). Metric selection for a new study must be based on the study's objectives, the system's spatial characteristics, and the ecological processes being studied (Gustafson 1998). In addition, they should be computed on process-appropriate maps (Kunz 2006a; Bailey et al. 2007).

Wang and Xu (2009) used landscape metrics of undisturbed and disturbed forests after Hurricane Katrina such as number of patches (NP), patch density (PD), patch area mean (AREA MN), patch area standard deviation, largest patch index, total core area, total edge (TE), edge density (ED), and landscape shape index (LSI) and found that forest types, forest coverage and stand density, and soils groups contributed to 85% of accuracy in modeling the probability of tree mortality.

Study area and methodology of research

Study area

Tuchola Forest Biosphere Reserve (TFBR), established on 2nd June 2010 under Man and Biosphere Program (MaB), is the tenth and the biggest biosphere reserve in Poland. It is located in the northwest part of the country and it covers an area of 319,525 ha (Fig. 1). Over 60% of the TFBR area is covered by forests. There are 13 Forest Districts managed within that area: Czersk, Dąbrowa, Kaliska, Kościerzyna, Lipusz, Osie, Osusznica, Przymuszewo, Rytel, Tuchola, Trzebciny, Woziwoda and Zamrzenica (Nienartowicz et al. 2010; Nienartowicz, Kunz 2018).

Every year, over a dozen cases of anemological phenomena are recorded over Poland. Most often these are strong blasts of wind. Selective monitoring of these phenomena makes it difficult to conduct multi-faceted research related to this subject. The current warning system against wind phenomena is not fully effective, as the messages concern too large an area of the country – usually selected voivodeships. So far, the detection of tornadoes in Poland is difficult due to their local nature. Although these phenomena appear rarely, unfortunately, they can be devastating (Poplawska 2014; Taszarek, Gromadzki 2017). The occurrence of extreme meteorologic events is influenced by many factors such as location of the baric systems, direction of inflow and type of air mass or even direction and velocity of the jet stream wind (Sulik 2021).

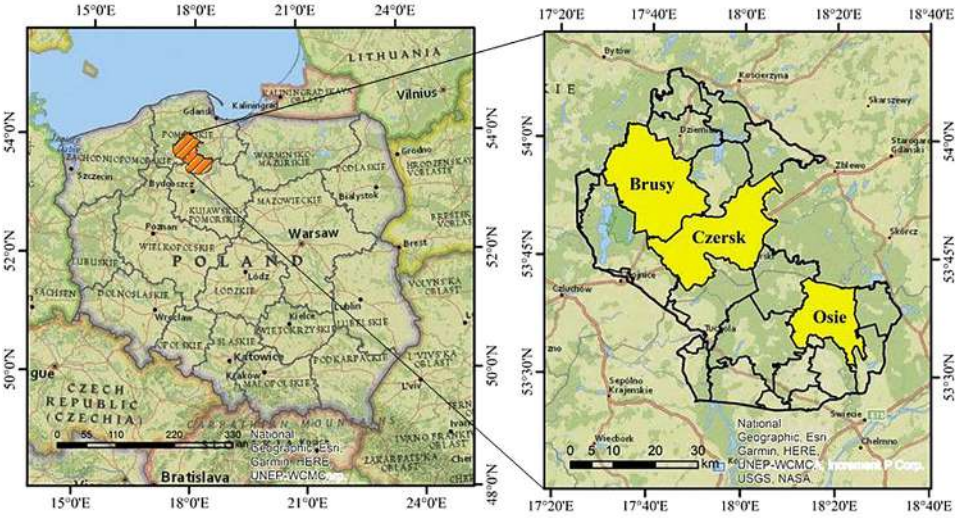

Fig. 1. Location of Tuchola Forest Biosphere Reserve and the three Communes – Brusy, Czersk and Osie

The north western province of Poland is most susceptible to windstorms that created havoc in the last two decades. On 14 July 2012, an isolated cyclic supercell thunderstorm occurred in north central Poland and produced a few tornadoes near the Tuchola Forest which destructed around 500 ha of forests (Taszarek et al. 2016). A derecho event that occurred in Poland on 11 August 2017, destroyed and partially damaged 79,700 ha of forest. Wind gusts of extreme intensity destroyed a significant part of the Tuchola Forest, including around 8,000 ha of forest in the Rytel Forest District and 6,000 ha of forest in the Lipusz Forest District. According to the accounts of some witnesses, the entire forest sections in the area of Tuchola, Chojnice, Bytów, Koscierzyna, and Lębork were swept away within a few minutes (Figurski et. al. 2017; Taszarek et. al. 2019). The meteorological station in Elblag recorded a peak wind gust of 42 ms^{-1}, while the station in Lębork had 31 ms^{-1}). At the end of July 2021, another hurricane destroyed over 1,000 hectares of forest, primarily in the Osie Forest District (Osie Commune). The greatest damage was inventoried in the vicinity of the villages of Tleń and Osie.

Thus the authors have selected the entire TFBR to analyse the overall effect of spatio temporal changes and validate the same in the most effected communes, considering that not all communes can have an equal impact of a disaster. The methodology has been depicted in Fig. 2 and elaborated in the following paragraphs.

Corine Land Cover database

Corine Land Cover (CLC) was specified to standardize land data collection in Europe to support the development of environmental policy. Images captured by

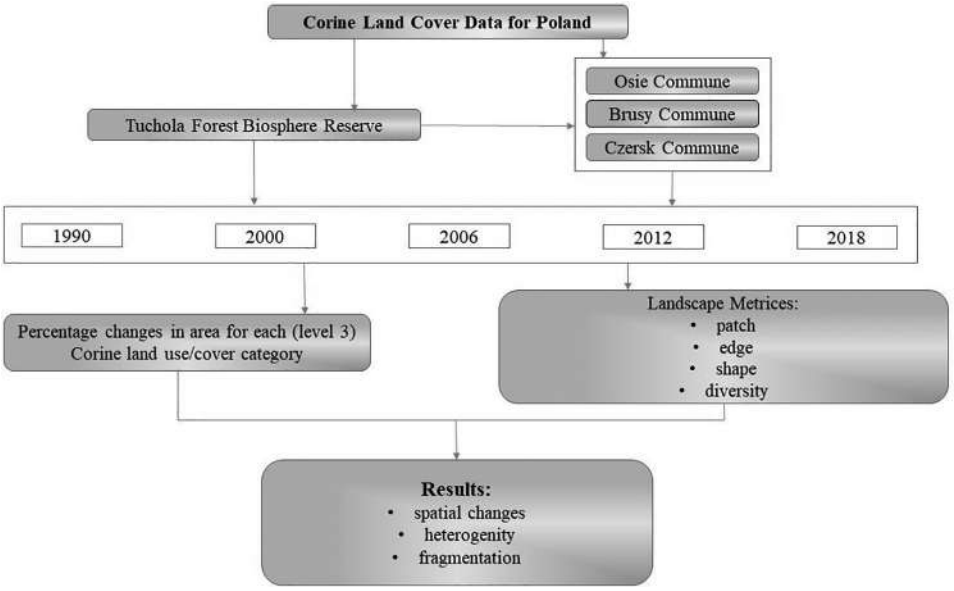

Fig. 2. Methodological scheme of the research process

Earth Observation (EO) satellites serve as the primary data source for determining land cover and land use (EEA Task Force 1992). The standard Corine Land Cover vector data for years 1990, 2000, 2006, 2012 and 2018 were downloaded freely from http://clc.gios.gov.pl/index.php/9-gorne-menu/clc-informacje-ogolne/59-produkty-2. Datasets were clipped to the extent of the Tuchola Forest Biosphere Reserve boundary given by the official website in 2010 in ArcGIS 10.7.1 and mapped to visually interpret the changes throughout the years (see Fig. 3) and 15 categories from third level were identified (see Table 1).

For temporal land cover change evaluation, the frequency of pixels in each category for each year was determined and merged within the attribute table of ArcGIS 10.7.1 to calculate the total area for each level three category and finally producing a land use/cover map for the entire biosphere reserve (see Fig. 3). This datasheet was then exported to excel for calculating the percentage change and plotting bar diagrams of area in square kilometre (Fig. 4). The purpose of the bar diagrams was to evaluate the extent of changes throughout the period and to determine which year and which particular commune records the most significant transition types. To calculate the percentage change in Microsoft Excel 2016, 1990 Corine Land Cover database was used as the base year, and 2000 was used for the later and then divided by the base year (1990) to be multiplied by 100. This was repeated for all the years in each category but only the Czersk Commune has been selected for representation because of its highest amount of change (see Figs. 5 and 6). Codes described in level 3 of CLC legend (refer to Table 1) are used for plotting the bar diagrams and line charts in Figures 4, 5 and 6.

Table 1. Corine Land Cover categories present in Tuchola Forest Biosphere Reserve

Level 1	Level 2	Level 3
1. Artificial surfaces	1.1. Urban fabric	1.1.2. Discontinuous urban fabric
	1.2. Industrial, commercial and transport units	1.2.1. Industrial or commercial units
		1.2.2. Road and rail networks and associated land
	1.4. Artificial non-agricultural vegetated areas	1.4.2. Sport and leisure facilities
2. Agricultural areas	2.1. Arable land	2.1.1. Non-irrigated arable land
	2.3. Pastures	2.3.1. Pastures
	2.4. Heterogeneous agricultural areas	2.4.2. Complex cultivation patterns
		2.4.3. Land principally occupied by agriculture with significant areas of natural vegetation
3. Forest and semi natural areas	3.1. Forests	3.1.1. Broad-leaved forest
		3.1.2. Coniferous forest
		3.1.3. Mixed forest
	3.2. Scrub and/or herbaceous vegetation associations	3.2.4. Transitional woodland-shrub
4. Wetlands	4.1. Inland wetlands	4.1.1. Inland marshes
		4.1.2. Peat bogs
5. Water bodies	5.1. Inland waters	5.1.2. Water bodies

Landscape metrices to study forest landscape fragmentation

Using the two land cover categorization datasets and the landscape pattern analysis extension Patch Analyst 3.1 for Esri Software, class-level and landscape-level measures were calculated (Rempel et al. 2012). To assess landscape pattern, the extension generated hundreds of patch-, class-, and landscape-level measurements. Typically, a subset of metrics is chosen based on the analysis's objectives. For this study, a number of previous studies (Kunz 2006; Kjelland et al. 2007; Gardner et al. 2008; Wang, Xu 2009; Kelly et al. 2011; Reif, Swannack 2014) have been thoroughly reviewed and evaluated to select the metrics according to their usability and importance in understanding ecological processes. The metrics considered for this investigation are summarized in Table 2. The vector data derived from the CLC land use/cover third level classes were analysed to obtain these metrics.

Table 2. Summary of landscape metrics used in the study

Name	Matric	Desription	Unit
Patches	Number of patches	NP>1, without limit, NP = 1 when a landscpae or class type contains one patch; number of patches corresponding to class type at a landscape	–
	Mean patch size	the average area of patches corresponding to the forest cover type; greater MPS indicate slightly fragmented forests	ha
Edge	Edge density	edge density (ED) standardizes edge to a per unit area basis that facilitates comparisons among landscape of varying size	m/ha
Shape	Mean shape index	shape complexity	
Diversity	Shannon's diversity index	measure of relative patch diversity	–

Results

Spatial patterns of land cover change

The impact of severe storms on forests is evaluated on a regional scale through a temporal series of maps from 1990 to 2018. After making landfall, hurricanes

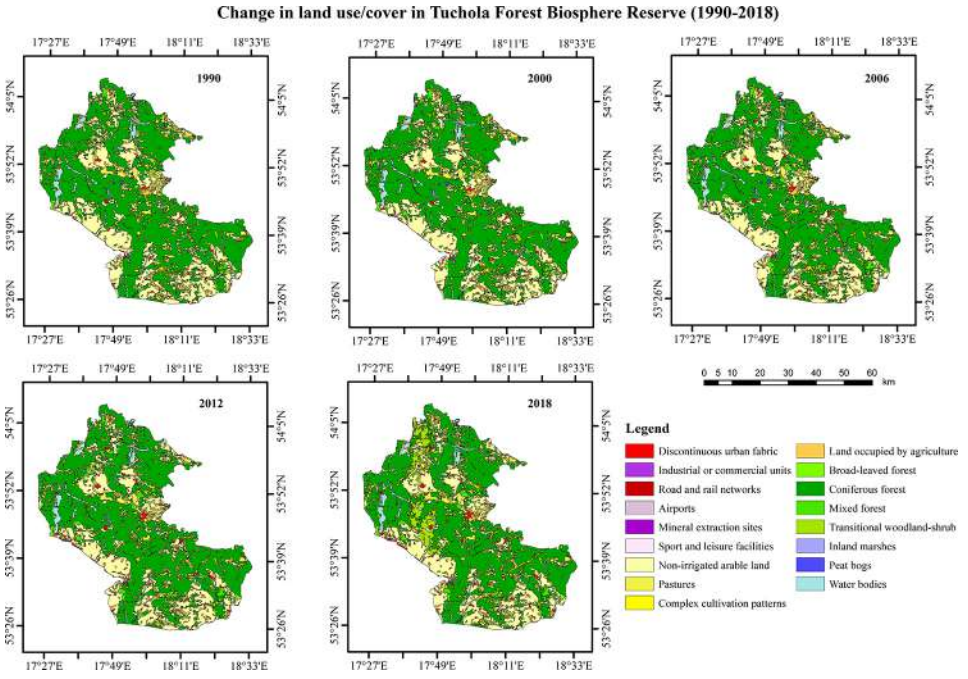

Fig. 3. Changes in land use/cover in Tuchola Forest Biosphere Reserve between 1990–2018

can significantly alter the landscape through wind damage, precipitation, and storm surge. Following the three recorded windstorms, significant changes within each CLC category has been shown spatially for the entire Tuchola Forest Biosphere Reserve (Fig. 3).

To validate the land use/cover changes within each commune particularly, the three selected communes (see Fig. 4) and the entire TFBR were compared using

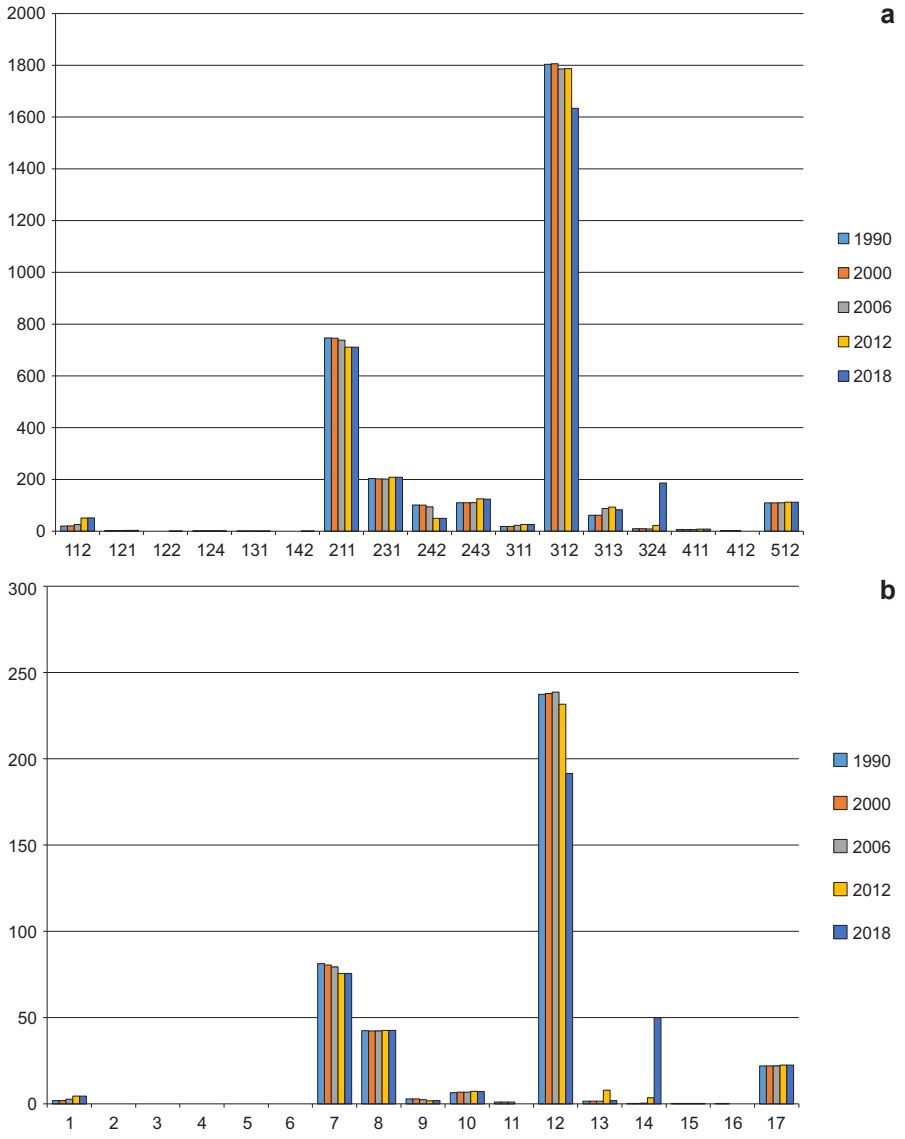

Fig. 4. Change in area for each category from 1990 to 2018 in: (a) Tuchola Forest Biosphere Reserve, (b) Brusy Commune

bar diagrams. The LULC produced by the CLC data from 1990–2018 shows similarity of categorical changes within each commune as well as the entire TFBR. The interpretation of landscape statistics (Fig. 4) and the resulting landscape map (Fig. 3), along with prior information of the research area, allowed for a detailed description of the landscape typologies that comprise the land use/cover. The pillar landscapes include non-irrigated arable land (code 211), pastures (code 231),

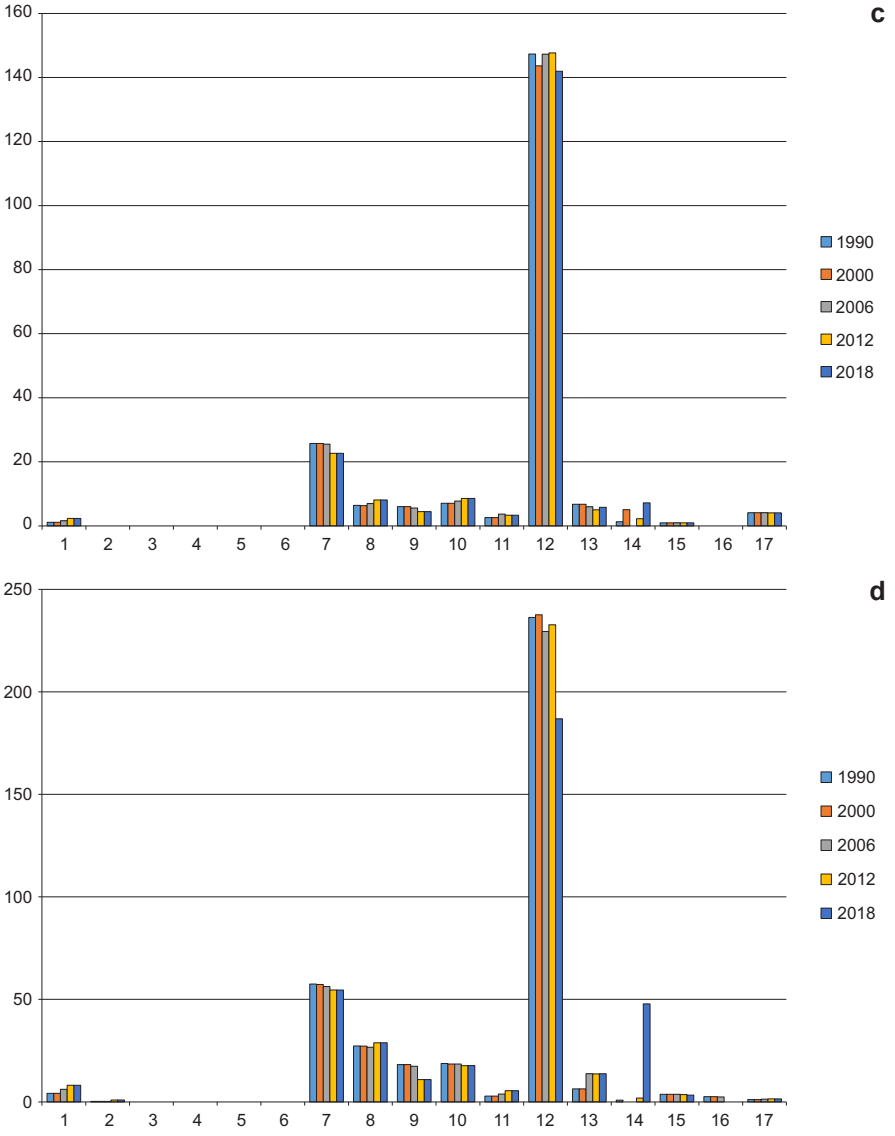

Fig. 4. Change in area for each category from 1990 to 2018 in: (c) Osie Commune, (d) Czersk Commune

land principally occupied by agriculture (code 243), coniferous forest (code 312), mixed forest (code 313), water bodies (code 512). The entire biosphere reserve hosts a diverse and complex set of CLC categories than individual communes. The adjacency bar graph illustrates the spatial links between the landscape types of the individual communes (b, c, and d) and the entire forest region (a), nevertheless the individual communes has a lower number of land use/cover classes compared to the entire landscape which comprises of 17 categories. Brusy and Osie has 12 categories each while Czersk has 13 categories.

To analyse the percentage change among each categories, two line diagrams are represented (Fig. 5 and 6). From Figure 4 it had been deduced that among the three communes, Czersk showed the highest amount of changes in land cover (Fig. 6), where coniferous forest (code 312) records 20.90% decrease while broadleaved forest and mixed forest increased gradually. Non-irrigated arable land (211) and complex cultivation patterns (code 242) shows approximately 5% and 41.74% decrease respectively. Transitional woodland/shrub (code 324) records 5,468.53% increase from 1990–2018. Inland marshes and waterbodies remain more or less unaffected.

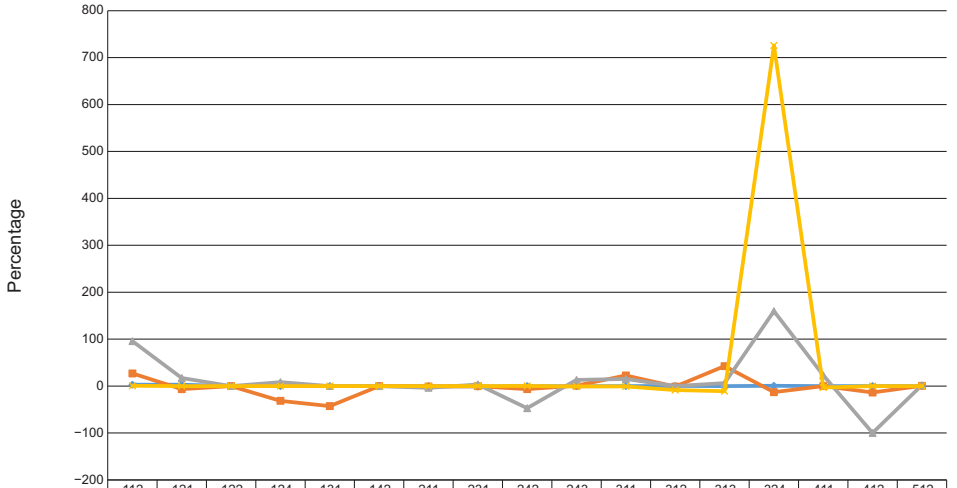

	112	121	122	124	131	142	211	231	242	243	311	312	313	324	411	412	512
1990–2000	2.84	2.95	0	0	0	0	−0.13	−0.81	−0.07	−0.38	0	0.13	0	0.53	0	0	0
2000–2006	26.88	−6.62	0	−31.44	−42.65	0	−1.01	−0.26	−6.48	0.86	22.61	−1.11	42.44	−13.01	0	−13.75	0.47
2006–2012	95.75	17.16	0	8.33	0	0	−3.70	3.47	−47.21	12.99	15.05	0.04	6.22	159.52	23	−100	1.82
2012–2018	0.74	0	0	0	0	0	0.03	0	0.42	−0.77	−0.59	−8.56	−10.93	725.86	3.06	0	0

Fig. 5. Trend showing percentage change in land use/cover in Tuchola Forest Biosphere Reserve (1990–2018)

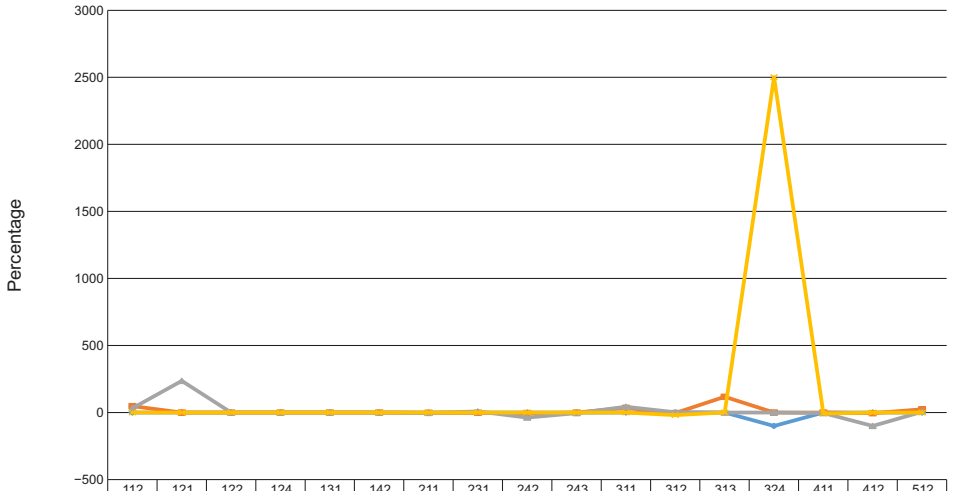

	112	121	122	124	131	142	211	231	242	243	311	312	313	324	411	412	512
1990–2000	0	0	0	0	0	0	−0.29	−0.25	0	−1.22	0	0.56	0	−100	0	0	0
2000–2006	47.48	0	0	0	0	0	−1.81	−1.97	−4.33	0.08	35.3	−3.43	117.37	0	0	−5.05	23.45
2006–2012	32.03	235.94	0	0	0	0	−2.99	8.09	−37.32	−4.38	43.1	1.42	−0.38	0	−4.1	−100	5.26
2012–2018	0	0	0	0	0	0	0	0	0	0.36	0	−19.69	0.55	2501.36	−7.13	0	0

Fig. 6. Trend showing percentage change in land use/cover in Czersk Commune (1990–2018)

Spatial analysis of forest structure

For quantifying the land cover changes in the Tuchola Forest Biosphere Reserve after the three aforementioned hurricanes, the authors decided to use: number of patches, mean patch size, total edge, edge density, mean shape index, area weighted mean patch fractal dimension and Shannon's diversity index.

Table 3. Landscape pattern indices for each year in Tuchola Forest Biosphere Reserve

Years	Number of patches	Mean patch size	Edge density	Mean shape index	Shannon's diversity index
1990	1,194	2,679,550.81	0.00351	1.981	1.879
2000	1,195	2,677,308.51	0.00348	1.978	1.878
2006	1,236	2,588,497.14	0.00352	1.964	1.902
2012	1,343	2,382,265.43	0.00357	1.912	1.952
2018	1,405	2,277,141.55	0.00376	1.929	2.019

Landscape metrics provided valuable data regarding forest changes, particularly fragmentation, connectivity, and heterogeneity measured at the landscape or class level. The total number of patches at the landscape scale increased from 1,194 to 1,405 between 1990 and 2018, while the mean patch size (MPS)

decreased by 15.02 percent. The MPS analysis indicates that the forest landscape in 2018 was highly fragmented.

Even though they are not spatially explicit, edge metrics are typically viewed as the best representation of landscape configuration. It is observed that, as the number of patches increases, so does the edge density, which once again confirms high fragmentation. Mean Shape Index values are typically greater than or equal to 1. When nearly all patch shapes are square-like, shape mn's value is 1, and as patch shapes become more irregular, shape mean's value increases proportionally. In this case, the mean shape index is relatively uniform, with a slight decrease.

Shannon's diversity index (SDI) initially (years 1990–2000) exhibited no significant change; however, from 2006 to 2018, SDI increased gradually, indicating an increase in diversity or heterogeneity.

Table 4. Landscape pattern indices for each year in Czersk Commune

Years	Number of patches	Mean patch size	Edge density	Mean shape index	Shannon's diversity index
1990	204	1,860,812.27	0.0037	1.989	1.875
2000	200	1,898,028.52	0.0036	1.988	1.853
2006	204	1,860,812.27	0.0037	1.949	1.907
2012	218	1,741,310.57	0.0037	1.928	1.933
2018	241	1,575,127.41	0.0041	1.937	2.034

Discussion

The Landscape Change Index (LCI) was defined by Woodward et al. (2001) as the total change in vegetation and land use at the landscape level by integrating the absolute average changes of all land-cover types into one value. In this way, LCI is characterized by a single value that represents the consequence of all types of changes occurring in the landscape's background over a specific time period. According to the applicability of Landscape Change Index, the authors identified that the highest amount of changes were analysed post 2006, owing to the disasters that occurred after 2012. There is an evident decrease in non-irrigated arable land (code 211) and broad-leaved forest (code 312) throughout the time period (see Figs. 4 and 5). Another striking change is noticed with transitional woodland/shrub (code 324) which increased about 725% and can be a result of woodland degradation after 2012 and 2017 windstorms, forest regeneration/recolonization, or natural succession. Peat bogs (code 412) which used to have a considerable amount of decomposed vegetation matter till 2006, suddenly disappeared in 2012, which could also be a direct influence of disasters. Coniferous forest (code 312) consisting of pine trees, the most dominating vegetation in the biosphere reserve registers a gradual fall throughout the years since 1990 with –8% in 2018. This can also be seen in terms of Shannon's diversity index where after the disastrous events of 2012 and 2017, the diverse number of categories increased to 6.15% after 2006, owing to the high number of transitional

woodland, discontinuous urban fabric, and water bodies which could be a direct consequence of storm events and heavy precipitation. Another notable change detected is the 157.29% increase in the Discontinuous urban fabric (code 112). Project Copernicus distinguishes between continuous and discontinuous urban fabric based on a distance of less than 300 m between the houses and associated with green spaces and bare surfaces among them.

In terms of forest sustainability and management policies, quantitative assessments of forest fragmentation and heterogeneity using spatial and temporal patterns constitute a valuable tool. The authors anticipate the release of the next series of Corine Land Cover data base in 2024, which will allow for better comparison. In addition, satellite imagery with a higher spatial resolution, such as Sentinel, or active sensors such as LiDAR, provides the opportunity to work in much greater detail.

This research also made us question whether administrative boundaries, such as communes, should be taken into account when conducting comparative research, given that nature knows no bounds.

Conclusion

In this study, multi-temporal data base from the Corine Land Cover datasets were used to identify the spatio-temporal patterns of land use and land cover changes after three catastrophic hurricanes. This study provided deforestation/degradation and regeneration statistics for the Tuchola Forest Biosphere Reserve over a 28-year period, with a focus on the communes in the path of windstorms (1990–2018). According to the results, 140.84 km^2 of forest cover was lost within the biosphere reserve.

Landscape indices for the entire Tuchola Forest and the Czersk Commune confirm fragmentation and heterogeneity as a result of an increase in patch size and edge density. The impact of the hurricane of 2021 on the landscape structure in the vicinity of Osie and Tleń can be determined using the updated CLC spatial database in 2024.

The diversity in both of these study regions has also increased significantly. This study has only examined the spatial and temporal changes in forest cover, without delving deeply into the underlying causes of hurricane-induced forest degradation. However, as discussed, previous research confirms a direct proportional relationship between forest land fragmentation and wind gusts. Therefore, this demonstrates the need for conservation efforts to focus on better forest management.

Overall, the change detection statistics and metrics exemplify how quantitative measures can be applied to land cover data to analyze broad land cover characteristics as well as the underlying structure, aggregation, and shape properties. This huge array of change measures was evaluated in the research area spanning the northern portion of Poland, and displays change mostly linked with the storms of 2012, 2017, and 2021 reviewed in the 2012 and 2018 imageries.

References

Adamczyk J., Tiede D., 2017. Zonalmetrics – A python toolbox for zonal landscape structure analysis. Computers & Geosciences, 99: 91–99 (https://doi.org/10.1016/j.cageo.2016.11.005).

Assaf C., Adams C., Ferreira F.F., França H., 2021. Land use and cover modeling as a tool for analyzing nature conservation policies – a case study of Juréia-Itatins. Land Use Policy, 100: 104895 (https://doi.org/10.1016/j.landusepol.2020.104895).

Bailey D., Herzog F., Augenstein I., Aviron S., Billeter R., Szerencsits E., Baudry J., 2007. Thematic Resolution Matters: Indicators of landscape pattern for European agro-ecosystems. Ecological Indicators, 7(3): 692–709 (https://doi.org/10.1016/j.ecolind.2006.08.001).

Boose E.R., Foster D.R., Fluet M., 1994. Hurricane impacts to tropical and temperate forest landscapes. Ecological Monographs, 64(4): 369–400 (https://doi.org/10.2307/2937142).

Brice Mora B., Tsendbazar N.E., Herold M., Arino O., 2014. Chapter 2: Global Land Cover Mapping: Current Status and Future Trends. In: M. Braun, I. Manakos (eds.), Land use and land cover mapping in Europe: Practices & Trends, Essay. Springer Netherlands, p. 22–38.

Buttner G., 2014. CORINE Land Cover and Land Cover Change Products. In: I. Mahakos, M. Braunhofer (eds.), Land use and land cover mapping in Europe: Practices & Trends, Essay. Springer Netherlands, p. 64–83.

Chamorro A., Giardino J.R., Granados-Aguilar R., Price A.E., 2015. A terrestrial landscape ecology approach to the Critical Zone. Developments in Earth Surface Processes, p. 203–238 (https://doi.org/10.1016/b978-0-444-63369-9.00007-0).

EEA Task Force, 1992. CORINE Land Cover. A European community project.

Emanuel K., 2005. Increasing destructiveness of tropical cyclones over the past 30 years. Nature, 436(7051): 686–688 (https://doi.org/10.1038/nature03906).

Figurski M., Nykiel G., Jaczewski A., Bałdysz Z., Wdowikowski M., 2017. The impact of initial and boundary conditions on severe weather event simulations using a high-resolution WRF model. Case study of the derecho event in Poland on 11 August 2017. Meteorology Hydrology and Water Management.

Gardner R.H., Lookingbill T.R., Townsend P.A., Ferrari J., 2008. A new approach for rescaling land cover data. Landscape Ecology, 23(5): 513–526.

Gustafson E.J., 1998. Minireview: Quantifying Landscape Spatial Pattern: What is the state of the art? Ecosystems, 1(2): 143–156 (https://doi.org/10.1007/s100219900011).

Hulshoff R.M., 1995. Landscape indices describing a Dutch landscape. Landscape Ecology, 10(2): 101–111 (https://doi.org/10.1007/bf00153827).

Hurricanes and climate change. Center for Climate and Energy Solutions, 2020 (https://www.c2es.org/content/hurricanes-and-climate-change/).

Joorabian Shooshtari S., Silva T., Raheli Namin B., Shayesteh K., 2019. Land use and cover change assessment and dynamic spatial modeling in the Ghara-su basin, northeastern Iran. Journal of the Indian Society of Remote Sensing, 48 (1): 81–95 (https://doi.org/10.1007/s12524-019-01054-x).

Juárez R.I., Chambers J.Q., Zeng H., Baker D.B., 2008. Hurricane driven changes in land cover create biogeophysical climate feedbacks. Geophysical Research Letters, 35(23) (https://doi.org/10.1029/2008gl035683).

Karra K., Kontgis C., Statman-Weil Z., Mazzariello J.C., Mathis M., Brumby S.P., 2021. Global land use/land cover with Sentinel 2 and deep learning. 2021 IEEE International Geoscience and Remote Sensing Symposium IGARSS, p. 4704–470.

Kelly M., Tuxen K.A., Stralberg D., 2011. Mapping changes to vegetation pattern in a restoring wetland: Finding pattern metrics that are consistent across spatial scale and time. Ecological Indicators, 11(2): 263–273.

Kjelland M.E., Kreuter U.P., Clendenin G.A., Wilkins R.N., Wu X.B., Afanador E.G., Grant W.E., 2007. Factors related to spatial patterns of rural land fragmentation in Texas. Environmental Management, 40 (2): 231–244.

Kucsicsa G., Popovici E.A., Bălteanu D., Grigorescu I., Dumitrașcu M., Mitrică B., 2019. Future land use/cover changes in Romania: regional simulations based on CLUE-S model and CORINE land cover database. Landscape and Ecological Engineering, 15(1): 75–90.

Kuntz S., Schmeer E., Jochum M., Smith G., 2014. Towards an European Land Cover Monitoring Service and High-Resolution Layers. In: I. Manakos, M. Braun (eds.), Land use and land cover mapping in Europe Practices & Trends, Essay. Springer, Netherlands, p. 53–62.

Kunz M., 2006. Standaryzacja danych kartograficznych i teledetekcyjnych do analizy zmian struktury krajobrazu. Roczniki Geomatyki, 4(3): 119–127.

Kunz M., 2006. Zmienność wzorca przestrzennego krajobrazu w świetle interpretacji dostępnych materiałów kartograficznych i teledetekcyjnych. Archiwum Fotogrametrii, Kartografii i Teledetekcji, 16: 373–384.

Kunz M., 2008. Application of State referential data and Corine Land Cover Database to estimation of landscape structure variety in selected protected areas in Kujawsko-Pomorskie Voivodeship. In: J. Plit, V. Andreychouk (eds.), Methods of landscape research. Dissertations Commission of Cultural Landscape, 8: 207–215.

Kunz M., Nienartowicz A., 2004. Landscape structure characterization with the application of NDVI and fractal dimension of remote sensing imageries in Zabory Landscape Park. In: R. Goossens (ed.), Remote Sensing in Transition. Millpress Science Publishers, Rotterdam, Netherlands, p. 435–441.

Lam N.N., Liu K.B., Liang W., Bianchette T.A., Platt W.J., 2011. Effects of hurricanes on the Gulf Coast Ecosystems: a remote sensing study of land cover change around Weeks Bay, Alabama. Journal of Coastal Research, p. 1707–1711.

Land use and land cover estimates for the United States. USDA ERS – Land Use and Land Cover Estimates for the United States (n.d.) (https://www.ers.usda.gov/about-ers/partnerships/strengthening-statistics-through-the-icars/land-use-and-land-cover-estimates-for-the-united-states/; retrieved: May 21, 2022).

McGarigal K., Marks B.J., 1995. Spatial pattern analysis program for quantifying landscape structure. Gen. Tech. Rep. PNW-GTR-351. US Department of Agriculture, Forest Service, Pacific Northwest Research Station, p. 1–122.

Messerli P., Heinimann A., Epprecht M., 2009. Finding homogeneity in heterogeneity – A new approach to quantifying landscape mosaics developed for the Lao PDR. Human Ecology, 37(3): 291–304.

Mladenoff D.J., DeZonia B.E., 2004. IAN – raster image analysis software programme.

Nienartowicz A., Domin D.J., Kunz M., Przystalski A., 2010. Rezerwat Biosfery Bory Tucholskie. Formularz Nominacyjny/Biosphere Reserve Tuchola Forest. Nomination Form. LGD Sandry Brdy, Chojnice.

Nienartowicz A., Kunz M., 2018. Tuchola Forest Biosphere Reserve 2.0 – the grounds and the scope of the proposed changes/Rezerwat Biosfery Bory Tucholskie 2.0 – uzasadnienie wniosku o powiększenie i zakres proponowanych zmian. LGD Sandry Brdy, Chojnice.

Pan-European. Copernicus Land Monitoring Service at a glance. (2020, December 2) (https://land.copernicus.eu/pan-european; retrieved: May 21, 2022).

Peng J., Wang Y., Zhang Y., Wu J., Li W., Li Y., 2010. Evaluating the effectiveness of landscape metrics in quantifying spatial patterns. Ecological Indicators, 10(2): 217–223 (https://doi.org/10.1016/j.ecolind.2009.04.017).

Popławska J., 2014. Tornada superkomórkowe w Polsce – studium przypadku z 15 sierpnia 2008. Prace i Studia Geograficzne, 56.

Popovici E.A., Bălteanu D., Kucsicsa G., 2013. Assessment of changes in land-use and land-cover pattern in Romania using Corine Land Cover Database. Carpathian Journal of Earth and Environmental Sciences, 8(4): 195–208.

Reed K.A., Wehner M.F., Zarzycki C.M., 2022. Attribution of 2020 hurricane season extreme rainfall to human-induced climate change. Nature Communications, 13 (1) (https://doi.org/10.1038/s41467-022-29379–1).

Reif M.K., Swannack T.M., 2014. Development of landscape metrics to support process-driven ecological modeling. Engineer Research and Development Center, Vicksburg Ms Environmental Lab.

Rempel R.S., Kaukinen D., Carr A.P., 2012. Patch Analyst and Patch Grid. Retrieved from Ontario Ministry of Natural Resources. Centre for Northern Forest Ecosystem Research, Thunder Bay, Ontario.

Riitters K., Vogt P., Soille P., Estreguil C., 2009. Landscape patterns from mathematical morphology on maps with contagion. Landscape Ecology, 24(5): 699–709.

Rodgers J.C., Murrah A.W., Cooke W.H., 2009. The impact of Hurricane Katrina on the coastal vegetation of the Weeks Bay Reserve, Alabama from NDVI Data. Estuaries and Coasts, 32(3): 496–507 (https://doi.org/10.1007/s12237-009-9138-z).

Senf C., Seidl R., 2018. Natural disturbances are spatially diverse but temporally synchronized across temperate forest landscapes in Europe. Global Change Biology, 24(3): 1201–1211.

Sulik S., 2021. Formation factors of the most electrically active thunderstorm days over Poland (2002–2020). Weather and Climate Extremes, 34: 100386.

Taszarek M., Czernecki B., Walczakiewicz S., Mazur A., Kolendowicz L., 2016. An isolated tornadic supercell of 14 July 2012 in Poland – A prediction technique within the use of coarse-grid WRF simulation. Atmospheric Research, 178: 367–379.

Taszarek M., Gromadzki J., 2017. Deadly tornadoes in Poland from 1820 to 2015. Monthly Weather Review 145 (4): 1221–1243.

Taszarek M., Pilguj N., Orlikowski J., Surowiecki A., Walczakiewicz S., Pilorz W., Półrolniczak M., 2019. Derecho evolving from a mesocyclone. A study of 11 August 2017 severe weather outbreak in Poland: Event analysis and high-resolution simulation. Monthly Weather Review, 147(6): 2283–2306.

Turner M.G., 2005. Landscape ecology: what is the state of the science? Annu. Rev. Ecol. Evol. Syst. 36: 319–344.

Turner M.G., Gardner R.H., 1991. Quantitative methods in landscape ecology: An introduction. Ecological Studies, p. 3–14 (https://doi.org/10.1007/978-1-4757-4244-2_1).

Walsh K.J., McBride J.L., Klotzbach P.J., Balachandran S., Camargo S.J., Holland G., Sugi M., 2016. Tropical cyclones and climate change. Wiley Interdisciplinary Reviews: Climate Change, 7(1): 65–89.

Wang F., Xu Y.J., 2008. Hurricane Katrina-induced forest damage in relation to ecological factors at landscape scale. Environmental Monitoring and Assessment, 156(1–4): 491–507 (https://doi.org/10.1007/s10661-008-0500-6).

Wang F., Xu Y.J., 2009. Hurricane Katrina-induced forest damage in relation to ecological factors at landscape scale. Environmental Monitoring and Assessment, 156(1): 491–507.

Woodward A.J., Fuhlendorf S.D., Leslie D.M., Shackford J., 2001. Influence of landscape composition and change on lesser prairie-chicken (*Tympanuchus pallidicinctus*) populations. The American Midland Naturalist, 145(2): 261–274.
Wu J., 2006. Landscape Ecology, cross-disciplinarity, and Sustainability Science. Landscape Ecology, 21(1): 1–4 (https://doi.org/10.1007/s10980-006-7195-2).
Wu J., Hobbs R., 2002. Key issues and research priorities in landscape ecology: an idiosyncratic synthesis. Landscape Ecology, 17(4): 355–365.
Wu J.G., 2000. Landscape ecology: pattern, process, scale and hierarchy. Higher Education Press, Beijing, China.
Wu L., Wang B., 2008. What has changed the proportion of intense hurricanes in the last 30 years? Journal of Climate, 21(6): 1432–1439 (https://doi.org/10.1175/2007jcli1715.1).
Xi W., Peet R.K., Urban D.L., 2008. Changes in forest structure, species diversity and spatial pattern following hurricane disturbance in a Piedmont North Carolina Forest, USA. Journal of Plant Ecology, 1(1): 43–57 (https://doi.org/10.1093/jpe/rtm003).

NICOLAUS COPERNICUS UNIVERSITY IN TORUŃ

Bulletin of Geography. Physical Geography Series, No. 26 (2024): 19–33
http://doi.org/10.12775/bgeo-2024-0002

Landscape metrics of the Brusy Commune before and after wind-storm: an assessment of the extent of changes based on Landsat-8 data

Sanjana Dutt[a*], **Mieczysław Kunz**[b]

Nicolaus Copernicus University in Torun, Faculty of Earth Sciences and Spatial Management, Department of Geomatics and Cartography, Torun, Poland

*Correspondence e-mail: sanjana.dutt@doktorant.umk.pl

[a]https://orcid.org/0000-0002-3845-6922, [b]https://orcid.org/0000-0002-3334-5238

Abstract. Monitoring the change in land cover in disaster-affected areas, such as forests, has become a conventional forest management practice, particularly in protected areas. Most change detection and fragmentation studies rely on single-dated satellite images even while investigating changes over a long temporal span. This study aims to move a step further to compare fragmentation before and after a derecho event that occurred in August 2017 using 23 Landsat-8 images of Brusy Commune within the Tuchola Forest Biosphere Reserve. The supervised classification was carried out in the Google Earth Engine using the machine learning algorithm of random forests within the summer months of 2017 and 2018. The high overall accuracy of 0.92 was obtained for the two images which were then analysed with landscape metrics such as mean patch size, number of patches, total edge and edge density using Patch Analyst. These landscape metrics facilitated the characterisation of landscape fragmentation at both the class and landscape levels. Shannon's Diversity Index was employed to assess heterogeneity across the landscape. The findings indicate significant fragmentation, particularly in the forest and pasture classes, with overall low diversity. This study underscores the potential for future research to employ advanced machine learning techniques and non-parametric classifiers, such as neural networks, to enhance the prediction of fragmentation across various spatial scales.

Key words:
landscape fragmentation,
landscape metrics,
LULC changes,
Landsat-8,
wind-storm,
Google Earth Engine

Introduction

The perception of forest landscapes varies significantly across different scales and is influenced by the observer's experiences and the methodological approach adopted in its study. This variability is particularly evident in remote sensing, where landscapes are interpreted through various resolutions – spatial, radiometric, spectral and temporal. These resolutions frame our understanding of the landscape's structure, dynamics and function. Natural disasters and human impacts have been consistently responsible for modifying the landscape, and it has thus become increasingly crucial to study the various changes occurring within the landscape using various remote-sensing and GIS tools on various scales (Haines-Young and Chopping 1996; Gustafson 1998; Frohn 2018; McGarigal and Cushman 2002; Vogt et al. 2007). When monitoring natural or human-induced events, change detection involves four steps: detecting the change, determining its nature, measuring its area and assessing its spatial pattern (Macleod and Congalton 1998).

Based on many remotely sensed images at various spatial resolutions and assessments of landscape metrics, researchers have been able to quantify the influence of spatial scale on landscape patterns (Kunz and Nienartowicz 2002, 2004, 2007;

Wu and Hobbs 2002; Saura 2004; Zhu et al. 2006; Gan et al. 2009). Indicators or metrics that consider the pattern, area and geometrical aspects of the landscape are used for change detection analysis (Kunz and Nienartowicz 2002). Turner et al. (2001) proposed methods for analysing landscape and forest patterns. In practice, the majority of forest fragmentation indicators are driven by either the ideas of adjacency or connectivity at the pixel level (Musick and Grover 1991). To meet requirements for the comparability of data and indicators across wide geographic regions, the input data for assessments are often derived from remote sensing and consist of land cover maps (Vogt et al. 2007).

Feng and Liu (2015) analysed raster datasets from 30 m to 330 m, at 30-m intervals, finding that landscape metrics' sensitivity to cell size varies, with some metrics significantly affected and others showing minimal sensitivity. This result is consistent with previous literature highlighting the correlation with metrics and scales (Kunz and Nienartowicz 2002; Millington et al. 2003; Uuemaa et al. 2005). Recent methodologies to analyse scale impacts have been utilised in case studies to examine scale constraints in landscape ecology (Alhamad et al. 2011; Forzieri and Catani 2011; Feng et al. 2013; Lü et al. 2013).

Forest disturbance mapping at medium resolution faced constraints until 2008, when Landsat imagery was made freely available. From a scientific perspective, the authors found it essential to not rely solely on single images from satellite sensors. Instead, they utilised a median composite of all cloud-free data for classification on Google Earth Engine (GEE). GEE is a free cloud-computing platform for satellite-data processing (Landsat, Sentinel-2, MODIS) and planetary-scale analysis (Gorelick et al. 2017). Since the first major work on the topic was published in 2013 (Hansen et al. 2013), the amount of research using GEE has risen sharply, with more than 397,000 results in Google Scholar as of April, 2024. The applications range from vegetation monitoring to land cover mapping, disaster management and agricultural applications (Kennedy et al. 2018; Mutanga and Kumar 2019; Amani et al. 2020; Orusa et al. 2023).

This research explores the suitability of Landsat's 30-m resolution for analysing landscape fragmentation, focusing on the Brusy Commune forest in northern Poland, which experienced a derecho stemming from a mesocyclone on August 11, 2017. It critically examines the impact of scale on landscape metrics and their sensitivity when employing GEE for satellite-based forest monitoring.

Materials and methods

Study area

The Brusy Commune, serving as the focal area for this study's detailed land use/land cover (LULC) changes analysis, is situated within the Chojnice Poviat of the Pomeranian Voivodeship, northern Poland (see Fig. 1). Spanning an area of 400.74 km^2, it is predominantly rural, with nearly 99% of its expanse dedicated to rural landscapes and a minor fraction (5.1 km^2) constituting the urban area of the town of Brusy. As of 2017, the commune had a population of ~14,500, resulting in a density of 36 individuals per km^2. The commune is composed of 100 settlement units, encompassing major villages, minor settlements and the urban centre of Brusy (Kunz and Nienartowicz 2023).

Within the Brusy Commune, the Przymuszewo Forest District is the predominant State Forest economic unit, encompassing 80.53% of the area, with the Czersk and Rytel Forest Districts following in contribution. Land cover/usage analysis reveals forests as the largest category, occupying 23,684 hectares or 59.1% of the commune's terrain. Agricultural spaces make up 30.4% of the land, with arable fields accounting for 20.5% of this. Water bodies, including six lakes each over 100 hectares, constitute 6.2% of the area. Built-up and transport infrastructures cover 2.1%, while areas with scattered trees and shrubbery account for roughly 0.2%. The forest landscape is mainly characterised by coniferous ecosystems, predominantly dry and fresh pine stands, with deciduous forests making up about 12% of the forestry. The average age of these forest stands is 62 years (Kunz and Nienartowicz 2023).

The Brusy Commune's forest regions are distinguished by a variety of protected areas, including the Zaborski Landscape Park located in its western sector (see Fig. 1). Within the commune boundaries, there exist eight nature reserves encompassing forest, peat bog and aquatic ecosystems, alongside 42 ecological sites.

Additionally, Brusy is among 22 communes within the Tuchola Forest Biosphere Reserve (TFBR), which was inaugurated on June 2, 2010 as part of the Man and Biosphere Programme (MaB), marking it as Poland's eleventh and largest biosphere reserve. Occupying 319,525 hectares in the country's north-west, the TFBR is predominantly forested, accounting for over 60% of its area. This significant forest cover positions the Tuchola Forest natural district as one of Poland's most extensive forested areas (Nienartowicz et al. 2010; Nienartowicz and Kunz 2018).

The Tuchola Forest Biosphere Reserve is segmented into three distinct zones: core, buffer and transit, as illustrated in Figure 1. The core zone, deemed the most critical, encompasses the "Tuchola Forest" National Park and 25 nature reserves. Following this is the buffer zone, primarily composed of four landscape parks, including the Zaborski Landscape Park, which predominantly falls within the Brusy Commune. The transit zone, the largest, extends over the territories of 22 communes (13 from the Kuyavian-Pomeranian Voivodeship and 9 from the Pomeranian Voivodeship) and the city of Tuchola, covering an area exceeding 206,000 hectares – nearly double the size of the buffer zone. This structure is a unique characteristic of the Tuchola Forest Biosphere Reserve. Nevertheless, in August 2017, the reserve, particularly within the Brusy Commune's administrative boundaries, was struck by a devastating derecho, leading to significant alterations in the landscape's structure (see figure 2)(Taszarek et al. 2019; Kunz et al. 2023).

Derecho event in Tuchola Forest Biosphere Reserve

European Severe Weather Database records 600 severe convective wind gusts annually in Poland (Dotzek et al. 2009). Such occurrences are most prevalent from May through August, with a typical peak in the late afternoon of July (Celiski-Mysaw and

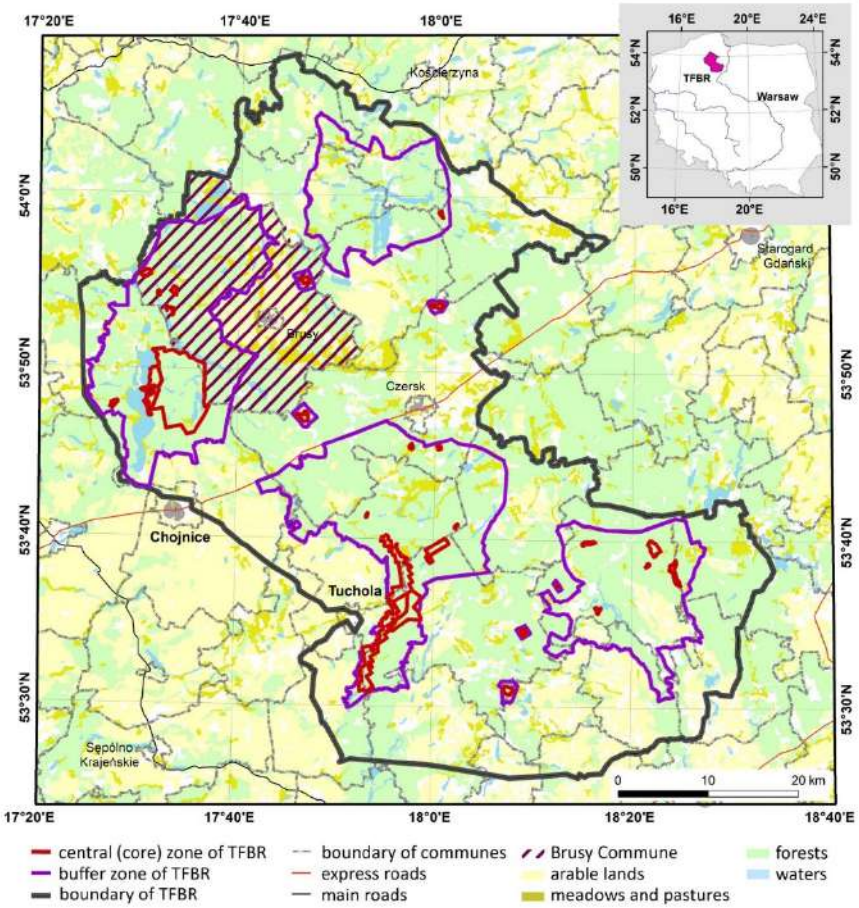

Fig. 1. Location of the Brusy Commune in the Tuchola Forest Biosphere Reserve

Palarz 2017; Taszarek et al. 2019; Sulik and Kejna 2020). These winds, capable of causing significant damage, commonly result from thunderstorm outflows and are frequently linked to supercells and mesoscale convective systems (MCS) (Zipser 1982; Doswell and Burgess 1993; Houze 1993).

Johns and Hirt (1987) were the inaugural scientists to outline the criteria for derechos, a term referring to intense downburst clusters associated with forward-propagating mesoscale convective systems (MCS) characterised by mesoscale vortices and inflow jets. According to Corfidi et al. (2016), for an event to be classified as a derecho, the damage path must maintain a width of at least 100 km and extend over a length of 650 km, predominantly driven by a mature, cold-pool MCS following the initial storm development. Annually, Poland witnesses an average of ten bow echoes and one derecho, indicative of the country's susceptibility to such severe weather phenomena. Notably, the derecho on August 11, 2017 exemplified this destructive capability, generating substantial wind damage with gusts exceeding 42 m/s (Celiski-Mysaw and Matuszko 2014; Celiski-Mysaw and Palarz 2017; Taszarek et al. 2019; Sulik and Kejna 2020).

Materials and methods

The methodological scheme has been illustrated in Figure 3 and described in detail in the following section.

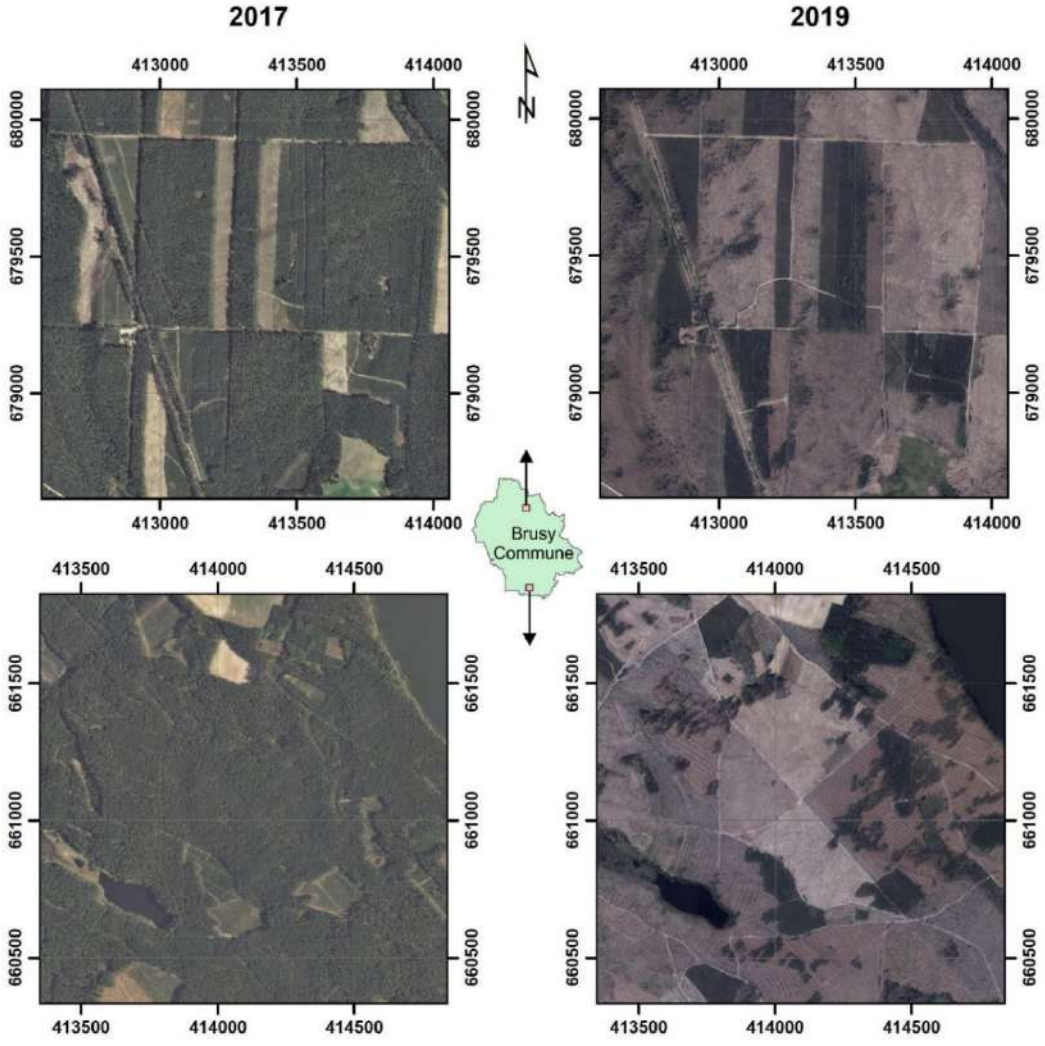

Fig. 2. Examples in aerial imageries of deforestation resulting from the derecho of August 11, 2017 (source of remote-sensing data – geoportal.gov.pl)

 Citation: Bulletin of Geography. Physical Geography Series 2024, 26, http://doi.org/10.12775/bgeo-2024-0002

Satellite data

This research employed multispectral satellite imagery from the Landsat-8 Operational Land Imager (OLI), focusing on orthorectified surface reflectance data processed through Google Earth Engine (GEE) to conduct land use and land cover (LULC) classification in Brusy, North Poland, specifically during the summer period of April, May, June, and July. Landsat-8's moderate spatial resolution of 30 meters, coupled with its global reach, has facilitated its widespread adoption for various land cover delineation tasks, including the identification of agricultural lands and wetland areas, since its launch (Giri et al. 2013; Schultz et al. 2015; Gilbertson et al. 2017). For the purpose of classification, this study selected only the blue, green, red, and near-infrared (NIR) bands, given their similar Spectral Response Functions (SRF). The criteria for image selection included a cloud cover of less than 10%. The dataset comprised 10 Landsat-8 surface reflectance (SR) images collected between March 30 and July 30, 2017, as pre-disaster evidence, and 13 images from the corresponding dates in 2018 as post-disaster evidence. For each set of yearly images, a median composite was generated to represent the summer season's land cover state.

Classification method

Reference data, including both training and validation samples, were collected from Landsat imagery for the specified time frames. Reflecting the objectives of this study and the real-world conditions of the study area, six distinct land cover types were identified for sampling: water bodies, forest, damaged forest area, bare land, pastures and built-up areas. To ensure a non-biased assessment of classification accuracy, validation samples were acquired at least one week subsequent to the collection of training samples. For the purpose of training, ~1500 samples for each land cover category were compiled. Conversely, the number of validation

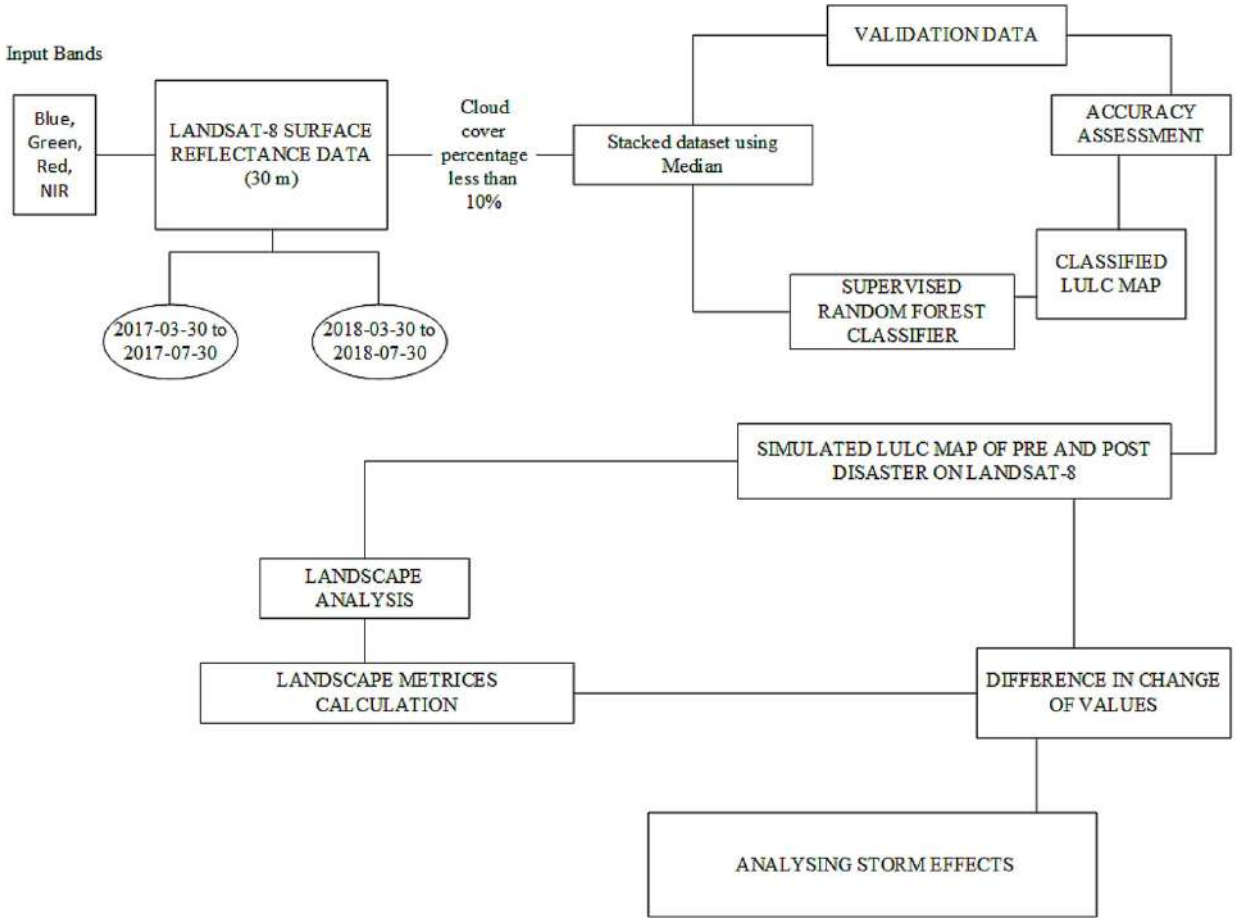

Fig. 3. Methodological scheme of work

samples was significantly lower, emphasising quality over quantity in assessing the model's performance.

Random forest classifier

In this research, the Random Forest (RF) algorithm was selected for the task of classification, recognised for its robustness in handling various satellite imagery types (Jin et al. 2019; Xu et al. 2020). Random Forest operates on the principle of Ensemble Learning, amalgamating multiple decision trees to improve the classification outcome. Each decision tree, constructed from a randomly sampled subset of the training data, contributes equally to the final decision through a process of majority voting on the classification of unlabelled samples.

Notably, the RF classifier is acclaimed for its swift training process, exceptional accuracy, resilience to outliers and resistance to overfitting, as highlighted in previous studies (Rodriguez-Galiano et al. 2012; Zhong et al. 2014). For the purposes of this study, the classifier was configured with 50 trees, a decision aimed at optimising the trade-off between computational efficiency and classification precision. All other parameters within the Google Earth Engine (GEE) framework were maintained at their default settings, ensuring a standardised approach to the classification process.

Accuracy evaluation

The evaluation of precision stands as a pivotal aspect of the classification workflow, with accuracy assessment being integral to verifying the correct categorisation of land cover types from sampled pixels (Rwanga and Ndambuki 2017). This process encompasses a variety of techniques designed to measure the thematic accuracy of land cover classifications. Among these, the confusion matrix serves as a fundamental tool, facilitating the calculation of Overall Accuracy (OA). OA is derived by dividing the number of correctly classified pixels by the total pixel count, offering a straightforward metric of classification success (Foody 2010). This measure provides a quantifiable means to assess the effectiveness of the classification algorithm in accurately identifying land cover from satellite imagery.

Landscape pattern analysis

The LULC classes can be mapped and their structural properties computed with the use of landscape ecological concepts and metrics. The authors used the term landscape metrics and indices simultaneously. Quantifying LULC patch distribution patterns and geographical analysis is crucial to understanding the direction and magnitude of landscape changes. Landscape pattern analysis can provide valuable information regarding LULC change (Zhang et al. 2011; Huang and Song 2016; Jaafari et al. 2016; Wang et al. 2018; Motlagh et al. 2020; Tariq et al. 2023; Tran et al. 2023). Forest fragmentation involves separating contiguous ecosystems into smaller sections called "patches" (Dutt and Kunz 2022). According to Forman (1995), a patch is defined as a relatively homogeneous area. The term "class" encompasses various categories of patches, including those defined by land cover/land use, habitat or vegetation types. Rutledge (2003) notes that fragmentation typically results in an increased number of patches, a reduction in the average size of these patches and an augmentation in the total length of their edges.

Fragmentation indices

Landscape indices are commonly categorised into two types: non-spatial and spatial (Gustafson 1998). Non-spatial indices quantify the composition of the landscape by measuring the classes of patches or the proportions of area they occupy. In contrast, spatial indices assess fragmentation by detailing the properties of these patches. Rutledge (2003) suggests that spatial indices are indicative of patch composition, shape and configuration. It is important to note that, strictly speaking, only patch composition is directly associated with fragmentation. However, the conventional concept of ecosystem fragmentation also encompasses the reduction of area and the additional indices previously discussed. The fundamental fragmentation landscape indices encompass composition, form and configuration. The selection of specific indices depends on authors' discretion and the metrics' applicability derived from prior studies. Composition indicators elucidate the foundational properties of fragmentation. Metrics such as the number of patches and mean patch area serve as

primary measures of fragmentation (McCarigal et al. 2002). However, these metrics are inadequate in capturing fragmentation comprehensively, as it also entails considerations of patch sizes.

Shape indices gauge patch complexity, with shapes like circles or squares featuring fewer edges and more core area (Forman 1995). Fractal dimension serves as another prominent metric for assessing shape and complexity (Krummel et al. 1987; O'Neill et al. 1988; Kunz and Nienartowicz 2007).

Patch configuration indices quantify the connectivity within landscape patches (Tischendorf and Fahrig 2000). The Shannon's Diversity Index (SHDI) offers a more robust measure of abundance, while the number of patches is termed "richness" (Turner 1990). A Shannon diversity index of zero indicates uniform distribution of space among patches across the entire landscape. Traditionally, composition analysis has utilised the Shannon metric (Effati et al. 2021).

The metrics for this landscape study are listed in Table 1 and were calculated using Patch Analyst 3.1 for Esri Software based on criteria from the literature. These metrics were determined by analysis of the vector data produced from the supervised classification both at the landscape level and the class level. For the landscape-level change metrics, the authors calculated the percentage value to plot all the matrices in the same graph for better visual interpretation.

Results and discussion

LULC change analysis

Windstorms can significantly alter the landscape through mechanisms such as wind damage, precipitation and storm surge (Dutt et al. 2024). Spatial variations resulting from a recorded derecho event have been distinctly observed within these categories (Dutt and Kunz 2022). Given the capabilities of Google Earth Engine, which includes a range of machine learning techniques, it was considered advantageous to evaluate whether this application programming interface could reliably compute forest fragmentation. Accordingly, imagery

Table 1. Description and implication of metrics

Name of metrics	Definition	Implication
Number of Patches (NP)	Total number of landscape patches, if *Analyse by Landscape* is selected, or the Number of Patches for each class, if *Analyse by Class* is selected.	Describes the fragmentation of the landscape, the higher the number, the more fragmentation.
Mean Patch Size (MPS)	Mean of all patch areas belonging to class *i*.	Defines landscape composition. Diversity index and mean patch size are inversely associated (Kumar et al. 2006). As the number of classes grows, the mean patch size decreases at a landscape scale (Li et al. 2005).
Total Edge (TE)	Length of edges in the surface area; an edge is the boundary between two distinct types of land cover.	Fragmentation produces a greater edge (Rutledge 2003).
Edge Density (ED)	Total edge density index is a ratio of total edges (number of cells at patch boundary) to total area (total cells).	Total edge density represents the level of fragmentation, it begins to increase rapidly at the landscape scale, but the rate slows as the number of classes increases (Li et al. 2005) species richness is sometimes positively correlated with edge density (Kumar et al. 2006).
Area Weighted Mean Patch Fractal Dimension (AWMPFD)	Shape complexity adjusted for shape size.	Rectangles, squares, and circles have fractal dimension 1, whereas irregular shapes approach 2. Human perturbations reduce the landscape's fractal dimension.
Shannon's Diversity Index (SHDI)	Number of land cover and land use types in a landscape; when normalised, this index value ranges from 0 to 1.	A high score suggests a fairly equal proportion of land cover types. Low values signify that a single land cover category dominates.

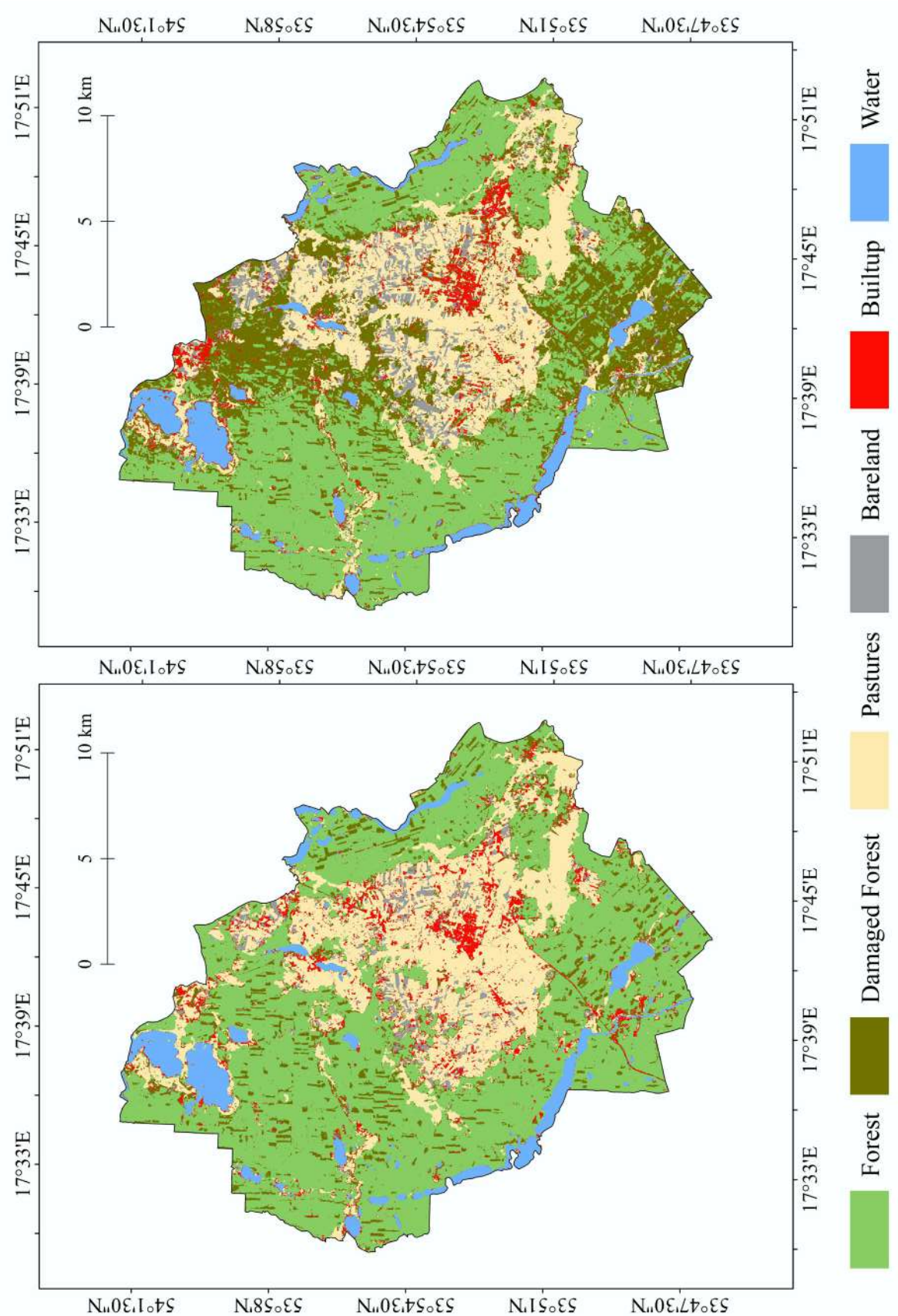

Fig. 4. Land use/land cover map of pre-disaster (left), and post-disaster (right)

from pre- (2017) and post-disaster (2018) scenarios was utilised. However, relying solely on a single database to observe these changes is inadequate for determining whether landscape metrics offer additional insights beyond conventional satellite imagery. Consequently, the authors employed supervised classification schemes to categorise Landsat images from 2017 and 2018, as illustrated in Figure 4. Post-classification, it is essential to assess and validate cartographic accuracy. Since the creation of ideal classification maps is unfeasible, a certain degree of error is anticipated. Thus, it is crucial to acknowledge the limitations imposed by user preferences, geographic regions or sensor specifications.

Figure 4 depicts land cover change trajectories in the Brusy Commune region. The trend analysis (Fig. 5A) shows a 177.52% increase in damaged forest, followed by a 79.59% increase in bare land. The forest cover decreased by 25.16%. Pastures, built-up and water had negligible change. Considering the two datasets, the predicted changes between the pre-disaster and post-disaster scenarios depict a satisfactory image of a disturbed landscape affected by windstorms.

A detailed examination of the satellite image classifications before and after the 2017 disaster, depicted in Figure 3, reveals significant vegetation loss in the north-west and south-east sections of the study area consequent to the derecho event. This data also facilitates the efficient determination of the storm's path. Notably, the region already exhibited signs of forest damage before the 2017 event, traceable to a tornado in 2012, as evidenced by the pre-disaster classified map (left) where short straight lines inside the forest patches vividly depict regions of secondary forest growth.

Errors in the classification process were noted, with omission errors present in water, pastures and bare land, while commission errors affected settlements and forests. These misclassifications, typically not expected in real-world scenarios, did not influence the water or settlement classes despite the storm events, and were thus deemed negligible by the authors. Additionally, the apparent decline in built-up areas is hypothesised to result from human classification errors, where highways and smaller settlements were likely misidentified as bare land or damaged forest.

Given the Landsat dataset's 30-m resolution, it is possible that machine learning techniques misclassified some open land as damaged forest or bare land. This scenario prompts a re-evaluation of the dataset's reliability for forest change studies and raises the question of whether higher-resolution data should be utilised for more accurate forest management analyses. These annual assessments prove crucial for identifying the impacts of recurrent events.

Fragmentation analysis at class level

According to Jiao et al. (2012), there is a significant linkage between land use and land cover (LULC) and landscape metrics. These metrics are instrumental in defining the landscape characteristics associated with LULC classes, as highlighted by Gudmann et al. (2020). Generally, the development of fragmentation indices mirrors advances in landscape ecology. This connection is succinctly captured in the title of Turner's seminal 1989 review, "Landscape Ecology: The Effect of Pattern on Process", which underscores the critical interplay between landscape patterns and ecological processes. The popularity and effectiveness of landscape pattern analysis have been enhanced by tools such as FRAGSTAT (McGarigal and Marks 1995) and Patch Analyst (Rempel et al. 1999). These tools have not only facilitated detailed measures of individual patches, classes and the entire landscape but their continued utilisation underscores their enduring relevance and utility. The analysis focuses on class-level changes across six dominant element types: damaged forest, forest, pastures, built-up area, barren land and water. Landscape metrics have yielded valuable insights into changes within the forest, particularly in terms of fragmentation, connectivity and heterogeneity. From 2017 to 2018, the total number of patches (NP) increased from 21,375 to 29,579, marking a 38.38% rise. This significant increase is partly attributable to interventions in the damaged forest landscape, where heavy equipment used for debris removal and subsequent restoration activities created numerous small, open spaces. These areas may be mistakenly identified as built-up areas in satellite imagery. Additionally, the presence of sandy surfaces and remains of devastated vegetation can further exacerbate these misclassifications.

In addition, there was a notable decrease in the mean patch size (MPS) by 30.05%, as shown in Figure 5C. This reduction, along with the results from other indicators, suggests that the landscape became increasingly fragmented during the study period. Figure 5A summarises the metrics generated for the area per land cover class at the class level, highlighting the substantial changes within the landscape. Notably, the category of damaged forest exhibited the most significant alterations. Concurrently, the MPS for pastures and forest land in Brusy also declined (Fig. 5C). This reduction in MPS occurred alongside a decrease in the total class areas (CA) (Fig. 5A) and an increase in the number of patches (NP) and edge density (ED) (Figs. 5B and 5D). These changes collectively indicate that fragmentation was most pronounced in the pastures and forest lands.

Fragmentation analysis at landscape level

Planners and policymakers often address the adverse effects of landscape fragmentation, which can arise through two primary mechanisms as identified by Burel and Baudry (2003): the reduction in the overall size of a habitat and the division of a habitat class into smaller patches. This process may also coincide with an increase in the total amount of edge, further complicating landscape integrity (Yu and Ng 2006; Dutt et al. 2024).

In this study, fragmentation was assessed using several indices, including Mean Patch Size (MPS), Number of Patches (NP), Total Edge (TE) and Edge Density (ED), as shown in Figure 6. The pre-disaster scenario exhibited a landscape where MPS was at its maximum, while TE, ED and NP were relatively low, indicating minimal fragmentation. In contrast, the post-disaster scenario showed a significant reversal in these metrics, clearly signalling increased landscape fragmentation.

Furthermore, measuring landscape heterogeneity, which encompasses patch variety and spatial complexity, is crucial for understanding landscape evolution (Burel and Baudry 2003). Despite the storm, Shannon's Diversity Index (SHDI), calculated to assess heterogeneity, showed no significant changes between pre- (1.64) and post-disaster (1.62) scenarios, as presented in Figure 6. This stability suggests that no substantial shifts in land cover types occurred within the short study period. The similar

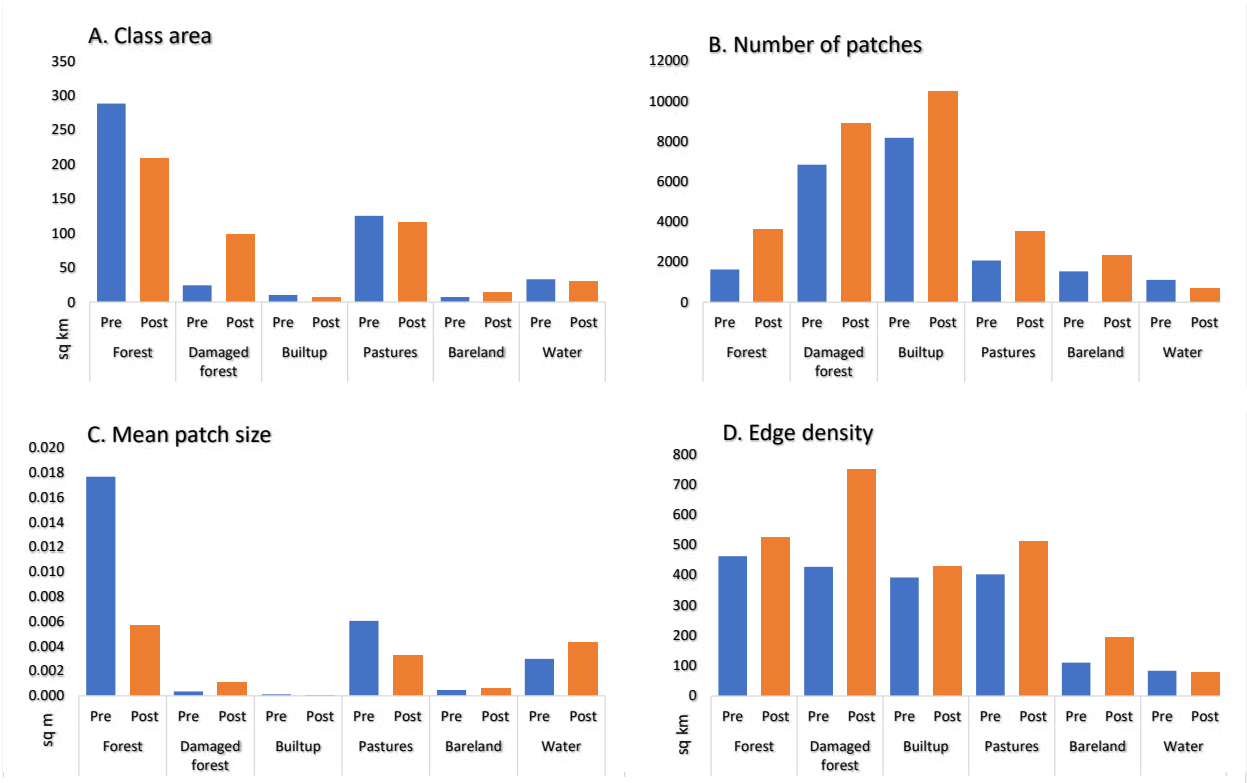

Fig. 5. Selected landscape indices: A. class area (CA), B. number of patches (NP), C. mean patch size (MPS), and D. edge density (ED)

 Citation: Bulletin of Geography. Physical Geography Series 2024, 26, http://doi.org/10.12775/bgeo-2024-0002

values of this index imply that while the structural dominance of land cover categories changed, it did not significantly impact overall diversity.

In general, the areas that remained forested despite the storm event are located at a considerable distance from roads and settlements, as well as from pastures (Fig. 4). This shows that there are many complex and interconnected processes behind recent land cover change.

Conclusion

The patterns found in the landscape as a result of our research show a direct relationship between land use and land cover. Within the research area, forests are generally located at a distance from human populations, roads, and pastures. This configuration may indicate the vulnerability of vegetation that remains closer to open lands and built-up structures, a finding consistent with what Dutt et al. (2024) identified in their study on forest fragmentation susceptibility. The methods employed within the study combine satellite images with landscape metrics, allowing us to assess and analyse changes in land use patterns in the study region. The utilisation of machine learning ensemble methods of stacked images covering the entire summer season of 2017 and 2018 with relevant metrics enables a deep investigation of dynamic landscapes that would have otherwise appeared static using single-date land cover analysis approaches. Although remote sensing is increasingly used to research land cover change (Feng et al. 2013; Gilbertson et al. 2017; Gin et al. 2019), few studies relate land cover change trajectories using multiple-dated imageries with landscape patterns.

The alleged lack of interpretability of numerous landscape metrics has always been a key issue (Haines-Young and Chopping 1996) in estimating which metrics are the most appropriate to which type of landscape and spatial resolution. Although this technique has also been applied to imagery with a medium resolution, the objective has remained the same: to investigate an area of interest and gather information about the texture of an image. The methodologies utilised here provide information on forest disturbance in the study area; spatial analysis of forest fragmentation at the class and landscape levels; land cover-change analysis through the incorporation of data from multiple images; and comparison of spatial patterns before and after the storm event. It is also worth noting that medium-resolution Landsat data are sufficient to determine forest fragmentation in this region.

This research blends environmental sciences and landscape ecology with remote sensing, GIS and machine learning techniques bringing us a step

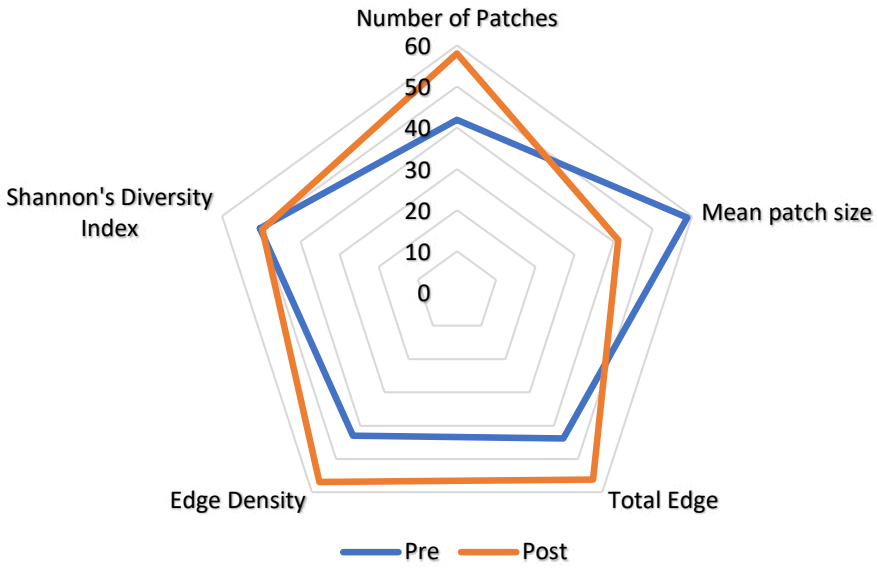

Fig. 6. Fragmentation and diversity analysis at landscape level

forward from the past forest disturbance studies. Further integration of methodologies and interpretations across disciplines is required if we are to fully comprehend and consequently mitigate the effects of global and local change on the environment.

Future studies should: (1) look into non-parametric classifiers like neural networks and decision trees that might improve LULC classification accuracy; (2) analyse specified landscape metrics using more scales, such as 4 m, 10 m, 90 m, 250 m, 500 m and 1000 m; (3) establish the scale influence on surface processes and LULC changes; (4) assess LULC changes at different spatial and temporal scales using efficient feature algorithms from various types of sensors; and (5) further integrate GIS and remote sensing and expert systems in detecting, visualising and monitoring LULC changes in disturbed forest environments.

Disclosure statement

No potential conflict of interest was reported by the authors.

Author contributions

Study design: SD, MK; data collection: SD, MK; statistical analysis: SD; result interpretation: SD, MK; manuscript preparation: SD, MK; literature review: SD, MK.

References

ALHAMAD MN, ALRABABAH MA, FEAGIN RA AND GHARAIBEH A, 2011, Mediterranean drylands: the effect of grain size and domain of scale on landscape metrics. *Ecological Indicators* 11(2): 611–621.

AMANI M, GHORBANIAN A, AHMADI SA, KAKOOEI M, MOGHIMI A, MIRMAZLOUMI SM and BRISCO B, 2020, Google Earth Engine cloud computing platform for remote sensing big data applications: A comprehensive review. *IEEE Journal of Selected Topics in Applied Earth Observations and Remote Sensing* 13: 5326–5350.

CELIŃSKI-MYSŁAW D and MATUSZKO D, 2014, An analysis of selected cases of derecho in Poland. *Atmospheric research* 149: 263–281. DOI: https://doi.org/10.1016/j.atmosres.2014.06.016.

CELIŃSKI-MYSŁAW D and PALARZ A, 2017, The occurrence of convective systems with a bow echo in warm season in Poland. *Atmospheric Research* 193: 26–35. DOI: https://doi.org/10.1016/j.atmosres.2017.04.015.

Corfidi SF, Coniglio MC, Cohen AE and Mead CM, 2016, A proposed revision to the definition of "derecho". *Bulletin of the American Meteorological Society* 97(6): 935–949.

DOSWELL CA and BURGESS DW, 1993, Tornadoes and tornadic storms: A review of conceptual models. *Geophysical Monograph-American Geophysical Union* 79: 161–161.

DOTZEK N, GROENEMEIJER P, FEUERSTEIN B and HOLZER AM, 2009, Overview of ESSL's severe convective storms research using the European Severe Weather Database ESWD. *Atmospheric research* 93(1–3): 575–586. DOI: https://doi.org/10.1016/j.atmosres.2008.10.020.

DUTT S, BATAR AK, SULIK S and KUNZ M, 2024, Forest ecosystem on the edge: Mapping forest fragmentation susceptibility in Tuchola Forest, Poland. *Ecological Indicators* 111980. DOI: https://doi.org/10.1016/j.ecolind.2024.111980.

DUTT S and KUNZ M, 2022, Land use/cover changes using Corine Land Cover data following hurricanes in the last 10 years: a case study on Tuchola Forest Biosphere Reserve. In: Młynarczyk A. (ed.), *Środowisko przyrodnicze jako obszar badań. Vol. 4*, 25-42, Bogucki Wydawnictwo Naukowe.

EARTHENGINE, 2023, AVailable at: earthengine.google.com.

EFFATI F, KARIMI H and YAVARI A, 2021, Investigating effects of land use and land cover patterns on land surface temperature using landscape metrics in the city of Tehran, Iran. *Arabian Journal of Geosciences* 14(13): 1–13.

FENG Y and LIU Y, 2015, Fractal dimension as an indicator for quantifying the effects of changing spatial scales on landscape metrics. *Ecological Indicators* 53: 18–27.

FENG,Y, LIU Y, ZHOU Q and HAN Z, 2013, A fractal based quantification analysis of spatial grain characteristics and its variation in landscape fragmentation of Shanghai, China. *Journal of Environmental Sciences* 22(3): 443–450.

FOODY G, 2010, Assessing the accuracy of remotely sensed data: principles and practices. *The Photogrammetric Record* 130(25): 204–205.

FORMAN RTT, 1995, *Land mosaics: the ecology of landscapes and regions*. Cambridge University Press, Cambridge, UK.

FORZIERI G and CATANI F, 2011, Scale-dependent relations in land cover biophysical dynamics. *Ecological modelling* 222(17): 3285–3290. DOI: https://doi.org/10.1016/j.ecolmodel.2011.06.010.

FROHN RC, 2018, Remote sensing for landscape ecology: new metric indicators for monitoring, modelling, and assessment of ecosystems. CRC Press.

GAN X, ZHU M, LI J, YANG Q and HUANG J, 2009, Effects of sensor spatial resolutions and classification themes on urban landscape analysis: a case study in Shanghai, China. *Canadian Journal of Remote Sensing* 35(4): 357–368. DOI: https://doi.org/10.5589/m09-031.

GILBERTSON JK, KEMP J and VAN NIEKERK A, 2017, Effect of pan-sharpening multi-temporal Landsat-8 imagery for crop type differentiation using different classification techniques. *Computers and Electronics in Agriculture* 134: 151–159.

GIRI C, PENGRA B, LONG J and LOVELAND TR, 2013, Next generation of global land cover characterization, mapping, and monitoring. *International Journal of Applied Earth Observation and Geoinformation* 25: 30–37. DOI: https://doi.org/10.1016/j.jag.2013.03.005.

GORELICK N, HANCHER M, DIXON M, ILYUSHCHENKO S, THAU D and MOORE R, 2017, Google Earth Engine: Planetary-scale geospatial analysis for everyone. *Remote Sensing of Environment* 202: 18–27. DOI: https://doi.org/10.1016/j.rse.2017.06.031.

GUDMANN A, CSIKÓS N, SZILASSI P and MUCSI L, 2020, Improvement in satellite image-based land cover classification with landscape metrics. *Remote Sensing* 12(21): 3580. DOI: https://doi.org/10.3390/rs12213580.

GUSTAFSON EJ, 1998, Quantifying landscape spatial pattern: what is the state of the art? *Ecosystems* 1(2): 143–156.

HAINES-YOUNG R and CHOPPING M, 1996, Quantifying landscape structure: a review of landscape indices and their application to forested landscapes. *Progress in Physical Geography* 20(4): 418–445. DOI: https://doi.org/10.1177/030913339602000040.

HANSEN MC, POTAPOV PV, MOORE R, HANCHER M, TURUBANOVA SA, TYUKAVINA A and TOWNSHEND J, 2013, High-resolution global maps of 21st-century forest cover change. *Science* 342(6160): 850–853.

HOUZE RA Jr, 1993, *Cloud Dynamics*. Academic Press.

HUANG C and SONG K, 2016, Forest cover change detection using Support Vector Machines, [in:] Chandra P. Giri (ed.) *Remote Sensing of Land Use and Land Cover. Principles and Applications*, 191–205, CRC Press, Boca Raton.

JAAFARI S, SAKIEH Y, SHABANI AA, DANEHKAR A and NAZARISAMANI AA, 2016, Landscape change assessment of reservation areas using remote sensing and landscape metrics (case study: Jajroud reservation, Iran). *Environment, Development and Sustainability* 18(6): 1701–1717.

JIAO L, LIU Y and LI H, 2012, Characterizing land-use classes in remote sensing imagery by shape metrics. *ISPRS Journal of Photogrammetry and Remote Sensing* 72: 46–55.

JIN Z, AZZARI G, YOU C, DI TOMMASO S, ASTON S, BURKE M and LOBELL DB, 2019, Smallholder maize area and yield mapping at national scales with Google Earth Engine. *Remote Sensing of Environment* 228: 115–128. DOI: https://doi.org/10.1016/j.rse.2019.04.016.

JOHNS RH and HIRT WD, 1987, Derechos: Widespread convectively induced windstorms. *Weather and Forecasting* 2(1): 32–49.

KENNEDY RE, YANG Z, GORELICK N, BRAATEN J, CAVALCANTE L, COHEN WB and HEALEY S, 2018, Implementation of the LandTrendr algorithm on Google Earth Engine. *Remote Sensing* 10(5): 691. DOI: https://doi.org/10.3390/rs10050691.

KRUMMEL JR, GARDNER RH, SUGIHARA G, O'NEILL RV and COLEMAN PR, 1987, Landscape patterns in a disturbed environment. *Oikos* 48: 321–324.

KUNZ M and NIENARTOWICZ A, 2002, Remote sensing imagery in monitoring spatial pattern changes in forest landscape. IN: Begni G. (ed.), *Observing our Environment from Space - New Solutions for a New Millenium*, 391–398, Balkema Publishers.

KUNZ M and NIENARTOWICZ A, 2004, Landscape structure characterization with the application of NDVI and fractal dimension of remote sensing imageries in Zabory Landscape Park. In: Goossens R. (ed.), *Remote Sensing in Transition*, 435-441, Millpress Science Publishers, Rotterdam Netherlands.

KUNZ M and NIENARTOWICZ A, 2007, The influence of past human activity gradient on present variation of NDVI and texture indices in Zabory Landscape Park. In: Bochenek Z. (ed.), *New Developments and Challenges*

in Remote Sensing, 171–184, Millpress Science Publishers, Rotterdam, Netherlands.

KUNZ M, and NIENARTOWICZ A., 2008, Variation of NDVI in seminatural and secondary forest: a case study of Zaborski Landscape Park. In: Gomarasca MA (ed.), *Geoinformation in Europe*, 227–234, Millpress Science Publishers, Rotterdam, Netherlands.

KUNZ M, NIENARTOWICZ A and KAMIŃSKI D, 2023, Loss in CO_2 assimilation by forest stands relative to its emissions generated by the economic sector as an indicator of ecological consequences of a windstorm in the municipality of Brusy, NW Poland. *Bulletin of Geography. Socio-economic Series* 59: 41–56. DOI: https://doi.org/10.12775/bgss-2023-0003.

LI X, HE HS, BU R, WEN Q, CHANG Y, HU Y and LI Y, 2005, The adequacy of different landscape metrics for various landscape patterns. *Pattern Recognition* 38(12): 2626–2638. DOI: https://doi.org/10.1016/j.patcog.2005.05.009.

LÜ Y, FENG X, CHEN L and FU B, 2013, Scaling effects of landscape metrics: a comparison of two methods. *Physical Geography* 34(1): 40–49.

MACLEOD RD and CONGALTON RG, 1998, A quantitative comparison of change-detection algorithms for monitoring eelgrass from remotely sensed data. *Photogrammetric Engineering and Remote Sensing* 64(3): 207–216.

MCCARIGAL K, CUSHMAN SA, NEEL MC and ENE E, 2002, *FRAGSTATS: Spatial pattern analysis program for categorical maps, version 3.0*. University of Massachusetts, Amherst, Massachusetts.

MCCARIGAL K and MARKS BJ, 1995, FRAGSTATS: spatial pattern analysis program for quantifying landscape structure. US Department of Agriculture, Forest Service, General Technical Report PNW-GTR-351.

MCGARIGAL K and CUSHMAN SA, 2002, Comparative evaluation of experimental approaches to the study of habitat fragmentation effects. *Ecological Applications* 12(2): 335–345. DOI: https://doi.org/10.1890/1051-0761(2002)012[0335:CEOEAT]2.0.CO;2.

MILLINGTON AC, VELEZ-LIENDO XM and BRADLEY AV, 2003, Scale dependence in multitemporal mapping of forest fragmentation in Bolivia: implications for explaining temporal trends in landscape ecology and applications to biodiversity conservation. *ISPRS Journal of Photogrammetry and Remote Sensing* 57(4): 289–299.

MOTLAGH ZK, LOTFI A, POURMANAFI S, AHMADIZADEH S and SOFFIANIAN A, 2020, Spatial modeling of land-use change in a rapidly urbanizing landscape in central Iran: Integration of remote sensing, CA-Markov, and landscape metrics. *Environmental Monitoring and Assessment* 192(11): 1–19.

MUSICK HB and GROVER HD, 1991, Image textural measures as indices of landscape pattern. *Ecological Studies* 82: 77–101.

MUTANGA O and KUMAR L, 2019, Google Earth Engine applications. *Remote Sensing* 11(5): 591. DOI: https://doi.org/10.3390/rs11050591.

NIENARTOWICZ A, DOMIN DJ, KUNZ M and PRZYSTALSKI A, 2010, *Rezerwat Biosfery Bory Tucholskie, Formularz Nominacyjny* (Biosphere Reserve Tuchola Forest, Nomination Form – in Polish). LGD Sandry Brdy, Chojnice.

NIENARTOWICZ A and KUNZ M, 2018, *Tuchola Forest Biosphere Reserve 2.0 – the grounds and the scope of the proposed changes* (Rezerwat Biosfery Bory Tucholskie 2.0 – uzasadnienie wniosku o powiększenie i zakres proponowanych zmian – in Polish). LGD Sandry Brdy, Chojnice.

O'NEILL RV, KRUMMEL JR, GARDNER RH, SUGIHARA G, JACKSON B, DEANGELIS DL, MILNE BT, TURNER MG, ZYGMUNT B, CHRISTENSEN SW, DALE VH and GRAHAM RL, 1988, Indices of landscape pattern. *Landscape Ecology* 1: 153–162.

ORUSA T, VIANI A, CAMMARERI D AND BORGOGNO MONDINO E, 2023, A Google Earth Engine Algorithm to Map Phenological Metrics in Mountain Areas Worldwide with Landsat Collection and Sentinel-2. *Geomatics* 3(1): 221–238. DOI: https://doi.org/10.3390/geomatics3010012.

REMPEL RS, CARR A and ELKIE P, 1999, Patch analyst and patch analyst (grid) function.

RODRIGUEZ-GALIANO VF, GHIMIRE B, ROGAN J, CHICA-OLMO M and RIGOL-SANCHEZ JP, 2012, An assessment of the effectiveness of a random forest classifier for land-cover classification. *ISPRS Journal of Photogrammetry and Remote Sensing* 67: 93–104.

RUTLEDGE DT, 2003, Landscape indices as measures of the effects of fragmentation: can pattern reflect process?

RWANGA SS and NDAMBUKI JM, 2017, Accuracy assessment of land use/land cover classification using remote sensing and GIS. *International Journal of Geosciences* 8(04): 611. DOI: 10.4236/ijg.2017.84033.

SAURA S and MARTINEZ-MILLAN J, 2001, Sensitivity of landscape pattern metrics to map spatial extent. *Photogrammetric engineering and remote sensing* 67(9): 1027–1036.

SAURA S, 2004, Effects of remote sensor spatial resolution and data aggregation on selected fragmentation indices. *Landscape Ecology* 19(2): 197–209.

SCHULTZ B, IMMITZER M, FORMAGGIO AR, DEL'ARCO SANCHES I, JOSÉ BARRETO LUIZ A and ATZBERGER C, 2015, Self-guided segmentation and classification of multi-temporal Landsat-8 images for crop type mapping in Southeastern Brazil. *Remote Sensing* 7(11): 14482–14508.

SULIK S and KEJNA M, 2020, The origin and course of severe thunderstorm outbreaks in Poland on 10 and 11 August, 2017. *Bulletin of Geography. Physical Geography Series* 18: 25–39. DOI: DOI: https://doi. org/10.2478/bgeo-2020-0003.

TARIQ A, JIANGO Y, LI Q, GAO J, LU L, SOUFAN W, ALMUTAIRI K and HABIB-UR-RAHMAN M, 2023, Modelling, mapping and monitoring of forest cover changes, using support vector machine, kernel logistic regression and naive bayes tree models with optical remote sensing data. *Heliyon* 9(2): e13212.

TASZAREK M, ALLEN J, PÚČIK T, GROENEMEIJER P, CZERNECKI B, KOLENDOWICZ L and SCHULZ W, 2019, A climatology of thunderstorms across Europe from a synthesis of multiple data sources. *Journal of Climate* 32(6): 1813–1837. DOI: https://doi.org/10.1175/JCLI-D-18-0372.1.

TASZAREK M, PILGUJ N, ORLIKOWSKI J, SUROWIECKI A, WALCZAKIEWICZ S, PILORZ W and PÓŁROLNICZAK M, 2019, Derecho evolving from a mesocyclone – A study of 11 August 2017 severe weather outbreak in Poland: Event analysis and high-resolution simulation. *Monthly Weather Review* 147(6): 2283–2306. DOI: https://doi.org/10.1175/MWR-D-18-0330.1.

TISCHENDORF L and FAHRIG L, 2000, On the usage and measurement of landscape connectivity. *Oikos* 90: 7–19.

TURNER MG, 1990, Spatial and temporal analysis of landscape patterns. *Landscape ecology* 4(1): 21–30.

TURNER MG, GARDNER RH and O'NEILL RV, 2001, *Landscape ecology in theory and practice, Vol. 401*. Springer New York.

TURNER MG, 1989, Landscape ecology: the effect of pattern on process. *Annual Review of Ecology and Systematics* 20: 179–197.

TRAN QC, TRAN NT, NGUYEN VL, LE TH and VAN TY, 2023, Assessment of forest status change based on normalized difference vegetation index in Aluoi district, Thua Thien Hue province. *Hue University Journal of Science: Agriculture and Rural Development* 132(3A): 183–193.

UUEMAA E, ROOSAARE J and MANDER Ü, 2005, Scale dependence of landscape metrics and their indicatory value for nutrient and organic matter losses from catchments. *Ecological indicators* 5(4): 350–369.

VOGT P, RIITTERS KH, ESTREGUIL C, KOZAK J, WADE TG and WICKHAM JD, 2007, Mapping spatial patterns with morphological image processing. *Landscape ecology* 22(2): 171–177.

WANG C, WANG Y, WANG R and ZHENG P, 2018, Modeling and evaluating land-use/land-cover change for urban planning and sustainability: A case study of Dongying city, China. *Journal of Cleaner Production* 172: 1529–1534.

WU J and HOBBS R, 2002, Key issues and research priorities in landscape ecology: an idiosyncratic synthesis. *Landscape ecology* 17(4): 355–365.

XU F, LI Z, ZHANG S, HUANG N, QUAN Z, ZHANG W and PRISHCHEPOV AV, 2020, Mapping winter wheat with combinations of temporally aggregated Sentinel-2 and Landsat-8 data in Shandong Province, China. *Remote Sensing* 12(12): 2065. DOI: https://doi.org/10.3390/rs12122065.

YU X and NG C, 2006, An integrated evaluation of landscape change using remote sensing and landscape metrics: a case study of Panyu, Guangzhou. *International Journal of Remote Sensing* 27(6): 1075–1092.

ZIPSER EJ, 1982, Use of a conceptual model of the life cycle of mesoscale convective systems to improve very-short-range forecasts. Nowcasting.

ZHANG Q, BAN Y, LIU J and HU Y, 2011, Simulation and analysis of urban growth scenarios for the Greater Shanghai Area, China. *Computers, Environment and Urban Systems* 35(2): 126–139.

ZHONG L, GONG P and BIGING GS, 2014, Efficient corn and soybean mapping with temporal extendability: A multi-year experiment using Landsat imagery. *Remote Sensing of Environment* 140: 1–13.

ZHU M, JIANG N, LI J, XU J and FAN Y, 2006, The effects of sensor spatial resolution and changing grain size on fragmentation indices in urban landscape. *International Journal of Remote Sensing* 27(21): 4791–4805.

Received 10 November 2023
Accepted 15 April 2024

Ecological Indicators 161 (2024) 111980

Contents lists available at ScienceDirect

Ecological Indicators

journal homepage: www.elsevier.com/locate/ecolind

Forest ecosystem on the edge: Mapping forest fragmentation susceptibility in Tuchola Forest, Poland

Sanjana Dutt [a,*], Amit Kumar Batar [b], Sławomir Sulik [a], Mieczysław Kunz [a]

[a] Faculty of Earth Sciences and Spatial Management, Nicolaus Copernicus University, Lwowska 1, 87-100, Toruń, Poland
[b] National Institute for Environmental Studies, 16-2 Onogawa, Tsukuba, Ibaraki, Japan

ARTICLE INFO

Keywords:
Forest fragmentation
Ecosystem integrity
Remote sensing
Susceptibility mapping
Wind storm

ABSTRACT

Forest ecosystems, vital for maintaining global biodiversity and ecological balance, are increasingly threatened by fragmentation. This study addresses the critical issue in the Tuchola Forest of Poland, examining the effects of natural and human factors on forest fragmentation. Our objective was to identify the most suitable dataset for monitoring forest fragmentation from 2015 to 2020, ascertain the primary drivers of fragmentation, and map the areas at high risk. Utilizing the PALSAR (25 m resolution) and Dynamic World (10 m resolution) datasets, we discovered PALSAR's enhanced ability to detect changes in forest structure, particularly evident after a significant windstorm in 2017. This dataset proved crucial in highlighting the escalating trend of forest fragmentation, reinforcing its importance for environmental monitoring and policy formulation. Our analysis identified key factors influencing fragmentation, such as proximity to croplands, tree height and age, wind speed, and vegetation water content, with areas near croplands and having younger, shorter trees being most susceptible. Employing a Weight-of-Evidence (WOE) Bayesian modeling technique, we mapped forest fragmentation susceptibility, demonstrating our methodology's effectiveness through high accuracy validation (AUC of 0.82 and Kappa Index of 0.68). Our innovative approach in mapping susceptibility to fragmentation, especially after extreme weather events, marks a pioneering contribution in Poland. This research advances the understanding of forest fragmentation dynamics and offers a scalable model for global application, emphasizing the urgent need for targeted conservation strategies to preserve the integrity of forest ecosystems amidst climatic risk and anthropogenic pressures.

1. Introduction

Forest fragmentation is a major concern in landscape ecology, significantly impacting the structure and functionality of forest ecosystems. This phenomenon not only threatens biodiversity, including wildlife habitats, water and nutrient cycles, and ecosystem resilience, but also fosters the creation of edge zones (Forman, 1996; Fischer et al., 2021). These zones escalate carbon emissions through increased tree mortality, with studies indicating that 70 % of remaining forests are within 1 km of an edge, thus highly susceptible to fragmentation's detrimental effects. These effects include a reduction in biodiversity by 13 to 75 % and impairment of ecosystem functions, notably biomass and nutrient cycles (Haddad et al., 2015; Brinck et al., 2017).

The complexity of fragmentation's impact extends to species interactions, disproportionately affecting mutualisms like pollination and seed dispersal more than antagonistic interactions. Such differential impacts necessitate a nuanced understanding of fragmentation's multifaceted effects on species persistence, distribution, and ecological interactions (Magrach et al., 2014). The scale-dependent nature of fragmentation patterns further demands a multi-scaled analytical approach, highlighting the urgency for conservation and restoration efforts to enhance landscape connectivity and mitigate extinction rates (Forman, 1996; Taubert et al., 2018; Haddad et al., 2015).

Technological advancements have revolutionized our ability to analyze forest fragmentation. Tools like FRAGSTATS, Patch Analyst for ArcGIS, and the GUIDOS Toolbox, with its Morphological Spatial Pattern Analysis (MSPA), provide sophisticated methodologies for assessing landscape connectivity and quantifying spatial heterogeneity (McGarigal, Cushman, & Ene, 2012; Rempel et al., 2012; Soille, 2003; Vogt et al., 2007; Vogt & Riitters, 2017). Yet, the effectiveness of these tools is contingent upon selecting an appropriate spatial resolution. This decision critically influences the detection and characterization of forest

* Corresponding author.
E-mail address: sanjana.dutt@doktorant.umk.pl (S. Dutt).

https://doi.org/10.1016/j.ecolind.2024.111980
Received 22 January 2024; Received in revised form 20 March 2024; Accepted 30 March 2024
Available online 6 April 2024

versus non-forest elements, potentially altering perceived spatial patterns significantly when comparing high (0.5 m) and low (30 m) resolution data (Wickham & Riitters, 2019). As highlighted by Fynn and Campbell (2019), the choice between coarse and fine-resolution imagery not only affects the availability and cost but also the accuracy of fragmentation metrics. Such discernment in resolution selection is essential to ensure the ecological validity of fragmentation studies, particularly in complex landscapes where the distinction between vegetation and non-vegetation can be subtle yet significant.

The study contrasts the use of PALSAR-2 Global forest/non-forest maps, utilizing SAR radar with a 25 m resolution, against Dynamic World's forest class, which employs 10 m optical Sentinel-2 imagery. This comparison aims to evaluate their respective efficacies in monitoring and analyzing forest ecosystems. PALSAR-2's SAR radar is instrumental in providing robust measurements of forest structure and detecting disturbances under challenging climatic conditions (Atkins et al., 2023; Balling et al., 2023), while Dynamic World's use of Sentinel-2 imagery offers detailed insights into environmental changes, supporting effective management and conservation efforts (Brown et al., 2022). This comparative analysis sheds light on the strengths and limitations of SAR and optical imagery in capturing forest fragmentation dynamics, aiming to enhance our understanding of these complex processes.

Despite a considerable volume of research on forest fragmentation within Poland—encompassing historical evaluations of habitat distribution (Mazgajski et al., 2010), implications for timber resources and carbon sequestration (Budniak & Zięba, 2022), and the socio-economic drivers of forest structural changes (Żmihorski et al., 2009; Szramka & Adamowicz, 2020)—focused investigations into the Tuchola Forest Biosphere Reserve's (TFBR) vulnerability to fragmentation are notably lacking. Specifically, there have been no studies investigating the size and dynamics of edge boundaries within the TFBR, a gap this study aims to address. The devastating windstorm of 2017 accentuates the TFBR's vulnerability, emphasizing the need for focused research on its fragmentation dynamics. This study hypothesizes that storm disturbances, coupled with escalating demands for land conversion to agriculture, predominantly drive fragmentation in the TFBR.

In this research, we aim to rigorously evaluate the effectiveness of two distinct datasets—the microwave PALSAR-2 Global forest/non-forest imagery, and the optical imagery from sentinel's collection of Dynamic World, in monitoring forest fragmentation within Tuchola Forest from 2015 to 2020. Our primary objective is to ascertain which dataset provides the most accurate and detailed representation of fragmented patches during this period. Furthermore, we intend to determine the principal factors contributing to forest fragmentation, particularly focusing on the roles of wind disturbances and proximity to cropland and bareland, as identified in significant prior studies (Forzieri et al., 2020; Jung et al., 2016). Through this analysis, we aim not only to enhance our understanding of fragmentation dynamics but also to map the region's susceptibility to ongoing and future fragmentation. This research is anticipated to offer valuable insights for more effective monitoring and management of forest ecosystems, thereby contributing significantly to the discourse on forest ecology and conservation.

1.1. Study Area: Tuchola Forest, Poland

The Tuchola Forest Biosphere Reserve (TFBR), nestled within the greater Tuchola Forest in northern Poland, stands out for its exceptional biodiversity and a mix of broadleaf and coniferous forests (Nienartowicz et al., 2010). Covering an expanse of 3,195 square kilometers, (see

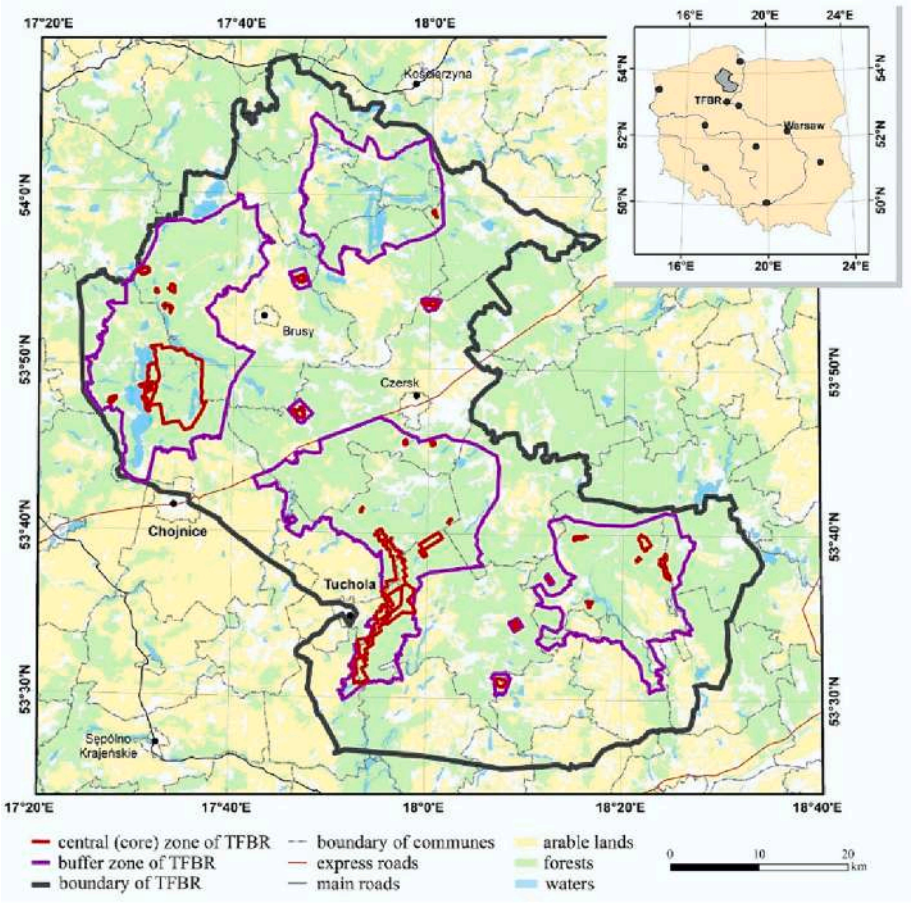

Fig. 1. The localization of the study area – Tuchola Forest Biosphere Resereve.

Fig. 1) this largely forested biosphere reserve plays a pivotal role in the UNESCO Man and Biosphere Programme, aiming at ecosystem conservation while promoting sustainable development (Nienartowicz & Kunz, 2020; Nienartowicz et al., 2010). Home to over 1,337 species of vascular plants and 1,250 phanerogams, the TFBR's ecological importance is highlighted by its rich biodiversity (Nienartowicz et al., 2010).

Historical research by Kunz (2012) indicates a significant increase in forest area within Western Pomerania, which includes the Tuchola Forest, from 16 % in 1618 to 37 % in the early 21st century. This reflects a transition from extensive deforestation due to logging and agriculture to systematic reforestation efforts since the 19th century. However, a 2017 storm notably impacted the forest's spatial structure, illustrating the dynamic nature of its landscape (Kunz, 2006; Dutt & Kunz, 2024).

The TFBR, encompassing 22 communes within two voivodeships, is recognized as Poland's most extensive UNESCO-designated biosphere reserve, predominantly covered by woodland, accounting for over 86 % of its area. It's strategically segmented into core, buffer, and transition zones, each dedicated to distinct conservation objectives and sustainable development initiatives. This zoning not only conserves a variety of ecosystems but also promotes ecological education, aligning with principles of sustainable development (Krawiec et al., 2022; Nienartowicz & Kunz, 2020).

The TFBR's landscape, shaped by its history and geological features, reflects the remnants of the ancient Tuchola Primeval Forest, with a composition that has evolved due to post-glacial climatic changes and human activities. Despite these changes, the reserve remains a sanctuary for rare and protected species, with its predominant forest types and diverse flora including a rich lichen community (Boiński, 1993; Boiński & Boińska, 2020).

Recent climatological research within the TFBR has revealed an increasing vulnerability to extreme weather events, including severe convective windstorms (Pacey et al., 2021) and whirlwinds that have caused significant forest destruction (Chojnacka-Ożga & Ożga, 2018). The 2017 windstorm, documented by Taszarek et al. (2019) and Chmielewski et al. (2020), highlights the severe impact of such climatic extremes, causing unprecedented forest damage and emphasizing the need for integrated climatic challenges into conservation strategies.

Acknowledging the historical context of deforestation and the ongoing challenges posed by climatic extremes, this study emphasizes the complex interplay between climate change and forest conservation efforts in the TFBR. The inclusion of recent climatic data and extreme weather event analyses offers a comprehensive overview, enhancing the understanding of the Tuchola Forest Biosphere Reserve's ecological dynamics and conservation priorities.

2. Data sources and processing

2.1. Rationale for time frame selection (2015–2020)

In selecting the analysis period of 2015–2020 for our study, we aimed to capture the dynamics of forest fragmentation both before and after a significant meteorological event: a derecho. A derecho is a widespread, long-lived windstorm that is associated with a band of rapidly moving showers or thunderstorms. Characterized by its intense straight-line winds, a derecho can cause substantial damage to landscapes, particularly forests, over a wide area (Chmielewski et al., 2020).

The rationale for focusing on this period is underpinned by the occurrence of one of Poland's most destructive storms on August 11, 2017. This derecho, as detailed by Chmielewski et al. (2020) and Taszarek et al. (2019), represents a catastrophic meteorological event in Poland's history. Originating as a mesoscale convective system on the border between the Czech Republic and Poland, it ravaged several provinces, causing unprecedented forest damage. Wind speeds during this event reached up to 130 km/h, and in some areas, they exceeded 150 km/h (Taszarek et al., 2019). The storm resulted in the loss of approximately 79,700 ha of forest, blocked and damaged over 1100 km of local and municipal roads, and left over 500,000 consumers without electricity (Chmielewski et al., 2020).

The period of 2015–2020 is crucial for understanding the scale of forest fragmentation attributable to such an extreme event. Prior to the derecho, the forests in Poland were already experiencing fragmentation; however, this six-year span provides a unique opportunity to quantify the magnitude of change that followed. Analyzing forest fragmentation in this timeframe not only allows for a pioneering investigation into the effects of the derecho but also offers a historic record of the fragmentation process. Such a record is invaluable in creating susceptibility maps, aiding in the prediction and management of future forest fragmentation under similar extreme events.

2.2. Remote sensing data

This study utilized a combination of synthetic aperture radar (SAR) and near-real-time (NRT) Land Use/Land Cover (LULC) datasets to assess forest/non-forest dynamics over six years, from 2015 to 2020. Two primary datasets, representing microwave and optical remote sensing technologies, were incorporated: the Advanced Land Observing Satellite (ALOS) Phased Array type L-band Synthetic Aperture Radar (PALSAR-2) for microwave remote sensing, and the Sentinel-2 L1C collection from the Dynamic World dataset for optical remote sensing. Comprehensive forest survey data, managed by the Bureau of Geodesy and Forest Management, were obtained from the Bank Danych Lasach (Forest Data Bank, BDL). This dataset encompasses detailed information on forests administered by the State Forests National Forests Holding, acquired through the BDL portal for specific forest inspectorates within the Regional Directorates of the State Forests in Gdańsk and Toruń.

The analysis of wind speed data sourced from the European Severe Storms Laboratory (ESSL) and the European Severe Weather Database (ESWD) (Dotzek et al., 2009) involved examining reports from 2015 to 2020 on severe wind gust events. The absence of specific wind speed measurements in some ESWD reports necessitated supplementary data from ERA5 reanalyses by the European Centre for Medium-Range Weather Forecasts (ECMWF) (Hersbach et al., 2020). This supplementary data was downscaled and integrated with the ESWD reports to estimate wind speeds at relevant locations within the study area (Sulik & Kejna, 2020). The approach facilitated a detailed examination of the climatic factors influencing forest dynamics, emphasizing the impact of severe wind gusts (Taszarek et al., 2019).

2.2.1. PALSAR-2 Forest/Non-Forest map

The PALSAR-2 datasets, utilizing Synthetic Aperture Radar (SAR) technology aboard the ALOS-2 satellite, provide critical data for environmental monitoring through microwave emissions and reflections. This SAR technology captures high-quality images under all weather conditions, day and night, by leveraging L-band microwaves capable of penetrating vegetation to some extent. The global forest/non-forest map is derived from SAR imagery at a 25 m resolution, the finest resolution available for these datasets, which classifies pixels based on backscatter intensity. Pixels with strong backscatter are labeled as 'forest,' and those with low backscatter as 'non-forest,' in line with the Food and Agriculture Organization's (FAO) definition of forest. This definition includes natural forest areas larger than 0.5 ha with a canopy cover of over 10 %.

To accommodate the study period from 2015 to 2020, data from two subsets were utilized. Initially, the Global 3-class PALSAR dataset (JAXA/ALOS/PALSAR/YEARLY/FNF) covered 2015 to 2017, providing classifications of forest, non-forest, and water. Subsequently, for 2018 to 2020, the more advanced Global 4-class PALSAR-2 dataset (JAXA/ALOS/PALSAR/YEARLY/FNF4) offered detailed classifications including dense forest, non-dense forest, non-forest, and water (Shimada et al., 2014). This approach aligns with the advancements in SAR capabilities, as highlighted by Awange & Kiema (2013), to overcome typical remote sensing limitations like cloud cover and limited daylight,

ensuring consistent and reliable environmental monitoring.

2.2.2. Dynamic World dataset forest cover map

In tandem with the SAR-based PALSAR-2 analysis, this study utilized the Dynamic World V1 dataset from Google Earth Engine (GOOGLE/DYNAMICWORLD/V1). Spanning from 2015 to the present, this dataset offers a near-real-time Land Use/Land Cover (LULC) classification at an unprecedented 10 m resolution (Brown et al., 2022), the highest available for such global monitoring applications. The study by Louzada et al. (2023) illustrates the effectiveness of integrating SAR with optical remote sensing data in environmental monitoring. For this study, the 'trees' band within the Dynamic World dataset was selected to identify forested areas, applying a threshold on the 'trees' probability band (greater than 0.6) to delineate forested regions from non-forest areas. This threshold was chosen based on the dataset's guidance to select pixels with high confidence in class prediction, aligning with the observed overall agreement of 73.8 % between Dynamic World model outputs and expert labels for high-confidence classes such as trees, indicating a robust delineation of forested versus non-forested areas (Brown et al., 2022). This approach enabled the examination of forest dynamics within the specified region of interest (ROI), leveraging the Dynamic World's capability to provide current and detailed LULC data, and complementing the SAR-based observations.

2.3. Analysis of forest fragmentation

Morphological Spatial Pattern Analysis (MSPA), a breakthrough in landscape ecology, offers a comprehensive approach to assessing landscape connectivity by studying the pixel arrangements (Soille, 2003; Vogt et al., 2007). The emergence of the GUIDOS Toolbox, with its user-friendly interface and broad applicability in environmental analyses, represents a further advancement in this field (Vogt & Riitters, 2017). Unlike traditional tools, GUIDOS is uniquely equipped to quantify spatial heterogeneity, a critical aspect in forest fragmentation studies, through sophisticated algorithms that provide a more nuanced understanding of fragmentation impacts.

In this study, we employed the GUIDOS Toolbox to assess forest fragmentation. This choice was motivated by the Toolbox's exceptional capability in spatial data analysis and land cover classification. Traditional methods, such as those proposed by Musick and Grover (1991) and Forman (1996), often relied on landscape-level concepts like patch-corridor-matrix or adjacency at the pixel level, which, while informative, lacked the ability to provide quantitative measures of fragmentation's degree or variation (Vogt, 2023). Moreover, these methods struggled in large-area assessments due to challenges in handling a vast number of patches and accurately representing patch sizes and shapes (Riitters et al., 2002; Heilman et al., 2002). In contrast, GUIDOS offers a robust methodology, proven in diverse research areas ranging from biodiversity impact studies to climate change effects on habitats (Rincón et al., 2022). Within this framework, fragmentation classes are defined based on the connectivity and adjacency of forest pixels, with special emphasis on categories like 'rare' and 'patchy', which indicate intense fragmentation and have significant implications for biodiversity and ecosystem health (Heilman et al., 2002). This approach not only resonates with Chavan et al. (2018) in tracking core area reduction but also aligns with Batar et al. (2021) in emphasizing the importance of understanding fragmentation drivers. Furthermore, our study leverages multi-temporal land cover data to analyze forest fragmentation, showcasing the GUIDOS Toolbox's versatility in a wide array of environmental assessments, including landslide risks and urban planning (Arrogante-Funes et al., 2021; Lin et al., 2021).

3. Predictive variables for forest fragmentation

To develop effective strategies for mitigating forest fragmentation risks, it's crucial to understand their predictive variables. Given the predominantly rural nature of the study area, this research focuses on the natural causes of fragmentation, acknowledging the limited yet not negligible human influence. The spatial representation of the ecological and geographical variables depicted in Fig. 2 serves as the basis for analyzing the factors contributing to forest fragmentation within the Tuchola Forest Biosphere Reserve (TFBR), Poland. The variables include wind speed, vegetation water content, tree age distribution, tree height, slope gradient, and distances from cropland, bare land, and roads (Fig. 2). The specific datasets from which these variables were derived are detailed in Table 1, which follows this figure. This table provides a comprehensive overview of the sources utilized for each factor.

3.1. Physical factors

Forest ecosystems' resilience and stability are significantly influenced by their physical environment. Factors such as slope angle play a crucial role in determining sunlight exposure and wind dynamics (Doane et al., 2023), which can heighten vulnerability to windthrow. The concept of forest structural diversity, which encompasses the spatial distribution of trees, species diversity, and variations in tree dimensions (size and height), is essential for understanding the impacts of wind on forest ecosystems. Forests with a higher degree of structural diversity, characterized by a mix of tree heights and species, can disrupt wind flow and potentially reduce the severity of wind damage, thereby influencing fragmentation patterns (Li et al., 2023). Furthermore, forest age and composition significantly affect fragmentation. Young and old-growth forests exhibit distinct fragmentation characteristics based on their composition and age structure, with older and taller trees, especially in conifer forests, being more susceptible to wind damage (Wulder et al., 2009). Severe wind events initiate a two-stage process of damage propagation in forests, starting with critical downward gusts and escalating as damaged areas expand (Dupont et al., 2015). Additionally, the study by Konings et al. (2021) on vegetation water content provides insights into how moisture levels impact forest resilience to environmental stressors. This comprehensive view highlights the importance of considering structural diversity and the physical factors contributing to fragmentation to enhance our understanding of forest ecosystem dynamics.

3.2. Human factors

Human activities significantly influence forest fragmentation, even in predominantly natural study areas (Haddad et al., 2015). The expansion of roads (Newman et al., 2014) and the introduction of croplands lead to land conversion and degradation, thereby disrupting forest continuity and intensifying fragmentation. Edge effects, where forests border non-forest areas, result in ecological consequences such as increased carbon emissions, as noted by Scanes (2018) and supported by findings from Haddad et al. (2015) and Mengist et al. (2022). Furthermore, Mitchell et al. (2014) explore how agricultural expansion and forest fragmentation impact ecosystem services, revealing the critical role of forest fragments in sustaining these services across agricultural landscapes. These studies collectively highlight the growing importance of addressing human factors in forest fragmentation and stress the need for managing habitat fragmentation and landscape structure to ensure the provision of multiple ecosystem services.

4. Methodology

The methodological schematic diagram depicted in Fig. 3, shows the workflow that had been carried out, it is further explained in the subsections below.

4.1. Image reclassification for fragmentation analysis

The initial step of our research entailed deriving vegetation cover

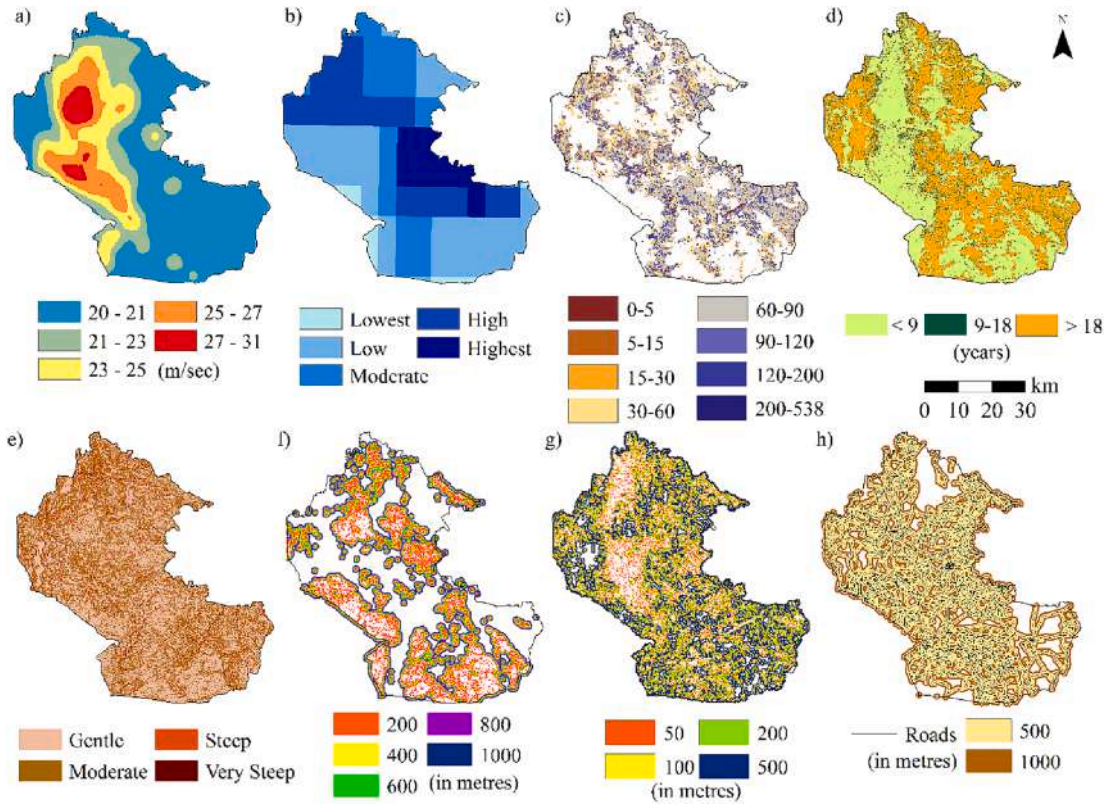

Fig. 2. Spatial representation of various ecological and geographical variables within the Tuchola Forest Biosphere Reserve (TFBR), Poland. Panels display (a) wind speed, (b) vegetation water content, (c) tree age distribution, (d) tree height, (e) slope gradient, (f) distance from cropland, (g) distance from bare land, and (h) distance from roads, derived from the different data source as mentioned in table 1.

Table 1
Data sources of predictive variables.

Factors	Source
Wind speed	ESSL, ESWD, ERA5 (ECMWF)
Vegetation water content	SMAP Enhanced L3 Radiometer Global and Polar Grid Daily 9 km EASE-Grid Soil Moisture, Version 5
Tree age	Bank Danych o Lasach (BDL) 2017
Tree height	Global Land Cover Facility, University of Maryland
Slope gradient	USGS SRTM DEM
Distance from cropland	Dynamic World image collection (2015–2020 average)
Distance from bare land	Dynamic World image collection (2015–2020 average)
Distance from roads	Global Roads Inventory Project - GRIP - version 4

maps from 2015 to 2020, as elaborated in Section 2.1. This phase utilized the PALSAR-2 Forest/Non-Forest Map in conjunction with the Dynamic World dataset, integrating Synthetic Aperture Radar (SAR) imagery analysis with near-real-time Land Use/Land Cover (LULC) data. This integration not only enhanced the accuracy of our vegetation mapping but also provided a comprehensive understanding of vegetative dynamics over the years, laying a solid foundation for our research.

Subsequently, the data from both datasets underwent a detailed reclassification into binary raster maps, a pivotal step for differentiating forest from non-forest areas. This reclassification was facilitated using Google Earth Engine (GEE), where the PALSAR-2 dataset, for the years 2015 to 2017, was reclassified with '1′ representing non-forest areas (including water bodies) and '2′ for forest areas. For data post-2017, the PALSAR data, now enriched with four bands, underwent a similar reclassification, merging Dense Forest and Non-dense Forest into a single Forest category ('2′), and Non-Forest and Water categories into a Non-Forest category ('1′). The Dynamic World dataset was also reclassified, applying a forest mask to the 'trees' band to designate forest areas as '2′ and non-forest areas as '1′, covering various land covers such as 'water', 'grass', 'flooded_vegetation', 'crops', 'shrub_and_scrub', 'built', 'bare', and 'snow_and_ice'. This methodological approach, using GEE for both datasets, enabled a nuanced analysis of different land covers, vital for accurately delineating forested from non-forested regions.

To standardize the projections and resolution, the PALSAR dataset was downloaded with a spatial resolution of 25 m and reprojected to the ETRS 1989 Transverse Mercator (EPSG:2180) coordinate system. Similarly, the Dynamic World data, with a finer scale of 10 m, was processed. Both datasets were then reclassified in GIS tools to uniform dimensions of 2550 by 2693 pixels and a cell size of 30x30 meters, ensuring consistency in spatial analysis across all images.

4.2. Forest area Density (FAD) analysis

The GUIDOS Toolbox (GTB) was pivotal in our study for analyzing forest fragmentation over six years using comprehensive datasets. Employing the Forest Area Density (FAD) function within GTB, which utilizes a per-pixel moving window technique, allowed for an assessment across variable observational scales: 7x7, 13x13, 27x27, 81x81, and 243x243 pixels. This multi-scalar analysis provided a nuanced view of forest structure and dynamics, integral to decoding ecosystem complexities (Vogt, 2023; Riitters et al., 2002, 2012a, b).

Our analysis specifically concentrated on the 'Rare' and 'Patchy' categories within the six-class categorization of Forest Area Density (FAD). These classes were chosen due to their representation of the most fragmented and disconnected forest zones. The 'Rare' class denotes areas with less than 10 % forest cover, while 'Patchy' refers to regions having 10 % to less than 40 % forest cover. The selection of these two classes was instrumental in providing evidence of forest fragmentation

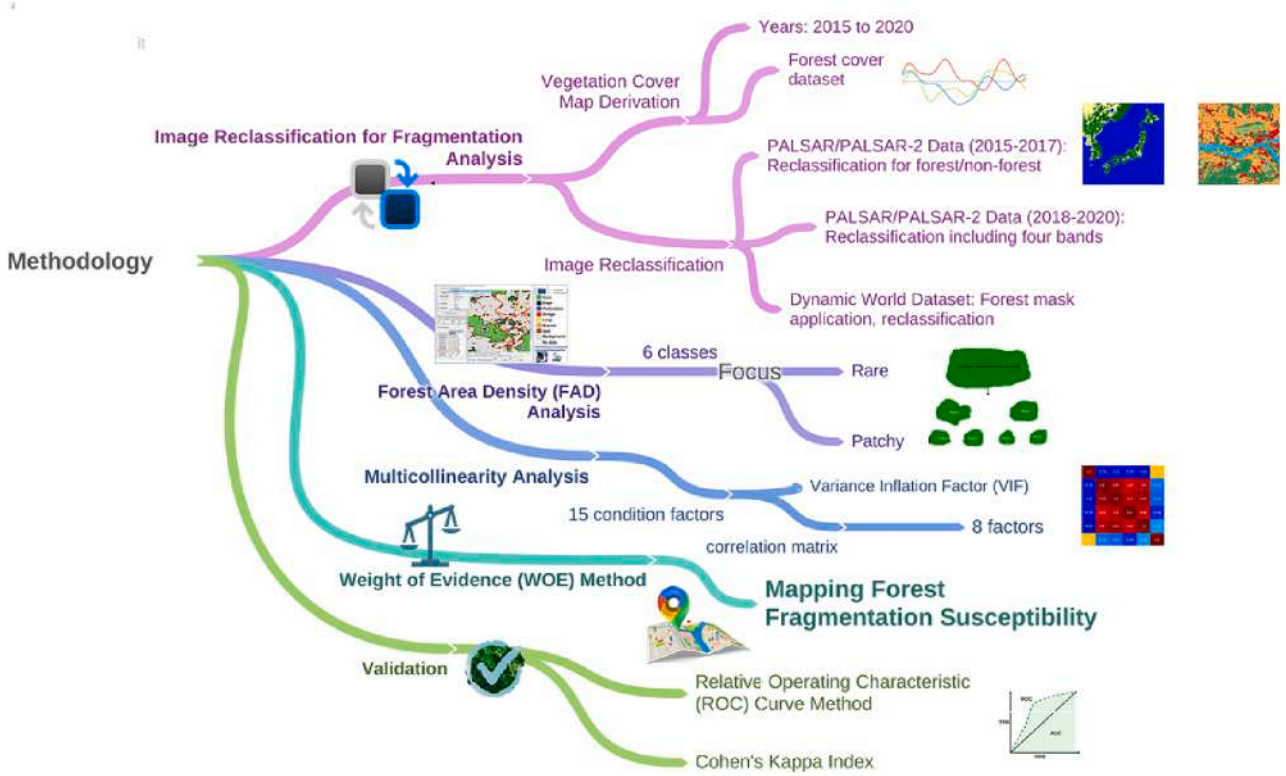

Fig. 3. Comprehensive methodological workflow. This figure presents the detailed methodological workflow employed in the study, starting from the derivation of vegetation cover maps using PALSAR-2 and Dynamic World datasets for the period 2015 to 2020. It illustrates the step-by-step process of image reclassification for forest/non-forest differentiation, forest area density (FAD) analysis focusing on 'Rare' and 'Patchy' fragmentation classes, multicollinearity analysis to refine predictive variables, and the application of the weight of evidence (WOE) method for mapping forest fragmentation susceptibility. Validation using the relative operating characteristic (ROC) curve method and Cohen's Kappa Index is included to confirm the robustness of the model.

in our model, highlighting areas significantly distanced from the core forest regions. This focus allowed for a detailed examination of the extent and impact of forest fragmentation, a key aspect of our study.

4.3. Predictive variables through multicollinearity analysis

In our study on forest fragmentation, we initially considered a diverse set of fifteen variables: tree species, aspect, tree age, forest type, elevation, slope, vegetation water content, soil type, tree height in 2015 and 2020, distance from road, cropland, bareland, forest, and wind speed. However, upon a detailed examination using both a Correlation Coefficient Matrix and the Variance Inflation Factor (VIF), we identified multicollinearity issues that could lead to unreliable statistical inferences, as they contravene the assumption of independent regressors (O'Brien, 2007). Notably, variables such as tree species, aspect, and forest type displayed linear relationships with other factors, indicating redundancy, and were thus excluded.

To enhance the precision of our model, we embarked on a rigorous exclusion process, following the guidelines recommended by García-Orozco et al. (2023) and incorporating fuzzy logic principles akin to those proposed by Omar et al. (2022). This refinement process resulted in the selection of eight independent factors deemed crucial for our model, as illustrated in Fig. 4: wind speed, vegetation water content, tree age, tree height in 2020, slope, distance from cropland, distance from bareland, and distance from roads. These variables were chosen due to their low correlation matrix scores and significant relevance to the fragmentation patterns observed from 2015 to 2020. During this period, numerous areas previously classified as patchy forest transitioned to bareland or cropland, pinpointing the importance of these selected factors in reflecting the current landscape conditions.

This methodical selection process bolsters the robustness of our model by mitigating multicollinearity, a crucial aspect for ensuring the validity of regression-based predictions. Our approach aligns with the best practices in ecological modeling, aimed at providing reliable data to support informed forest management and conservation strategies. The final selection of variables represents a deliberate balance between comprehensive data inclusion and statistical integrity, recognizing that each factor independently contributes to our understanding of forest fragmentation dynamics. By refining the variables, our model's predictive accuracy for areas at risk is significantly enhanced, which is vital for developing targeted conservation interventions. Our methodology showcases the adaptability required in ecological studies, ensuring that our conclusions are grounded in statistically sound practices and lay a solid foundation for ongoing and future forest management efforts.

4.4. Construction of the forest fragmentation susceptibility map

The methodical extraction of patchy areas, as discussed in section 4.2, was crucial for the construction of the Forest Fragmentation Susceptibility Map. This process involved correlating the eight variables detailed in Fig. 2—wind speed, vegetation water content, tree age, tree height in 2020, slope, distance from cropland, distance from bareland, and distance from roads—with these patchy zones (Fig. 7). This step was fundamental in providing an incisive investigation into the association between environmental factors and fragmentation susceptibility. By employing the weight-of-evidence approach, detailed in the subsequent section, our study precisely evaluated the susceptibility of these forested areas to fragmentation. This process enhanced our understanding of forest fragmentation dynamics, laying the groundwork for future discussions on the implications of our findings.

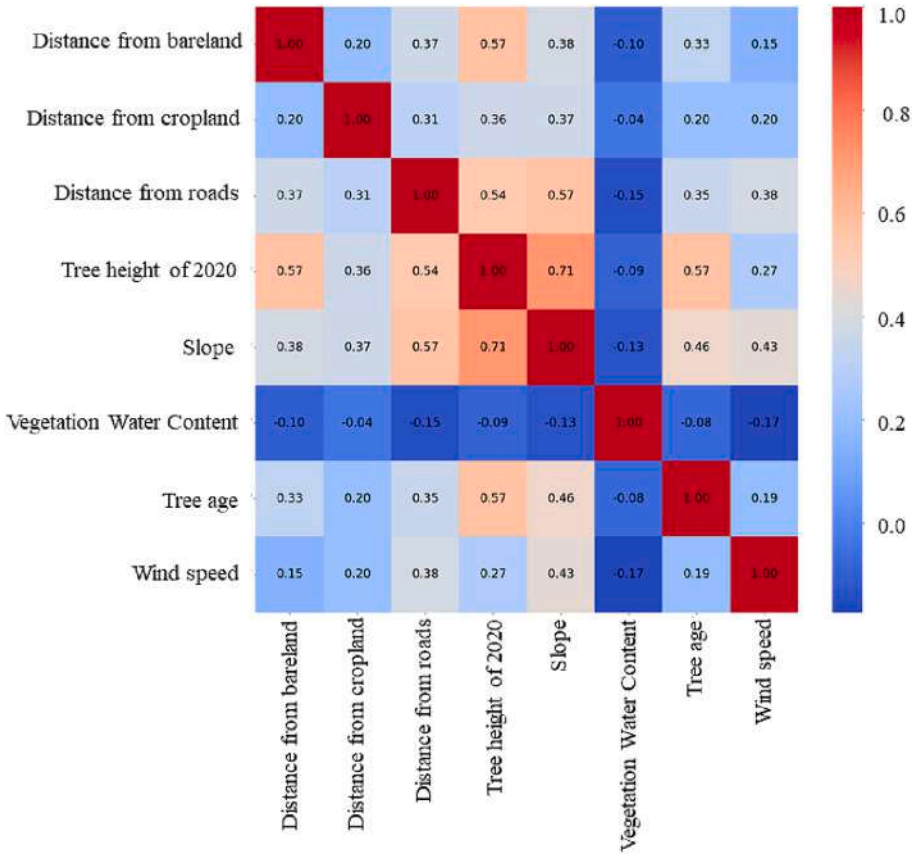

Fig. 4. Correlation matrix displaying Pearson correlation coefficients for eight predictive variables. The variables are ordered as follows: distance from bareland, distance from cropland, distance from roads, tree height of 2020, slope, vegetation water content, tree age, and wind speed. High values represent higher correlation in red and vice versa.

4.5. *Weight of evidence (WOE) method*

In our study, we utilize the Weight-of-Evidence (WOE) method, a Bayesian modeling technique, to map forest fragmentation susceptibility. This quantitative approach, initially developed in the field of mineral exploration (Bonham-Carter, 1990), has been widely applied in ecological studies due to its effectiveness in evaluating spatial associations between variables and observed phenomena.

We calculate the positive (W +) and negative weights (W −) for each variable class related to patch forests, using the method refined by Sterlacchini et al. (2011). These weights are determined using the following formulas:

$$W^{+} = \log_e\left(\frac{P(B|D)}{P(\overline{B}|\overline{D})}\right)$$

$$W^{-} = \log_e\left(\frac{P(\overline{B}|D)}{P(\overline{B}|\overline{D})}\right)$$

Here, P denotes probability, B the presence of a class of patch forest predictive variable, $\overline{B}$ its absence, D the presence of a patch forest, and $\overline{D}$ the absence of a patch forest (Fan et al., 2011).

The contrast between these weights, known as the weight contrast (C), is defined as:

$$C = W^{+} - W^{-}$$

This measure reflects the spatial association strength between the variables and patch forests. To refine our analysis, we calculate the standardized weight contrast (Wstd) as the ratio of C to its standard deviation, S(C):

For the standard deviation of the weight contrast $S(C)$:

$$S(C) = \sqrt{S^2(W^{+}) + S^2(W^{-})}$$

For the variances $S^2(W^{+})$ and $S^2(W^{-})$:

$$S^2(W^{+}) = \frac{1}{N_{B\cap D}} + \frac{1}{N_{B\cap\overline{D}}}$$

$$S^2(W^{-}) = \frac{1}{N_{\overline{B}\cap D}} + \frac{1}{N_{\overline{B}\cap\overline{D}}}$$

The standardized weight contrast (Wstd) is then calculated:

$$Wstd = \frac{C}{S(C)}$$

A positive Wstd value indicates a factor's favourable influence on forest fragmentation, while a negative value suggests an unfavourable influence. A value close to zero indicates a minimal relation to forest fragmentation. Finally, the Forest Fragmentation Susceptibility Index (FFSI) is derived by summing the standardized weight contrasts (Wstd) for each variable:

$$FFSI = \sum Wstd$$

This detailed formulation of the WOE method, incorporating rigorous statistical analysis, ensures a robust approach for understanding and predicting patterns of forest fragmentation. This calculation methodology is consistent with the approach described by Batar et al. (2021). Our application aligns with the principles of objective and transparent scientific inquiry, as advocated in broader ecological studies (Dekant &

Bridges, 2016).

4.6. Validation of the forest fragmentation susceptibility map

The validation of predictive models is a fundamental step in ecological research, particularly when addressing critical issues such as forest fragmentation. Given the complexity of forest ecosystems and the multifaceted influences leading to fragmentation, our approach integrates both the Relative Operating Characteristic (ROC) curve method and Cohen's Kappa Index to offer a comprehensive evaluation of the Forest Fragmentation Susceptibility Map.

4.6.1. Validation by ROC method

To validate our forest fragmentation susceptibility map, we employed the relative operating characteristic (ROC) curve method. This standard approach evaluates model performance by analyzing the area under the curve (AUC), which assesses a classifier's overall ranking capability across all possible classification thresholds. Such a measure is crucial for comparing learning algorithms and optimizing model construction (Fawcett, 2006; Mingote et al., 2020). The ROC-AUC's utility stems from its ability to provide a single, comprehensive value representing model accuracy, with values closer to 1 indicating higher accuracy and values near 0.5 suggesting limited predictive capability (Fawcett, 2006; Batar et al., 2021).

The AUC formula for a two-class problem is:

$$AUC = \frac{\sum \text{rankings of positive samples} - \frac{n_p(n_n+1)}{2}}{n_p n_n}$$

Here, n_p and n_n represent the counts of positive and negative samples, respectively. The AUC of the ROC reflects the quality of the probabilistic model in predicting the occurrence or non-occurrence of an event (Fawcett, 2006).

4.6.2. Validation by Cohen's Kappa Index

The AUC-ROC method, while widely used, is not without its limitations, particularly in its potential to obscure model performance in specific operational contexts (Lobo et al., 2007; Vakhshoori and Zare, 2018). As such, to complement our ROC curve analysis, we conducted a confused matrix and Cohen's kappa index for validation. This statistical tool is essential for measuring the concordance between observed and predicted classifications within the forest fragmentation susceptibility map, while correcting for chance agreement (Cohen, 1960; Vakhshoori and Zare, 2018).

Cohen's Kappa (κ) is calculated to measure the agreement between two raters, adjusting for chance agreement. The formula is:

$$\kappa = \frac{P_{obs} - P_{exp}}{1 - P_{exp}}$$

where (P_{obs}) is the observed agreement among raters, and (P_{exp}) is the expected agreement by chance. Our dataset, (P_{obs}) and (P_{exp}) are derived as follows:

$$P_{obs} = \frac{TP + TN}{N}$$

$$P_{exp} = \frac{(TP + FN) \times (TP + FP) + (FP + TN) \times (FN + TN)}{N^2}$$

Here, TP, TN, FP, and FN represent true positives, true negatives, false positives, and false negatives, respectively, with N being the total number of observations.

5. Results

5.1. Comparison of remote sensing datasets

The comparative analysis of PALSAR (25 m resolution) and Dynamic World (10 m resolution) datasets in mapping forest fragmentation in Tuchola Forest, Poland, from 2015 to 2020, demonstrates a clear preference for the PALSAR dataset. This is particularly evident in Fig. 5, which presents the trends in the 'Dominant' and 'Interior' classes (representing low and very low fragmentation, respectively) in both datasets. The line graphs for these classes in datasets (a) PALSAR and (b) Dynamic World reveal significant shifts post the 2017 derecho event, with the PALSAR dataset more markedly capturing the changes in forest structure. These shifts identify PALSAR's enhanced capability to detect subtle and significant alterations in the forest landscape, especially in response to sudden environmental disturbances.

Building upon these insights, Fig. 6 delves deeper into the 'Rare' (very high fragmentation) and 'Patchy' (high fragmentation) classes. Prior to 2017, the levels of fragmentation in these classes were almost negligible. However, post-2017, there was a significant rise, with the 'Rare' class in PALSAR data increasing from virtually 0 % in the years preceding 2017 to 38.68 % by 2020. Similarly, the 'Patchy' class also showed a substantial increase, rising from 7.7 % in 2017 to 30.7 % by 2020. In contrast, the Dynamic World dataset depicted these changes to a lesser extent, with the 'Rare' class peaking at 23.47 % and the 'Patchy' class at 20.32 % in 2020.

These findings, illustrated through Figs. 5 and 6 are not mere statistical variances but reflect the intrinsic capacity of the PALSAR dataset to accurately depict environmental dynamics, even during acute natural events. The implications of these results are substantial for forest conservation efforts and policy-making, highlighting the critical need for selecting appropriate remote sensing tools that can faithfully represent environmental changes.

5.2. Results of the multicollinearity analysis

Our correlation coefficient matrix, refer to Fig. 4, indicates a predominantly low to moderate interdependence among the environmental factors related to forest fragmentation. Most predictive variables show low correlation coefficients (mostly blue shades), suggesting their independence.

Particularly, "Vegetation Water Content" is the most independent variable, displaying minimal correlation with others, while "Tree age" and "Wind speed" also show low intercorrelations. Despite some moderate correlations between "Distance from cropland" and "Distance from roads" with "Tree height of 2020″ and "Slope," these are not substantial enough to indicate problematic multicollinearity. These findings affirm that the chosen variables in our model maintain their integrity for an unbiased analysis.

5.3. Rare and patchy forest fragmentation assessment

Utilizing the Forest Area Density (FAD) function within GTB using PALSAR, our analysis identified 'Rare' and 'Patchy' fragmentation classes as areas with FAD below 40 %. These classifications denote non-continuous and extensively fragmented forest sections. Subsequent spatial analysis for the period 2015–2020 quantified these patchy forests at 175.6 km2, equating to 5.49 % of the study's total area. Over time, some of these regions have undergone further fragmentation, transitioning into bareland or cropland, thus being excluded from further analysis.

Incorporating the 2023 forest layer with a 10 m resolution allowed us to identify persistent rare and patchy forest fragments within the current forest boundaries. These areas, totaling 30.10 km^2, constitute 0.94 % of the total study region and are integral to the subsequent susceptibility analysis. The forest cover has decreased by approximately 33.23 square

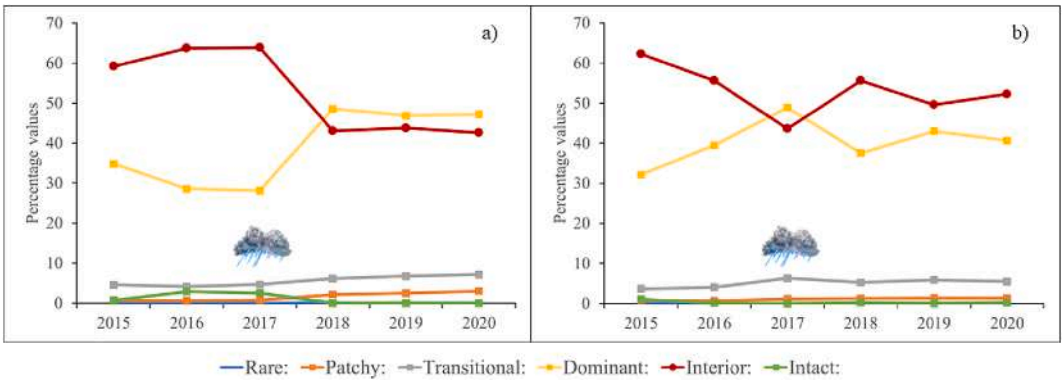

Fig. 5. FAD values through the years 2015–2020 in datasets a) Palsar b) Dynamic World.

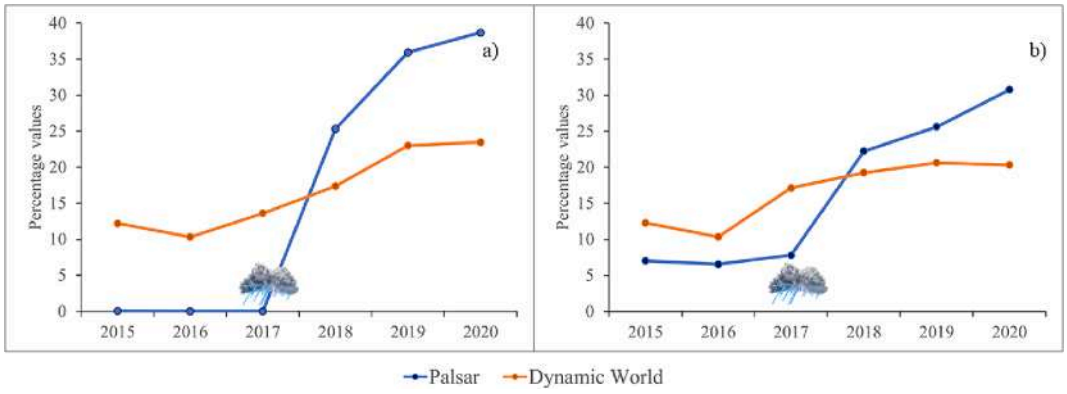

Fig. 6. FAD values in the two datasets through the years 2015–2020 for a) rare class b) patchy class.

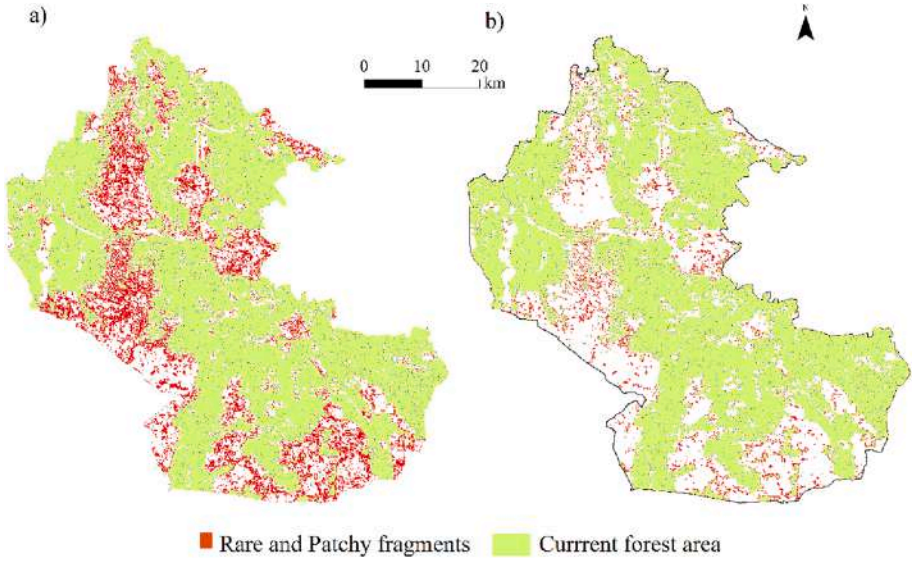

Fig. 7. Rare and patchy fragments in a) entire study region (2015–2020) and b) current forest areas of 2023.

kilometers from the year 2020 to 2023. This represents a percentage change of approximately −1.89 %, indicating a continued trend of forest fragmentation and loss within the study area. The utilization of the 2023 forest layer was pivotal in our study to understand susceptible zones in the future, focusing on the rare and patchy fragments that were present in the 2023 forest cover layer for a comprehensive analysis of the landscape's vulnerability. Fig. 7a and 7b illustrate the geographical distribution of these forests within the Tuchola Forest, showcasing the contrasts before and after the extraction process, and highlighting the changes in forest fragmentation susceptibility from the final year of the study period up until the current time.

5.4. *Forest fragmentation susceptibility analysis*

The forest fragmentation susceptibility map (Fig. 8) presents a detailed visualization of the areas within the Tuchola Forest that are

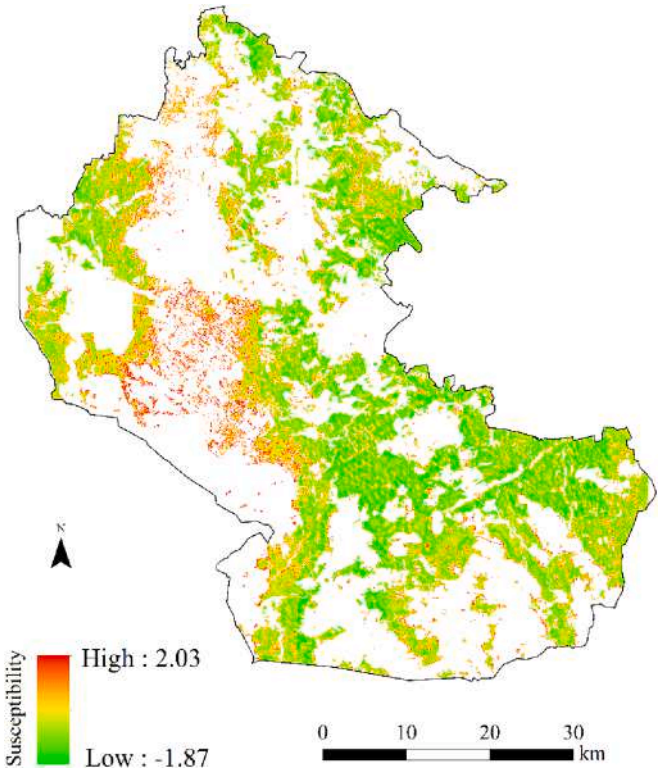

Fig. 8. Forest fragmentation susceptibility map.

particularly vulnerable to fragmentation, integrating an exhaustive analysis that takes into account a variety of predictive variables. The importance of these factors has been quantitatively assessed using the Weight of Evidence (WoE) method (Table 2), with the results indicating significant influencers on forest fragmentation susceptibility. The analysis revealed that the nearest distance from cropland, specifically within 200 m, has the most substantial positive influence on forest fragmentation susceptibility, evidenced by a WoE value of 0.54. This finding illustrates that forest areas in closer proximity to croplands are at a higher risk of fragmentation. Other significant factors contributing to increased susceptibility include the closest distances from bareland (50 m), tree height within the < 9 m range, and tree ages between 5 and 15 years, highlighting the nuanced interplay of various environmental and anthropogenic elements in forest fragmentation. Additionally, external environmental conditions such as high wind speeds (25–27 km/h) and moderate vegetation water content further exacerbate the susceptibility to fragmentation.

On the contrary, factors such as steeper slopes and greater distances from cropland and bareland correlated with reduced forest fragmentation risk. The gentlest slopes were associated with the lowest susceptibility (WoE value: −0.63), suggesting these areas are less likely to undergo fragmentation (see table 2).

Overall, the results reveal the intricate interplay between various environmental factors and their impact on forest fragmentation susceptibility. The findings from Table 1, coupled with the ROC analysis, provide a robust foundation for targeted conservation efforts aimed at mitigating the risks of further fragmentation within the Tuchola Forest landscape.

5.5. Validation of forest fragmentation susceptibility map

The validation of the Forest Fragmentation Susceptibility Map is further reinforced through comprehensive analyses, incorporating both the ROC curve and Cohen's Kappa Index to evaluate model performance. The ROC curve analysis, illustrated in Fig. 9, demonstrates the model's reliability in predicting susceptibility, achieving an AUC value of 0.82. This high discriminative capacity signifies the model's adeptness at distinguishing between areas susceptible and not susceptible to fragmentation.

The Cohen's Kappa calculation yielded an index of 0.68, indicating substantial agreement beyond chance. These metrics offer compelling evidence of the model's accuracy in classifying areas according to their fragmentation susceptibility, affirming the effectiveness of our methodological approach in forest conservation planning (see Table 3).

6. Discussion

6.1. Implication of fragmentation (FAD) in different datasets

Our comparative analysis between the PALSAR and Dynamic World datasets reveals PALSAR's superior sensitivity in detecting 'Rare' and 'Patchy' forest fragmentation post-2017, an observation echoed by Atkins et al. (2023) and Balling et al. (2023). These studies highlight the advanced radar technologies, like PALSAR, for their nuanced detection of environmental changes and shifts in forest structure, especially following significant disturbances such as the 2017 windstorm. Microwave remote sensing, as employed by PALSAR, offers distinct advantages across various environmental settings. Awange & Kiema (2013) elucidate the critical role of microwave sensing in overcoming the limitations posed by persistent cloud cover and dense vegetation, notably in tropical regions where optical remote sensing faces significant challenges. This technology's ability to penetrate vegetation canopies and function effectively under conditions of high cloud cover, such as during wet seasons, is indispensable for comprehensive fragmentation studies, particularly after severe weather events.

Furthermore, the integration of SAR and optical remote sensing methods, as demonstrated by Louzada et al. (2023), supports our findings and emphasizes the necessity of selecting the appropriate remote sensing technology tailored to specific environmental conditions and research objectives. Similarly, Meraner et al. (2020) highlight the potential of SAR-optical data fusion in removing clouds from optical imagery, using deep learning approaches to preserve the integrity of surface observations beneath cloud cover.

The effectiveness of PALSAR's microwave remote sensing in accurately capturing changes in forest structure, despite its lower resolution compared to high-resolution optical sensing from Dynamic World, demonstrates its utility in forest fragmentation analysis. This is especially relevant in post-disturbance scenarios, emphasizing the importance of choosing SAR technologies like PALSAR for forest cover and fragmentation studies. Our research not only reinforces the significance of PALSAR in forest conservation and decision-making processes but also aligns with the broader scientific consensus on the adaptability and effectiveness of SAR technology in addressing the challenges of optical remote sensing limitations.

6.2. Influence of environmental factors on forest fragmentation susceptibility

6.2.1. Integrated analysis of forest fragmentation factors

Challenging the conventional wisdom, Morreale et al. (2021) suggest that temperate forest edges may demonstrate increased growth and biomass compared to their tropical counterparts, casting new light on edge-induced vulnerability. This revelation underpins our investigation into the Tuchola Forest, where we dissect the influence of both environmental and anthropogenic factors on forest fragmentation.

Our findings highlight proximity to cropland as a significant anthropogenic influence. Forest fragments within 200 m of cropland demonstrate the highest susceptibility to fragmentation, supporting global patterns observed by Haddad et al. (2015). The role of agricultural expansion and its impact on the floristic composition at the forest-cropland interface (Ribeiro et al., 2019) calls for a nuanced approach to

Table 2
Weight of Evidence (WoE) values for forest fragmentation susceptibility factors.

Variable	Subdivision	WoE values
Distance from Cropland	200	0.54
Distance from Bareland	50	0.37
Tree height	9-18	0.36
Tree age	5-15	0.28
Wind Speed	25 - 27	0.19
Distance from Bareland	100	0.18
Vegetation Water Content	Moderate	0.16
Wind Speed	27 - 31	0.16
Slope	Steep	0.13
Tree age	0-5	0.12
Tree age	15-30	0.11
Vegetation Water Content	Low	0.09
Slope	Moderate	0.09
Vegetation Water Content	Lowest	0.08
Tree age	30-60	0.04
Wind Speed	21 - 23	0.03
Slope	Very Steep	0.03
Distance from Road	500	0.01
Tree height	0-9	0.01
Wind Speed	23 - 25	0.00
Tree age	200-538	0.00
Distance from Road	1000	-0.01
Tree age	120-200	-0.04
Vegetation Water Content	Highest	-0.07
Distance from Cropland	400	-0.10
Distance from Bareland	200	-0.18
Tree age	90-120	-0.19
Slope	Gentle	-0.19
Vegetation Water Content	High	-0.19
Tree age	60-90	-0.23
Distance from Cropland	600	-0.24
Wind Speed	20 - 21	-0.24
Distance from Cropland	1000	-0.26
Distance from Cropland	800	-0.26
Tree height	18-26	-0.33
Distance from Bareland	500	-0.41

land-use planning that considers ecological impacts. Our results from the Tuchola Forest corroborate these observations and echo similar fragmentation patterns noted by Mengist et al. (2022) across Poland, emphasizing the enduring legacy of historical land-use on present-day forest structure and biodiversity (Mazgajski et al., 2010).

Tree characteristics, notably height and age, emerged as pivotal natural factors. Our data indicates that younger forests (5–15 years) and shorter trees (less than 9 m) are more vulnerable to fragmentation. This is in line with the findings of Rodrigues et al. (2016), who observed long-term structural changes in forest canopies and the impact of anthropogenic disturbances on tree height and spatial structure. Moreover, Wulder et al. (2009) provide insight into how forest age and fragmentation are interrelated, further suggesting the influence of these factors on the ecological dynamics of forest landscapes.

Wind speed and vegetation water content are additional natural determinants of fragmentation risk. High wind speeds (25–27 km/h) and moderate water content conditions were associated with increased fragmentation risks, implying the necessity of incorporating meteorological and hydrological considerations into forest management (Konings et al., 2021; Doane et al., 2023; Li et al., 2023).

Additionally, the influence of topography on fragmentation susceptibility is accentuated by our findings. Guo et al. (2024) found that extensively burned forest patches are often located at higher elevations, while more fragmented patches tend to occur in areas with gentle slopes. Our results corroborate this pattern, suggesting that less steep slopes may facilitate the spread of fragmentation.

The interplay between forests and their topographic context is further elaborated by Doane et al. (2023), who delve into the concept of topographic roughness as a natural archive of wind events. Their work suggests that forests coevolve with their environment, with topography influencing the resilience of forests to windthrow events.

In summary, our integrated analysis of forest fragmentation factors in the Tuchola Forest emphasizes the multifaceted nature of susceptibility. It highlights the urgency of incorporating a diverse range of ecological and physical variables into forest management and conservation strategies to ensure resilience against ongoing and future environmental challenges.

6.2.2. *Tree specie characteristics*

In the Tuchola Forest, the composition of tree species, including the predominance of Scots pine (*Pinus sylvestris*) (82.78 %), followed by Silver birch (*Betula pendula*) (7.39 %) and English oak (*Quercus robur*) (1.29 %), suggests a landscape largely shaped by the resilience and susceptibility of these species to fragmentation (see Figure S1). Despite not being the primary factors in our correlation analysis, the species characteristics significantly contribute to the nuanced ecological dynamics of the forest. Scots pine (*Pinus sylvestris*), with its notable resilience, contrasts with the heightened vulnerability of Silver birch (*Betula*

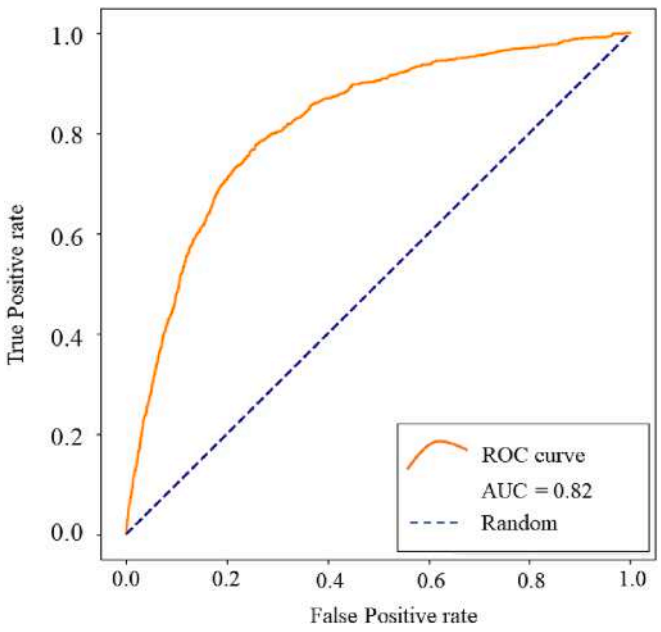

Fig. 9. The accuracy of the forest fragmentation susceptibility map.

Table 3
Summary of classification metrics for Cohen's Kappa Index.

Metric	Value
True Negative (TN)	1,494,224
False Positive (FP)	2013
False Negative (FN)	426
True Positive (TP)	2551
Cohen's Kappa Index	0.68

pendula) and English oak (*Quercus robur*) near forest edges. This distinction is crucial for understanding the intricate effects of fragmentation and is supported by the findings of Konôpka et al. (2020) and Budniak & Zięba (2022), which emphasize variable impacts on different species within Polish forests. Their findings resonate with our investigation into species-specific susceptibility and highlight importance of informed management practices tailored to the unique ecological roles and physiological needs of each species.

Pimentel et al. (2013) and Roche and Campagne (2017) advocate for an ecosystem integrity framework that incorporates both species diversity and environmental factors into forest management decisions. This approach is vital for addressing the specific needs of Scots pine (*Pinus sylvestris*), Silver birch (*Betula pendula*), and English oak (*Quercus robur*). The genetic robustness of Scots pine (Pinus sylvestris), as discussed by González-Díaz et al. (2017), may underpin its resilience, offering insights into adaptive strategies for forest conservation. Conversely, the pioneering nature of Silver birch (*Betula pendula*), highlighted by Oksanen (2021) suggests a vulnerability to edge effects that necessitates careful consideration in forest management practices. Similarly, the decline of English oak (*Quercus robur*) in altered disturbance regimes, as noted by Knoot et al. (2010), calls for a nuanced understanding of its ecological and physiological sensitivities.

Coates et al. (2018) contribute to this discourse by differentiating the effects of partial harvesting on species-specific windthrow susceptibility, particularly near forest edges. This aspect is crucial for managing fragmented landscapes, where selective interventions and the recognition of tree-level heterogeneity can influence the overall resilience of forest ecosystems to storm events.

By integrating these varied perspectives, our discussion offers a comprehensive examination of the physiological, ecological, and genetic dimensions that define the responses of Scots pine (*Pinus sylvestris*), Silver birch (*Betula pendula*), and English oak (*Quercus robur*) to fragmentation. Such a multifaceted approach is essential for developing forest management practices that are sensitive to the distinct characteristics of each species, ensuring their continued health and viability in changing environmental conditions. Through this lens, we aim to enhance the resilience of forest ecosystems, mitigating the impacts of fragmentation and promoting sustainable forest landscapes.

6.2.3. Holistic approach to forest management

Incorporating diverse factors into our model not only enhances predictive accuracy but also aligns with the ecosystem integrity framework crucial for the resilience of forests like the Tuchola Forest. This holistic approach, informed by our findings and echoed by the comprehensive analyses of forest fragmentation in Poland by Referowska-Chodak & Kornatowska (2021), stresses the importance of considering both species diversity and environmental factors in forest management strategies. The integration of development and conservation policies, as discussed by Szramka & Adamowicz (2020), becomes paramount, offering insights for anticipating high-risk fragmentation areas and emphasizing sustainable management practices that prioritize long-term ecosystem integrity and resilience.

6.3. Methodological adaptation and predictive model refinement

The refinement of variables in our study marked a pivotal transition towards an enhanced model for predicting forest fragmentation susceptibility. Initial analyses using 15 variables were fine-tuned to focus on the current vegetation state, leading to the exclusion of non-vegetated areas formerly identified as susceptible. Ground-truthing revealed that the earlier model overestimated susceptibility in areas no longer forested. Subsequent multicollinearity analysis informed the removal of highly interdependent variables such as soil type, and less impactful ones like forest type and species, as well as aspect and elevation in this relatively flat region.

A discernible shift in the susceptibility patterns was evident when comparing the previous and current maps. Where the initial model indicated heightened susceptibility at the forest edges, the refined model demonstrated more dispersed susceptibility zones, particularly in central areas with the highest wind speeds recorded between 2015 and 2020 (Fig. 2). This adaptation not only corroborated the significant role of wind in forest fragmentation but also resulted in a notable increase in model accuracy, with the ROC curve's accuracy improving from 0.64 to 0.82 which suggests an accurate and reliable model along with the Cohen's Kappa Index calculation.

The adjustment of our analytical framework, informed by empirical evidence and expert field knowledge, illustrates the dynamic nature of ecological modeling. It highlights the importance of iterative analysis and underlines the value of precise variable selection in developing models with high predictive accuracy, crucial for the formulation of effective forest management and conservation strategies.

7. Conclusion

Our study in the Tuchola Forest region not only highlights the specific challenges faced by this area but also serves as a microcosm for the broader, global imperative for adaptive forest management in the face of climate change. The heightened susceptibility of forests to windthrow events, particularly near croplands and barelands, coupled with the pivotal role of species diversity in bolstering ecosystem resilience, emphasizes the universal relevance of our findings. This global perspective reinforces the necessity of implementing adaptive management strategies worldwide to safeguard forest ecosystems against the escalating threats posed by wind disturbances and other climate change-related stressors.

Drawing on insights from Forzieri et al. (2020) regarding the increasing intensity of wind disturbances and Sanginés de Cárcer et al.

(2021) on effective post-windstorm management, our work highlights the necessity of integrating empirical data with best forestry practices. Customized strategies that consider specific forest types and site conditions are essential.

Future research should explore the balance between ecological impacts and salvage logging, incorporating climate change considerations more explicitly into forest management plans. The findings from the Joint Research Centre (JRC) on forest landscape patterns and fragmentation in Europe highlight the need for comprehensive plans addressing spatial patterns and connectivity (European Commission, Joint Research Centre (JRC), 2023; Sanginés de Cárcer et al., 2021).

In summary, our study advocates for dynamic forest management approaches that meld in-depth research, existing literature, and practical insights. Such strategies are critical to maintain the ecological integrity of forests like the Tuchola Forest, enhancing ecosystem services and ensuring resilience amidst evolving environmental challenges (Pimentel et al., 2013).

8. Declaration of Generative AI and AI-assisted technologies in the writing process

During the preparation of this work the author(s) used ChatGPT for language polishing and editing the manuscript. After using this tool/service, the author(s) reviewed and revised the content as needed and take(s) full responsibility for the content of the publication.

CRediT authorship contribution statement

Sanjana Dutt: Writing – review & editing, Writing – original draft, Visualization, Validation, Software, Resources, Methodology, Investigation, Funding acquisition, Formal analysis, Data curation, Conceptualization. **Amit Kumar Batar:** Writing – review & editing, Conceptualization, Data curation, Formal analysis, Methodology, Software, Supervision. **Sławomir Sulik:** Data curation. **Mieczysław Kunz:** Visualization, Supervision.

Declaration of competing interest

The authors declare that they have no known competing financial interests or personal relationships that could have appeared to influence the work reported in this paper.

Data availability

Data will be made available on request.

Acknowledgements

We extend our deepest gratitude to the European Severe Storms Laboratory (ESSL) and the team at the European Severe Weather Database (ESWD) for providing critical data that significantly contributed to the research presented in this article. Special thanks are extended to Thomas Schreiner and Igor Laskowski at ESSL for their invaluable support and guidance.

Our heartfelt appreciation goes to Marcin Myszkowski from the Bank Danych o Lasach (Forest Data Bank) at Biuro Urządzania Lasu i Geodezji Leśnej. His assistance in providing essential forest data and translating from Polish to English, played a pivotal role in the success of our study.

We are also immensely grateful to Karolina Lubińska, Chief Nature Conservation Specialist at the National Park "Tuchola Forest". Her insights and expertise in the area of nature conservation were instrumental in shaping our understanding of the Tuchola Forest region.

This work was supported by a grant for open access provided by the 'Excellence Initiative - Research University' program. The contributions of all these individuals and organizations have been fundamental to our research, and we are truly thankful for their cooperation and support. This study would not have been possible without the collaborative spirit and generous sharing of knowledge and resources by these dedicated professionals and institutions. Their commitment to advancing scientific research and conservation is deeply appreciated.

Appendix A. Supplementary data

Supplementary data to this article can be found online at https://doi.org/10.1016/j.ecolind.2024.111980.

References

Arrogante-Funes, P., Bruzón, A.G., Arrogante-Funes, F., Ramos-Bernal, R.N., Vázquez-Jiménez, R., 2021. Integration of vulnerability and hazard factors for landslide risk assessment. Int. J. Environ. Res. Public Health 18 (22). https://doi.org/10.3390/ijerph182211987. Article 11987.

Atkins, J.W., Bhatt, P., Carrasco, L., Francis, E., Garabedian, J.E., Hakkenberg, C.R., Krause, K., 2023. Integrating forest structural diversity measurement into ecological research. Ecosphere 14 (9). https://doi.org/10.1002/ecs2.4633. Article e4633.

Awange, J., & Kiema, J., 2013. Microwave remote sensing. In Environmental Science and Engineering (pp. 133–144). https://doi.org/10.1007/978-3-642-34085-7_9.

Balling, J., Herold, M., Reiche, J., 2023. How textural features can improve SAR-based tropical forest disturbance mapping. Int. J. Appl. Earth Obs. Geoinf. 124, 103492 https://doi.org/10.1016/j.jag.2022.103492.

Batar, A.K., Shibata, H., Watanabe, T., 2021. A novel approach for forest fragmentation susceptibility mapping and assessment: a case study from the indian himalayan region. Remote Sens. (Basel) 13 (20). https://doi.org/10.3390/rs13204090. Article 4090.

Boiński, M., Boińska, U., 2020. Interesting plant species and communities of wdecki Landscape Park and its environs. In: Kunz, M. (Ed.), Rola i Funkcjonowanie Parków Krajobrazowych w Rezerwatach Biosfery. Wydawnictwo UMK, pp. 247–270.

Boiński, M., 1993. Rezerwat Biosfery "Bory Tucholskie". In: Proceedings of the Bory Tucholskie: Walory Przyrodnicze, Problemy Ochrony, Przyszłość, Bachorze, Poland, 17–20 September 1992, pp. 361–375. Nicolaus Copernicus University.

Bonham-Carter, G.F., Agterberg, F.P., & Wright, D.F., 1990. Weights of evidence modeling: A new approach to mapping mineral potential. In: F. P. Agterberg, & G. F. Bonham-Carter (Eds.), Statistical applications in the earth sciences, pp. 171–183. Geological Survey of Canada. https://doi.org/10.4095/128059.

Brinck, K., Fischer, R., Groeneveld, J., Lehmann, S., De Paula, M.D., Pütz, S., Sexton, J.O., Song, D., Huth, A., 2017. High resolution analysis of tropical forest fragmentation and its impact on the global carbon cycle. nature. Communications 8 (1). https://doi.org/10.1038/ncomms14855.

Brown, C.F., Brumby, S.P., Guzder-Williams, B., Birch, T., Hyde, S.B., Mazzariello, J., Tait, A.M., 2022. Dynamic world, Near real-time global 10 m land use land cover mapping. Sci. Data 9 (1). https://doi.org/10.1038/s41597-022-01580-5. Article 251.

Budniak, P., Zięba, S., 2022. Effects of forest fragmentation on the volume of wood resources in managed. Pine-Dominated Forests in Poland. Forests 13 (4), 590. https://doi.org/10.3390/f13040590.

Chavan, S.B., Reddy, C.S., Rao, S.S., Rao, K.K., 2018. Assessing and predicting decadal forest cover changes and forest fragmentation in kinnerasani wildlife sanctuary, telangana, India. J. Indian Soc. Remote Sens. 46, 729–735.

Chmielewski, T., Szer, J., Bobra, P., 2020. Derecho wind storm in Poland on 11–12 august 2017: results of the post-disaster investigation. Environ. Hazards 19 (5), 508–528. https://doi.org/10.1080/17477891.2020.1730154.

Chojnacka-Ożga, L., Ożga, W., 2018. Meteorological conditions of the occurrence of wind damage on august 11–12, 2017 in the forests of central-western Poland. Sylwan 162 (3), 200–208.

Coates, K.D., Hall, E.C., Canham, C.D., 2018. Susceptibility of trees to windthrow storm damage in partially harvested complex-structured multi-species forests. Forests 9 (4), 199.

Cohen, J., 1960. A coefficient of agreement for nominal scales. Educ. Psychol. Meas. 20 (1), 37–46. https://doi.org/10.1177/001316446002000104.

Dekant, W., Bridges, J., 2016. A quantitative weight of evidence methodology for the assessment of reproductive and developmental toxicity and its application for classification and labeling of chemicals. Regul. Toxicol. Pharm. 82, 173–185.

Doane, T.H., Yanites, B.J., Edmonds, D.A., & Novick, K.A., 2023. Hillslope roughness reveals forest sensitivity to extreme winds. Proceedings of the National Academy of Sciences of the United States of America, 120(3). https://doi.org/10.1073/pnas.2212105120.

Dotzek, N., Groenemeijer, P., Feuerstein, B., Holzer, A.M., 2009. Overview of ESSL's severe convective storms research using the european severe weather database ESWD. Atmos. Res. 93, 575–586.

Dupont, S., Pivato, D., Brunet, Y., 2015. Wind damage propagation in forests. Agric. For. Meteorol. 214–215, 243–251. https://doi.org/10.1016/j.agrformet.2015.07.010.

Dutt, S., & Kunz, M., 2024. Landscape metrics of the Brusy Commune before and after wind-storm: assessment of the extent of changes based on Landsat-8 data. Bulletin of Geography. Physical Geography Series, 26: in press.

European Commission, Joint Research Centre (JRC), 2023, January. Quantifying Forest Fragmentation [PDF file]. GuidosToolbox. Retrieved November 8, 2023, from https://ies-ows.jrc.ec.europa.eu/gtb/GTB/psheets/GTB-Fragmentation.pdf.

Fan, D.M., Cui, X., Yuan, D., Wang, J., Yang, J., Wang, S., 2011. Weight of evidence method and its applications and development. Procedia Environ. Sci. 11, 1412–1418.
Fawcett, T., 2006. An introduction to ROC analysis. Pattern Recogn. Lett. 27 (8), 861–874.
Fischer, R., Taubert, F., Müller, M., Groeneveld, J., Lehmann, S., Wiegand, T., Huth, A., 2021. Accelerated forest fragmentation leads to critical increase in tropical forest edge area. science. Advances 7 (37). https://doi.org/10.1126/sciadv.abg7012.
Forman, R.T., 1996. Land mosaics: the ecology of landscapes and regions. Cambridge University Press.
Forzieri, G., Pecchi, M., Girardello, M., Mauri, A., Klaus, M., Nikolov, C., Beck, P.S., 2020. A spatially explicit database of wind disturbances in european forests over the period 2000–2018. Earth Syst. Sci. Data 12 (1), 257–276.
Fynn, I.E.M., Campbell, J.B., 2019. Forest fragmentation analysis from multiple imaging formats. Journal of Landscape Ecology 12 (1), 1–15. https://doi.org/10.2478/jlecol-2019-0001.
García-Orozco, S., Vargas-Gutiérrez, G., Ordóñez-Sánchez, S., Silva, R., 2023. Using multi-criteria decision making in quality function deployment for offshore renewable energies. Energies 16 (18), 6533.
González-Díaz, P., Jump, A.S., Perry, A., Wachowiak, W., Лапшина, Е.Д., Cavers, S., 2017. Ecology and management history drive spatial genetic structure in scots pine. For. Ecol. Manage. 400, 68–76. https://doi.org/10.1016/j.foreco.2017.05.035.
Guo, L., Wu, Z., Li, S., Xie, G., 2024. The relative impacts of vegetation, topography and weather on landscape patterns of burn severity in subtropical forests of southern China. J. Environ. Manage. 351, 119733 https://doi.org/10.1016/j.jenvman.2023.119733.
Haddad, N.M., Brudvig, L.A., Clobert, J., Davies, K.F., Gonzalez, A., Holt, R.D., Lovejoy, T.E., Sexton, J.O., Austin, M.P., Collins, C.D., Cook, W.M., Damschen, E.I., Ewers, R.M., Foster, B.L., Jenkins, C.N., King, A.J., Laurance, W.F., Levey, D.J., Margules, C., Townshend, J.R.G., 2015. Habitat fragmentation and its lasting impact on Earth's ecosystems. science. Advances 1 (2). https://doi.org/10.1126/sciadv.1500052.
Heilman, G.E., Strittholt, J.R., Slosser, N.C., Dellasala, D.A., 2002. Forest fragmentation of the conterminous United States: assessing forest intactness through road density and spatial characteristics. Bioscience 52 (5), 411–422.
Hersbach, H., Bell, B., Berrisford, P., Hirahara, S., Horányi, Á., Muñoz-Sabater, J., Nicolas, J.P., Peubey, C., Radu, R., Schepers, D., Simmons, A.J., Soci, C., Abdalla, S., Abellan, X., Balsamo, G., Bechtold, P., Biavati, G., Bidlot, J., Bonavita, M., Thépaut, J., 2020. The ERA5 global reanalysis. Q. J. R. Meteorolog. Soc. 146 (730), 1999–2049. https://doi.org/10.1002/qj.3803.
Jung, C., Schindler, D., Albrecht, A.T., Buchholz, A., 2016. The role of highly-resolved gust speed in simulations of storm damage in forests at the landscape scale: a case study from southwest Germany. Atmos. 7 (1), 7.
Knoot, T.G., Schulte, L.A., Tyndall, J., Palik, B.J., 2010. The state of the system and steps toward resilience of disturbance-dependent oak forests. Ecol. Soc. 15 (4) https://doi.org/10.5751/es-03589-150405.
Konings, A.G., Saatchi, S., Frankenberg, C., Keller, M., Leshyk, V.O., Anderegg, W.R.L., Humphrey, V., Matheny, A.M., Trugman, A.T., Sack, L., Agee, E., Barnes, M.L., Binks, O., Cawse-Nicholson, K., Christoffersen, B., Entekhabi, D., Gentine, P., Holtzman, N., Katul, G.G., Zuidema, P.A., 2021. Detecting forest response to droughts with global observations of vegetation water content. Glob. Chang. Biol. 27 (23), 6005–6024. https://doi.org/10.1111/gcb.15872.
Konôpka, B., Pajtík, J., Šebeň, V., Merganičová, K., Surový, P., 2020. Silver birch aboveground biomass allocation pattern, stem and foliage traits with regard to intraspecific crown competition. Central European Forestry Journal 66 (3), 159–169.
Krawiec, A., Wysocki, W., Jamorska, I., Belzyt, S., 2022. Geoturist evaluation of geosites in the Tuchola Forest biosphere reserve (N Poland). Resources 11 (2), 13. https://doi.org/10.3390/resources11020013.
Kunz, M., 2006. Zmienność wzorca przestrzennego krajobrazu w świetle interpretacji dostępnych materiałów kartograficznych i teledetekcyjnych [Variability of the spatial pattern of the landscape in the light of the interpretation of available cartographic and remote sensing materials]. archiwum fotogrametrii. Kartografii i Teledetekcji [archives of Photogrammetry, Cartography and Remote Sensing] 16, 373–384.
Kunz, M., 2012. Zmiany lesistości pomorza zachodniego w ostatnich 400 latach [changes in the forest cover of Western Pomerania in the last 400 years]. Roczniki Geomatyki [annals of Geomatics] X, 4 (56), 145–156.
Li, J., Morimoto, J., Hotta, W., Suzuki, S.N., Owari, T., Toyoshima, M., Nakamura, F., 2023. The 30-year impact of post-windthrow management on the forest regeneration process in northern Japan. Landsc. Ecol. Eng. 19 (2), 227–242.
Lin, Y., An, W., Gan, M., Shahtahmassebi, A., Ye, Z., Huang, L., Wang, K., 2021. Spatial grain effects of urban green space cover maps on assessing habitat fragmentation and connectivity. Land 10 (10), 1065.
Lobo, J.M., Jiménez-Valverde, A., Real, R., 2007. AUC: a misleading measure of the performance of predictive distribution models. Glob. Ecol. Biogeogr. 17 (2), 145–151. https://doi.org/10.1111/j.1466-8238.2007.00358.x.
Louzada, R.O., Reis, L.K., De Souza Diniz, J.M.F., De Oliveira Roque, F., Gama, F.F., Bergier, I., 2023. Combining optical and microwave remote sensing for assessing gullies in human-disturbed vegetated landscapes. Catena 228, 107127. https://doi.org/10.1016/j.catena.2023.107127.
Magrach, A., Laurance, W.F., Larrinaga, A.R., Santamaría, L., 2014. Meta-analysis of the effects of forest fragmentation on interspecific interactions. Conserv. Biol. 28 (5), 1342–1348. https://doi.org/10.1111/cobi.12304.
Mazgajski, T.D., Żmihorski, M., Abramowicz, K., 2010. Forest habitat loss and fragmentation in Central Poland during the last 100 years. Silva Fennica 44 (4). https://doi.org/10.14214/sf.136.
McGarigal, K., Cushman, S., Ene, E., 2012. FRAGSTATS v4: spatial pattern analysis program for categorical and continuous maps. University of Massachusetts, Amherst. Retrieved from https://www.umass.edu/landeco/research/fragstats/fragstats.html.
Mengist, W., Soromessa, T., Feyisa, G.L., 2022. Forest fragmentation in a forest biosphere reserve: implications for the sustainability of natural habitats and forest management policy in Ethiopia. Resources, Environment and Sustainability 8, 100058. https://doi.org/10.1016/j.resenv.2022.100058.
Meraner, A., Ebel, P., Zhu, X.X., Schmitt, M., 2020. Cloud removal in Sentinel-2 imagery using a deep residual neural network and SAR-optical data fusion. ISPRS J. Photogramm. Remote Sens. 166, 333–346. https://doi.org/10.1016/j.isprsjprs.2020.05.013.
Mingote, V., Miguel, A., Ortega, A., Lleida, E., 2020. Optimization of the area under the ROC curve using neural network super-vectors for text-dependent speaker verification. Comput. Speech Lang. 63, 101078.
Mitchell, M.G.E., Bennett, E.M., Gonzalez, A., 2014. Forest fragments modulate the provision of multiple ecosystem services. J. Appl. Ecol. 51 (4), 909–918. https://doi.org/10.1111/1365-2664.12241.
Morreale, L.L., Thompson, J.R., Tang, X., Reinmann, A.B., Hutyra, L.R., 2021. Elevated growth and biomass along temperate forest edges. nature. Communications 12 (1). https://doi.org/10.1038/s41467-021-27373-7.
Musick, H.B., Grover, H.D., 1991. Image textural measures as indices of landscape pattern. Ecological Studies 82, 77–101.
Newman, M.E., McLaren, K., Wilson, B.S., 2014. Assessing deforestation and fragmentation in a tropical moist forest over 68 years; the impact of roads and legal protection in the cockpit country, Jamaica. For. Ecol. Manage. 315, 138–152. https://doi.org/10.1016/j.foreco.2013.12.033.
Nienartowicz, A., Domin, D.J., Kunz, M., Przystalski, A., 2010. Biosphere reserve –Tuchola Forest. Sandry Brdy.
Nienartowicz, A., Kunz, M., 2020. 10 lat funkcjonowania rezerwatu biosfery bory tucholskie. In: Rola i Funkcjonowanie Parków Krajobrazowych w Rezerwatach Biosfery. Wydawnictwo UMK, pp. 13–38.
Oksanen, E., 2021. Birch as a model species for the acclimation and adaptation of northern Forest ecosystem to changing environment. Frontiers in Forests and Global Change 4. https://doi.org/10.3389/ffgc.2021.682512.
Omar, M., Janada, K., Soltan, H., 2022. FAQT: a precise system for welding process selection. Int. J. Fuzzy Syst. 24 (3), 1605–1618.
Pacey, G.P., Schultz, D.M., Garcia-Carreras, L., 2021. Severe convective windstorms in Europe: climatology, preconvective environments, and convective mode. Weather Forecast. 36 (1), 237–252. https://doi.org/10.1175/waf-d-20-0075.1.
Pimentel, D., Westra, L., Noss, R.F., 2013. Ecological integrity: integrating environment, conservation, and health. Island Press.
Referowska-Chodak, E., Kornatowska, B., 2021. Effects of forestry transformation on the landscape level of biodiversity in Poland's forests. Forests 12 (12), 1682. https://doi.org/10.3390/f12121682.
Rempel, R.S., Kaukinen, D., Carr, A.P., 2012. Patch analyst and patch grid. Ontario Ministry of Natural Resources, Centre for Northern Forest Ecosystem Research, Thunder Bay, Ontario.
Ribeiro, J.C.T., Nunes-Freitas, A.F., Fidalgo, E.C.C., Uzêda, M.C., 2019. Forest fragmentation and impacts of intensive agriculture: responses from different tree functional groups. PLoS One 14 (8), e0212725.
Riitters, K.H., Wickham, J.D., O'Neill, R.V., Jones, K.B., Smith, E., Coulston, J.W., Wade, T.G., Smith, J.A., 2002. Fragmentation of continental United States forests. Ecosystems 5 (8), 815–822.
Riitters, K.H., Coulston, J.W., Wickham, J.D., 2012. Fragmentation of forest communities in the eastern United States. For. Ecol. Manage. 263, 85–93.
Riitters, K.H., Wickham, J.D., 2012. Decline of forest interior conditions in the conterminous United States. Sci. Rep. 2. Article 653.
Rincón, V., Velázquez, J., Pascual, Á., Herráez, F., Gómez, I., Gutiérrez, J., Sánchez-Mata, D., 2022. Connectivity of natura 2000 potential natural riparian habitats under climate change in the Northwest Iberian Peninsula: implications for their conservation. Biodivers. Conserv. 31 (2), 585–612.
Roche, P.K., Campagne, C.S., 2017. From ecosystem integrity to ecosystem condition: a continuity of concepts supporting different aspects of ecosystem sustainability. Curr. Opin. Environ. Sustain. 29, 63–68.
Rodrigues, D.R., Bovolenta, Y.R., Pimenta, J.A., Bianchini, E., 2016. Height structure and spatial pattern of five tropical tree species in two seasonal semideciduous forest fragments with different conservation histories. Revista Arvore 40 (3), 395–405.
Sanginés de Cárcer, P., Mederski, P.S., Magagnotti, N., Spinelli, R., Engler, B., Seidl, R., Schweier, J., 2021. The management response to wind disturbances in european forests. Current Forestry Reports 7, 167–180.
Scanes, C.G., 2018. Human activity and habitat loss: destruction, fragmentation, and degradation. In Elsevier eBooks 451–482.
Shimada, M., Itoh, T., Motooka, T., Watanabe, M., Shiraishi, T., Thapa, R., Lucas, R., 2014. New global forest/non-forest maps from ALOS PALSAR data (2007–2010). Remote Sens. Environ. 155, 13–31.
Soille, P., 2003. Morphological image analysis: principles and application. Springer-Verlag.
Sterlacchini, S., Ballabio, C., Blahůt, J., Masetti, M., Sorichetta, A., 2011. Spatial agreement of predicted patterns in landslide susceptibility maps. Geomorphology 125 (1), 51–61. https://doi.org/10.1016/j.geomorph.2010.09.004.
Sulik, S., Kejna, M., 2020. The origin and course of severe thunderstorm outbreaks in Poland on 10 and 11 august, 2017. Bulletin of Geography: Physical Geography Series 18 (1), 25–39. https://doi.org/10.2478/bgeo-2020-0003.
Szramka, H., Adamowicz, K., 2020. Forest development and conservation policy in Poland. Folia Forestalia Polonica 62 (1), 31–38. https://doi.org/10.2478/ffp-2020-0004.

Taszarek, M., Pilguj, N., Orlikowski, J., Surowiecki, A., Walczakiewicz, S., Pilorz, W., Piasecki, K., Pajurek, Ł., Półrolniczak, M., 2019. Derecho evolving from a Mesocyclone—A study of 11 august 2017 severe weather outbreak in Poland: event analysis and high-resolution simulation. Mon. Weather Rev. 147 (6), 2283–2306. https://doi.org/10.1175/mwr-d-18-0330.1.

Taubert, F., Fischer, R., Groeneveld, J., Lehmann, S., Müller, M., Rödig, E., Wiegand, T., Huth, A., 2018. Global patterns of tropical forest fragmentation. Nature 554 (7693), 519–522. https://doi.org/10.1038/nature25508.

Vakhshoori, V., Zare, M., 2018. Is the ROC curve a reliable tool to compare the validity of landslide susceptibility maps? Geomat. Nat. Haz. Risk 9 (1), 249–266. https://doi.org/10.1080/19475705.2018.1424043.

Vogt, P., 2023. GuidosToolbox (GTB) user guide (3.2 rev. 0). European Commission, Joint Research Centre (JRC). https://ies-ows.jrc.ec.europa.eu/gtb/GTB/GuidosToolbox_Manual.pdf.

Vogt, P., Riitters, K.H., 2017. GuidosToolbox: universal digital image object analysis. European Journal of Remote Sensing 50 (1), 352–361. https://doi.org/10.1080/22797254.2017.1330650.

Vogt, P., Riitters, K.H., Estreguil, C., Kozak, J., Wade, T.G., Wickham, J.D., 2007. Mapping spatial patterns with morphological image processing. Landsc. Ecol. 22, 171–177. https://doi.org/10.1007/s10980-006-9013-2.

Wickham, J.D., Riitters, K.H., 2019. Influence of high-resolution data on the assessment of forest fragmentation. Landsc. Ecol. 34 (9), 2169–2182. https://doi.org/10.1007/s10980-019-00820-z.

Wulder, M.A., White, J.C., Andrew, M.E., Seitz, N., Coops, N.C., 2009. Forest fragmentation, structure, and age characteristics as a legacy of forest management. For. Ecol. Manage. 258 (9), 1938–1949. https://doi.org/10.1016/j.foreco.2009.07.041.

Żmihorski, M., Chylarecki, P., Rejt, Ł., Mazgajski, T.D., 2009. The effects of forest patch size and ownership structure on tree stand characteristics in a highly deforested landscape of central Poland. Eur. J. For. Res. 129 (3), 393–400. https://doi.org/10.1007/s10342-009-0344-9.

To whom it may concern,

I, **Sanjana Dutt**, confirm that my manuscript has been **successfully submitted** to **GIScience & Remote Sensing (Taylor & Francis)**.

- **Title:** *How Does Fragmentation Reshape Forests? Tracking Dominant Ecological Processes Across Core, Transitional, and Rare Zones*
- **Submission ID: 254801274**
- **Corresponding author:** Sanjana Dutt (sanjana.dutt@doktorant.umk.pl)

Due to a **temporary technical issue on the Taylor & Francis Submission Portal**—specifically, a persistent banner stating that *"PDF file(s) are unavailable for preview"*—the system has **not generated the compiled "submitted PDF"** on my author dashboard. I have therefore attached **screenshots** showing: the **submission-confirmation screen** with the Submission ID, and

This letter is provided as interim **proof of submission** for inclusion in my PhD thesis materials. I will supply the **official compiled PDF** (or publisher-issued submission confirmation) as soon as it becomes available.

Thank you for accepting this statement for doctoral documentation purposes.

Sincerely,
Sanjana Dutt
Faculty of Earth Sciences and Spatial Management
Nicolaus Copernicus University in Toruń
Email: sanjana.dutt@doktorant.umk.pl


Taylor & Francis
Taylor & Francis Group

Dear Sanjana Dutt,

Thank you for your submission.

Submission ID	254801274
Manuscript Title	How Does Fragmentation Reshape Forests? Tracking dominant ecological processes across core, transitional, and rare zones
Journal	GIScience & Remote Sensing

Sanjana Dutt
Digitally signed by Sanjana Dutt
DN: cn=Sanjana Dutt, o=Nicolaus Copernicus University, Toruń, Poland., ou=Department of Geomatics and Cartography, Faculty of Earth Sciences and Spatial Management., email=sanjana.dutt@doktorant.umk.pl, c=PL
Date: 2025.09.24 14:01:27 +02'00'

How Does Fragmentation Reshape Forests? Tracking dominant ecological processes across core, transitional, and rare zones

Sanjana Dutt*[1], Jakub Wojtasik[2], Dimitri Justeau-Allaire[3], Mieczysław Kunz[1]

[1] Faculty of Earth and Environmental Sciences, Nicolaus Copernicus University, Toruń, Poland
[2] Centre for Statistical Analysis, Nicolaus Copernicus University, Toruń, Poland
[3] AMAP Laboratory (BotAny and Modeling of Plant Architecture and Vegetation), Montpellier, France
Corresponding author*. E-mail address: sanjana.dutt@doktorant.umk.pl

Abstract

Forest fragmentation reshapes ecological dynamics, yet its zone-specific impacts remain poorly quantified. We assess degradation, moisture stress, habitat quality, and structural maturity in the Tuchola Forest Biosphere Reserve (Poland) across three Foreground Area Density (FAD) classes—Core (≥90%), Transitional (40–60%), and Rare (≤10%). Leveraging open Sentinel-2 data and field-based ecological attributes from the Polish Forest Data Bank, we integrate FAD zoning with interpretable ensembles (ET, LGBM) to model vegetation condition for 2016, 2020, and 2024. Partial dependence analyses reveal consistent ecological contrasts across zones: Rare areas show pronounced early-stage degradation tied to edge exposure and reduced connectivity, whereas Core areas maintain stable moisture regimes and structural maturity. Site-type responses and stand-age signals further indicate that spectral confusion in fragmented edges can mimic maturity, emphasizing the value of structural information in future applications. Validated against field observations, the workflow provides a spatially explicit, reproducible approach to diagnose fragmentation effects from open data. Results translate directly to management: strict protection for Core interiors, adaptive buffer and corridor strategies in Transitional zones, and targeted restoration/rewilding in Rare zones to enhance connectivity and drought resilience. The framework advances geospatial science by operationalizing FAD-aware, interpretable remote sensing for zone-specific conservation in temperate forests.

Keywords: forest fragmentation; ecological processes; Sentinel-2; Foreground Area Density (FAD); machine learning; temperate forests

1. Introduction

Forest fragmentation—the division of continuous forest into smaller, more isolated patches—disrupts ecological processes governing biodiversity, hydrological regulation, and biomass productivity (Haddad et al., 2015; Wang et al., 2025). Fragmentation *per se* (independent of habitat loss) alters patch configuration and increases edge exposure, intensifying microclimatic stress through higher insolation, wind, and desiccation, and elevating fire susceptibility (Arroyo-Rodríguez et al., 2017; Fletcher et al., 2018). These pressures are especially acute in the Tuchola Forest Biosphere Reserve (TFBR), a pine-dominated landscape where even-aged Scots pine (Pinus sylvestris) stands (>90% of area) exhibit uniform canopy structure and shallow rooting, heightening vulnerability to edge-driven moisture stress, bark beetle outbreaks, and fire relative to mixed or deciduous systems (Wulder et al., 2009; Britton et al., 2024). Resulting changes—canopy thinning, moisture stress, and reduced connectivity—constrain dispersal of forest-interior specialists that depend on large, contiguous patches (Blake & Karr, 1984; Fahrig et al., 2019). While small patches can function as stepping stones for some taxa, large patches remain critical for sustaining interior specialists and population stability (Blake & Karr, 1984; Fahrig et al., 2019; Wang et al., 2025).

Sentinel-2's 10 m multispectral record enables repeated monitoring of vegetation condition via indices (VIs) that capture gradients in greenness/biomass, canopy water content, and pigment dynamics (Lausch et al., 2016). Indices such as NDVI and EVI (greenness/biomass), NDMI (moisture), and CIred-edge/NDRE (pigment dynamics) are sensitive to structural and disturbance regimes that co-vary with fragmentation (Wang et al., 2010; Xue & Su, 2017). However, few studies jointly integrate multi-temporal Sentinel-2 data, Foreground Area Density (FAD)–based fragmentation zoning, and field-based ecological attributes (FEAs) to model zone-specific processes, limiting our understanding of how fragmentation effects differ across dense, mixed, and sparse forest contexts (Wang et al., 2010; Lausch et al., 2017). Stratifying by local forest density using FAD—into Core (≥90%), Transitional (40–60%), and Rare (≤10%) zones—helps disentangle ecological signal from spectral noise by conditioning analysis on neighborhood context (Vogt & Riitters, 2017; Wang et al., 2025).

Here, we develop a framework for assessing fragmentation effects in TFBR, a system shaped by windstorms, silviculture, and historical land use (Łuców et al., 2021; Dutt et al., 2024). TFBR's homogeneity—dominated by even-aged pine—reduces beta-diversity and may dampen species-level variability in spectral responses, yet increased edge density can magnify stress exposure (Wulder et al., 2009; Kozak et al., 2018; Fahrig et al., 2019). We integrate multi-temporal Sentinel-2 (2016, 2020, 2024) with FEAs from the Polish Forest Data Bank (degradation, soil moisture, site type, stand age) to model forest condition across FAD-defined zones spanning stable interiors to highly fragmented edges (Kozak et al., 2018). Our contribution is a spatially explicit, reproducible GIS workflow that combines FAD zoning, Sentinel-2 VIs, and interpretable ensembles to diagnose fragmentation-linked ecological processes from open data.

Our objectives are to:

1. ***identify sensitive indicators***—determine which VIs best capture biomass productivity, moisture stress, pigment dynamics, and understory conditions in a fragmented landscape;
2. ***map zone-specific patterns***—quantify how VI–FEA relationships vary across Core, Transitional, and Rare zones under differing configuration pressures; and
3. ***assess predictive power***—evaluate how accurately VIs predict field-observed attributes using interpretable ensemble learning across zones and years.

By combining Sentinel-2 with FAD-based zoning and interpretable models, we provide a scalable tool for monitoring fragmentation-linked ecological dynamics and for informing zone-specific conservation and restoration strategies under increasing climate pressures (González-Ávila et al., 2023; Wang et al., 2025).

2. Materials and Methods

2.1. Study Area

The Tuchola Forest Biosphere Reserve (TFBR; 53°30′N, 17°50′E; ~3,195 km²) occupies nutrient-poor fluvioglacial sands on the Pomeranian outwash plain of northern Poland and contains >900 kettle lakes and Sphagnum peatlands that generate sharp hydrological and edaphic gradients (Łuców et al., 2021). TFBR is dominated by even-aged Pinus sylvestris plantations (>90%), with minor Betula spp., Quercus robur, and Alnus glutinosa. Fragmentation arises primarily from silvicultural clear-cuts and salvage logging, compounded by biotic outbreaks (e.g., *Panolis flammea*) and extreme events—the 2012 F3 tornado and the 2017 derecho are notable examples (Budniak & Zięba, 2022; Dutt et al., 2024).

As Dutt et al. (2024) show using Bayesian mapping, edge expansion in TFBR is strongly associated with cropland proximity, younger stands, and high wind exposure. This configuration-driven change has progressed even where total forest area remains relatively stable, a pattern consistent with fragmentation-per-se effects emphasized by Fahrig (2017) and observed in other Polish landscapes by

Kozak et al. (2018). These characteristics make TFBR an apt natural laboratory for examining how local forest density and neighborhood context modulate ecological processes under fragmentation.

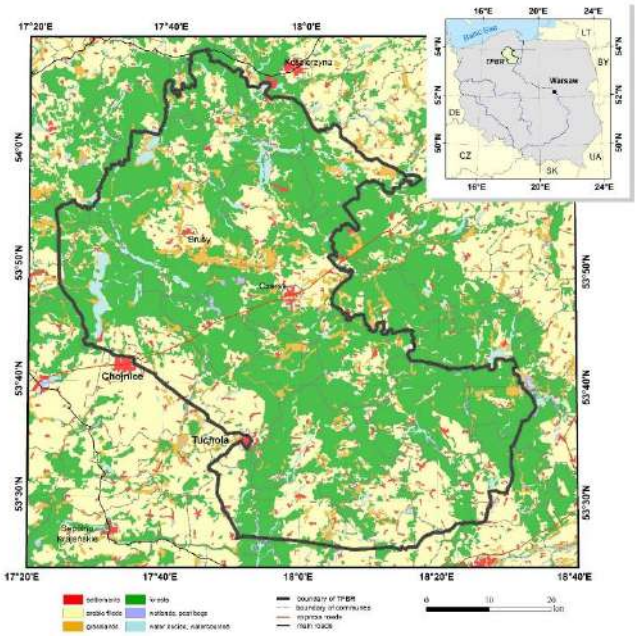

Figure 1. Location of the Tuchola Forest Biosphere Reserve (TFBR) in northern Poland, overlaid with CORINE land cover types (2018), major roads, and commune boundaries.

2.2. Data Collection

2.2.1. Sentinel-2 Imagery

We used Sentinel-2 Level-2A surface reflectance for the growing season (May 1–August 31) in 2016, 2020, and 2024. Where Level-2A was unavailable in 2016, the corresponding Level-1C scenes were converted to L2A using ESA's Sen2Cor (atmospheric correction from top-of-atmosphere to surface reflectance; also produces the Scene Classification Layer, SCL). We removed cloud-affected pixels using the SCL by excluding class 3 (cloud shadow), 8 (cloud—medium probability), 9 (cloud—high probability), and 10 (thin cirrus). For consistency, we also excluded class 11 (snow/ice), although snow is rare in May–August in Poland. We retained bands *B2, B3, B4, B5, B8, B11* due to their sensitivity to vegetation biochemistry and structure (Lausch et al., 2016; Xue & Su, 2017). The overall workflow—preprocessing, vegetation-index (VI) calculation, FAD-based zoning, model fitting, and interpretation—is outlined in Figure 2.

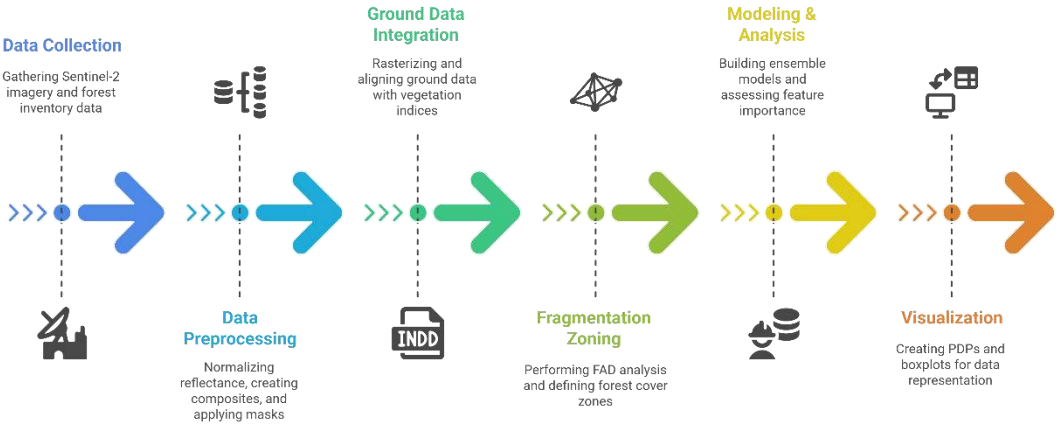

Figure 2: Forest Fragmentation Analysis Workflow. Overview of the methodology combining Sentinel-2 imagery and forest inventory data, preprocessing steps, vegetation index calculation, FAD-based fragmentation zoning, ensemble modeling (Extra Trees, LightGBM), and visualization through PDPs and boxplots.

2.2.2. Field Data

Forest inventory data from the Polish Forest Data Bank (BDL) provided polygon-level attributes—degradation, moisture content, forest site type, and stand age—hereafter field-based ecological attributes (FEAs). Polygons correspond to operational management units (e.g., stands/compartments) delineated by the State Forests National Forest Holding for planning and monitoring. These attributes, recorded by professional foresters using standardized protocols, serve as the reference for evaluating how well Sentinel-2 VIs represent on-the-ground ecological conditions (cf. Peters et al., 2007; Nguyen et al., 2020). The semantics and numeric encodings for categorical FEAs are summarized in Supplementary Tables S2–S4. Procedures for spatial alignment with the Sentinel-2 composites (CRS, grid, and rasterization choices) and preparation for modeling are detailed in Section 2.5.1.

2.3. Data Processing

2.3.1. Image Preprocessing

All inputs are Sentinel-2 Level-2A surface reflectance (0–1). We produced annual median composites in Google Earth Engine to reduce cloud/phenology noise and reprojected them to PUWG 1992 (EPSG:2180) at 10 m. 20 m bands (B5, B11) were upsampled to 10 m with bilinear interpolation to preserve radiometric continuity; nearest-neighbor was used only for categorical layers (e.g., masks, classes). To restrict analyses to forested pixels, we applied a binary mask from Dynamic World "trees" probability with a primary threshold of 0.60 (Brown et al., 2022; Dutt et al., 2024). We note that simple threshold sensitivity checks (e.g., 0.50/0.60/0.70) can further assess robustness and are recommended for future extensions.

2.3.2. Vegetation Indices and Field Data Integration

We computed 17 VI's (Table 1) in Python (rasterio 1.3; NumPy 1.26) spanning greenness/biomass (e.g., NDVI, EVI, EVI2, GNDVI, GRNDVI, GSAVI, LAI, DVI), moisture (NDMI, GVMI), pigment/chlorophyll (GARI, MCARI, MTVI2, NDRE, GBNDVI), and indices addressing soil/shadow effects (CVI, MSAVI). Formal definitions and Sentinel-2 band mappings are provided in Supplementary Table S1 (see Xue & Su, 2017; Wang et al., 2010; Lausch et al., 2016).

Polygon-level FEAs (degradation, moisture content, site type, stand age) from BDL were rasterized to 10 m with nearest-neighbor to preserve categorical labels and aligned to the Level-2A composite grid. This ensured congruence between FEAs and VI rasters while avoiding interpolation artefacts in class data. Where polygon boundaries did not coincide exactly with pixel edges, attributes were assigned to the pixel containing the polygon centroid, and simple overlay checks were used to flag potential misalignments for QA/QC (Budniak & Zięba, 2022; Brown et al., 2022).

Table 1: Sentinel-2 Vegetation Indices Used in the Study

Functional Domain	Indices	Ecological Focus	References
Greenness/Biomass	NDVI, EVI, EVI2, GNDVI, GRNDVI, GSAVI, LAI, DVI	Leaf area, productivity, biomass	Xue & Su, 2017; Wang et al., 2010
Moisture Stress	NDMI, GVMI	Canopy water content, drought	Wang et al., 2010
Pigment/Chlorophyll	GARI, MCARI, MTVI2, NDRE, GBNDVI	Chlorophyll, nutrient status	Lausch et al., 2016
Soil/Shadow Correction	CVI, MSAVI	Soil background, shadow	Xue & Su, 2017; Lausch et al., 2016

2.4. Landscape Stratification

Foreground Area Density (FAD) was computed in GuidosToolbox (Vogt & Riitters, 2017) using a moving square window on the 10 m grid. The primary window was 243 × 243 pixels (i.e., 2.43 km per side; 5.90 km²), which emphasizes neighborhood forest amount/configuration and highlights areas with sparse cover (low FAD) (Figure 3). We selected the 243 × 243 window to better resolve sparsely forested neighborhoods (the Rare class) while preserving local context at ~2.4 km, a scale relevant to edge-driven processes and operational planning. We applied the binary forest mask from Section 2.3.1 (Dynamic World "trees" probability, threshold 0.60) prior to FAD calculation. From the six native FAD classes, we retained Core (FAD ≥ 90%), Transitional (40–60%), and Rare (≤ 10%) given their ecological relevance in TFBR (Dutt et al., 2024; Brown et al., 2022). While FAD provides a compact, spatially explicit descriptor of neighborhood forest density, it does not fully disentangle habitat amount from configuration; complementary metrics—such as edge density (boundary complexity) and patch cohesion (connectedness)—can refine fragmentation assessment (Fahrig, 2017; Riitters & Wickham, 2012; cf. González-Ávila et al., 2023). Sensitivity to alternative window sizes (e.g., 121 × 121 and 365 × 365) is recommended for future robustness checks. See Supplementary Figure S1 for temporal

overlaps among zones (2016, 2020, 2024).

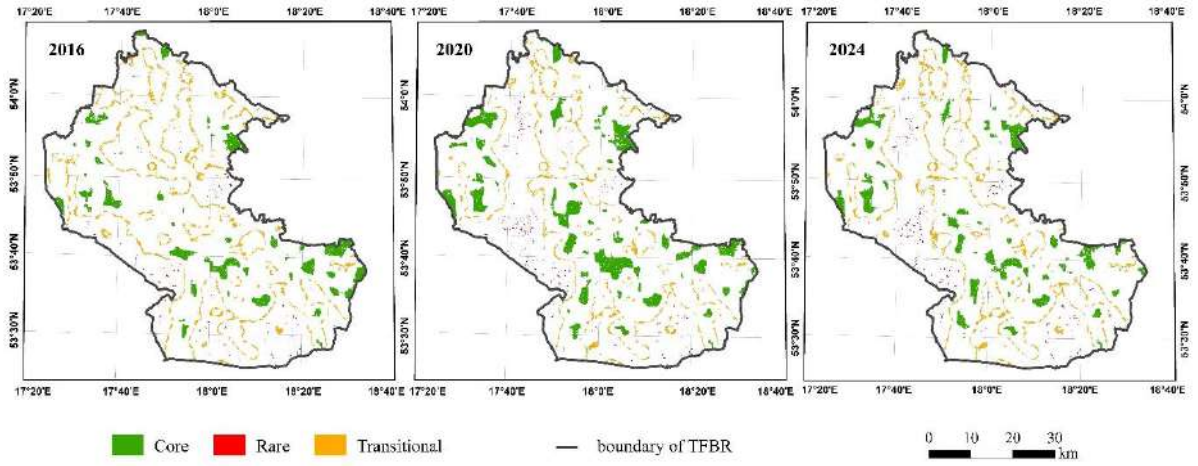

Figure 3. Foreground Area Density (FAD)-derived fragmentation zones—Core (green, ≥90% forest cover), Transitional (orange, 40–60%), and Rare (red, ≤10%)—mapped across TFBR in 2016, 2020, and 2024, showing spatial patterns of forest density.

2.5.1 Data Preprocessing and Feature Engineering

FEAs (degradation, moisture content, site type, stand age) were linked to FAD classes (Core, Transitional, Rare) for 2016, 2020, 2024, then rasterized to the 10 m grid of the Sentinel-2 L2A composites for pixel-wise modelling. Rasterization of categorical labels used nearest-neighbor to preserve class integrity.

- ***Degradation:*** eight ordered classes from *Degraded* to *Transformed* (Table S2).
- ***Moisture content:*** thirteen ordered classes from *very wet bogs* to *fresh soils* (Table S3).
- ***Site type***: fifteen nominal categories spanning *soil–moisture gradients* (Table S4).
- ***Stand age***: continuous years of growth, also summarized into developmental stages.

The combined L2A-based dataset was >99% complete; pixels with missing spectral or ancillary values (<1%) were removed. No outliers were discarded, to avoid biasing models away from ecologically meaningful extremes.

For modelling, ordinal FEAs (degradation, moisture) were integer-encoded to retain rank; site type was one-hot encoded; stand age remained numeric. VI sensitive to pigment loss (e.g., NDRE, GARI), moisture stress (e.g., NDMI), and canopy structure/pigment contrast (e.g., CIred-edge) were derived from Sentinel-2, composited to midsummer for each year (Section 2.3.2; Table S1). Tree-based models required no additional feature scaling (Pedregosa et al., 2011).

2.5.2. Variable Importance and Effect Interpretation

Our geocomputational focus was on interpretable ensemble learning. Following Breiman's seminal perspective on variable importance in tree ensembles, we combined impurity-based importance (from Extra Trees) with Permutation Importance (PI) to diagnose drivers across FAD zones and years (Breiman, 2001; cf. Grömping, 2009; Nicodemus et al., 2010). Impurity scores summarize split-level reductions (e.g., variance) but may favor high-cardinality features; PI provides a model-agnostic estimate by shuffling a feature and recording the error increase (MSE), which better reflects out-of-sample impact.

To assess stability, we repeated PI with multiple random permutations per feature and summarized the resulting spread; this emphasizes robust patterns rather than single-run artefacts. Interpretation leveraged partial dependence plots (PDPs)—including 2D PDPs for key VI pairs—to visualize nonlinear and zone-specific responses, aiding ecological interpretation and transfer to management (Molnar, 2019). We report importance rankings for each FEA × year × FAD class (Supplementary Figs. S3, S5, S7, S9), highlighting indices recurrently associated with degradation, moisture, site type, and stand age in temperate forests (e.g., NDRE, NDMI, NDVI; see Lausch et al., 2016; Xue & Su, 2017; Yu et al., 2021; Britton et al., 2024).

2.5.3. Model Comparison and Selection

We compared two ensemble regressors widely used in spatial data mining—Extra Trees (ET) and LightGBM (LGBM)—to predict FEAs within Core, Transitional, and Rare zones across 2016, 2020, 2024 (Geurts et al., 2006; Ke et al., 2017). Regression was preferred over multinomial classification because several ordered levels (e.g., degradation, moisture) are uneven or absent in certain zones; treating them as quasi-continuous preserves rank information and avoids extrapolating to unseen categories (cf. Pedregosa et al., 2011).

To mitigate spatial autocorrelation, hyperparameters were tuned under spatial k-fold cross-validation with non-overlapping geographic partitions, and evaluated on held-out folds. This scheme reduces leakage between train/test and better reflects mapping use-cases in GIS. Key ET hyperparameters (number of trees, features per split, min samples to split/leaf) were optimized per FEA × zone × year (Supplementary Table S5). Model performance (MSE/MAE) is summarized in Supplementary Table S6, and ET was selected for downstream interpretation due to its stability and transparency (see also Łoś et al., 2021). For completeness, predictions were subsequently mapped back to management classes for interpretation in Results; agreement metrics beyond MSE/MAE (e.g., RMSE, R^2, Spearman's ρ, Weighted Kappa) are noted as complementary perspectives.

2.5.4. Partial Dependence Plots (PDPs)

We used partial dependence plots (PDPs) to visualize how VIs influence model predictions after averaging over the distribution of all other features (Molnar, 2019). Let $f(\cdot)$ denote the trained model and split the features into a set of interest x_S and its complement x_cThe partial dependence of f with respect to x_S is

$$F_{s(z)} = \int f(z, x_c)p(x_c)dx_c = E_{\{X_c\}[f(z,X_c)]}$$

where $p(x_C)$ is the marginal distribution of the complementary features. In practice, we approximate this expectation using the brute-force empirical average over the observed dataset:

$$\hat{F}_s(z) = (1/n) \sum_{\{i=1\}}^{n} f\left(z, x_{\{c,i\}}\right)$$

where $x_{\{C,i\}}$ are the observed values of the complementary features for sample i, and n is the number of samples used in the average.

Because fragmentation effects are context-dependent, we emphasized 2D PDPs (i.e., $|S| = 2$) to capture nonlinear responses and interactions between key VI pairs for each FEA: e.g., NDRE–GARI (degradation), NDRE–NDMI (moisture content), NDVI–NDRE (site type), and CVI–NDRE (stand age). To support direct comparison across conditions, PDPs were organized in 3×3 grids—rows: FAD classes (Rare, Transitional, Core); columns: years (2016, 2020, 2024). We implemented PDPs using scikit-learn's brute method, evaluating grids within observed feature ranges to avoid extrapolation.

2.5.6: Model Accuracy Assessment

The predictive performance of ET and LGBM models was assessed using Mean Squared Error (MSE) and Mean Absolute Error (MAE), computed separately for training and test datasets to evaluate model fit and generalization. For each FEA predicted values $\hat{y}_i$ were compared against ground-truth values y_i derived from the Polish Forest Data Bank, rasterized at 10 m resolution to align with Sentinel-2 L2A imagery (Section 2.3.1). MSE was calculated as the average squared difference between predicted and actual values, emphasizing larger errors:

$$MSE = \left(\frac{1}{n}\right)\sum(i = 1\ to\ n)(y_i - \hat{y}_i)^2$$

MAE was computed as the average absolute difference, providing an interpretable metric in the original units of the GI:

$$MAE = \left(\frac{1}{n}\right)\sum(i = 1\ to\ n)|y_i - \hat{y}_i|$$

Here, n represents the number of sampled pixels per fragmentation zone (10% stratified random sample). Metrics were computed per FEA, per zone (Rare, Transitional, Core), and per year (2016, 2020, 2024) to preserve ecological context. We also summarized error distributions with boxplots of predictions versus ground truth to assess stability across zones. All values are reported in Supplementary Table S6.

3. Results

3.1. Model Performance Across Fragmentation Zones

The ET model, tuned via hyperparameters such as number of trees and split thresholds (Supplementary Table S5; Section 2.5.3), predicted FEAs across Core, Transitional, and Rare zones for 2016, 2020, and 2024. Its performance was compared with LGBM on held-out test data (Supplementary Table S6; Section 2.5.6). As shown in Figure 4, ET produced lower or more stable errors for most FEAs—particularly degradation, site type, and stand age—while LGBM was occasionally lower for moisture in specific zones but more variable overall. Boxplots of prediction errors (Supplementary Figure S2) confirm ET's narrower error spread and fewer extremes across zones and years, supporting its selection for interpretability in Section 3.2. Full training and test metrics for both models are reported in

Supplementary Table S6.

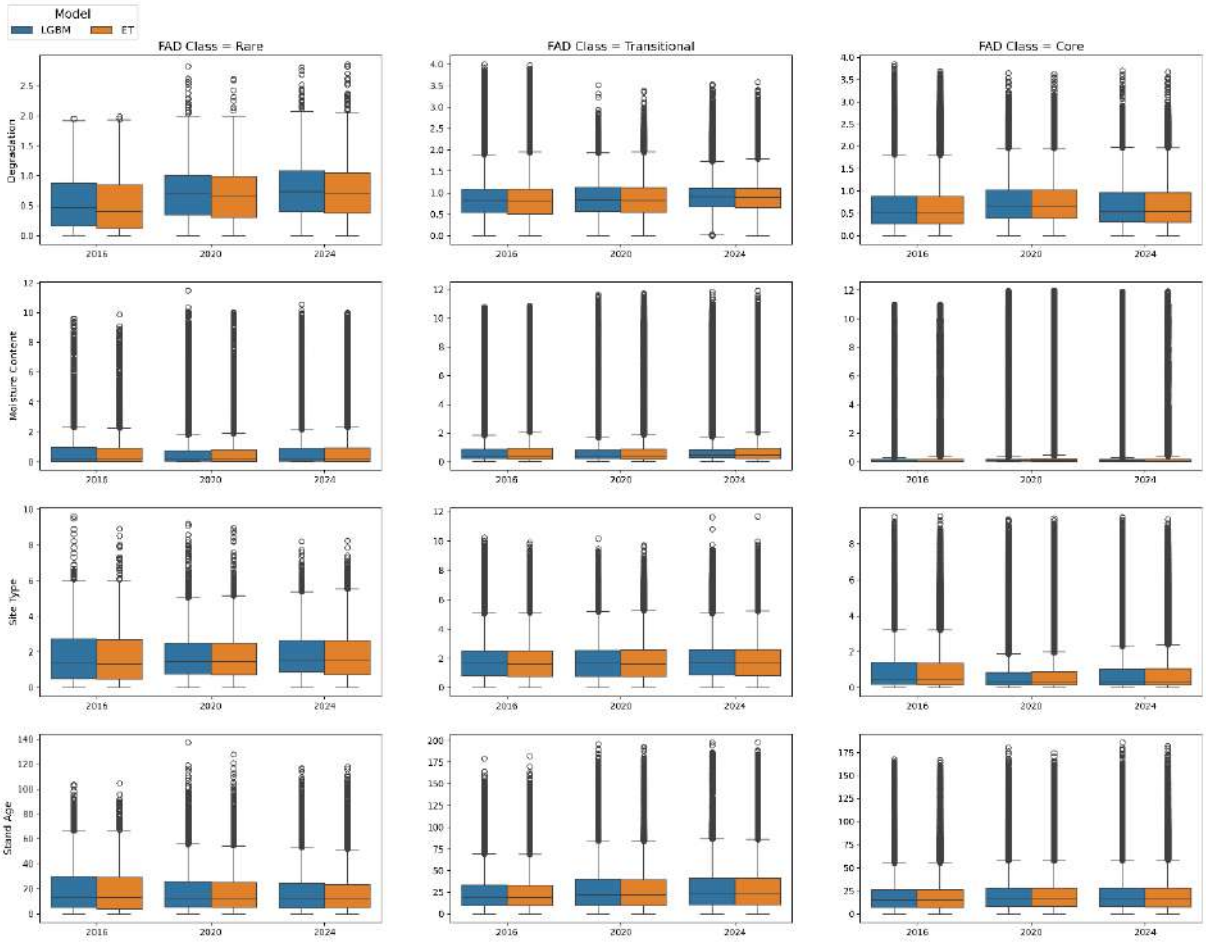

Figure 4. Test-set error distributions (raw units) for ET (orange) and LGBM (blue) across FAD classes (Rare, Transitional, Core) and years (2016, 2020, 2024), shown per FEA (Degradation, Moisture, Site Type, Stand Age).

3.2. FEA Prediction Performance

For each FEA, we selected a representative VI pair based on PI rankings (Section 2.5.2; Supplementary Figures **S3, S5, S7, S9**). This approach ensures interpretability and consistency across fragmentation classes and years while retaining ecological relevance. Selected pairs were: NDRE + GARI (Degradation), NDRE + NDMI (Moisture Content), NDVI + NDRE (Site Type), and CVI + NDRE (Stand Age). Additional VI pairs and detailed PDP layouts are provided in Supplementary Figures S4, S6, S8, and S10.

3.2.1. Degradation

PI analysis (Supplementary Figure S3) identifies NDRE as the most influential VI for degradation prediction, particularly significant in Rare zones, while GARI and GRNDVI also consistently rank high in fragmented contexts.

PDPs for NDRE + GARI (Figure 5) illustrate:

- **Core zones** consistently represent natural or semi-natural forest conditions, exhibiting minimal degradation signals throughout the studied period.

- **Transitional zones** progressively shift towards distorted or strongly degraded forest states by 2024, evidenced by brighter regions indicating intensified canopy stress and pigment deterioration.
- **Rare zones** prominently feature transformed or devastated conditions, as indicated by pronounced bright regions, clearly reflecting increased fragmentation-induced ecological stress and significant canopy loss.

Alternative influential indices, such as GRNDVI and NDWI, demonstrate similar ecological trends, particularly in Rare zones, as shown in Supplementary Figure S4.

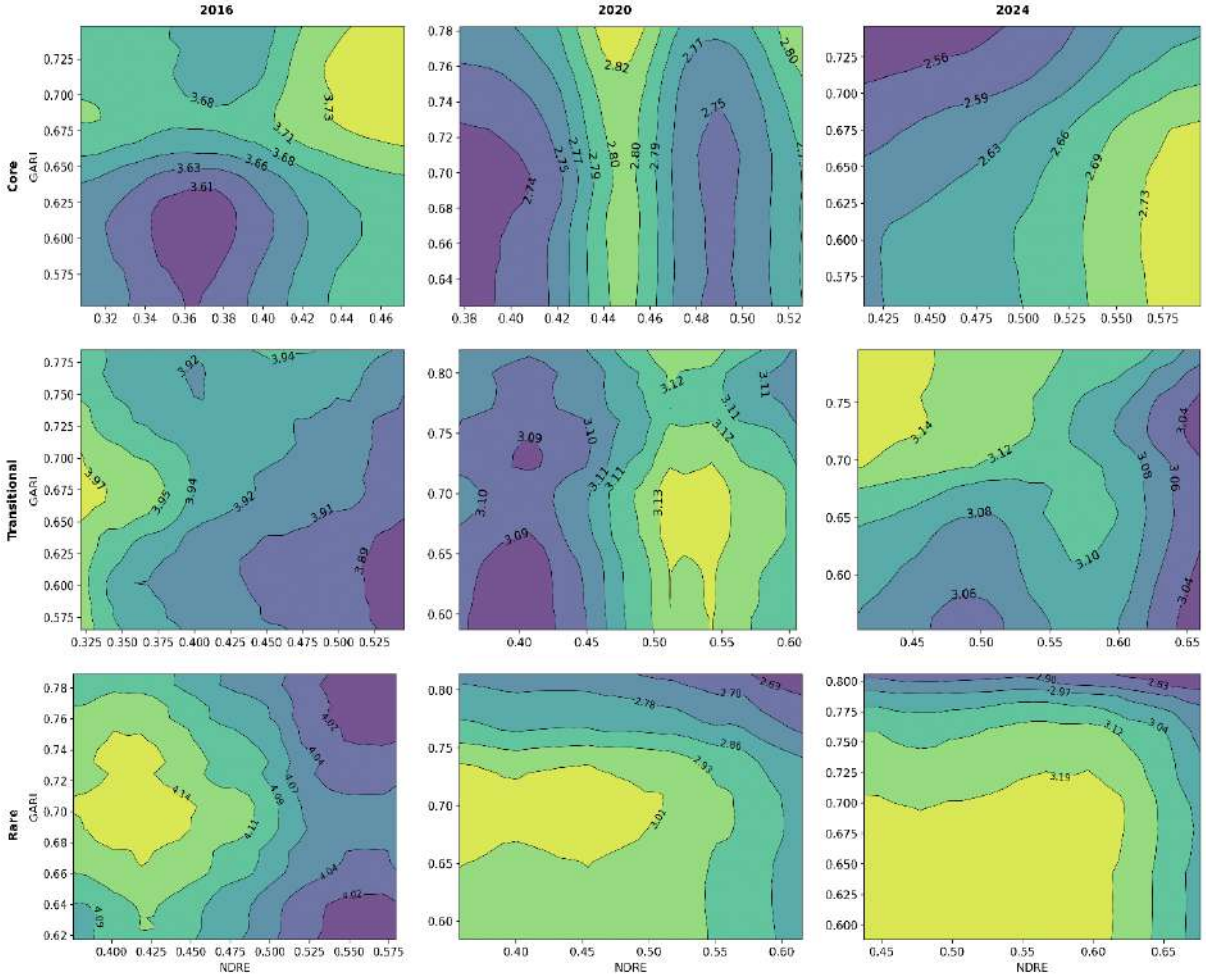

Figure 5. PDPs illustrating degradation using NDRE + GARI across Core, Transitional, and Rare zones (2016, 2020, 2024). Brighter areas indicate more severe degradation (see Supplementary Table S2 for degradation classes).

3.2.2. Moisture Content

PI rankings (Supplementary Figure S5) highlight NDMI and NDRE as key predictors, notably during drier conditions (2020), when moisture stress intensified in Rare zones.

PDPs for NDRE + NDMI (Figure 6) show:

- **Core zones** predominantly characterized by fresh or moist soil conditions, maintaining consistent moisture levels across years.

- **Transitional zones** display increasing variability and heterogeneity, transitioning between moist and fresh soils by 2024, indicative of altered hydrological patterns due to fragmentation.
- **Rare zones** exhibit clear transitions towards drier or partially drained soil conditions, signaling intensified moisture stress associated with exposure and fragmentation.

Alternative indices sensitive to moisture variations, including NDWI and CIred-edge, are presented in Supplementary Figure S6.

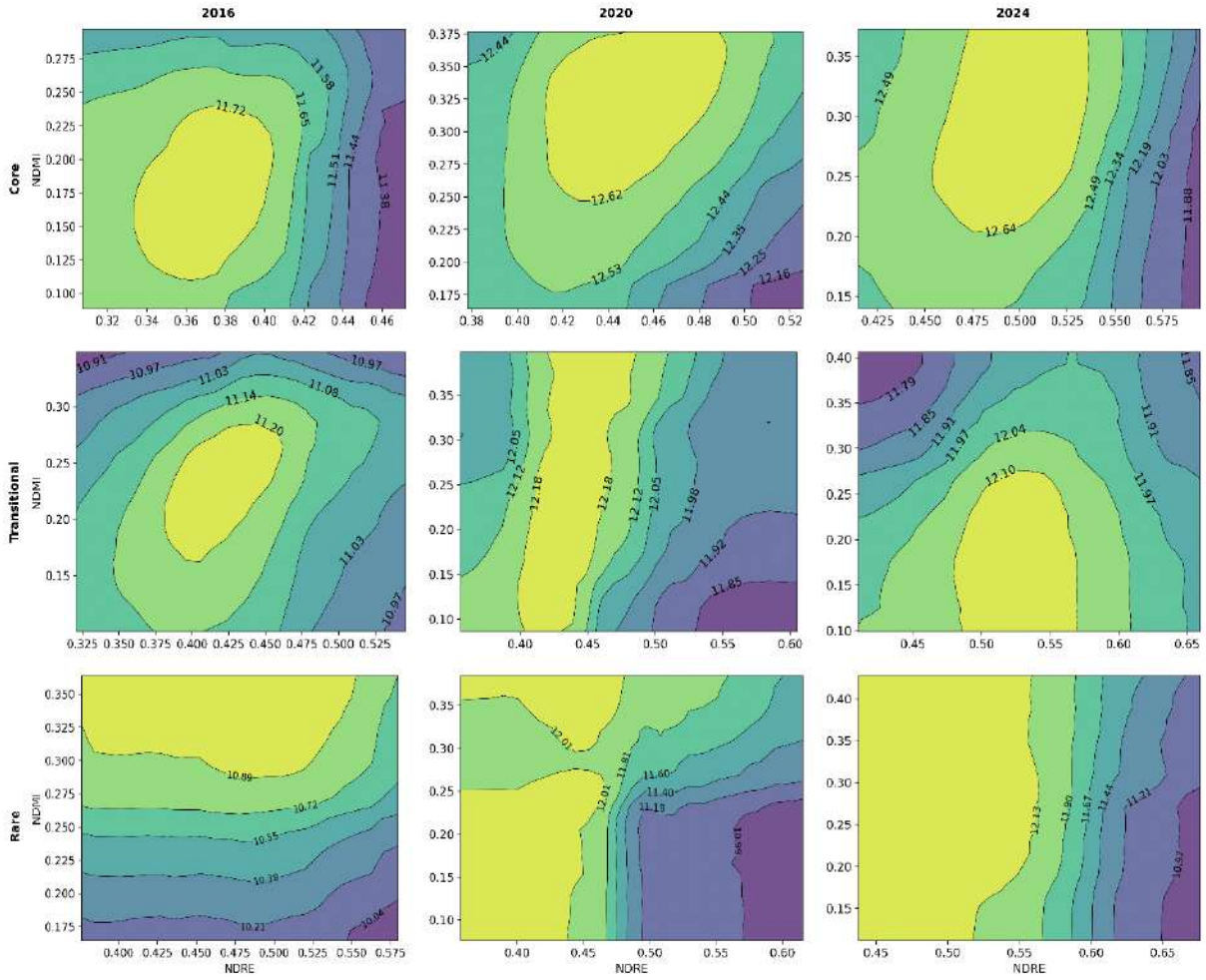

Figure 6. PDPs depicting moisture content using NDRE + NDMI across Core, Transitional, and Rare zones (2016, 2020, 2024). Brighter regions represent drier conditions (refer to Supplementary Table S3 for detailed moisture classes).

3.2.3. Site Type

PI analysis (Supplementary Figure S7) emphasizes NDVI and NDRE as the primary predictors for site type classification, with CIred-edge becoming significant particularly in fragmented forest zones.

PDPs for NDVI + NDRE (Figure 7) reveal:

- **Core zones** consistently associated with fresh or moist broadleaf and coniferous forest habitats, reflecting stable ecological conditions.
- **Transitional zones** exhibit intermediate habitat heterogeneity, progressively shifting towards mixed moist broadleaf or swamp forest types by 2024.

- **Rare zones** present pronounced contrasts, notably transitioning towards bog forests and riparian floodplain habitats, indicative of significant ecological disruptions linked to fragmentation.

Supplementary Figure S8 provides additional vegetation index pairs used for site type prediction.

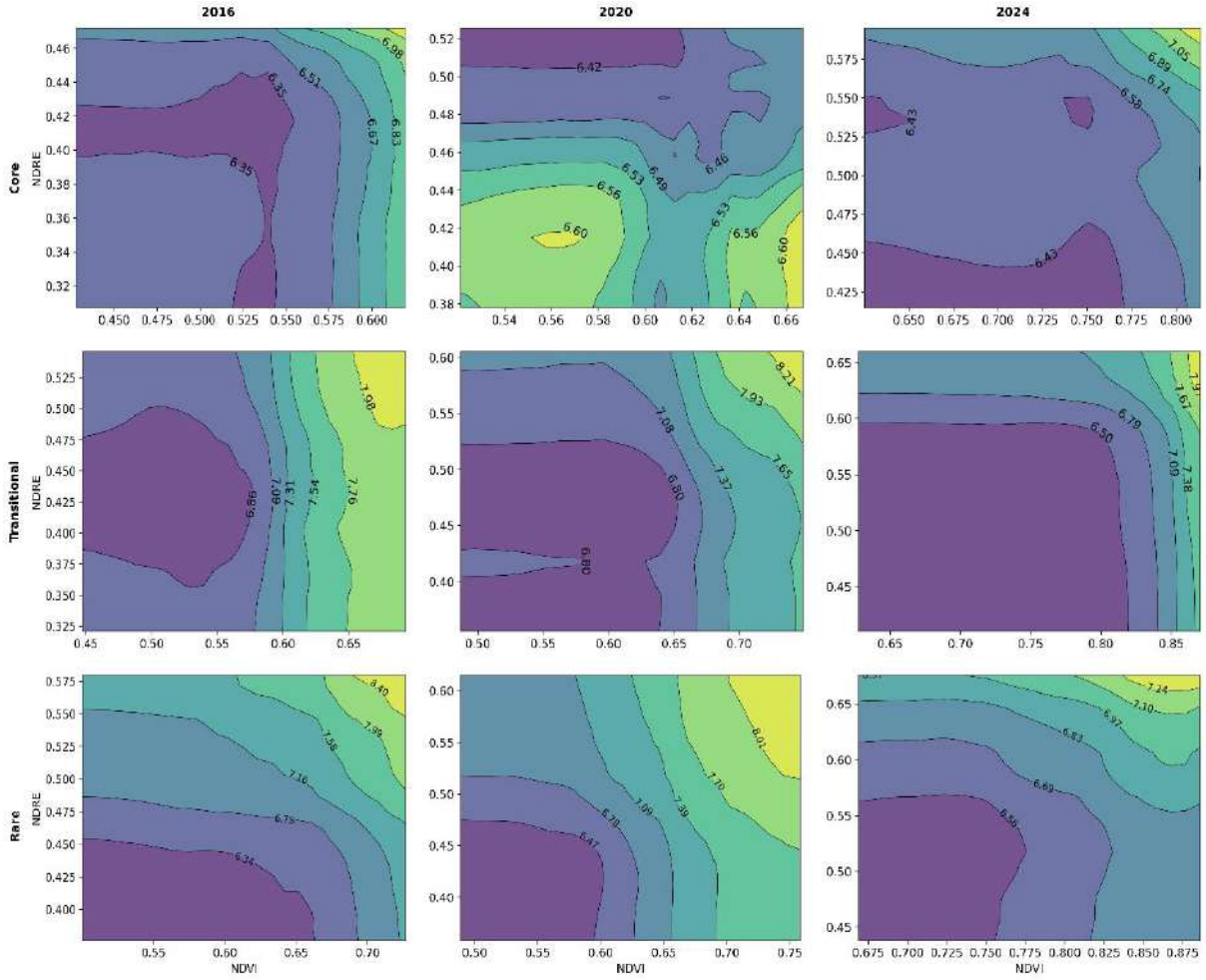

Figure 7. PDPs illustrating site type conditions using NDVI + NDRE across Core, Transitional, and Rare zones (2016, 2020, 2024). Brighter regions indicate habitats with more fertile and fresh conditions, whereas darker regions represent bog or swamp habitats (see Supplementary Table S4 for detailed site type categories).

3.2.4. Stand Age

PI analysis (Supplementary Figure S9) identifies CVI as the leading predictor of stand age in Core and Transitional zones, while NDRE emerges as essential in Rare zones, capturing younger regrowth dynamics.

PDPs for CVI + NDRE (Figure 8) illustrate:

- **Core zones** prominently represent older, mature stands, indicated by stable bright regions reflecting relatively undisturbed forest conditions.
- **Transitional zones** highlight varied age structures, showing mixed-age stands reflective of selective disturbances and ongoing regrowth.
- **Rare zones** clearly show younger stands interspersed with isolated older remnants, consistent with fragmented forest landscapes and repeated disturbances.

Supplementary Figure S10 provides additional vegetation index pairings utilized for stand age prediction.

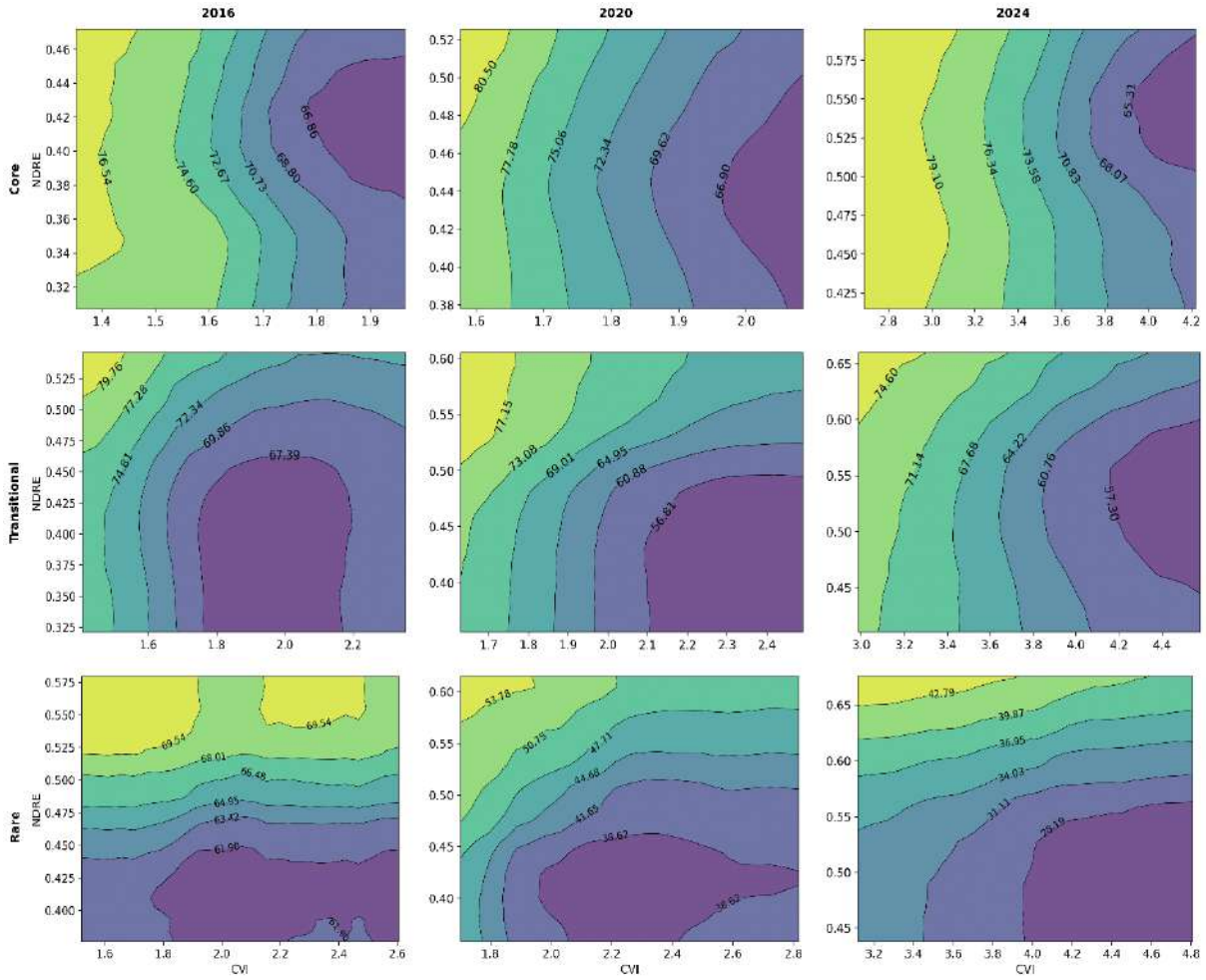

Figure 8. PDPs illustrating stand age patterns using CVI + NDRE across Core, Transitional, and Rare zones (2016, 2020, 2024). Brighter regions indicate older forest stands.

4. Discussion

4.1. Ecological Drivers and Degradation Trends Across FAD Zones

Across fragmentation zones, NDRE, GARI, and GRNDVI consistently captured canopy stress, reflecting their sensitivity to pigment decline and early warning signals (Lausch et al., 2016; Rossini et al., 2006). Treating degradation as a continuous gradient helped reveal subtle shifts before major structural change, in line with trait-based remote sensing calls for anticipatory indicators (Trumbore et al., 2015; Wang et al., 2010).

In Core areas, PDPs were notably stable—consistent with buffered microclimates and structural continuity that reduce edge stress and aid dispersal of wide-ranging species (Hanski, 2015). By contrast, Transitional and Rare zones showed steeper, more variable PDP gradients, symptomatic of heightened microclimatic variability, nutrient depletion, and wind exposure near edges (Briant et al., 2010; Arroyo-Rodríguez et al., 2017). These patterns echo global evidence that edge effects accelerate pigment degradation and moisture stress, especially where habitat falls below critical thresholds of ~20–30% (Haddad et al., 2015; Fahrig, 2017).

The strong performance of NDRE and GARI in Rare zones supports their use as *operational early-warning indicators* of functional decline, enabling interventions before biomass losses accrue. By linking pigment-sensitive indices to fragmentation gradients, this study shows how open-access Sentinel-2 data can form a *reproducible early-warning system* for canopy decline, directly addressing the challenge of detecting subtle degradation before structural loss becomes visible.

4.2. Moisture Dynamics and Spectral Predictability

Moisture responses diverged by zone: NDMI and NDRE consistently ranked as the most informative indices for soil–canopy interactions under disturbance (Peters et al., 2007; He et al., 2013). Core zones retained stable, fresh–moist conditions—consistent with closed canopies and mature root systems that buffer drought (Schwartz et al., 2019). Rare zones, in contrast, displayed sharp moisture contrasts and higher variability, pointing to localized drying under reduced canopy cover and altered evapotranspiration—hallmarks of fragmentation-driven desiccation risk (Briant et al., 2010; Wei et al., 2022).

A brightening of PDP signals in Rare areas by 2024 may indicate secondary hydrological recovery after thinning or disturbance, a dynamic noted elsewhere (He et al., 2013; Schwartz et al., 2019). These results emphasize the importance of *rewilding Rare zones* with deeper-rooted, mixed plantings to enhance soil-water retention, and *adaptive thinning in Transitional zones* to dampen extremes. The clear separation of hydrological dynamics across zones also underscores the value of FAD-based stratification, which disentangles fragmentation signals otherwise obscured in whole-forest averages, offering a *scalable approach* for climate resilience assessments.

4.3. Site Type as a Landscape Filter

Fragmentation reshaped habitat quality gradients, with NDVI and NDRE emerging as primary predictors and CIred-edge distinguishing pigment-related fertility differences. Core zones exhibited homogeneous PDP responses—consistent with fertile, moist broadleaf–conifer conditions and the value of intact interiors (Lausch et al., 2017). Transitional and Rare zones, however, showed marked heterogeneity, reflecting shifts in soils and successional stages driven by disturbance histories (Nguyen et al., 2020; Budniak & Zięba, 2022).

Modeling site type on a continuous scale aided comparative reading across zones but may blur fine-scale heterogeneity—particularly in Rare fragments mixing pioneer regrowth with remnant mature patches. A pragmatic extension is to combine vegetation indices with LiDAR-derived structure or detailed soils to sharpen habitat delineation (Alonzo et al., 2016). In extensive forests lacking detailed inventories, NDVI and NDRE still offer an *efficient proxy* for fertility mapping, while targeted ground checks in high-risk or disturbed areas remain necessary. The framework therefore *advances forest ecology* by operationalizing fragmentation-sensitive indices into zone-specific habitat filters, bridging spatial modeling with practical monitoring.

4.4. Stand Age and Structural Maturity

Stand age patterns linked CVI and NDRE closely with canopy developmental stages, reflecting pigment dynamics during forest succession. Core and Transitional zones showed stable PDPs indicative of mature and uniform stand ages, confirming that optical indices remain *reliable age predictors* in low-disturbance contexts (Wulder et al., 2009). Rare zones, however, posed greater predictive challenges: regenerating edges often spectrally resembled older stands, risking misinterpretation of maturity—a difficulty previously noted in fragmented forests (Dobor et al., 2018).

Incorporating structural metrics from LiDAR or GEDI alongside vegetation indices could significantly enhance accuracy in fragmented, heterogeneous landscapes (Bauer et al., 2024; Burns, Hakkenberg, & Goetz, 2024). In practice, prioritizing Rare zones for *integrated structural–spectral assessment* can help

avoid misallocation of restoration resources to stands that appear mature optically but remain ecologically young.

4.5. From Process Detection to Management Application

The fragmentation processes identified in this study translate directly into zone-specific management strategies. Core zones, with their stable conditions, require *strict protection* to sustain carbon sequestration potential and safeguard interior specialists dependent on large, contiguous habitats (Blake and Karr, 1984; Fahrig et al., 2019). Transitional zones, which exhibited intermediate and variable ecological responses, call for *adaptive approaches* such as selective thinning and corridor creation to stabilize pigment and moisture dynamics, echoing recommendations from Fletcher et al. (2018). Rare zones, by contrast, showed pronounced ecological stress, emphasizing the need for *targeted restoration* and passive rewilding to restore connectivity, reduce desiccation risk, and support the persistence of edge-sensitive species.

This framework is consistent with global findings that even small, well-managed patches can significantly strengthen connectivity and biodiversity outcomes across fragmented landscapes (Fahrig, 2017; González-Ávila et al., 2023). Remote sensing adds a practical dimension to these strategies: indices such as NDRE, NDMI, and NDVI provide cost-effective monitoring tools, enabling managers to detect stress early and act before irreversible declines occur. Because the data used are open-access and globally available, the same playbook—*protect Core, adapt in Transitional, restore Rare*—can be readily applied to other temperate forest systems.

4.6. Limitations and Methodological Considerations

Several methodological considerations temper the interpretation of these results. Treating categorical FEAs (degradation, moisture, site type) as continuous variables facilitated the detection of ecological gradients, yet risks obscuring sharp thresholds—especially in edge-dominated Rare zones where variability in species composition, soil conditions, wind exposure, and microclimatic dynamics may play disproportionate roles. This limitation has practical implications, as restoration often depends on identifying *precise thresholds* beyond which ecological collapse is likely.

Resolution presents another challenge. Sentinel-2's 10 m pixel size may fail to capture microhabitat heterogeneity, particularly in species-rich stands or highly fragmented mosaics. As Alonzo et al. (2016) and Burns et al. (2024) note, integrating UAV- or LiDAR-derived data could complement spectral indices by providing finer structural detail. Managers may therefore require such information before committing restoration resources in heterogeneous forests.

Finally, transferability beyond temperate pine-dominated systems may be constrained. In more diverse tropical or broadleaf systems, spectral confusion between canopy species can reduce predictive accuracy, necessitating careful local calibration (Fahrig, 2003; Lausch et al., 2017).

Despite these caveats, the integration of Extra Trees with permutation importance and PDPs proved effective in linking fragmentation to ecological processes. The workflow itself—built on *open-access data* and reproducible tools—offers a *scalable template* for forest monitoring. Future developments could involve hybrid approaches combining climate, soil, and structural covariates, or radiative transfer model–machine learning hybrids, to refine predictions and improve resilience forecasting under diverse disturbance regimes.

5. Conclusion

This study demonstrates how fragmentation reshapes key ecological processes—*degradation, moisture dynamics, habitat quality, and structural maturity*—across Core, Transitional, and Rare zones in the Tuchola Forest Biosphere Reserve, using Sentinel-2 vegetation indices. Pigment-sensitive indices such

as NDRE and GARI emerged as early-warning signals of degradation in Rare zones, where edge stress and connectivity loss precede structural decline, particularly affecting forest interior specialists reliant on stable habitats (Blake and Karr, 1984). Moisture-sensitive indices like NDMI captured hydrological stability in Core zones and sharp variability in Rare areas, reflecting cumulative disturbance and rooting-depth limitations tied to the monodominant Scots pine structure, which reduces beta-diversity and stabilizes responses but heightens edge vulnerability (Fahrig et al., 2019; Wulder et al., 2009). Site type predictions distinguished fertile core habitats from fragmented mosaics, while stand age modeling revealed a critical risk of misinterpreting edge regrowth as maturity—highlighting the need to integrate structural metrics for accurate assessment.

By combining *FAD-based zoning* with interpretable machine learning (Extra Trees and PDPs), this study establishes an *operational framework* for linking spectral traits to ecological processes under fragmentation. Beyond diagnosis, the results translate into clear, zone-specific strategies: (1) strict protection of Core zones to sustain carbon storage and interior biodiversity; (2) adaptive management in Transitional areas through corridor planting and selective thinning; and (3) intensive restoration of Rare zones via passive rewilding and stepping-stone creation to reduce edge stress and reconnect habitats.

Future research should validate this framework across diverse ecological contexts and explore integration with structural and climatic datasets to enhance predictive accuracy and applicability. Because it is grounded in *open-access Sentinel-2 data* and reproducible workflows, the approach is readily transferable to other temperate and boreal landscapes. In doing so, it aligns with global biodiversity and climate targets by enabling cost-effective, scalable monitoring of fragmentation impacts. Ultimately, integrating vegetation indices with zone-based planning transforms remote sensing into a *practical tool* for anticipating ecological decline and guiding resilience-oriented forest management under accelerating climate and land-use pressures (González-Ávila et al., 2023; Wang et al., 2025).

Declaration of Generative AI in the Writing Process

The authors used generative AI tools (*ChatGPT by OpenAI* and *Grok*) solely to improve the language and readability of the manuscript. No sections of text, figures, or analyses were generated automatically. All content was reviewed, edited, and approved by the authors to ensure accuracy and integrity. The authors take full responsibility for the content of this work.

Data Availability Statement

All inputs are *open access*. Sentinel-2 Level-2A imagery (and 2016 L1C scenes corrected with Sen2Cor) and Dynamic World "trees" probabilities were accessed via *Google Earth Engine*. Field-based ecological attributes (degradation, moisture, site type, stand age) were obtained from the *Polish Forest Data Bank (BDL)*.

To support reproducibility, the manuscript and supplements include:

- complete model hyperparameters and random seeds (Table S5),
- the exact preprocessing and modeling steps (Sections 2.2–2.5), and
- Google Earth Engine / Python scripts (Supplementary Listings).

A minimal example dataset (10×10 km tiles per FAD class for each year) and the full script bundle are available from the corresponding author upon reasonable request for academic, non-commercial use. Large full-extent rasters can be regenerated directly from open sources using the provided scripts.

Acknowledgements

The authors express their gratitude to *Dr. Melaine Aubry Kientz* and *Prof. Grégoire Vincent* for valuable advice and guidance during the internship at the AMAP Laboratory, Montpellier. We also thank the *Statistical Analysis Center at Nicolaus Copernicus University* for providing access to their computational cluster and expert statistical feedback. Additionally, we acknowledge the *Bank Danych o Lasach – Lasy Państwowe (Forest Data Bank – State Forests)* for providing high-quality forest inventory data collected by professional foresters.

CRediT Author Statement

- *Sanjana Dutt*: Conceptualization, Data curation, Formal analysis, Investigation, Methodology, Project administration, Resources, Software, Validation, Visualization, Writing – original draft, Writing – review & editing.
- *Jakub Wojtasik*: Software, Formal analysis, Visualization, Validation, Writing – review & editing.
- *Dimitri Justeau-Allaire*: Supervision, Writing – review & editing.
- *Mieczysław Kunz*: Resources, Supervision, Visualization (maps), Writing – review & editing.

Funding Statement

This research did not receive any specific grant from funding agencies in the public, commercial, or not-for-profit sectors.

Disclosure Statement

The authors report *no competing interests* to declare.

References

1. Alonzo, M., McFadden, J.P., Nowak, D.J., Roberts, D.A., 2016. Mapping urban forest structure and function using hyperspectral imagery and lidar data. Urban For. Urban Green. 17, 135–147. https://doi.org/10.1016/j.ufug.2016.04.003
2. Arroyo-Rodríguez, V., Saldana-Vazquez, R.A., Fahrig, L., Santos, B.A., 2017. Does forest fragmentation cause an increase in forest temperature? Ecol. Res. 32, 81–88. https://doi.org/10.1007/s11284-016-1411-6
3. Bauer, L.P.L., Huth, A., Bogdanowski, A., Müller, M., Fischer, R., 2024. Edge effects in Amazon forests: Integrating remote sensing and modelling to assess changes in biomass and productivity. Remote Sens. 16(3), 501. https://doi.org/10.3390/rs16030501
4. Blake, J.G., Karr, J.R., 1984. Species composition of bird communities and the conservation benefit of large versus small forests. Biol. Conserv. 30(2), 173–187. https://doi.org/10.1016/0006-3207(84)90065-X
5. Breiman, L., 2001. Random forests. Mach. Learn. 45, 5–32. https://doi.org/10.1023/A:1010933404324
6. Briant, G., Gond, V., Laurance, S.G., 2010. Habitat fragmentation and the desiccation of forest canopies: Eastern Amazonia. Biol. Conserv. 143(11), 2763–2769. https://doi.org/10.1016/j.biocon.2010.07.024
7. Brinck, K., Fischer, R., Groeneveld, J., Lehmann, S., de Paula, M.D., Pütz, S., Huth, A., 2017. High-resolution analysis of tropical forest fragmentation and its impact on the global carbon cycle. Nat. Commun. 8, 14855. https://doi.org/10.1038/ncomms14855
8. Britton, J., Abatzoglou, J.T., et al., 2024. Explaining MODIS NDVI drought responses with tree-based models and SHAP. J. Appl. Serv. Climatol. 2024(5), e009001. https://doi.org/10.46275/JOASC.2024.09.001

9. Broggio, I.S., Silva-Junior, C.H., Nascimento, M.T., Villela, D.M., Aragão, L.E.O.C., 2024. Quantifying landscape fragmentation and forest carbon dynamics over 35 years in the Brazilian Atlantic Forest. Environ. Res. Lett. 19(3), 034047. https://doi.org/10.1088/1748-9326/ad281c
10. Brown, C.F., Brumby, S.P., Guzder-Williams, B., et al., 2022. Dynamic World, near real-time global 10 m land use land cover mapping. Sci. Data 9, 251. https://doi.org/10.1038/s41597-022-01307-4
11. Budniak, P., Zięba, S., 2022. Effects of forest fragmentation on the volume of wood resources in managed pine-dominated forests in Poland. Forests 13(4), 590. https://doi.org/10.3390/f13040590
12. Burns, P., Hakkenberg, C.R., Goetz, S.J., 2024. Multi-resolution gridded maps of vegetation structure from GEDI. Sci. Data 11, 881. https://doi.org/10.1038/s41597-024-03668-4
13. Dobor, L., Hlásny, T., Rammer, W., Barka, I., Trombik, J., Pavlenda, P., Seidl, R., 2018. Post-disturbance recovery of forest carbon in a temperate forest landscape under climate change. Agric. For. Meteorol. 263, 308–322. https://doi.org/10.1016/j.agrformet.2018.08.028
14. Dutt, S., Batar, A.K., Sulik, S., Kunz, M., 2024. Forest ecosystem on the edge: Fragmentation susceptibility in Tuchola Forest, Poland. Ecol. Indic. 161, 111980. https://doi.org/10.1016/j.ecolind.2024.111980
15. Fahrig, L., 2003. Effects of habitat fragmentation on biodiversity. Annu. Rev. Ecol. Evol. Syst. 34, 487–515. https://doi.org/10.1146/annurev.ecolsys.34.011802.132419
16. Fahrig, L., 2017. Ecological responses to habitat fragmentation per se. Annu. Rev. Ecol. Evol. Syst. 48, 1–23. https://doi.org/10.1146/annurev-ecolsys-110316-022612
17. Fahrig, L., Arroyo-Rodríguez, V., Bennett, J.R., Boucher-Lalonde, V., Cazetta, E., Currie, D.J., Zeller, K.A., 2019. Is habitat fragmentation bad for biodiversity? Biol. Conserv. 230, 179–186. https://doi.org/10.1016/j.biocon.2018.12.026
18. Fletcher, R.J., Didham, R.K., Banks-Leite, C., Barlow, J., Ewers, R.M., Rosindell, J., Haddad, N.M., 2018. Is habitat fragmentation good for biodiversity? Biol. Conserv. 226, 9–15. https://doi.org/10.1016/j.biocon.2018.07.022
19. Geurts, P., Ernst, D., Wehenkel, L., 2006. Extremely randomized trees. Mach. Learn. 63(1), 3–42. https://doi.org/10.1007/s10994-006-6226-1
20. González-Ávila, S., Ortega, E., Martín, B., 2023. Potential priority areas for forest-dwelling species in Spain based on the degree of forest fragmentation. J. Maps 19(1), 2223597. https://doi.org/10.1080/17445647.2023.2223597
21. Grömping, U., 2009. Variable importance assessment in regression: Linear regression versus random forest. Am. Stat. 63(4), 308–319. https://doi.org/10.1198/tast.2009.08199
22. Haddad, N.M., Brudvig, L.A., Clobert, J., Davies, K.F., Gonzalez, A., Holt, R.D., Townshend, J.R., 2015. Habitat fragmentation and its lasting impact on Earth's ecosystems. Sci. Adv. 1(2), e1500052. https://doi.org/10.1126/sciadv.1500052
23. He, L., Ivanov, V.Y., Bohrer, G., Thomsen, J.E., Vogel, C.S., Moghaddam, M., 2013. Temporal dynamics of soil moisture in a northern temperate mixed successional forest after a prescribed intermediate disturbance. Agric. For. Meteorol. 180, 22–33. https://doi.org/10.1016/j.agrformet.2013.04.014
24. Hollberg, J.L., Schellberg, J., 2017. Distinguishing intensity levels of grassland fertilization using vegetation indices. Remote Sens. 9(1), 81. https://doi.org/10.3390/rs9010081
25. Ke, G., Meng, Q., Finley, T., Wang, T., Chen, W., Ma, W., Ye, Q., Liu, T.Y., 2017. LightGBM: A highly efficient gradient boosting decision tree. Adv. Neural Inf. Process. Syst. 30, 3146–3154.
26. Kozak, J., Ziółkowska, E., Vogt, P., Dobosz, M., Kaim, D., Kolecka, N., Ostafin, K., 2018. Forest-cover increase does not trigger forest-fragmentation decrease: Polish Carpathians. Sustainability 10(5), 1472. https://doi.org/10.3390/su10051472
27. Laurance, W.F., Camargo, J.L.C., Fearnside, P.M., Lovejoy, T.E., Williamson, G.B., Mesquita, R.C.G., Meyer, C.F.J., Bobrowiec, P.E.D., Laurance, S.G., 2018. An Amazonian rainforest and its fragments as a laboratory of global change. Biol. Rev. 93(1), 223–247. https://doi.org/10.1111/brv.12343
28. Lausch, A., Erasmi, S., King, D.J., Magdon, P., Heurich, M., 2016. Understanding forest health with remote sensing—Part I: Spectral traits, processes and characteristics. Remote Sens. 8(12), 1029. https://doi.org/10.3390/rs8121029

29. Lausch, A., Erasmi, S., King, D.J., Magdon, P., Heurich, M., 2017. Understanding forest health with remote sensing—Part II: Approaches and data models. Remote Sens. 9(2), 129. https://doi.org/10.3390/rs9020129
30. Liu, X., Liang, S., Li, B., Ma, H., He, T., 2021. Mapping 30 m fractional forest cover over China's Three-North Region with ensemble machine learning. Remote Sens. 13(13), 2592. https://doi.org/10.3390/rs13132592
31. Łoś, H., Mendes, G.S., Cordeiro, D., Grosso, N., Costa, H., Benevides, P., Caetano, M., 2021. Evaluation of XGBoost and LGBM performance in tree species classification with Sentinel-2 data. In: IGARSS 2021 - IEEE Int. Geosci. Remote Sens. Symp., 5803–5806. IEEE. https://doi.org/10.1109/IGARSS47720.2021.9553031
32. Łuców, D., Lamentowicz, M., Kołaczek, P., Łokas, E., Marcisz, K., Obremska, M., Słowiński, M., 2021. Pine forest management and disturbance in Northern Poland: Combining high-resolution paleoecology and remote sensing. Front. Ecol. Evol. 9, 747976. https://doi.org/10.3389/fevo.2021.747976
33. Molnar, C., 2019. Interpretable Machine Learning: A Guide for Making Black Box Models Explainable. Leanpub, Victoria, Canada. https://christophm.github.io/interpretable-ml-book
34. Nguyen, H.T., Nguyen, T.D., Kappas, M., 2020. Land cover and forest type classification by values of vegetation indices and forest structure of tropical lowland forests in central Vietnam. Int. J. For. Res. 2020, 8896310. https://doi.org/10.1155/2020/8896310
35. Nicodemus, K.K., Malley, J.D., Strobl, C., Ziegler, A., 2010. The behaviour of random forest permutation-based variable importance measures under predictor correlation. BMC Bioinform. 11, 110. https://doi.org/10.1186/1471-2105-11-110
36. Pedregosa, F., Varoquaux, G., Gramfort, A., Michel, V., Thirion, B., Grisel, O., Blondel, M., Prettenhofer, P., Weiss, R., Dubourg, V., Vanderplas, J., Passos, A., Cournapeau, D., Brucher, M., Perrot, M., Duchesnay, É., 2011. Scikit-learn: Machine learning in Python. J. Mach. Learn. Res. 12, 2825–2830.
37. Peters, J., De Baets, B., Verhoest, N.E.C., Samson, R., Degroeve, S., De Becker, P., Huybrechts, W., 2007. Random forests as a tool for ecohydrological distribution modelling. Ecol. Model. 207(2–4), 304–318. https://doi.org/10.1016/j.ecolmodel.2007.05.011
38. Primka, E.J., Smith, W.K., 2019. Synchrony in fall leaf drop: chlorophyll degradation, color change, and abscission layer formation in three temperate deciduous tree species. Am. J. Bot. 106(3), 377–388. https://doi.org/10.1002/ajb2.1247
39. Riitters, K., Wickham, J., 2012. Decline of forest interior conditions in the conterminous United States. Sci. Rep. 2, 653. https://doi.org/10.1038/srep00653
40. Rossini, M., Panigada, C., Meroni, M., Colombo, R., 2006. Assessment of oak forest condition based on leaf biochemical variables and chlorophyll fluorescence. Tree Physiol. 26(11), 1487–1496. https://doi.org/10.1093/treephys/26.11.1487
41. Schwartz, N.B., Budsock, A.M., Uriarte, M., 2019. Fragmentation, forest structure, and topography modulate impacts of drought in a tropical forest landscape. Ecology 100(6), e02677. https://doi.org/10.1002/ecy.2677
42. Vogt, P., Riitters, K., 2017. GuidosToolbox: Universal digital image object analysis. Eur. J. Remote Sens. 50(1), 352–361. https://doi.org/10.1080/22797254.2017.1330650
43. Wang, K., Franklin, S.E., Guo, X., Cattet, M., 2010. Remote sensing of ecology, biodiversity and conservation: A review from the perspective of remote-sensing specialists. Sensors 10(11), 9647–9667. https://doi.org/10.3390/s101109647
44. Wang, Z., Han, L., Wang, L., Shi, H., Luo, Y., 2025. Neighboring patch density or patch size? Which determines the importance of forest patches in maintaining overall landscape connectivity in Kanas, Xinjiang, China. Biology 14(7), 881. https://doi.org/10.3390/biology14070881
45. Wei, X., Giles-Hansen, K., Spencer, S.A., Ge, X., Onuchin, A., Li, Q., Hou, Y., 2022. Forest harvesting and hydrology in boreal forests: Under an increased and cumulative disturbance context. For. Ecol. Manage. 522, 120468. https://doi.org/10.1016/j.foreco.2022.120468
46. Wulder, M.A., White, J.C., Andrew, M.E., Seitz, N.E., Coops, N.C., 2009. Forest fragmentation, structure, and age characteristics as a legacy of forest management. For. Ecol. Manage. 258(9), 1938–1949. https://doi.org/10.1016/j.foreco.2009.07.041

47. Xue, J., Su, B., 2017. Significant remote sensing vegetation indices: A review of developments and applications. J. Sensors 2017, 1353691. https://doi.org/10.1155/2017/1353691
48. Yu, X., Xie, J., Jiang, R., Zhao, Y., Li, F., Liang, J., Wang, Y., 2021. Spatiotemporal variation and predictability of vegetation coverage in the Beijing–Tianjin–Hebei metropolitan region, China. Theor. Appl. Climatol. 145, 47–62. https://doi.org/10.1007/s00704-021-03616-x

Supplementary Material for ***How Does Fragmentation Reshape Forests? Tracking Dominant Ecological Processes Across Core, Transitional, and Rare Zones***

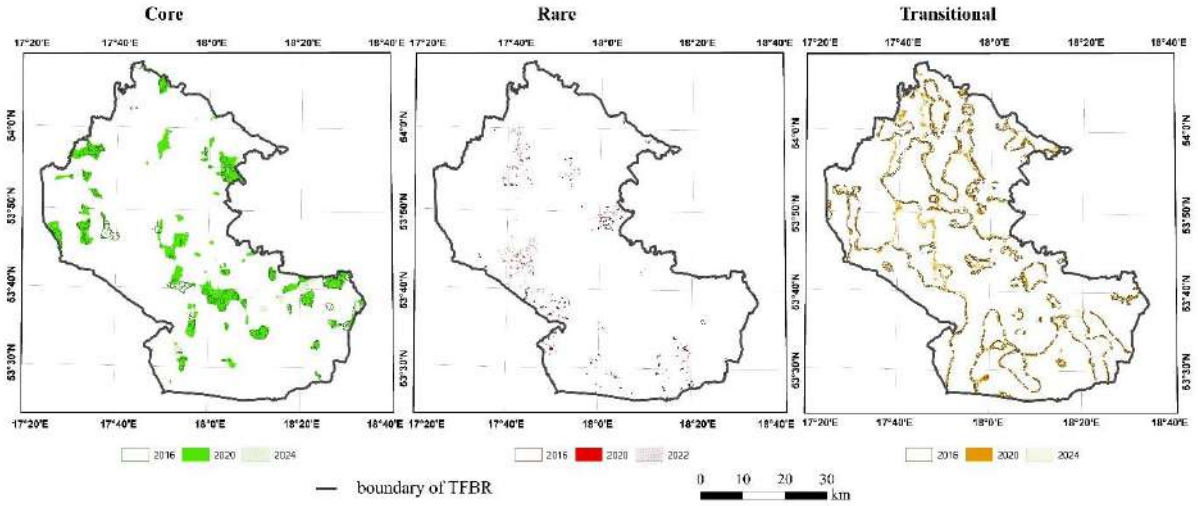

Supplementary Figure S1. Spatial persistence and transitions of Core, Rare, and Transitional zones in TFBR across 2016, 2020, and 2024. Color hues indicate temporal overlap and shifts of zone types, offering insight into fragmentation trajectory over time.

Supplementary Table S1. Vegetation Indices Used in This Study with Corresponding Formulas and Ecological Relevance

The table summarizes the vegetation indices computed from Sentinel-2 bands (B2–B11), grouped by their functional ecological domains. Each formula reflects the actual implementation used in this study, and the indices are categorized based on their relevance to greenness/biomass, moisture stress, pigment content, and soil or shadow correction.

🔶 **Greenness / Biomass Indices**

Index	*Formula*	*Notes*
NDVI	(B8 − B4) / (B8 + B4)	Normalized Difference Vegetation Index
EVI	2.5 × (B8 − B4) / (B8 + 6 × B4 − 7.5 × B2 + 1)	Enhanced Vegetation Index using Blue for atmospheric correction
EVI2	2.5 × (B8 − B4) / (B8 + 2.4 × B4 + 1)	Two-band EVI, avoids blue band
GNDVI	(B8 − B3) / (B8 + B3)	Green NDVI, more sensitive to chlorophyll content
GRNDVI	(B5 − B3) / (B5 + B3)	Red Edge NDVI, useful for early stress detection
GSAVI	((B8 − B4) × (1 + 0.5)) / (B8 + B4 + 0.5)	Green Soil-Adjusted Vegetation Index, L = 0.5
LAI	3.618 × ((B8 − B4) / (B8 + 6 × B4 − 7.5 × B2 + 1)) − 0.118	Proxy for Leaf Area Index, derived from EVI
DVI	B8 − B4	Difference Vegetation Index, simple reflectance gap

🔷 **Moisture Stress Indices**

Index	*Formula*	*Notes*

NDMI	(B8 − B11) / (B8 + B11)	Normalized Difference Moisture Index using NIR and SWIR
GVMI	(B8 + 0.1 − (B11 + 0.02)) / (B8 + 0.1 + (B11 + 0.02))	Global Vegetation Moisture Index, atmospheric-corrected variant

710

711 **Pigment / Chlorophyll Indices**

Index	*Formula*	*Notes*
GARI	(B8 − (B3 − (B2 − B4))) / (B8 + (B3 − (B2 − B4)))	Green Atmospherically Resistant Index, sensitive to chlorophyll
MCARI	((B5 − B4) − 0.2 × (B5 − B3)) × (B5 / B4)	Modified Chlorophyll Absorption Ratio Index
MTVI2	1.5 × [1.2 × (B5 − B3) − 2.5 × (B4 − B3)] / √[(2 × B5 + 1)² − (6 × B5 − 5 × √B4) − 0.5]	Modified Triangular Vegetation Index 2
NDRE	(B8 − B5) / (B8 + B5)	Normalized Difference Red Edge Index
GBNDVI	(B8 − (B3 + B2)) / (B8 + (B3 + B2))	Green-Blue NDVI, sensitive to nutrient/pigment shifts

712

713 **Soil / Shadow Correction Indices**

Index	*Formula*	*Notes*
CVI	(B8 × B4) / (B3²)	Chlorophyll Vegetation Index, proxy for vegetation cover density
MSAVI	(2 × B8 + 1 − √[(2 × B8 + 1)² − 8 × (B8 − B4)]) / 2	Modified Soil-Adjusted Vegetation Index, soil background minimized

714

715 **Band Mapping (Sentinel-2)**

716 - **B2** – Blue (490 nm)
717 - **B3** – Green (560 nm)
718 - **B4** – Red (665 nm)
719 - **B5** – Red Edge 1 (705 nm)
720 - **B8** – Near Infrared (842 nm)
721 - **B11** – Shortwave Infrared (1610 nm)

722

723 **Supplementary Table S2.** Degradation Codebook

Code	*English Description*	*Assigned Number*
D1	Degraded	1
D2	Strongly degraded	2
D3	Devastated	3
N1	Natural	4

N2	Semi-natural	5
Z1	Distorted	6
Z2	Strongly distorted	7
Z3	Transformed	8

724
725
726 **Supplementary Table S3.** Moisture Content Codebook

Code	***Description***	***Assigned Number***
BBM	Very wet bog	1
BM	Wet bog	2
BO	Drained bog	3
BSO	Strongly drained bog	4
SU	Dry soils	5
SŚ	Very fresh soils	6
WO	Drained moist soils	7
WSW	Very moist soils	8
WW	Moist soils	9
ŁP	Floodplain forest (flooded/drained)	10
ŁZ	Floodplain forest (flooded)	11
Ś	Fresh soils	12

727 **Supplementary Table S4.** Site Type Codebook

Code	***Description***	***Assigned Number***
BB	Bog coniferous forest	1

BMB	Mixed bog forest	2
BMW	Mixed moist coniferous forest	3
BMŚW	Mixed fresh coniferous forest	4
BS	Dry coniferous forest	5
BW	Moist coniferous forest	6
BŚW	Fresh coniferous forest	7
LMB	Mixed swamp forest	8
LMW	Mixed moist broadleaf forest	9
LMŚW	Mixed fresh broadleaf forest	10
LW	Moist broadleaf forest	11
LŁ	Riparian floodplain forest	12
LŚW	Fresh broadleaf forest	13
OL	Alder swamp forest	14
OLJ	Ash-alder swamp forest	15

Supplementary Table S5: Extra Trees Settings for Predicting Field-Based Ecological Attributes

Below are the tuned settings for Extra Trees models, organized by field-based ecological attribute (FEA), fragmentation zone (Core, Transitional, Rare), and year (2016, 2020, 2024). Settings include: Number of Trees (trees in the model), Features for Decisions (number of input features considered), Min Samples to Split (minimum samples to split a decision point), and Min Samples per Node (minimum samples in a final node).

a) Degradation

Zone	*Year*	*Number of Trees*	*Features for Decisions*	*Min Samples to Split*	*Min Samples per Node*
Rare	2016	1000	16	2	1
Rare	2020	1000	9	2	1
Rare	2024	1000	9	2	1
Transitional	2016	1000	17	18	1
Transitional	2020	1000	17	20	4
Transitional	2024	1000	17	20	4
Core	2016	1000	15	20	1
Core	2020	878	17	6	10
Core	2024	474	16	18	7

b) Stand Age

Zone	*Year*	*Number of Trees*	*Features for Decisions*	*Min Samples to Split*	*Min Samples per Node*
Rare	2016	1000	13	2	1
Rare	2020	1000	11	10	1
Rare	2024	1000	13	10	1
Transitional	2016	978	10	20	1
Transitional	2020	1000	8	20	2
Transitional	2024	1000	10	20	1
Core	2016	1000	12	20	1
Core	2020	1000	9	20	5
Core	2024	1000	12	20	1

c) Moisture Content

Zone	*Year*	*Number of Trees*	*Features for Decisions*	*Min Samples to Split*	*Min Samples per Node*
Transitional	2016	822	14	13	3
Transitional	2020	1000	15	20	4
Transitional	2024	822	14	13	3
Core	2016	822	14	13	3
Core	2020	1000	17	20	4
Core	2024	1000	17	20	5

d) Site Type

Zone	*Year*	*Number of Trees*	*Features for Decisions*	*Min Samples to Split*	*Min Samples per Node*
Rare	2016	1000	17	2	1
Rare	2020	1000	9	6	1
Rare	2024	1000	17	2	2
Transitional	2016	1000	17	20	1
Transitional	2020	1000	17	20	5
Transitional	2024	1000	17	20	5
Core	2016	1000	17	20	1
Core	2020	1000	17	20	4
Core	2024	1000	12	18	1

Supplementary Table S6: Mean Squared Error (MSE) and Mean Absolute Error (MAE) values from Extra Trees and LightGBM models trained to predict four ecological ground indices (Degradation, Moisture Content, Site Type, and Stand Age) across FAD fragmentation classes (Rare, Transitional, Core) and years (2016, 2020, 2024). Values are presented separately for training and test sets. These results guided model selection for subsequent feature importance and interpretability analyses.

Ground validation	**year**	**metric**	**set**	**rare**		**transitional**		**core**	
				Extra Trees	**LGBM**	**Extra Trees**	**LGBM**	**Extra Trees**	**LGBM**
Degradation	**2016**	**MSE**	**train**	**0.0000**	0.3167	**0.3800**	0.8457	**0.2979**	0.5777
			test	**0.4911**	0.5279	**0.9247**	0.9420	**0.6316**	0.6417
		MAE	**train**	**0.0000**	0.4306	**0.5276**	0.7977	**0.4263**	0.5985
			test	**0.5245**	0.5625	**0.8286**	0.8423	**0.6257**	0.6311
	2020	**MSE**	**train**	**0.0000**	0.4801	**0.4824**	0.8213	**0.5137**	0.7235
			test	**0.6481**	0.6825	**0.8907**	0.8954	**0.7463**	0.7521
		MAE	**train**	**0.0000**	0.5846	**0.6215**	0.8175	**0.6061**	0.7226
			test	**0.6711**	0.7014	**0.8478**	0.8534	**0.7316**	0.7365
	2024	**MSE**	**train**	**0.0000**	0.4850	**0.5011**	0.8782	**0.4142**	0.6342
			test	**0.7421**	0.7705	**0.9254**	0.9338	**0.6733**	0.6781
		MAE	**train**	**0.0000**	0.5970	**0.6422**	0.8568	**0.5240**	0.6501
			test	**0.7335**	0.7557	**0.8760**	0.8838	**0.6701**	0.6724
Moisture Content	**2016**	**MSE**	**train**	**0.0000**	1.0585	**1.7015**	3.2823	**0.5173**	0.8878
			test	**3.3411**	3.7551	**3.5456**	3.6115	**1.0064**	1.0239
		MAE	**train**	**0.0000**	0.4931	**0.6683**	0.9437	**0.1860**	0.2468
			test	**0.8570**	0.9317	**0.9812**	0.9886	0.2665	**0.2654**
	2020	**MSE**	**train**	**0.3579**	2.1324	**2.4190**	3.5762	**0.8985**	1.3300
			test	**3.2964**	3.4204	**3.8757**	3.9129	**1.3901**	1.3988

		MAE	**train**	**0.2535**	0.6679	**0.7522**	0.9225	**0.2729**	0.3350
			test	**0.8222**	0.8384	0.9649	**0.9644**	0.3444	**0.3428**
	2024	**MSE**	**train**	**0.3928**	3.1530	**2.0689**	3.8898	**0.7678**	1.0182
			test	**4.0947**	4.1929	**4.1683**	4.1982	**1.1778**	1.1846
		MAE	**train**	**0.2793**	0.8529	**0.7280**	1.0086	**0.2345**	0.2711
			test	**0.9463**	0.9663	1.0519	**1.0451**	0.2950	**0.2925**
Site Type	**2016**	**MSE**	**train**	**0.0000**	1.9109	**2.2577**	4.7335	**0.9002**	1.8913
			test	**5.2886**	5.6835	**5.2355**	5.3250	**2.0667**	2.1100
		MAE	**train**	**0.0000**	1.0254	**1.2079**	1.7744	**0.6082**	0.9005
			test	**1.7347**	1.8018	**1.8396**	1.8715	**0.9208**	0.9399
	2020	**MSE**	**train**	**0.5164**	3.0805	**3.0707**	4.9907	**0.9378**	1.5775
			test	**4.8349**	5.0059	**5.3062**	5.3329	**1.6627**	1.6764
		MAE	**train**	**0.5562**	1.4202	**1.4073**	1.8230	**0.5783**	0.7604
			test	**1.7519**	1.7903	**1.8583**	1.8765	**0.7718**	0.7782
	2024	**MSE**	**train**	**0.3550**	3.2902	**3.1324**	5.1645	**0.8189**	1.7311
			test	**5.3478**	5.4392	**5.5047**	5.5089	**1.8546**	1.8734
		MAE	**train**	**0.4502**	1.4702	**1.4347**	1.8707	**0.5519**	0.8120
			test	**1.8459**	1.8957	**1.9095**	1.9253	**0.8335**	0.8381
Stand Age	**2016**	**MSE**	**train**	**0.0000**	268.9510	**405.2102**	769.3967	**281.4542**	562.2617
			test	**747.3080**	793.0772	**845.6752**	856.3144	**608.6250**	618.2795
		MAE	**train**	**0.0000**	11.9544	**16.0089**	22.1318	**12.7420**	18.1369
			test	**19.4408**	20.2882	**23.0373**	23.2354	**18.6947**	18.9155
	2020	**MSE**	**train**	**169.4794**	462.7494	**615.2930**	1030.3012	**431.9596**	651.3972
			test	**652.9835**	672.6903	**1094.1886**	1098.0216	**673.1787**	678.0556
		MAE	**train**	**9.0716**	15.4731	**19.6523**	25.5795	**16.0512**	19.9115
			test	**18.1192**	18.5197	**26.2680**	26.3333	**20.1023**	20.2300
	2024	**MSE**	**train**	**141.7045**	412.3192	**569.7954**	1097.1861	**327.6254**	654.1738
			test	**586.8752**	600.7807	**1183.4747**	1189.8587	**709.3864**	713.3502
		MAE	**train**	**8.2464**	14.4584	**18.9441**	26.3012	**13.8434**	19.6359
			test	**17.0806**	17.1967	**27.2026**	27.2870	**20.2769**	20.3625

746

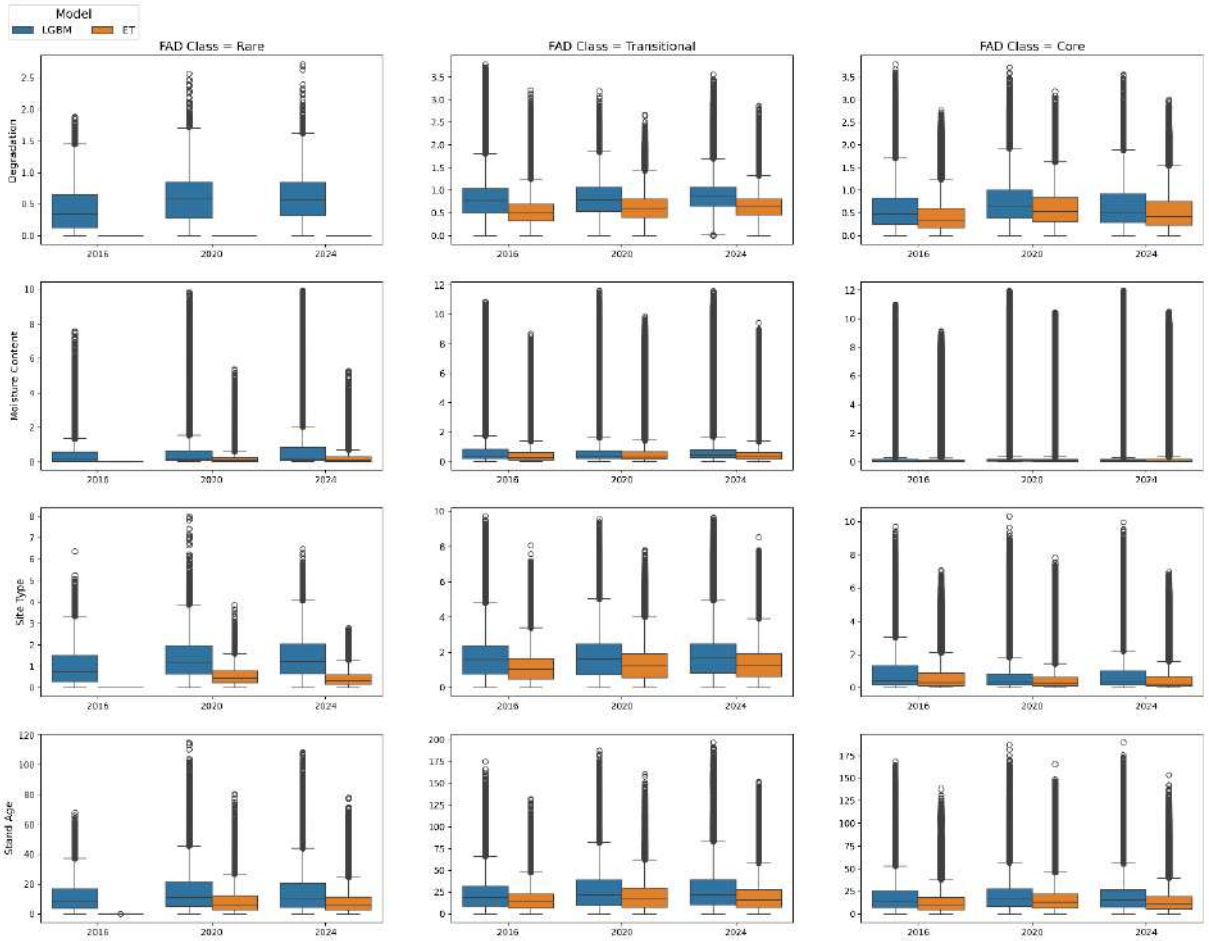

Supplementary Figure S2. Boxplots of prediction errors on the train set for Extra Trees (ET) and LightGBM (LGBM) models across three forest fragmentation classes (Rare, Transitional, Core) and years (2016, 2020, 2024), for each of the four ground indices

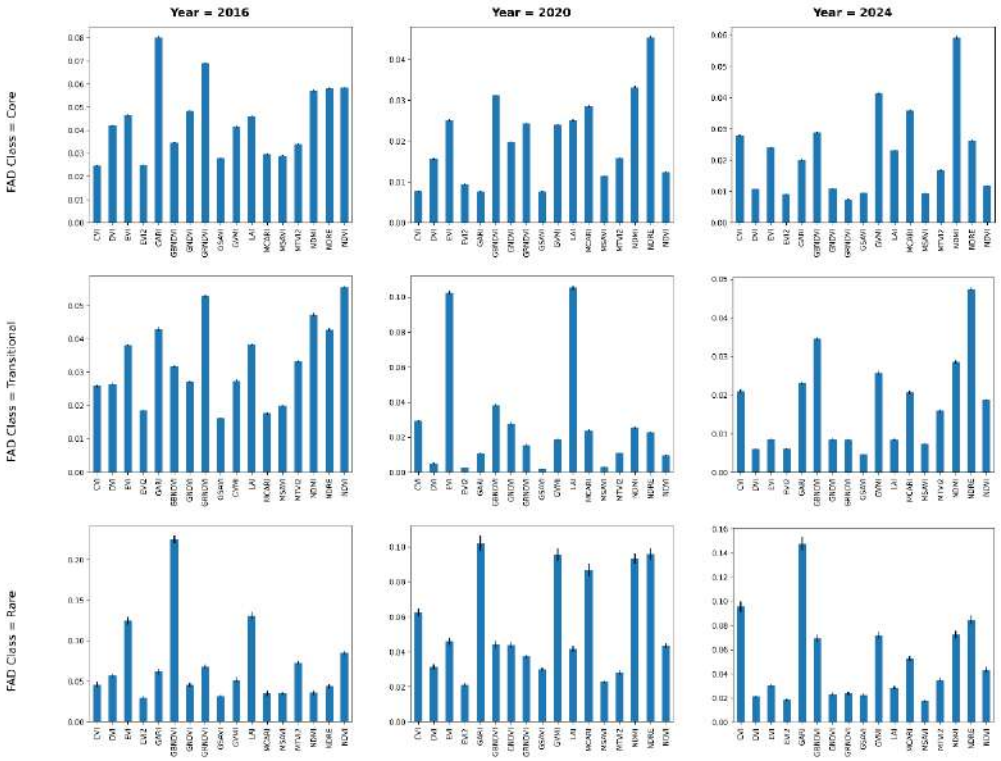

Supplementary Figure S3: Partial Importance (PI) grid showing the relative importance of vegetation indices used in predicting ***degradation levels*** across fragmentation classes (Core, Transitional, Rare) and years (2016, 2020, 2024), based on Extra Trees regressors. NDWI, GNDVI, and NDRE frequently emerged as key contributors.

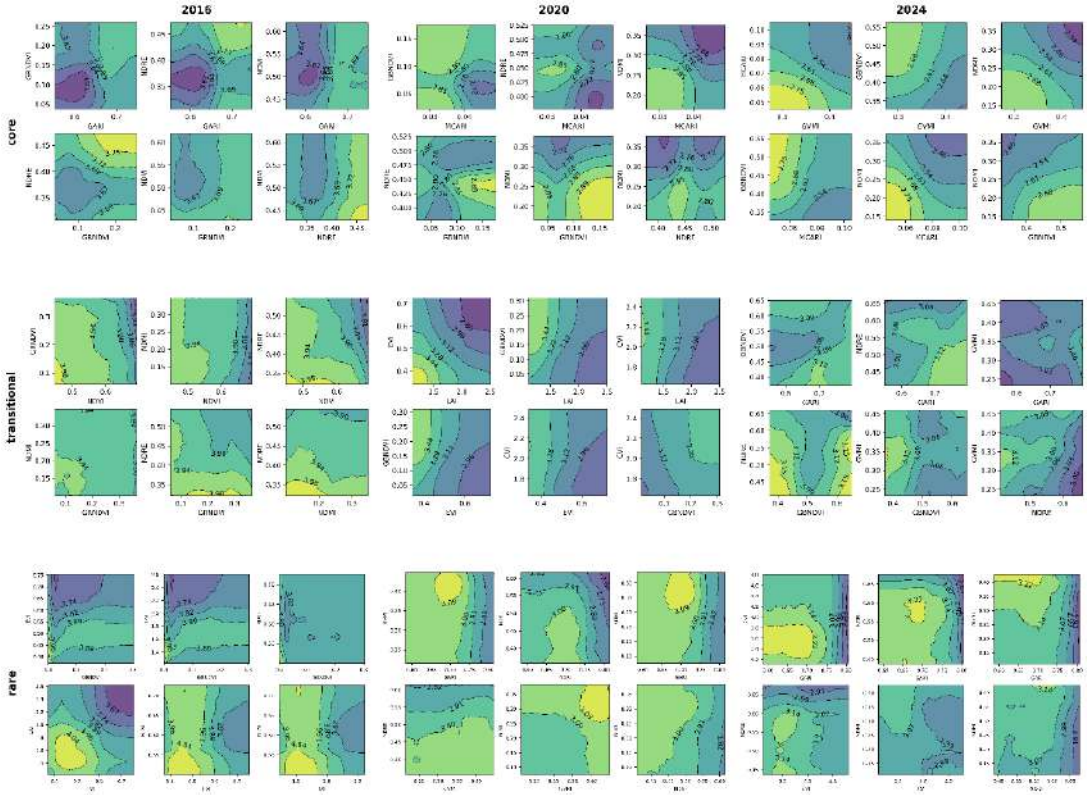

Supplementary Figure S4. Additional PDP layouts for ***degradation*** prediction, illustrating alternative VI pairs across zones and years.

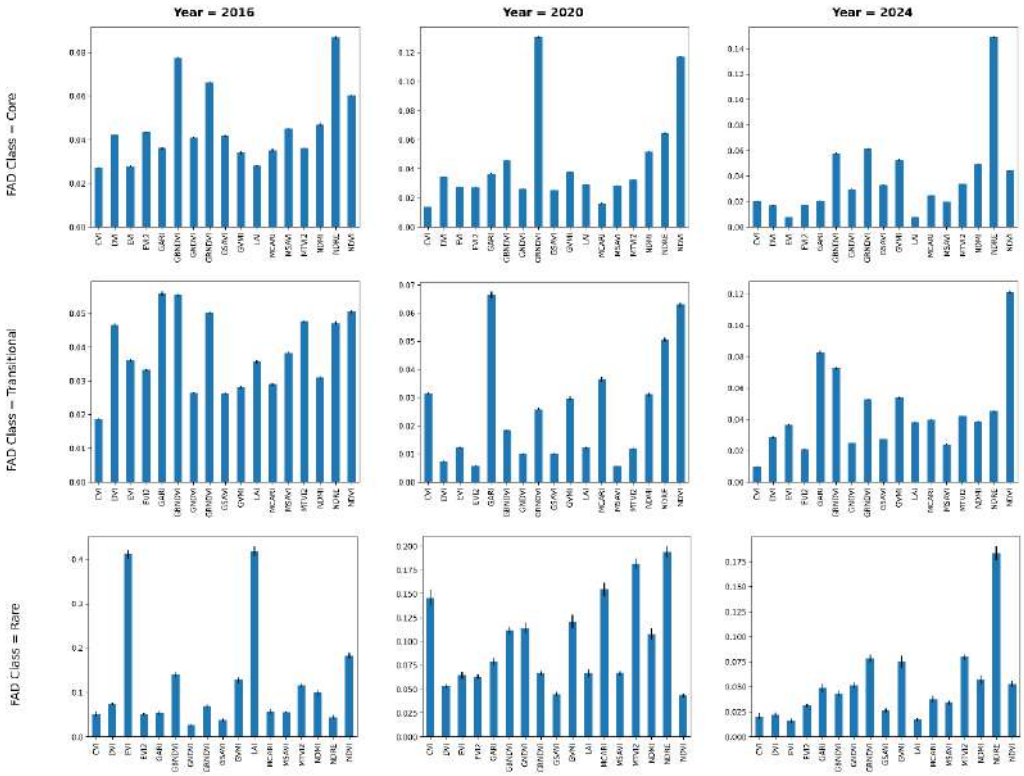

Supplementary Figure S5. Partial Importance (PI) grid for ***moisture content,*** summarizing vegetation index relevance for moisture predictions across zones and years. NDWI and NDRE emerged as the most important indices, particularly in less fragmented areas.

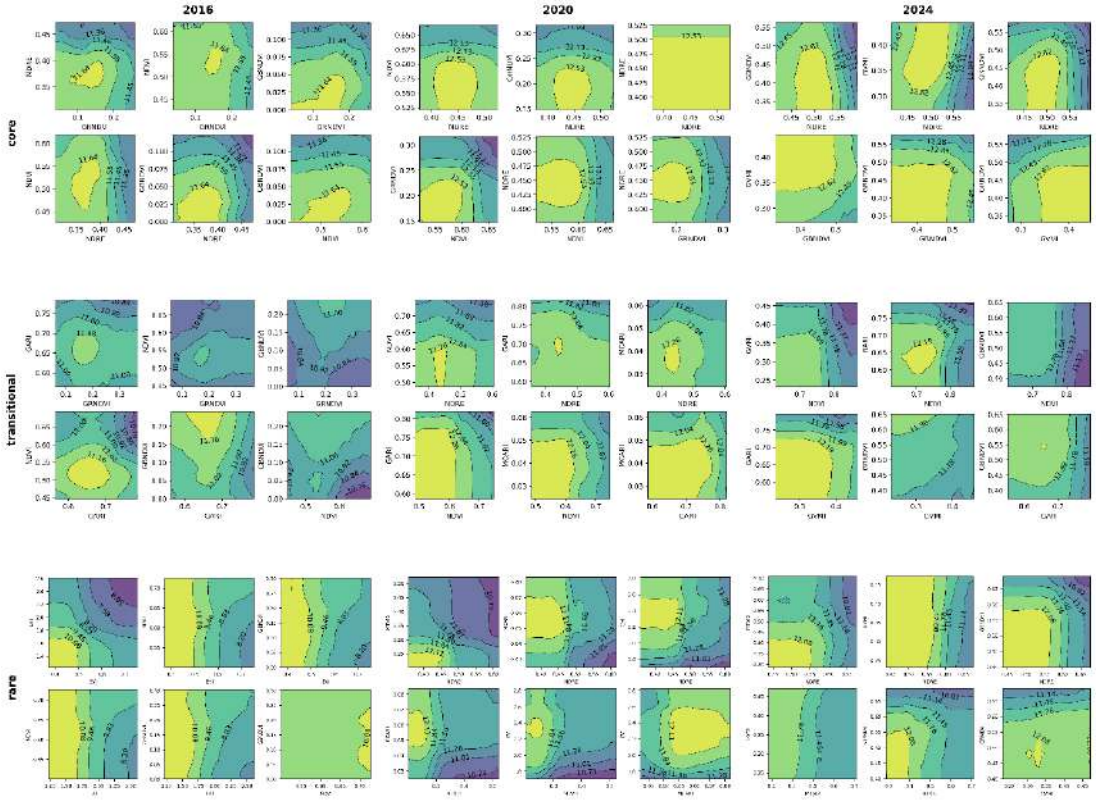

Supplementary Figure S6. Additional PDPs for ***moisture*** content, displaying alternative vegetation index pairings used to model moisture variation across FAD zones and time.

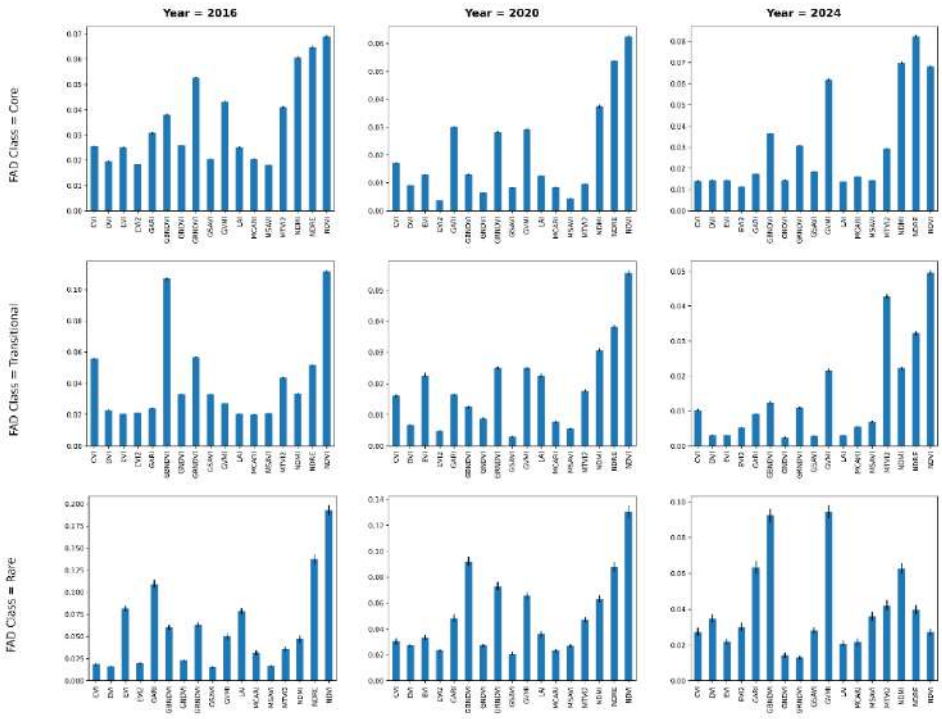

Supplementary Figure S7. Partial Importance (PI) grid showing the relative contribution of vegetation indices to ***Site Type*** predictions across fragmentation classes (Core, Transitional, Rare) and years (2016, 2020, 2024), based on Extra Trees regressors. NDVI, CIre, and NDWI emerged as consistent top predictors.

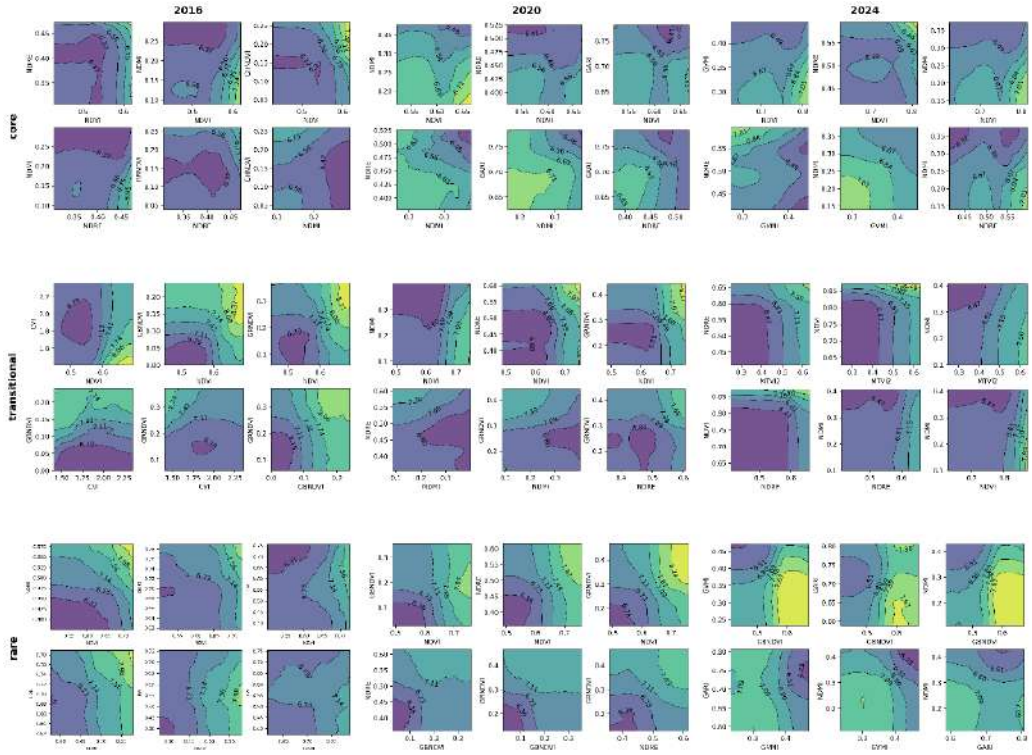

Supplementary Figure S8. PDP layouts for alternate VI pairs used for ***Site Type*** prediction across different FAD zones and years.

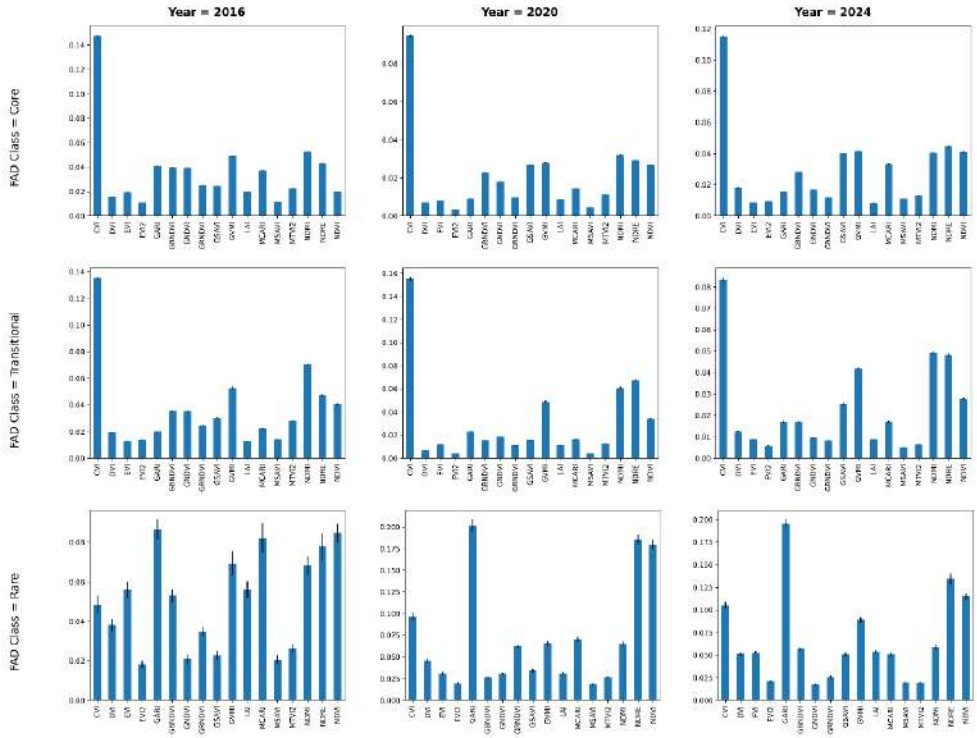

Supplementary Figure S9. Partial Importance (PI) grid showing the relative importance of vegetation indices used in predicting ***stand age*** across fragmentation classes (Core, Transitional, Rare) and years (2016, 2020, 2024), based on Extra Trees regressors. CIre, NDVI, and NDRE emerged as key predictors, with CIre particularly influential in fragmented areas.

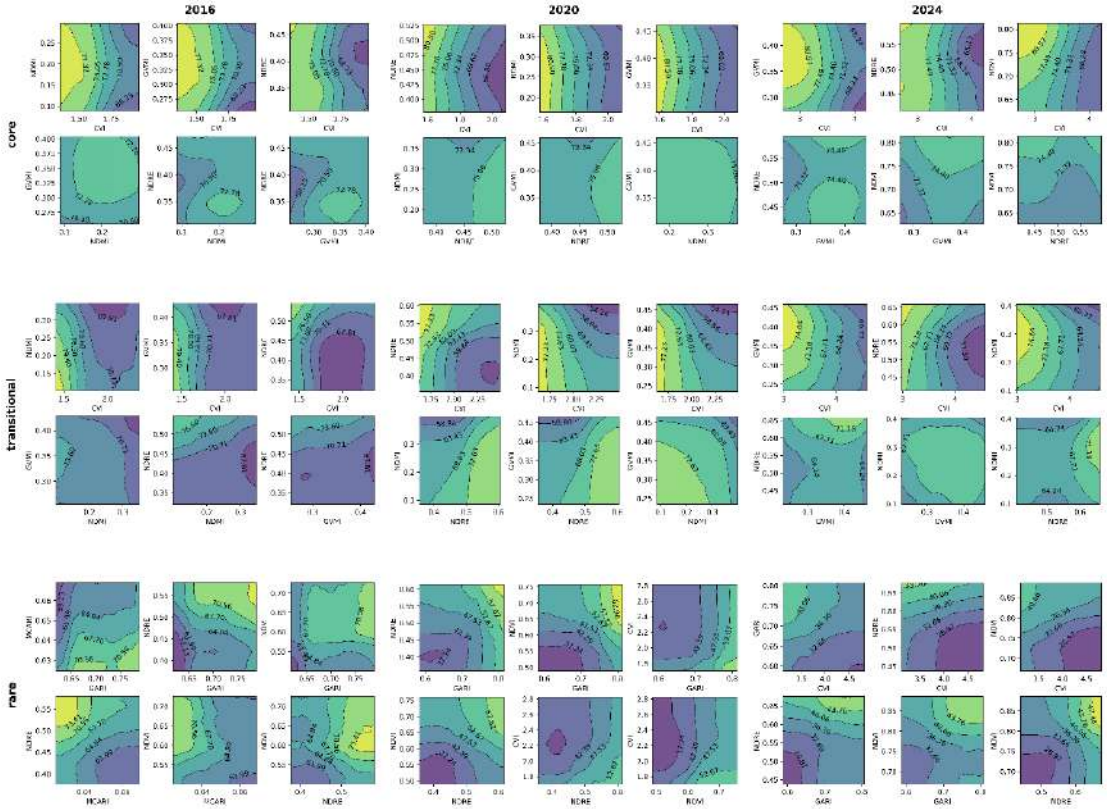

Supplementary Figure S10. PDP layouts for alternate VI pairs used for ***stand age*** prediction across different FAD zones and years.